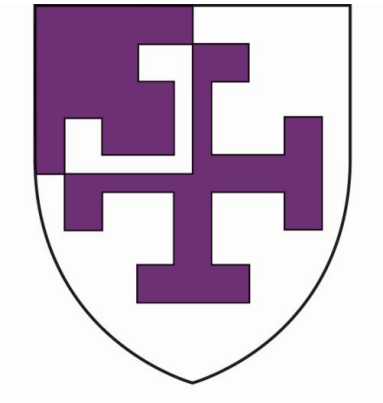
Geometrically Constrained Compounds of the Main-Group Elements for the Activation of Small Molecule Substrates





Lingyu Liu

St Cross College

University of Oxford

A thesis submitted for the degree of

Doctor of Philosophy in Inorganic Chemistry

Hilary 2022

Abstract

Geometrically Constrained Compounds of the Main-Group Elements for the Activation of Small Molecule Substrates

Lingyu Liu St Cross College
DPhil in Inorganic Chemistry Hilary 2022

This thesis is focused on the preparation of group 13 complexes stabilised by pincer ligands and their application in catalysis and small molecule activation.

Pincer stabilised gallium halides were synthesised, and their application as precursors in salt metathesis reaction was explored. Novel gallium hydrides with an $[ON(H)O]^{2-}$ ligand were prepared via the reaction of precursors and borane reagents. The use of gallium hydrides in the activation of compounds with carbonyl groups (such as aldehydes, ketones) was explored, resulting in bimetallic gallium alkoxide complexes.

Several gallium complexes were used as catalysts for the catalytic hydroboration of aldehydes, ketones, carbon dioxide, isocyanates and imines. With low catalyst loadings (0.05−1.0 mol%), substrates containing unsaturated bonds were hydroborated under ambient conditions with good efficiency. A mechanism is proposed for the catalytic hydroboration of ketones.

Transelementation reactions between gallium complexes and boron reagents are discussed. A series of boron complexes were prepared by the reaction of $[H_3(ONO)]$ and boranes. The exploration of the dehydrogenation reactivity of the boron complex [ON(H)O]BH is described. The Lewis acidity of some boron complexes is also discussed.

Additionally, pincer stabilised boron halides were prepared by reacting the $[H_3(ONO)]$ ligand and boron halides. Their reactivity towards bases was explored. The boron bromide complex

[ON(H)O]BBr was found to activate the C−O bond of cyclic ethers to give borate esters, which release HBr to give cyclic products possessing an N−B−O moiety.

Acknowledgments

I am immensely grateful to my supervisor, Prof. Jose Goicoechea, for his dedicated supervision throughout my D.Phil. project. He is motivated and helpful, and his enthusiasm for chemistry is inspiring. He has an amazing energy, and has made the laboratory a nice place to work. As he always says, I have matured a lot during my studies at Oxford (although I am still young).

Dr. Siu-Kwan Lo, Mr. Cory Smith and Ms. Rachel Bowld are acknowledged as very helpful collaborators. I would also like to thank the group members, Dr. Urwin, Mr. Feld and Dr. Wilson, for their patience in proof-reading my written work. In general, credit should be given to the Goicoechea and Aldridge labs, where I benefited a lot through daily discussions. Special thanks for Erica and Doruk for their daily gossip. In addition, I would like to acknowledge all the crystallographers in Goicoechea lab, they are amazing.

It has been a great pleasure to be a member of St. Cross College. The college has consistently offered nice food during lunches and formal dinners, and those meals are remarkable memories for me. Thank you, Mr David Khachaturov, for always being there for me.

I also want to thank many friends: Dr. Ching Lam who had the most dinners with me; Mr. Marcus Yu and Mr. Rex Huang who had the most lunches with me; Mr. Wales, Ms. McManus and Dr. Boyd who had most formals with me; Dr. Yuhang Shi who sent the most messages to me; Mr. Kelland Xu, Ms. Hannah Wu and Ms. Estrella Yin who I have known the longest at Oxford. Special thanks to Ms. Alice Yu and her family. I would like to say a special thank you to my best-friends-forever, Mr. Gengbin, Mr. Qi yang, Mr. Jonathan Lam and Ms. Iris Yip for their constant support and friendship. I also want to express my thanks to Dr. Lu Wei and Dr. Chao Zou who supervised me during my undergraduate study.

I would like to thank my family. My uncle, Mr. Kelvin Chan, has consistently offered me unreserved help since childhood, and the honour should be credited to him. My mum and her sisters offered me endless support and love to keep me going forward. Nobody has been more important to me than my family members.

List of abbreviations

$\{^1H\}$	^1H decoupled
$[ONO]^{3-}$	*N*,*N*-bis-(3,5-di-*tert*-butyl-2-phenoxy)amide
$[H_3(ONO)]$	*N*,*N*-bis(3,5-di-*tert*-butyl-2-phenol)amine
$[ON(H)O]^{2-}$	*N*,*N*-bis-(3,5-di-*tert*-butyl-2-phenoxy)amine
°	angles
°C	degrees Celsius
Å	Ångström
τ_5	geometry index or structural parameter for a five-coordinate complex
δ	chemical shift
Δ	difference or heating
γ	gyromagnetic or magnetogyric ratio
Σ	sum
μ	micro or bridging ligand
9-BBN dimer	9-borabicyclo[3.3.1]nonane dimer, $C_{16}H_{30}B_2$
Anal.	elemental analysis
AN	acceptor number

Ar	aryl
atm	atmosphere
br	broad
butyl	C_4H_9
B_2pin_3	2,2'-(2,3-dimethyl-2,3-butanediyldioxy)bis(4,4,5,5-tetramethyl-1,3,2-dioxaborolane, $C_{18}H_{36}B_2O_6$
BCF	tris(pentafluorophenyl)borane
Bz	benzyl
Cy	cyclohexyl
Calcd	calculated
CCD	charge-coupled device
CSD	Cambridge Structural Database
COD	1,5-cyclooctadiene
d	doublet
d_n	deuterated with n deuterium atoms
dba	dibenzylideneacetone, $C_{17}H_{14}O$
dioxane	1,4-dioxane, $C_4H_8O_2$
dpp-bian	1,2-bis[(2,6-diisopropylphenyl)imino]acenaphthene

DBU	1,8-diazabicyclo[5.4.0]undec-7-ene, $C_9H_{16}N_2$
DCM	dichloromethane, CH_2Cl_2
DFT	density functional theory
Dipp	2,6-diisopropylphenyl
^{Dipp}Nacnac	$HC[C(Me)N(2,6\text{-}^{i}Pr\text{-}C_6H_3)]_2$
DOSY	diffusion-ordered spectroscopy
ee	enantiomeric excess
eV	electronvolt
EI MS	electron impact mass spectrometry
ESI MS	electrospray ionisation mass spectrometry
Et	ethyl, CH_2CH_3
FIA	fluoride ion affinity
FLP	frustrated Lewis pair
g	gram
h	hour
HBA	hydrogen bond acceptor
HBpin	pinacolborane
HBCat	catecholborane

HIA	hydride affinity
HMDS	hexamethyldisilylamide, $N(SiMe_3)_2$
HMCTS	hexamethylcyclotrisiloxane
Hz	Hertz
I	nuclear angular momentum quantum number
^{i}Pr	isopropyl
IPr	1,3-bis(2,6-diisopropylphenyl)imidazol-2-ylidene, $:C(N(Dipp))_2(CH)_2$
J	Joule
J	coupling constant
k	kilo
K	Kelvin
Kα	radiation emitted on transition of an electron from an L shell to K shell
L	litre
m	milli or metre or multiplet
m/*z*	mass to charge ratio
min	minute
mol	mole
M	mega or molar, mol dm^{-3}

Me	methyl, CH_3
MeOTf	methyl trifluoromethanesulfonate
Mes	2,4,6-trimethylphenyl
MTB	monothiobinaphthol
$MTBH_2$	2-hydroxy-2´-mercapto-1,1´-binaphthyl
n	nano
nacnac	β-diketiminato
NOESY	nuclear overhauser effect spectroscopy
^{n}Bu	normal butyl, $CH_2CH_2CH_2CH_3$
NHC	*N*-heterocyclic carbene
NMR	nuclear magnetic resonance
OAc^-	acetate, $[CH_3COO]^-$
OTf^-	triflate, $[CF_3SO_3]^-$
OTs^-	tosylate group
ppm	parts per million
propyl	C_3H_7
py	pyridine, C_5H_5N
Ph	phenyl, C_6H_5

q	quartet
r	radius
rt	room temperature
R	hydrocarbonyl ligand
s	singlet
^{S}Bu	2-butyl, $CH(CH_2CH_3)(CH_3)$
SEGWE	Stokes-Einstein Gierer-Wirtz Estimation
SIPr	1,3-bis(2,6-diisopropylphenyl)imidazolidin-2-ylidene
t	triplet
^{t}Bu	tertiary butyl, $C(CH_3)_3$
tert	tertiary
TEMPO	(2,2,6,6-tetramethylpiperidin-1-yl)oxyl, $(CH_2)_3(CMe_2)_2NO$
TFP	tetrafluoropyridyl
THF	tetrahydrofuran, C_4H_8O
TOF	turnover frequency
TON	turnover number
TPM	triphenylmethane

Table of Contents

Table of Contents **1**

Chapter One Introduction **8**

1.1 Main group elements and catalysis 9

1.2 Group 13 hydrides (EH_3; E = B–Tl) 10

1.2.1 Binary hydrides of the group 13 elements 10

1.2.2 Amine stabilised gallium hydrides 11

1.3 Main group element catalysts in hydroboration 14

1.3.1 Magnesium and calcium catalysts in hydroboration reactions 17

1.3.2 Aluminium and gallium catalysts in hydroboration reactions 22

1.3.3 Germanium and tin catalysts in hydroboration reactions 28

1.3.4 Phosphorus and arsenic catalysts in hydroboration reactions 33

1.4 Dehydrogenation of amine-boranes 37

1.4.1 Acid mediated dehydrogenation of amine-boranes 38

1.4.2 Base mediated dehydrogenation of amine-boranes 41

1.4.3 Frustrated Lewis pair mediated dehydrogenation of amine-boranes 43

1.5 Project aims and summary 47

1.6 References 49

Chapter Two Synthesis of novel pincer-ligated gallium complexes and their use in the hydrogallation of small molecule substrates **58**

2.1 Introduction and objectives 59

2.2 Synthesis of $[ON(H)O]^{2-}$ stabilised gallium chloride complexes 63

2.3 Synthesis of gallium phosphaketene complex **2.3** 65

2.4 Reactivity of the gallium phosphaethynolate complex 67

2.5 Salt metathesis reactions of **2.3** 70

2.6 Dehydrocoupling of **2.7** and alcohols 74

2.7 Reaction of **2.8a** with boranes 77

2.8 Application of NMR techniques in the characterisation of **2.9** 80

2.9 A boryloxy-bridged side-product formed during the synthesis of **2.9** 87

2.10 Monomerisation of **2.9** to **2.7** using a coordinating solvent 89

2.11 Hydrogallation of aldehydes by complexes **2.7** and **2.9** 91

2.12 Hydrogallation of ketones by complexes **2.7** and **2.9** 96

2.13 Conclusions 101

2.14 References 103

Chapter Three Gallium hydride catalysts for the hydroboration of unsaturated substrates 106

3.1 Introduction and objectives 107

3.2 Gallium catalysed hydroboration of aldehydes 108

3.2.1 Catalytic hydroboration of aldehydes 108

3.2.2 Control experiments for the hydroboration of aldehydes 111

3.3 Gallium catalysed hydroboration of ketones 115

3.3.1 Catalytic hydroboration of ketones 116

3.3.2 Inhibition of ketone hydroboration by tetramethylethylenediamine (TMEDA) 119

3.3.3 Monitoring of hydroboration of 4′-nitroacetophenone with different catalysts 120

3.3.4 A simplified proposed mechanism for the hydroboration of aldehydes and ketones 122

3.3.5 Kinetic studies for the hydroboration of ketones 124

3.3.6 Simulation studies for the hydroboration of ketones 127

3.4 Catalytic hydroboration of carbon dioxide 128

3.5 Catalytic hydroboration of isocyanates 131

3.5.1 Catalytic hydroboration of isocyanates 133

3.6 Hydroboration of imines 138

3.7 Summary and perspective 142

3.8 References 144

Chapter Four Synthesis and reactivity of pincer stabilised boron complexes ... 147

4.1 Introduction and objectives 148
4.2 Transelementation reactions and the formation of borane complexes of $[ON(H)O]^{2-}$ 149
4.3 Synthesis of boron complexes stabilised by the $[ON(H)O]^{2-}$ ligand 152
4.4 Synthesis of novel amine-borane complexes as hydrogen carriers 158
4.5 Dehydrogenation studies of **4.6** 161
4.6 Catalytic dehydrogenation of **4.6** 165
4.7 Reaction of **4.6** towards unsaturated substrates 169
4.8 Determination of the Lewis acidity of **4.8** and **4.9** 171
4.9 Conclusions 175
4.10 References 177
Chapter Five Synthesis and reactivity of pincer stabilised boron halide complexes 180
5.1 Introduction and objectives 181
5.2 Synthesis of pincer stabilised boron halide complexes 183
5.3 Synthesis of Lewis base adducts of boron-halide complexes 188
5.4 Transfer hydrobromination of **5.2c** to an alkyne 192
5.5 Application of **5.2c** in C−O bond cleavage 193
5.6 Boron halides in water activation 201
5.7 Conclusions 202
5.8 References 204
Chapter Six Experimental Details 206
6.1 General considerations and starting materials 207
6.2 Experimental details for Chapter Two 211
6.2.1 Synthesis of $[H_3(ONO)]$ 211
6.2.2 Synthesis of Ga[ON(H)O]Cl(py) (**2.1**) 212

6.2.3 Synthesis of Ga[ON(H)O]Cl($NH_2{}^nPr$) (**2.2**) 213
6.2.4 Synthesis of Ga[ON(H)O]py(PCO) (**2.3**) 214
6.2.5 Synthesis of $Ga_3[ON(H)O]_2[ONO]py_2$ (**2.4**) and $[Ga(ONO)py]_2$ (**2.5**) 215
6.2.6 Synthesis of [ONO]$Ga(Na_2)(THF)_2(O^tBu)_2$ (**2.6**) 216
6.2.7 Synthesis of HGa(THF)[ON(H)O]·1.5BH_3:py (**2.7**·1.5BH_3:py) 217
6.2.8 Synthesis of $\{Ga[ON(H)O](OCH_2CH_3)\}_2$ (**2.8a**) 218
6.2.9 Synthesis of $\{Ga[ON(H)O](OCH_2Cy)\}_2$ (**2.8b**) 219
6.2.10 Synthesis of $H_2Ga[\mu^2$-ON(H)O]Ga[ON(H)O] (**2.9**) 220
6.2.11 Synthesis of $\{Ga[ON(H)O](OBpin)\}_2$ (**2.10**). 221
6.2.12 Synthesis of HGa(THF)[ON(H)O] (**2.7**) 222
6.2.13 General synthesis and characterisation data for $\{Ga[ON(H)O](OCH_2R)\}_2$ (**2.11a**–**e**). 224
6.2.14 Synthesis of $\{Ga[ON(H)O](OCH_2Ph)\}_2$ (**2.11a**) 224
6.2.15 Synthesis of $\{Ga[ON(H)O](OCH_2CHMe_2)\}_2$ (**2.11b**) 225
6.2.16 Synthesis of $\{Ga[ON(H)O](OCH_2C_6H_4$-4-OMe$)\}_2$ (**2.11c**) 225
6.2.17 Synthesis of $\{Ga[ON(H)O](OCH_2C_6H_4$-4-Br$)\}_2$ (**2.11d**) 226
6.2.18 Synthesis of $\{Ga[ON(H)O](OCH_2C_6H_2Me_3)\}_2$ (**2.11e**) 226
6.2.19 Synthesis of $\{Ga[ON(H)O](OCH(Ph)_2)\}_2$ (**2.12a**) 227
6.2.20 Synthesis of $\{Ga[ON(H)O](OCH(Me)_2)\}_2$ (**2.12b**) 228
6.2.21 Synthesis of $\{Ga[ON(H)O][OCH(CH_3)(C_6H_4$-4-OMe$)]\}_2$ (**2.12c**) 229
6.2.22 Synthesis of $\{Ga[ON(H)O][OCH(CH_3)(C_6H_4$-4-Br$)]\}_2$ (**2.12d**) 229
6.2.23 Synthesis of $\{Ga[ON(H)O](OCHC_8H_8)\}_2$ (**2.12e**) 230
6.2.24 Synthesis of $\{Ga[ON(H)O][OCH(CH_3)(C_6H_4$-4-$NO_2)]\}_2$ (**2.12f**) 231
6.3 Experimental details for Chapter Three 232
6.3.1 General procedure for the catalytic hydroboration of aldehydes and ketones 232
6.3.2 $PhCH_2OBpin$: product from hydroboration of benzaldehyde. 233
6.3.3 4-Br-$C_6H_4CH_2OBpin$: product from hydroboration of 4-bromobenzaldehyde 233
6.3.4 4-MeO-$C_6H_4CH_2OBpin$: product from hydroboration of 4-methoxybenzaldehyde 233
6.3.5 2,4,6-$Me_3C_6H_2CH_2OBpin$: product from hydroboration of mesitaldehyde 233
6.3.6 4-F-C_6H_4-CH_2OBpin: product from hydroboration of 4-fluorobenzaldehyde 234

6.3.7 4-Me-$C_6H_4CH_2OBpin$: product from hydroboration of 4-methylbenzaldehyde 234
6.3.8 (4-Br-C_6H_4)(CH_3)C(H)OBpin: product from hydroboration of 4'-bromoacetophenone 234
6.3.9 (4-MeO-C_6H_4)(CH_3)C(H)OBpin: product from hydroboration of 4'-methoxyacetophenone 235
6.3.10 $(CH_3)_2C(H)OBpin$: product from hydroboration of acetone 235
6.3.11 $(CH_3)_2C(H)CH_2OBpin$: product from hydroboration of isobutyraldehyde 235
6.3.12 (4-NO_2-C_6H_4)C(H)(CH_3)OBpin: product from hydroboration of 4'-nitroacetophenone 235
6.3.13 (4-I-C_6H_4)C(H)(CH_3)OBpin: product from hydroboration of 4'-iodoacetophenone 236
6.3.14 (4-Cl-C_6H_4)C(H)(CH_3)OBpin: product from hydroboration of 4'-chloroacetophenone 236
6.3.15 Preparation of a stock solution for carbon dioxide hydroboration 236
6.3.16 MeOBpin: product from the hydroboration of carbon dioxide 237
6.3.17 $O(Bpin)_2$: side product from the hydroboration of carbon dioxide 237
6.3.18 General procedure for the catalytic hydroboration of isocyanates 237
6.3.19 PhN(Me)Bpin: product from hydroboration of phenyl isocyanate. 238
6.3.20 MesN(Me)Bpin: product from hydroboration of 2,4,6-trimethylphenyl isocyanate 238
6.3.21 2-$CF_3C_6H_4$N(Me)Bpin: product from hydroboration of 2-(trifluoromethyl)phenyl isocyanate 238
6.3.22 4-MeC_6H_4N(Me)Bpin: product from hydroboration of *p*-tolyl isocyanate 239
6.3.23 CH_2=$CHCH_2$N(Me)Bpin: product from hydroboration of allyl isocyanate 239
6.3.24 $PhCH_2$N(Me)Bpin: product from hydroboration of benzyl isocyanate or *N*-benzylidenemethylamine 240
6.3.25 4-BrC_6H_4N(Me)Bpin: product from hydroboration of 4-bromophenyl isocyanate 240
6.3.26 General procedure for the catalytic hydroboration of imines 240
6.3.27 $PhCH_2N(^tBu)$Bpin: product from hydroboration of *N*-benzylidene-*tert*-butylamine 241
6.4 Experimental details for Chapter Four 241
6.4.1 Synthesis of [O(H)N(H)O]B(C_6F_5)$_2$ (**4.1**) 241
6.4.2 Synthesis of [ON(H)O]B(C_6F_5) (**4.2**) 242

6.4.3 Synthesis of $OPEt_3$·[ON(H)O]B(C_6F_5) (**4.2**·$OPEt_3$) 243
6.4.4 Synthesis of [ON(H)OH]B(C_6H_5)$_2$ (**4.3**) 244
6.4.5 Synthesis of [ON(H)O]B(C_6H_5) (**4.4**) 245
6.4.6 Synthesis of [O(H)N(H)O]B(pin) (**4.5**) 246
6.4.7 Synthesis of [ON(H)O]BH (**4.6**) 247
6.4.8 Synthesis of [ON(H)O]BH·$OPEt_3$ (**4.6**·$OPEt_3$) 248
6.4.9 Synthesis of [ON(H)O]BH·DMSO (**4.6**·DMSO) 249
6.4.10 Synthesis of [ONO]B($NH_2{}^n$Pr) (**4.7**) 250
6.4.11 Synthesis of [ONO]B[ONO]B·($NH_2{}^n$Pr) (**4.8**·$NH_2{}^n$Pr) 251
6.4.12 Preparation of [B(ONO)]$_2$ (**4.9**) 252
6.4.13 Synthesis of **4.8**·$OPEt_3$ and **4.9**·$OPEt_3$ 254
6.4.14 Synthesis of [ON(H)O]B(OCH_2-*p*-$C_6H_4CH_3$) (**4.11**) 255
6.4.15 Synthesis of [ON(H)O]B[$OCH(CH_3)$-*p*-$C_6H_4NO_2$] (**4.12**). 256
6.5 Experimental details for Chapter Five 257
6.5.1 Synthesis of [H_3(ONO)]·BF_3 (**5.1**) 257
6.5.2 Synthesis of [ON(H)O]BF (**5.2a**) 258
6.5.3 Synthesis of [ON(H)O]BCl (**5.2b**) 259
6.5.4 Synthesis of [ON(H)O]BBr (**5.2c**) 260
6.5.5 Synthesis of [ON(H)O]BCl·Et^{i}Pr$_2$N·HCl (**5.2b**·Et^{i}Pr$_2$N·HCl) 261
6.5.6 Synthesis of (ONO)BNEt_3 (**5.3a**) 262
6.5.7 Synthesis of (ONO)B(DBU) (**5.3b**) 263
6.5.8 Sythesis of (ONO)BNMe_3 (**5.3c**) 264
6.5.9 Synthesis of [ON(H)O]BOC_4H_8Br (**5.4**) 265
6.5.10 Synthesis of [ONO]BOC_4H_8 (**5.5**) 266
6.5.11 Synthesis of [ON(H)O]B$OC_2H_4OC_2H_4$Br (**5.6**) 267
6.5.12 Synthesis of [ON(H)O]BOC_2H_4Br (**5.7**) 268
6.5.13 Synthesis of [ONO]BOC_2H_4 (**5.8**) 269
6.5.14 Synthesis of {[ON(H)O]B}$_2$O (**5.9**) 270
6.6 References 271
Chapter Seven Conclusions and perspective 272
7.1 Conclusions and perspective 273
7.2 References 276
Appendix 277

Single crystal X-ray diffraction data.....277

Chapter One

Introduction

1.1 Main group elements and catalysis

A catalyst is a substance that offers an alternative reaction pathway, allowing a chemical reaction to proceed with a smaller energy barrier.[1] By definition, a catalyst is regenerated after the reaction is completed, i.e. it is not consumed during the reaction. Given the economic benefits of enabling facile chemical transformations by making chemical reactions more efficient, catalysts have been heavily employed in the chemical industry.

Historically, catalysis has focused on late transition metals (e.g. palladium, rhodium, and iridium),[2–4] which are often expensive and scarce. Transition metal catalysts have been extensively studied for many decades, and the impressive development of the field has been a key area of chemical research.

By contrast, main group elements (such as aluminium and silicon) are inexpensive, have a high crustal abundance and are potentially attractive for the development of novel catalysts.[5,6] The main obstacle facing these systems is that they are often unreactive, or for the specific transformations in which they can be used as catalysts, they often have low turnover numbers.[7] It was not until 2005 that the first example of a main group based system which showed reactivity towards the activation of dihydrogen was reported.[8] This breakthrough inspired a global research effort exploring small molecule activation using compounds based on the main group elements.

1.2 Group 13 hydrides (EH_3; E = B–Tl)

The group 13 (or IIIa) elements, also known as the boron group elements, are six chemical elements of the periodic table. These six elements are boron (B), aluminium (Al), gallium (Ga), indium (In), thallium (Tl) and the synthetic chemical element nihonium (Nh).[9,10]

The study of early group 13 element hydrides (particularly those of boron and aluminium) has been fuelled by their applications in chemical synthesis over the past years.[11,12] By contrast, the hydrides of the heavier elements (gallium, indium and thallium) remain under-explored. In all likelihood, this is due to the increased instability of the M–H bond on descending group 13, which is caused by ineffective orbital overlap.[13]

1.2.1 Binary hydrides of the group 13 elements

Boron hydride complexes are often reactive, moisture-sensitive and flammable. They remained unexplored until the development of high vacuum techniques by Stock around 1912.[14] Stock was a pioneer of borane chemistry, and first reported the preparation of a series of binary boranes.[15] Binary boranes, such as B_2H_6, B_4H_{10}, B_5H_9, B_5H_{11}, B_6H_{10}, $B_{10}H_{14}$, were all synthesised by Stock, via reaction of magnesium boride with aqueous acid solutions.[15,16] The monomeric borane BH_3 cannot be isolated under ambient conditions due to its electron deficiency and tendency to form a dimer, B_2H_6, through three-centre two-electron B−H−B bond.[16,17]

In contrast to the wide scope of binary boranes, low molecular weight binary alanes were not synthesised until much later.[18] The earliest documented example of the attempted synthesis of alanes dates back to the 1940s, and focused on the synthesis and

characterisation of the polymeric aluminium hydrides $(AlH_3)_n$.[12,19,20] In 2003, Andrews reported the synthesis and infrared spectroscopy of the aluminium hydride $H_2Al(\mu\text{-}H)_2AlH_2$. Condensed hydrogen gas was co-deposited with aluminium atoms (generated by pulsed-laser ablation) at 3.5 K to afford the binary dibridged alane. This compound was found to gradually release dihydrogen upon heating above 6.8 K.[18]

Heavier group 13 binary hydrides EH_3 (E = Ga, In, Tl) are generally unstable and decompose to the element and hydrogen gas at room temperature. Strong Lewis bases are needed to stabilise GaH_3 and InH_3.[21] So far, TlH_3 has not been synthesised in bulk, although research on the photoablation of thallium under an H_2 atmosphere provides evidence for the existence of this compound.[22]

Gallane (Ga_2H_6) was first synthesised as a chemically pure compound via the reaction of lithium gallium hydride with monochlorogallane in 1989, and fully characterised by Downs in 1991 (Scheme 1.1).[23,24] It is worth noting that digallane Ga_2H_6 is susceptible to aggregation in the condensed phase to form a tetramer $(GaH_3)_4$.[24]

$$0.5\ \text{eq}\ [H_2GaCl]_2 + LiGaH_4 \xrightarrow[\text{neat reagents or } n\text{-octane}]{-30\ ^\circ C} 1/x\ \text{eq}\ [GaH_3]_x + LiGaH_3Cl$$

Scheme 1.1: Synthetic procedure for the synthesis of gallane.[23,24]

1.2.2 Amine stabilised gallium hydrides

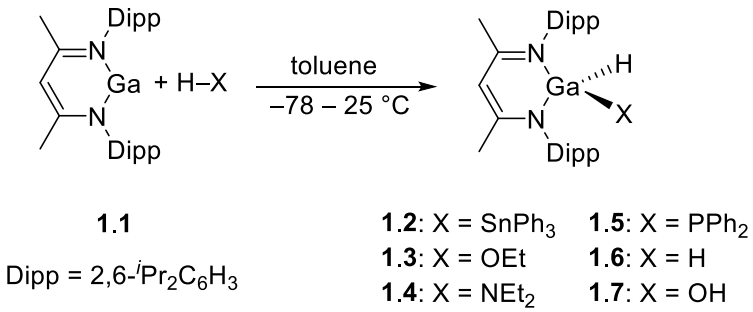
As gallane decomposes above −10 °C, more stable gallium hydride reagents, such as lithium gallium hydride or amine-GaH_3 adducts (e.g. $Me_3N{\cdot}GaH_3$), are more commonly used due to the ease with which they can be manipulated.[25–31]

Gallium hydrides with nitrogen donor ligands, such as amines, azides and hydrazine, are of interest as potential single source precursors for GaN (gallium nitride) films,

obtained via metal organic chemical vapour deposition (MOCVD).[32] GaN is widely used in electronics, as it has a wide band gap (E_g = 3.4 eV) which makes it a technologically important semiconductor.[33] It has found applications in LEDs, transistors, radars, nano-scale electronics and even in medical diagnostics.[34]

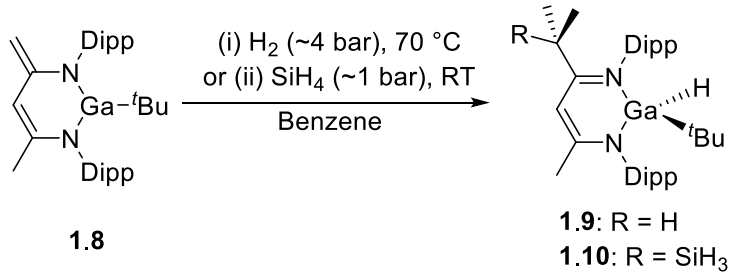
Adducts of gallium hydrides with primary and secondary amines such as L·GaH_3 (L = MeH_2N,[26,35–37] Me_2HN,[37] $^{i}PrH_2N$,[36] $^{s}BuH_2N$,[38] $^{t}BuH_2N$),[26] and cationic species such as $[H_2Ga(NH_2R)_2]Cl$ (R = Me, ^{i}Pr, ^{t}Bu, ^{s}Bu),[39] and {[2,6-$(Me_2NHCH_2)_2C_6H_3$]Ga(H)$(OTf)_2$}(OTf),[40] are chemically interesting as they have hydridic (Ga−H) and protic (N−H) hydrogen atoms in a same complex and can, in principle, eliminate dihydrogen.

A general approach for the synthesis of gallium hydride complexes is via the reaction of a ligand and gallium hydride reagents, such as $HGaCl_2$,[41] H_2GaCl,[23,30] $R_3N·GaH_3$,[26,27] and $LiGaH_4$.[23,35,39,40,42–44] By using this approach, the Ga–H bond is formed prior to the introduction of ligands.[45] As an exception, the air-stable, amide-bridged dimeric gallium hydride, $[^{t}Bu(H)Ga(\mu\text{-}NEt_2)]_2$, is synthesised by the reaction of *tert*-butyl lithium and $[Cl_2Ga(\mu\text{-}NEt_2)]_2$ (the hydride is formed by β-hydride elimination of a *tert*-butyl substituent).[46] A series of H−X bonds (X = $SnPh_3$, OEt, NEt_2, PPh_2, H, OH) can be activated by (^{Dipp}Nacnac)Ga **1.1** (^{Dipp}Nacnac = $HC[C(Me)N(2,6\text{-}^{i}Pr\text{-}C_6H_3)]_2$) to generate gallium hydride complexes **1.2**−**1.7** (Scheme 1.2).[47]



Scheme 1.2: Synthesis of gallium hydride complexes **1.2**–**1.7**.[47]

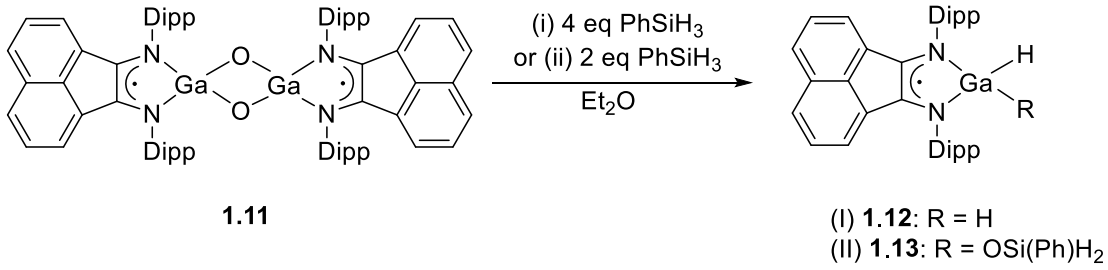
Gallium–hydride bond formation, in the case of [CH{C(R)NAr}$_2$Ga(^{t}Bu)(H)] (Ar = 2,6-^{i}Pr$_2$C$_6$H$_3$, R = CH$_3$ or CH$_2$SiH$_3$), is possible by addition of H$_2$ or SiH$_4$ at [CH{C(R)NAr}$_2$Ga(^{t}Bu)] (Ar = 2,6-^{i}Pr$_2$C$_6$H$_3$, R = CH$_2$), or simple use of K[BEt$_3$H] as a hydride source (Scheme 1.3).[48]



Scheme 1.3: Synthesis of gallium hydride complexes **1.9** and **1.10**.[48]

The dpp-Bian ligand (dpp-bian = 1,2-bis[(2,6-diisopropylphenyl)imino]acenaphthene) has also been used for the stabilisation of gallium hydrides. In this case, phenylsilane was used as a deoxygenating agent to afford ligand supported gallium hydrides **1.12** and **1.13** (Scheme 1.4).[41]

Other common hydride transfer reagents such as LiH, NaH, NaBH$_4$, LiAlH$_4$, NaBEt$_3$H, MeSiH$_3$ and AlH$_3$·NMe$_3$ have also been used for the formation of gallium–hydride bonds on reaction with gallium halides through hydride/halide exchange reactions.[39,44,49]

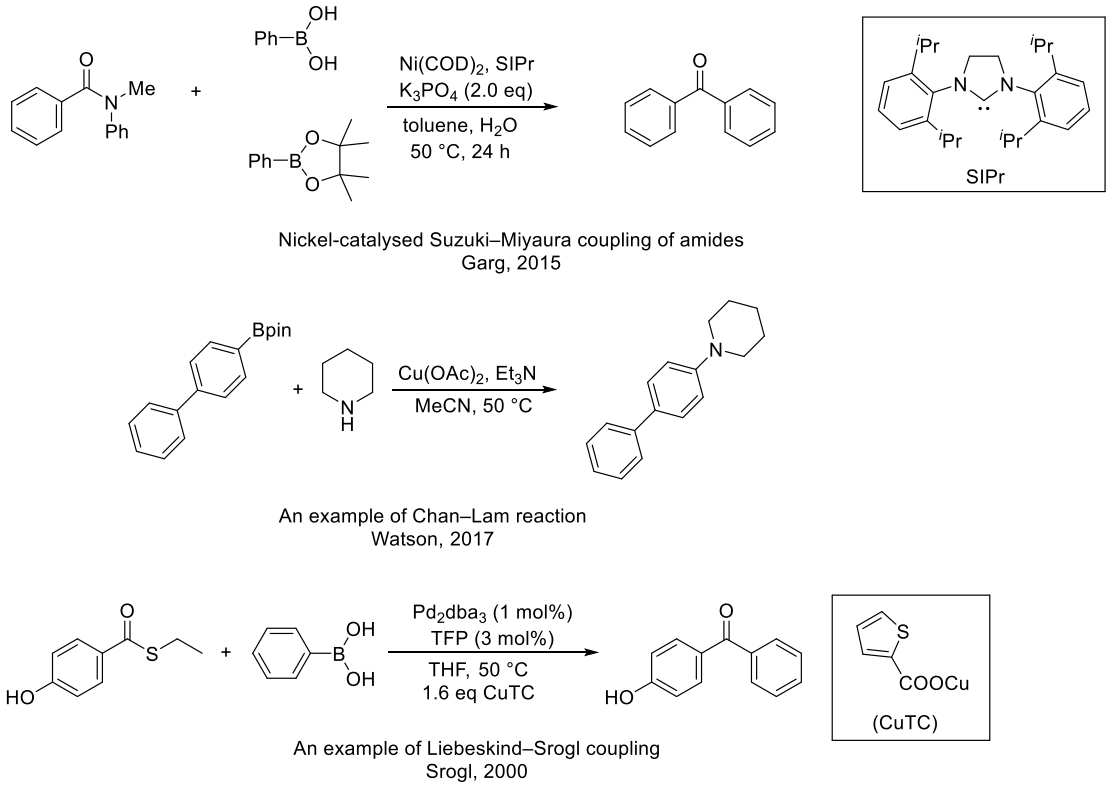


Scheme 1.4: Synthesis of gallium hydride complexes **1.12** and **1.13**.[41]

1.3 Main group element catalysts in hydroboration

Hydroboration is a ubiquitous chemical transformation that is particularly significant in the regioselective functionalisation of unsaturated carbon−carbon multiple bonds, to give boronic acids or boronic esters.[50,51] Boronic acids and boronic esters are both important reactants in organic reactions, particularly in C−C bond forming reactions such as the Suzuki–Miyaura reaction, Chan–Lam coupling, and Liebeskind–Srogl coupling (Scheme 1.5).[52–57] In this regard, developing novel synthetic methodologies for the synthesis of boronic esters will contribute to the development of synthetic chemistry.

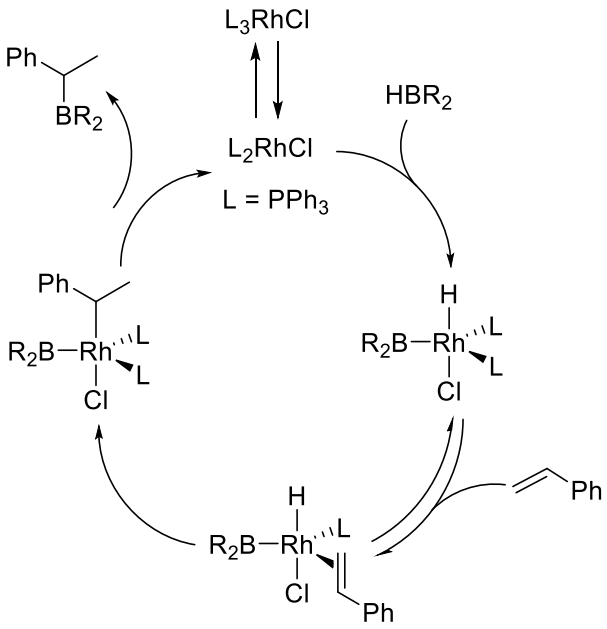
The first recorded direct hydroboration of aldehydes and ketones with diborane (B_2H_6) was reported by Brown in 1939.[60] Since then, hydroboration reagents with low toxicity and good stability have been developed. Sodium borohydride, for example, is relatively air- and moisture-stable and often used under mild conditions for the reduction of aldehydes and ketones.[61] In 1956, the direct addition of a B−H moiety to a C=C bond was introduced by Brown, using ($AlCl_3$ enhanced) sodium borohydride as reducing reagent.[62] As diborane is a pyrophoric gas, commercially available base-stabilised borane hydrides (BH_3·L, e.g. L=THF, SMe_2, NH_3, NMe_3, py, PPh_3) are more commonly used.



Scheme 1.5: Examples of the Suzuki-Miyaura reaction, Chan-Lam coupling and Liebeskind–Srogl coupling.[57–59]

Catalytic hydroboration was not well-developed until the 1980s due to the general high reactivity of borane–base adducts, $BH_3{\cdot}L$ (L = THF, SMe_2), that are active towards unsaturated C=C bonds in the absence of a catalyst. However, $BH_3{\cdot}L$ compounds are often air- and moisture-sensitive, unstable or generate malodorous by-products, such as SMe_2.[63] In view of this, more stable boranes, with greater air- and moisture-compatibility, were developed in the 1970s−1980s, to give sterically hindered boronic esters. Two of the most prominent boranes, catecholborane (HBcat) and pinacol borane (HBpin), are much less electrophilic and exhibit reduced reactivity towards substrates containing unsaturated bonds, compared to $BH_3{\cdot}L$ (L = THF, SMe_2). In order to circumvent this reduced reactivity, the development of catalysts for hydroboration reactions became a necessity.[64,65]

The synthesis of HBcat was reported by Brown and co-workers in 1971, with an emphasis on its use in alkene and alkyne hydroboration processes at elevated temperatures.[64,66,67] In 1975, Kono reported the oxidative addition of HBcat to Wilkinson's catalyst $(Ph_3P)_3RhCl$, which affords compounds with a metal−boron (Rh−B) σ-bond.[68] Nöth and co-workers described the catalytic hydroboration of 5-hexen-2-one (which was selective towards the carbonyl), using the Wilkinson's catalyst in 1985.[69] The mechanism for the hydroboration of alkenes using Wilkinson's catalyst was proposed to consist of the following steps: (1) dissociation of PPh_3 from Rh(I) centre; (2) oxidative addition of B−H bond to a 14 electron species; (3) coordination of alkene to the Rh(III) centre; (4) migratory insertion of alkene to the Rh−H moiety; (5) regeneration of the catalyst through reductive elimination of borylated alkane (Scheme 1.6).[69]



Scheme 1.6: Proposed mechanism for the rhodium (I) catalysed hydroboration of alkene.[69,70]

The dissociation step was further supported by Fu's research,[70] although the system was shown to be more complicated by Baker and co-workers, who highlighted the

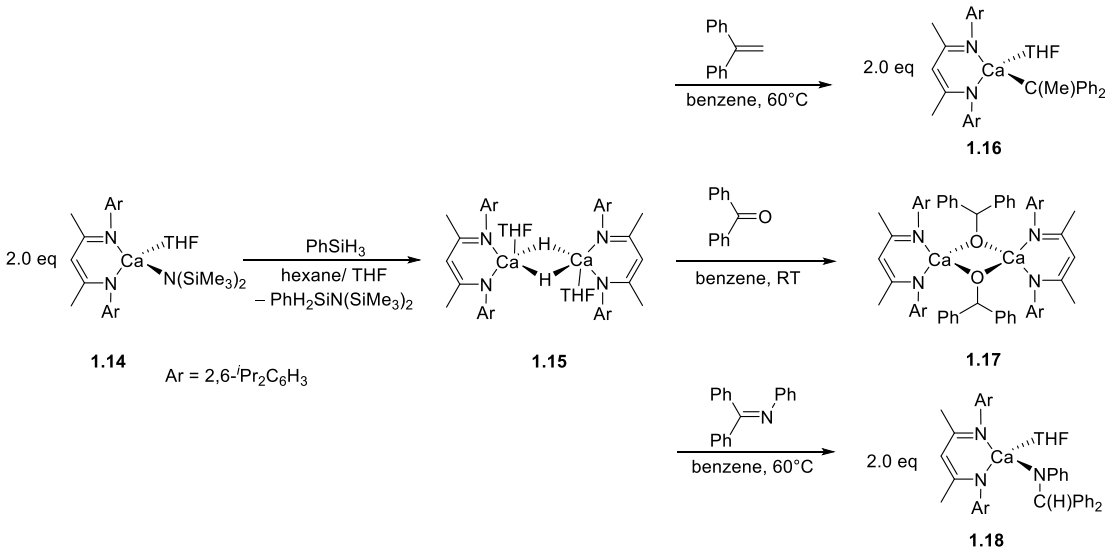
possibility of a rhodium-catalysed side reaction resulting in the degradation of HBcat to BH_3.[71] Despite its prominent role in the development of catalytic hydroboration processes, HBcat is not an ideal reagent as it is moisture sensitive and it easily decomposes to B_2cat_3 in the presence of a nucleophile.[72]

Another type of alkoxy substituted borane, HBpin, was synthesised by reacting pinacol and $BH_3{\cdot}SMe_2$ in dichloromethane, according to Knochel's report from 1992.[65] Although it was first reported that HBpin was an active reagent for alkyne hydroboration at room temperature in the absence of a catalyst,[65] it was later proven that trace amounts of an impurity (a BH_3 adduct) played a role as a 'hidden catalyst'.[73,74] Due to the inert nature of HBpin, many types of catalysts (most of them transition metal-based) have been developed which use it as a feedstock for the hydroboration of unsaturated substrates.[75] The resulting organoborane products, RBpin, are often stable in air and moisture, and can thus be further purified by chromatography. These are important precursors for C−C coupling reactions. Historically, research on catalytic hydroboration has mainly focused on developing novel transition metal catalysts, but in recent years, low toxicity, earth-abundant main group elements have been found to play an important role in hydroboration processes.[75]

1.3.1 Magnesium and calcium catalysts in hydroboration reactions

Recently, there has been a research focus on developing main group metal hydrides in catalysis. Amongst these, a handful of s-block metal hydrides have been reported.[76–82] A milestone in this area of research was the successful synthesis of a soluble dimeric Nacnac calcium hydride, **1.15**, by Harder in 2006. This compound was synthesised through the reaction of (^{Dipp}Nacnac)Ca[$N(SiMe_3)_2$](THF), **1.14**, with phenylsilane.[78] Solid calcium hydride CaH_2 is insoluble in common organic solvents, unreactive

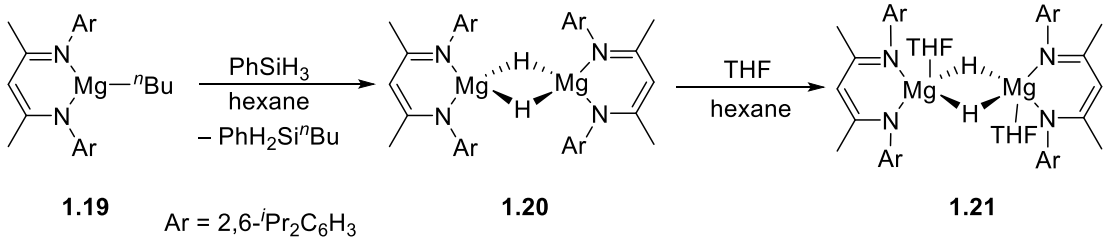
towards organic substrates and mainly used as a drying agent. In contrast, the soluble calcium hydride complex **1.15** is not only stable in non-polar solvents, but can also be used to activate unsaturated bonds under ambient conditions.[83] The reaction of calcium hydride **1.15** with compounds containing C=X bonds (X = C, O, N) results in the insertion of the unsaturated bond into the Ca–H σ-bond, to give **1.16**–**1.18** (Scheme 1.7). Calcium hydride **1.15** also reacts with C≡X bonds (X = C, N) affording calcium alkenyl (X = C), and calcium benzaldimide complexes (X = N). Harder and co-workers tried to use **1.15** as a catalyst for the catalytic hydroboration of 1,1-diphenylethylene, however, at the elevated operating temperatures used (100 °C), HBcat was found to decompose to B_2cat_3 and BH_3 first. The resulting product, $B(CH_2CHPh_2)_3$, was found to originate from the reaction of BH_3 with the alkene. The reaction of HBpin and **1.15** resulted into the formation of $[(^{Dipp}Nacnac)Ca(H_2Bpin)]_3$, thus no further catalytic hydroboration was explored.[84]



Scheme 1.7: Synthesis and reactivity of calcium hydride **1.15**.[83]

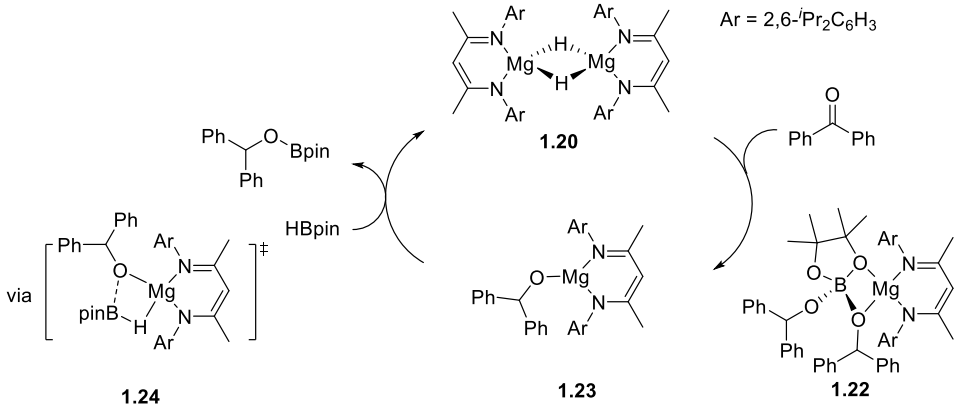
Similar to the methodology developed by Harder, a magnesium hydride bearing the same β-diketiminato ligand, $\{(^{Dipp}Nacnac)(\mu\text{-}H)Mg\}_2$, **1.20**, was synthesised by Jones

in 2008.[77] Reaction of phenylsilane or HBpin with the β-diketiminato-supported *n*-butylmagnesium complex **1.19** results into the formation of magnesium dihydride **1.20** (Scheme 1.8). Thus, in principle, complex **1.19** can be used as a pre-catalyst for transformations that rely on the formation of a hydride intermediate (**1.20**) such as hydroboration or hydrosilylation. Upon the addition of excess THF, complex **1.20** converts to a THF coordinated magnesium dihydride **1.21**.



Scheme 1.8: Synthesis of magnesium hydride complexes **1.20** and **1.21**.[77]

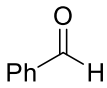
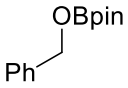
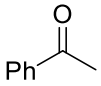
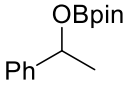
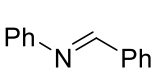
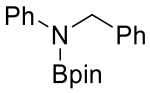
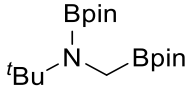
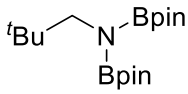
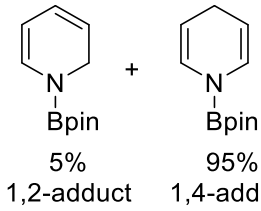
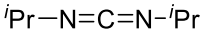
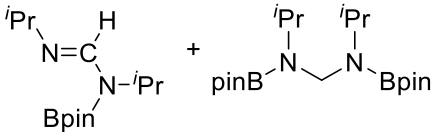
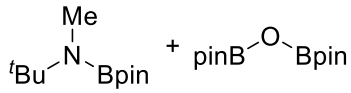
The magnesium dihydride **1.20** exhibits similar reactivity towards unsaturated bonds to that of the calcium dihydride **1.15** and will react to form a series of dimeric magnesium complexes. These reactions involve C=X (X = C, O, N) or C≡X (X = C, N) bond insertion into Mg−H bond. In the presence of excess borane, the resulting compounds will regenerate the magnesium hydride bond through a B−H/Mg−X (X = C, O, N) σ-bond metathesis reaction (Scheme 1.9).[77]



Scheme 1.9: Proposed catalytic cycle for the hydroboration of benzophenone using **1.20**.[85]

Jones and co-workers have shown that **1.20** is an efficient catalyst for the reduction of aldehydes, ketones, imines, carbodiimides, nitriles, isonitriles, pyridine, isocyanates, carbon dioxide and alkenes with boranes or silanes (Table 1.1).[85–93]

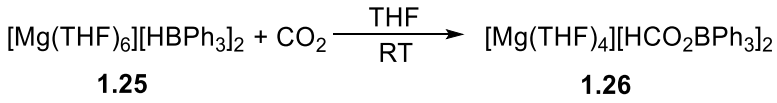
Table 1.1: Examples of catalytic hydroboration using pre-catalyst **1.19**.[85–93]

Entry	Substates	Products	Catalyst loading (mol%)	T (°C)	Time (h)	NMR yield (%)
1[a]			0.05	25	0.25	95
2[a]			1	25	4	94
3[a]			1	60	1	99
4[b]			5	60	5	99
5[b]			10	60	5.5	97
6[a]		 5% 1,2-adduct 95% 1,4-adduct	10	80	16	90
7[a]			10	60	15	90
8[c]			10	60	3.5	81

[a] Using one equivalent of HBpin, [b] Using two equivalents of HBpin, [c] Using three equivalents of HBpin.

Magnesium bis(hydridotriphenylborate), $[Mg(THF)_6][HBPh_3]_2$, **1.25**, was synthesised by reacting magnesium tetramethyldisilazide, $Mg[N(SiHMe_2)_2]_2$, with BPh_3. This reactions proceeds via a β-hydrogen abstraction from the Si−H bond of the amide in THF, according to a report by Okuda from 2016 (Scheme 1.10).[94]. In THF solution,

complex **1.25** reacts with carbon dioxide through a C=O bond insertion into the B−H bond to afford complex **1.26** as the product.

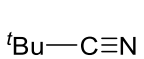
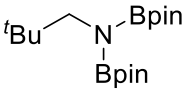
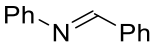
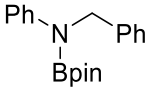
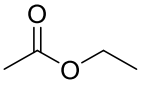
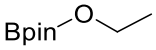
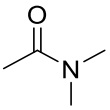
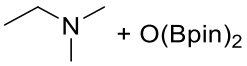
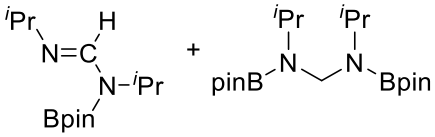
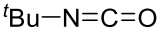
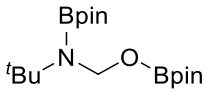


Scheme 1.10: The reaction of **1.25** and CO_2.[94]

Magnesium complex **1.25** has been shown to be catalytically active for the hydroboration of various substrates, such as aldehydes, ketones, imines, carbodiimides, nitriles, isonitriles, pyridine, isocyanates, sulfonyls and carbon dioxide (Table 1.2), however the mechanism by which it operates remains unclear. Although the catalyst is active for a wide substrates scope, catalysis often requires elevated temperatures (e.g. 60 °C), and the poor solubility of **1.25** in apolar solvents and THF has limited its further use.

The weak and highly polarised $^{\delta+}M-H^{\delta-}$ bonds of calcium hydride **1.15** and magnesium hydride **1.20** readily undergo insertion (1,2-hydrometallation) reactions with unsaturated bonds. This reaction plays a key role in catalytic hydroboration processes. In general, group 2 element metal hydrides are active towards a wide scope of substrates, for example, magnesium complexes **1.20** and **1.25** are active catalysts for the hydroboration of aldehydes, ketones, carbon dioxide, imines and isocyanates. However, these group 2 compounds are often difficult to manipulate and can react with excess borane resulting in catalyst decomposition, so other more stable systems are also worth exploring.

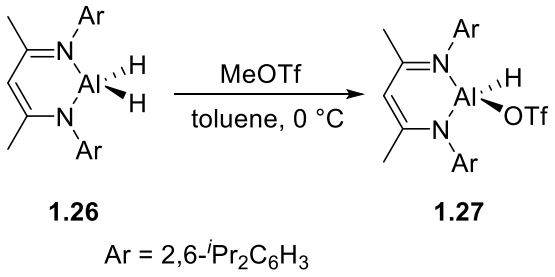
Table 1.2: Catalytic hydroboration by catalyst **1.25**.[94]

Entry	Substates	Products	Catalyst loading (mol%)	T (°C)	Time (h)[a]
1[b]			1	60	1
2[b]			1	60	24
3[b]			1	60	1
4[b]			1	60	8
5[c]	CO_2 (1 bar)	MeOBpin + $O(Bpin)_2$	10	25	3
6[b, d]			1	60	12
7[b]			1	60	0.5

[a] Time for over 99% consumption of substrates, [b] The catalysis is performed in a solution with **1.25** (2 mg), [substrate] 0.48 M, [HBpin] 1 M, 0.45 mL of solvent (THF : THF-d_8 = 2 : 1), [c] The catalysis is performed in a solution with **1.25** (2.37×10^{-2} M), [HBpin] 0.24 M, 0.45 mL of THF-d_8, [d] The reaction of one equivalent of HBpin with carbodiimide afford two products.

1.3.2 Aluminium and gallium catalysts in hydroboration reactions

Group 13 metal hydrides have been shown to be reactive towards small molecule substrates, but these hydrides are often unstable, air- and moisture-sensitive, and therefore not ideal catalysts.[24] Hence, the use of these compounds as potential catalysts is relatively recent. It was not until 2015, that an aluminium hydride was used as a catalyst for hydroboration.[95,96] Supported by a β-diketiminato ligand, the stable aluminium dihydride **1.26** was reported by Roesky. This compound was shown to react with methyl triflate to afford an aluminium monohydride triflate complex **1.27** (Scheme 1.11).



1.26 **1.27**

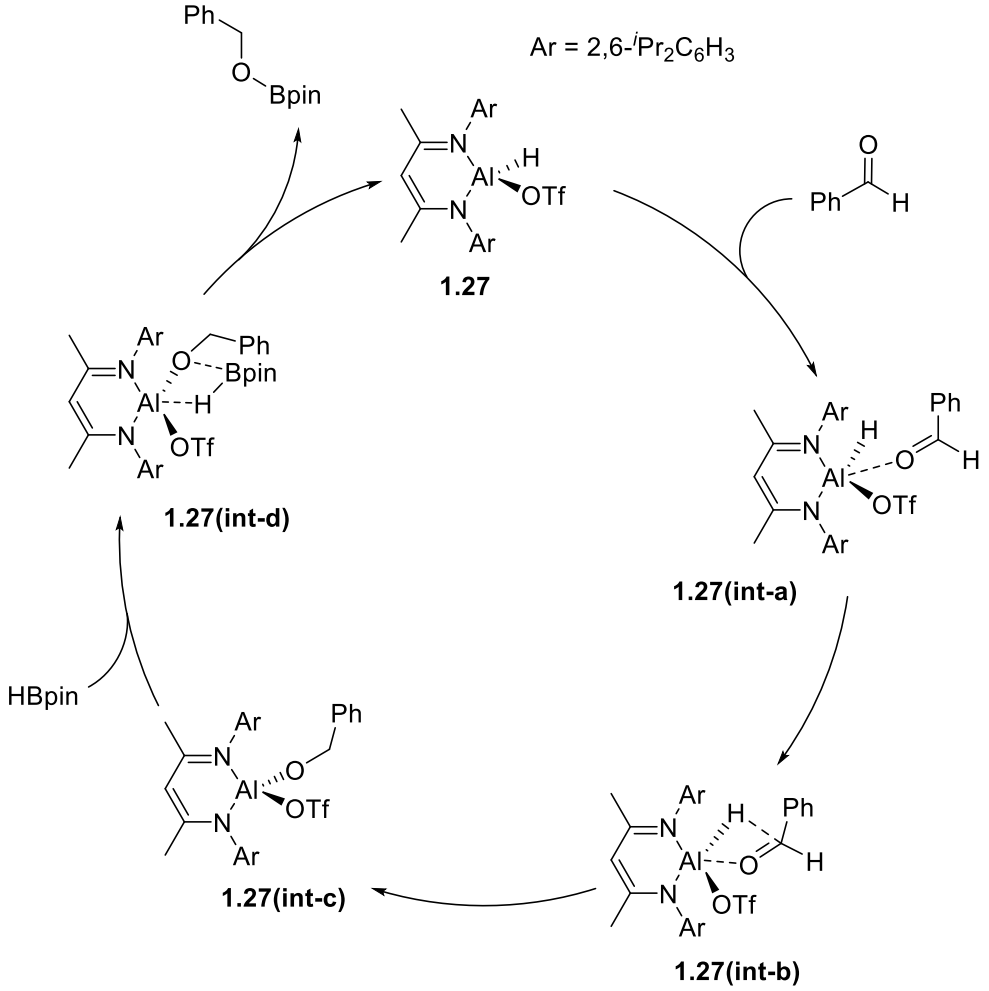
Ar = 2,6-^{i}Pr$_2$C$_6$H$_3$

Scheme 1.11: Aluminium hydride complexes supported by a β-diketiminato ligand.[95,96]

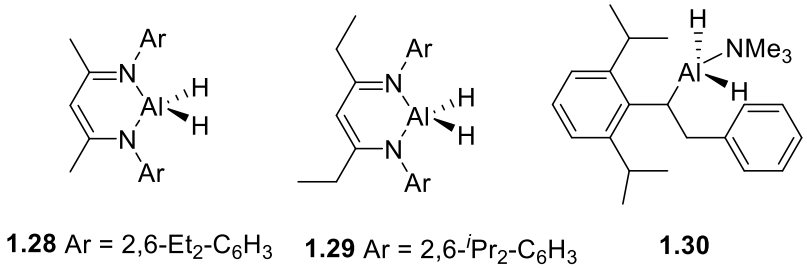
Complex **1.27** is catalytically active in the hydroboration of aldehydes and ketones, as well as trimethylsilyl cyanidation.[95] A mechanism has been proposed for the catalytic hydroboration with **1.27**, in which the carbonyl substrate coordinates to the aluminium centre **1.27(int-a)**. The carbonyl is then proposed to insert into the Al−H bond to afford an alkoxide **1.27(int-c)**. The final step involves the reaction of HBpin with the aluminium alkoxide through a B−H/Al−O σ-bond metathesis reaction to generate a borate ester and regenerate the aluminium hydride catalyst (Scheme 1.12).

One year later, with a slight ligand modification (Ar = 2,6-Et$_2$C$_6$H$_3$), aluminium dihydride complex **1.28** was found to facilitate the hydroboration of alkynes, and dehydrocoupling reactions of HBpin with amines, phenols and thiols (Scheme 1.13).[96] Further modification of the β-diketiminato ligand by replacing the backbone methyl groups with ethyl groups, i.e. {HC[C(Et)N(2,6-^{i}Pr-C$_6$H$_3$)]$_2$}, was used to afford a novel hydride, **1.29**. For comparison, an aluminium dihydride that was not supported by a β-diketiminato ligand, **1.30**, was also used (Scheme 1.13). At 80 °C and using the same catalyst loading (5.0 mol%), the hydroboration of benzonitrile reaches the highest conversions when employing **1.28** as the catalyst with 99% conversion within 6 hours, while **1.29** only reached 68% in the same time. By contrast, the performance of **1.30** as the catalyst was worse, as conversion of benzonitrile only reaches 28% after 24 h at

80 °C. Although a mechanistic model was proposed, with an initial insertion of the Al−H bond into the C≡N bond, no stable intermediates were successfully isolated.[97]

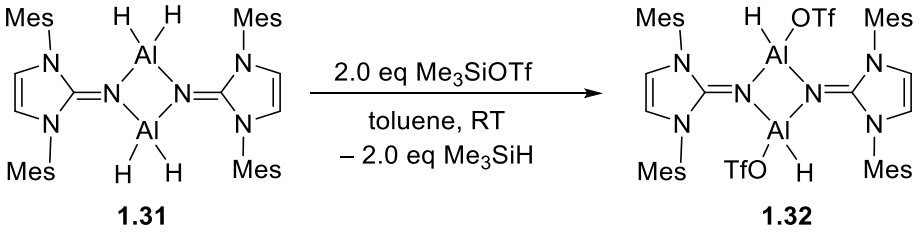


Scheme 1.12: Proposed mechanism for the catalytic hydroboration of benzaldehyde using **1.27**.[95]



Scheme 1.13: Aluminium complexes **1.28**−**1.30**.[97]

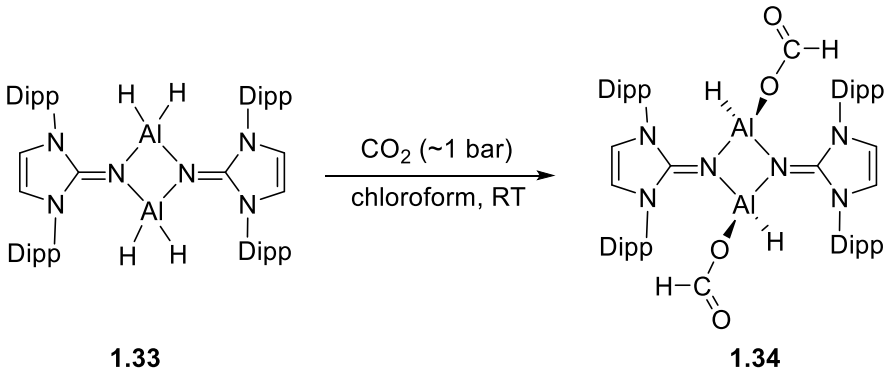
Dimeric imidazolin-2-iminato ligand supported aluminium dihydride complex **1.31** was first synthesised by Inoue in 2014, and its reactivity towards sulphur (S_8) and diphenyl sulfide was explored.[98] Two years later, **1.31** was found to react with Me_3SiOTf to afford a dimeric aluminium monohydride triflate complex **1.32** (Scheme 1.14).[99] Inspired by Roesky's hydroboration work, Inoue and co-workers investigated the role of **1.31** and **1.32**, in catalytic hydroboration reactions. They found that the triflate anion did not have a significant impact on the activity of the catalyst.[99]



1.31 **1.32**

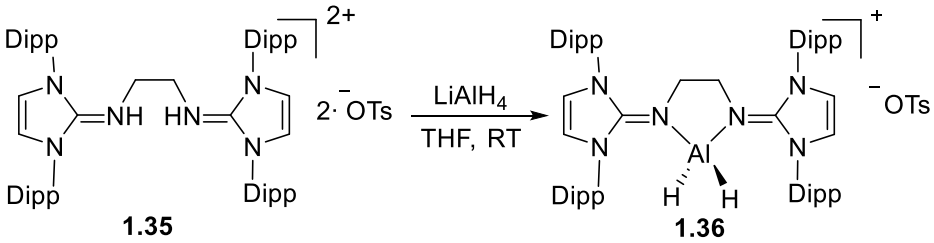
Scheme 1.14: Aluminium hydride complexes **1.31**−**1.32**.[99]

Carbon dioxide is one of the most stable carbonyl-containing substrates, however despite its unreactive nature it is an attractive C1 feedstock for a variety of organic transformations.[100] In 2019, Inoue showed that the dimeric NHI-supported aluminium dihydride **1.33** reacts with carbon dioxide (1 bar) at ambient temperature to afford aluminium carboxylate complex **1.34**.[101] This aluminium carboxylate complex is interesting on its own right, as it can further react with carbon dioxide to give an aluminium tetracaboxylate complex, or act as a formate transfer reagent on reaction with a strong Lewis acid (Scheme 1.15).[101]



Scheme 1.15: NHI supported aluminium hydride **1.33** and its reaction with carbon dioxide.[101]

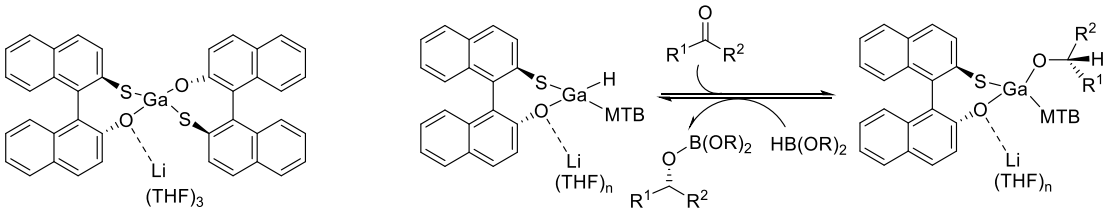
For comparison, Inoue also synthesised the aluminium dihydride **1.36** through the metallation of bulky bisimino ligand **1.35** with lithium aluminium hydride (Scheme 1.16). Employing catalyst **1.34** or **1.36**, under ~1 bar pressure carbon dioxide, HBcat could be converted to multiple borate esters such as HCO_2Bcat, $H_2C(OBcat)_2$ $H_3COBcat$ and $O(Bcat)_2$ without selectivity. The authors observed that **1.34** (4 h, 53% conversion) is a more efficient catalyst than **1.36** (4 h, 23% conversion).



Scheme 1.16: Synthesis of aluminium hydride complexes **1.36**.[101]

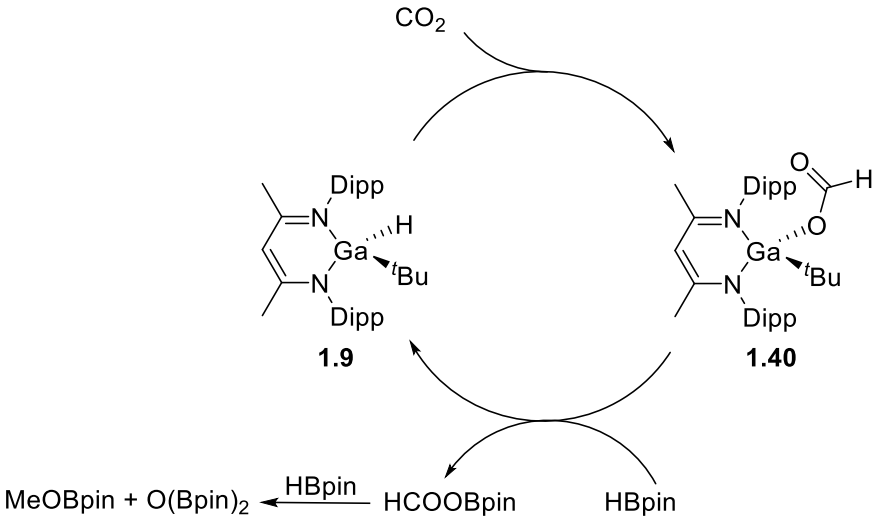
Despite the aforementioned studies on catalytic hydroboration using aluminium complexes that have been reported in recent few years, only a handful of gallium hydrides have been studied for such purposes. Gallium hydrides are generally unstable and are not commercially available, thus they need to be freshly prepared, which in all likelihood is why such compounds remain underexplored (Section 1.2). In 1999 and 2000, Woodward reported a novel strategy for the catalytic hydroboration of ketones

with HBcat using a combination of $LiGaH_4$ and 2-hydroxy-2'-mercapto-1,1'-binaphthyl ($MTBH_2$) as the catalyst.[102,103] A stochiometric reaction of $LiGaH_4$ and two equivalents of $MTBH_2$ afforded $[Li_2(MTB)][Ga_2(MTB)_3]$ in solution (as evidenced by NMR spectroscopy), whilst crystallisation of the reaction mixture afford single crystals of $[Li(THF)_3Ga(MTB)_2]$ **1.37** which is believed to act as a hydroboration pre-catalyst. A mechanistic model for catalytic hydroboration was proposed involving carbonyl insertion into the gallium hydride **1.38** (formed by in situ reaction of $LiGaH_4$ and $MTBH_2$) to give a gallium alkoxide complex **1.39**, followed by a B−H/Ga−O metathesis on reaction with the borane. This gives rise to the borate ester product and regenerates gallium hydride **1.38** (Scheme 1.17). It is worth noting that this catalyst is active using a variety of boranes, such as HBpin, BH_3·THF, $(^iPrO)_2BH$, oxazaborole and thiazaborole.[102,103]



Scheme 1.17: Catalyst **1.37** and proposed model for hydroboration.[102,103]

In 2015, Aldridge reported a β-diketiminato ligand supported gallium hydride complex **1.9** that reacts with carbon dioxide at room temperature to generate a gallium formate complex **1.40**. This species can react with HBpin to regenerate **1.9**. In the presence of HBpin at 60 °C, carbon dioxide can be catalytically hydroborated to a methanol equivalent, MeOBpin (Scheme 1.18).[48] This was the first example of carbon dioxide hydroboration using a gallium catalyst.[104]

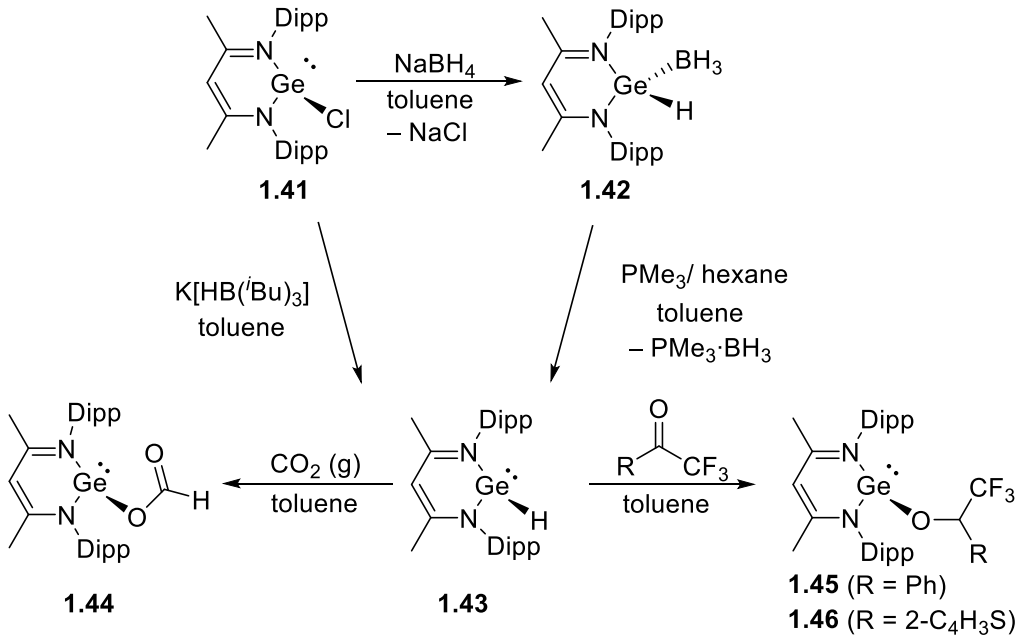


Scheme 1.18: Gallium hydride **1.9** and proposed mechanism for hydroboration of CO_2.[48]

Although examples of gallium catalysed hydroboration reactions remain limited, recently reported examples have shown that such species are promising candidates as catalysts.

1.3.3 Germanium and tin catalysts in hydroboration reactions

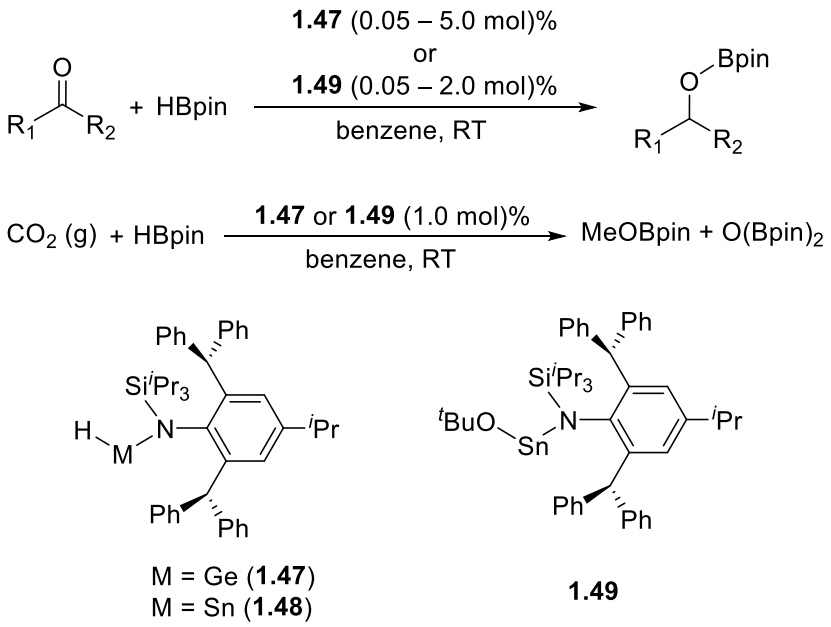
The first documented monomeric germanium (II) hydride complex **1.42** was reported by Roesky in 2001, prepared through hydride exchange of the β-diketiminato ligand supported germanium chloride complex **1.41** with sodium borohydride.[105] The borane substituent on the germanium complex **1.42** could be removed by adding trimethylphosphine (PMe_3), resulting in the formation of a stable three-coordinate germanium complex **1.43** (Scheme 1.19). Compound **1.43** can also be synthesised by reacting germanium chloride **1.41** with either $AlH_3{\cdot}NMe_3$ or $K[HB(^iBu)_3]$ (Scheme 1.19).[106,107] The reactivity of **1.43** towards carbon dioxide was examined and found to afford the germanium formate complex **1.44**. Similarly, reaction with ketones was found to give **1.45** and **1.46**. Complex **1.43** has also been found to be reactive towards other substrates, such as alkynes, nitrous oxide, azides and sulphur.[107,108]



Scheme 1.19: Synthesis and functionalisation of germanium hydride complexes.[105]

A theoretical study on the hydroelementation of ketones catalysed by complex **1.43** was shown to be energetically feasible by Sakaki and co-workers in 2013 before catalysis was experimentally performed.[109]

In 2014, Jones and co-workers first employed the low valent two-coordinate germanium and tin hydride complexes **1.47** and **1.48** in the catalytic hydroboration of aldehydes and ketones (Scheme 1.20).[110] While germanium hydride **1.47** is stable and can be used directly for catalysis, the tin hydride **1.48** decomposes gradually at room temperature over two days. Thus, for the catalysis studies, the corresponding *tert*-butoxide tin complex, LSn^{t}OBu **1.49** (L = −N(Ar)(Si^{i}Pr$_3$); Ar = $C_6H_2\{C(H)Ph_2\}_2{}^i$Pr-2,6,4)) was used as the pre-catalyst.

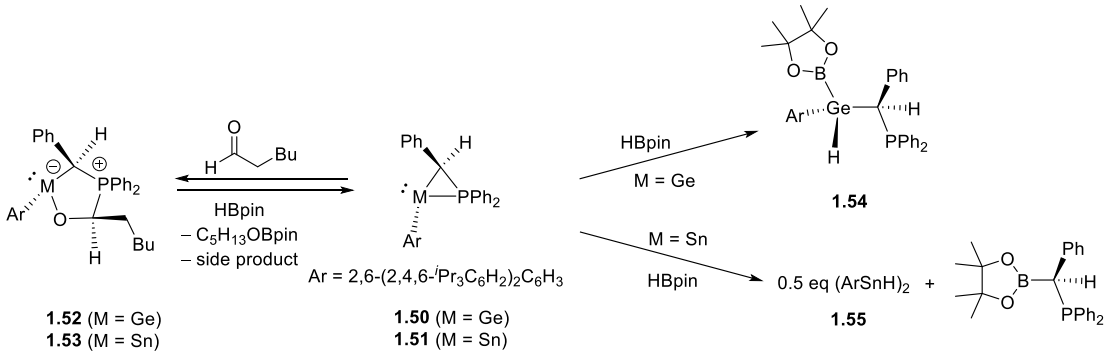


Scheme 1.20: Catalytic hydroboration of carbonyls by germanium/tin hydride complexes.[110]

The reaction of the germanium hydride **1.47** or tin hydride **1.48** with stochiometric amounts of aldehydes or ketones affords the corresponding metal alkoxide complexes. On addition of the HBpin, regeneration of metal hydrides was observed. This type of reactivity supports the pivotal role of the metal hydride in the catalytic hydroboration of carbonyls. In a later report catalytic hydroboration was extended to more inert substrates such as carbon dioxide.[111] In the presence of 1 mol% of **1.47** or **1.49**, carbon dioxide could be hydroborated by HBpin to a methanol equivalent CH_3OBpin and $O(Bpin)_2$, presumably through the formation of an intermediate metal formate.

When a Lewis acid and Lewis base cannot form an adduct due to steric hindrance, they are together known as a Frustrated Lewis Pair (FLP).[112] Intramolecular tetrylene Lewis pairs have been explored by Wesemann and co-workers since 2013, and they have shown that such compounds react with unsaturated substrates such as alkynes, aldehydes, alkenes, isonitriles and azides.[113–118] In 2017, Wesemann reported that the germylene **1.50** and stannylene **1.51** catalysed the hydroboration of aldehydes and

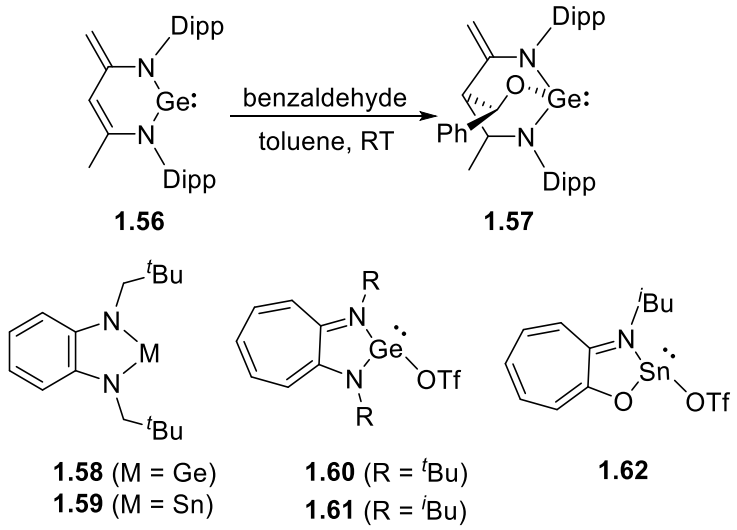
ketones. Addition of hexanal to either of these compounds resulted in the insertion of the carbonyl group into the M−P (M = Ge, Sn) bond to afford five-membered ring products **1.52** and **1.53** (Scheme 1.21). These can be converted back to **1.50** and **1.51** by adding HBpin. Interestingly, the reaction of germylene **1.50** with HBpin gives a B−H bond activation product, the germanium hydride **1.54**, while the reaction of stannylene **1.51** with HBpin afford a dimeric tin hydride complex **1.55** and a phosphine substituted alkyl borate, i.e. $PhC(H)(PPh_2)Bpin$.[117] With these findings in hand, the authors concluded that the **1.50** and **1.51** catalysed hydroboration reaction possibly follow two contrasting pathways, involving an FLP type and metal−hydride type mechanism.



Scheme 1.21: Reactivity of germylene **1.50** and stannylene **1.51**.[117]

Other examples of germanium and tin catalysts in hydroboration have been reported by Zhao in 2016, and Khan, Nagendran and Inoue in 2019 (Scheme 1.22).[119–123] The history of the β-diketiminato supported germylene **1.56** dates back to 2006, when it was first reported by Driess.[124] This compound was later shown to be active towards alkylhalides,[124] alkynes,[125] ammonia,[126] water, phenol, carboxylic acids,[127] boronate, boroxine,[128] and aldehydes.[119] The activation of benzaldehyde with **1.56** is unique, with C=O bond addition to the germanium centre and the γ-carbon atom of the ligand backbone, giving rise to the bicyclo[2,2,2]octane-like product **1.57** (Scheme

1.22). Although complexes **1.56** and **1.57** were both found to be catalytically active towards the hydroboration of aldehydes and ketones, the reaction of **1.57** with HBpin does not give any isolable products. Supported by the transformation from **1.56** to **1.57**, the authors argued that catalysis probably proceeds through a metal/ligand cooperative activation.[119]



Scheme 1.22: Reactivity of germylene **1.56** and structure of complexes **1.58**–**1.62**.[120–122]

Complexes **1.58** and **1.59** were shown to catalyse the hydroboration of aldehydes (Scheme 1.22), however, these reactions proceeded slowly when using 2 mol% catalyst loadings. Instead of proceeding via a metal-hydride intermediate, the authors postulated that hydroboration was facilitated by a Lewis acid type mechanism, as a mechanism involving formal oxidative addition of HBpin at the tetrel element center was calculated to be energetically unfavorable.[122] The aminotroponiminate-stabilised germanium complexes **1.60** and **1.61** have also been shown to be catalytically active towards the hydroboration of aldehydes and ketones, however, an elevated temperature (60 °C) for these transformations was often needed.[121] In contrast, at room temperature, with 0.025–0.25 mol% of the triflatostannylene **1.62**, hydroboration of aldehydes and

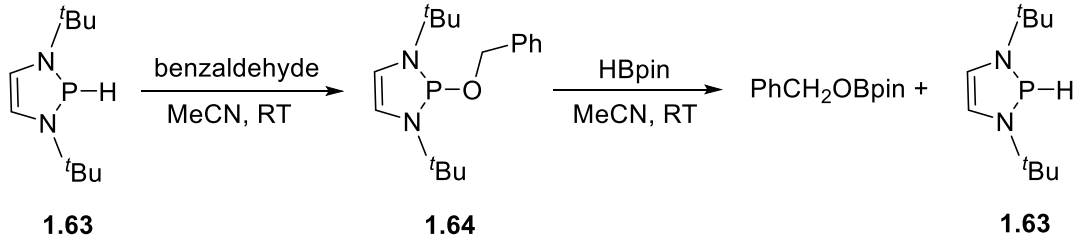
ketones could be achieved rapidly, (7840−30461 h^{-1} for aldehydes, 316−2475 h^{-1} for ketones). DFT calculation were performed and showed that a hydridostannylene intermediate is possibly involved in the catalytic cycle, that being said this species has not been isolated.[120]

To summarise, group 14 hydrides have been shown to be active in the hydroboration of a variety of substrates containing unsaturated bonds, including typically unreactive species such as carbon dioxide. In many cases, these reactions proceed with very low catalyst loadings and high TON. Mechanistic studies suggest that catalytic hydroboration can proceed through a variety of mechanisms, involving element−hydride intermediates, FLPs, or Lewis acid catalysis. These studies afford valuable insight for the design for future catalysts.

1.3.4 Phosphorus and arsenic catalysts in hydroboration reactions

As mentioned earlier, catalysis was once the exclusive domain of transition metal catalysts, and research into main group catalysis is a relatively recent field. In most cases, the main group elements in questions are metals, and cases of metal-free catalysis are very rare. In 2015 Kinjo reported the first metal-free catalytic hydroboration of aldehydes and ketones (Scheme 1.23).[129] The reaction of 1,3,2-diazaphospholene **1.63** with aldehydes and ketones was shown to afford phosphine alkoxide complexes.[129–131] The phosphine alkoxide **1.64** can further react with HBpin to regenerate the 1,3,2-diazaphospholene **1.63** and a borate ester Ph_2CH_2OBpin. After this initial observation, it was shown that complex **1.63** can be used as a catalyst for the hydroboration of a wide range of aldehydes and ketones. However, ketone hydroboration by **1.63** required high catalyst loading (10 mol%) and high temperatures (90 °C). In 2017, Speed extended the substrate scope of catalytic hydroboration to imines, and conjugated

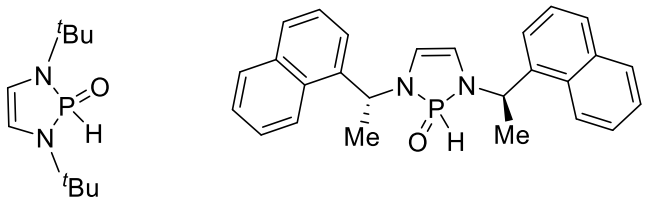
systems (α,β-unsaturated carbonyl derivatives).[132] It is also worth noting that 1,3,2-diazaphospholene can hydrophosphinate carbon dioxide to form phosphorus formate, this was exploited by Kinjo in 2015 for the catalytic *N*-formylation of amines.[133]



1.63 **1.64** **1.63**

Scheme 1.23: Reactivity of 1,3,2-diazaphospholene **1.63**.[129]

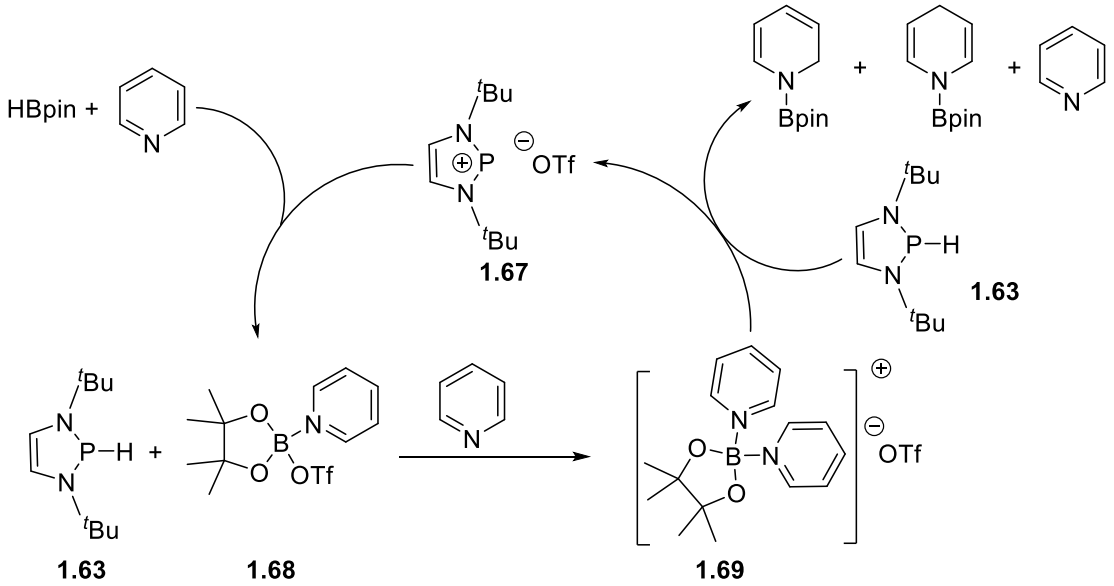
As 1,3,2-diazaphospholene reacts with moisture and air,[131,134] the air- and moisture-stable secondary phosphine oxides **1.65** and **1.66** were developed by Speed in 2020, as catalysts for the hydroboration of imines and pyridines (Scheme 1.24).[134]



1.65 **1.66**

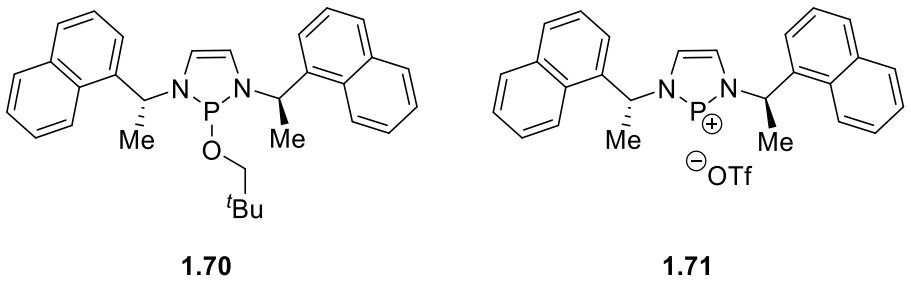
Scheme 1.24: Stable secondary phosphine oxides **1.65** and **1.66**.[134]

In 2018, Kinjo reported the application of phosphenium complexes **1.67** in the selective hydroboration of pyridine (Scheme 1.25). In the presence of pyridine, the hydride of HBpin can be abstracted by **1.67**, to give phospholene **1.63** and (py)(OTf)Bpin **1.68**. Solution and solid state studies support a mechanism in which a boronium salt intermediate, $[(py)_2Bpin]^+$ **1.69**, reacts with the pre-formed phospholene **1.63** to afford the 1,2- and 1,4-hydroboration products and regenerates the phosphenium catalyst.[135]



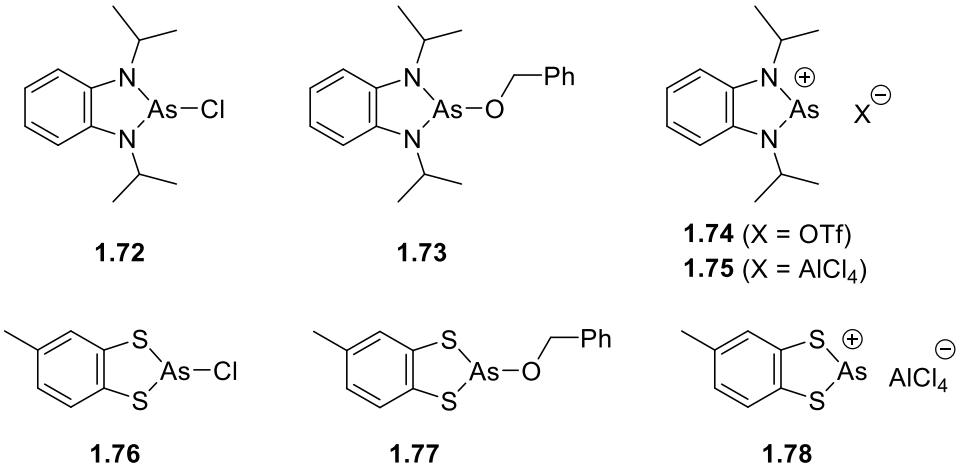
Scheme 1.25: Proposed model for the phosphenium catalysed hydroboration of pyridine.[135]

In 2019, Speed reported on the asymmetric catalytic hydroboration of imines using a chiral phosphenium catalyst (Scheme 1.26).[136] Compound **1.71** was shown to exhibit enhanced reactivity when compared to the phosphorus alkoxide compound **1.70**, and catalytic hydroboration was shown to be possible at low temperature (−35 °C), with low catalyst loadings (0.1 mol%), good regioselectivity, high conversion (98%) on a one gram scale. An imine-borenium intermediate was proposed for the imine reduction. The phosphenium cation is believe to abstract the hydride from the borane and deliver the P−H to imine-borenium, to regenerate the catalyst and afford the borylated product.



Scheme 1.26: Phosphorus alkoxide **1.70** and phosphenium **1.71**.[136]

In contrast to the successful application of phosphorus(III) complexes in catalysis, the study of related arsenic-containing compounds, is much more limited. In 2018, Melen and co-workers first reported the use of an arsenic complex in the catalytic hydroboration of aldehydes. In this study they compared the catalytic activity of a series arsenic complexes **1.72**−**1.78** towards 4-(trifluoromethyl)benzaldehyde (Scheme 1.27).[137–139] A possible mechanism for catalysis using **1.73** as a model system was proposed, and postulated to proceed through As−O/B−H metathesis, generating an arsane (detected by HRMS) and affording the borate ester as the product.



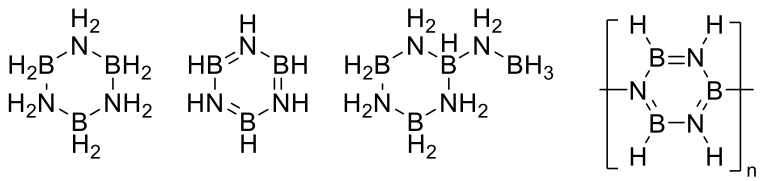
Scheme 1.27: Arsenic complexes **1.72**−**1.78**.[137–139]

Despite some interesting proof-of-concept results, group 15 element catalysts are not particularly reactive in the catalytic hydroboration of carbonyl-containing compounds, and the substrate scopes are rather limited. The exception is the phosphenium cation **1.71**, which was shown not only to be a reactive catalyst in catalytic hydroboration reactions, but also give good regioselectivity of the products.[136] The mechanism for the hydroboration using the aforementioned arsenic compounds has not been well established yet, and further study is needed.

1.4 Dehydrogenation of amine-boranes

Developing suitable hydrogen storage materials as a sustainable energy supply is an important aspect in order to use hydrogen as a fuel source. An ideal hydrogen storage material is stable at temperature, has a high gravimetric hydrogen storage capacity and only releases hydrogen on demand.[140]

Hydrogen rich materials containing B−N bonds have attracted considerable attention in recent decades, as they have the potential store and release hydrogen on demand. Specifically, amine-borane adducts have both protic (N−H) and hydridic hydrogen (B−H) bonds and they can release hydrogen under relatively mild conditions with the aid of a catalyst. In the context of hydrogen storage materials, ammonia-borane ($H_3N{\cdot}BH_3$) has received the most attention, due to its high gravimetric hydrogen content (19.6 wt%).[141,142] At room temperature, no observable decomposition of ammonia-borane is observable. At elevated temperatures (>120 °C), thermolysis occurs and result in decomposition and dihydrogen release.[141] Without the presence of catalyst, thermolysis of ammonia-borane result in multiple products, such as cyclotriborazanes **1.79**, borazines **1.80**, branched cyclotetraborazanes **1.81** and polymeric BN materials **1.82** (Scheme 1.28).[143–148]



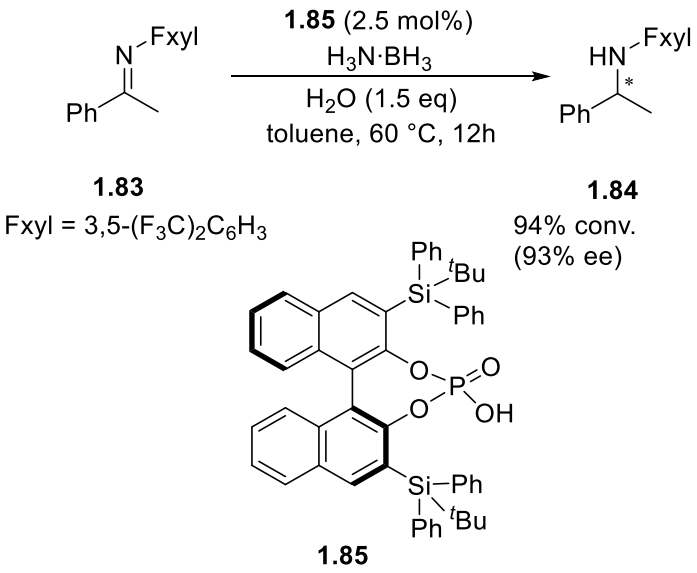
Scheme 1.28: Possible ammonia-borane dehydrogenation products.[143–148]

In order to effectively release hydrogen from ammonia-borane at ambient temperature and control selectivity over the dehydrogenation products, the use of a catalyst is necessary.[140] Most reports of amine-borane dehydrogenation catalysis, employ transition metal catalysts (examples include Y,[149] Zr,[150–153] Re,[154] Fe,[155–157] Ru,[158–165] Os,[166] and Ir).[167–170] More recently, in tandem with the development of fundamental main group element chemistry, a number of examples of main group compounds capable of ammonia-borane dehydrogenation have been reported. In the coming section, examples of non-transition metal facilitated dehydrogenation of amine-boranes are discussed.

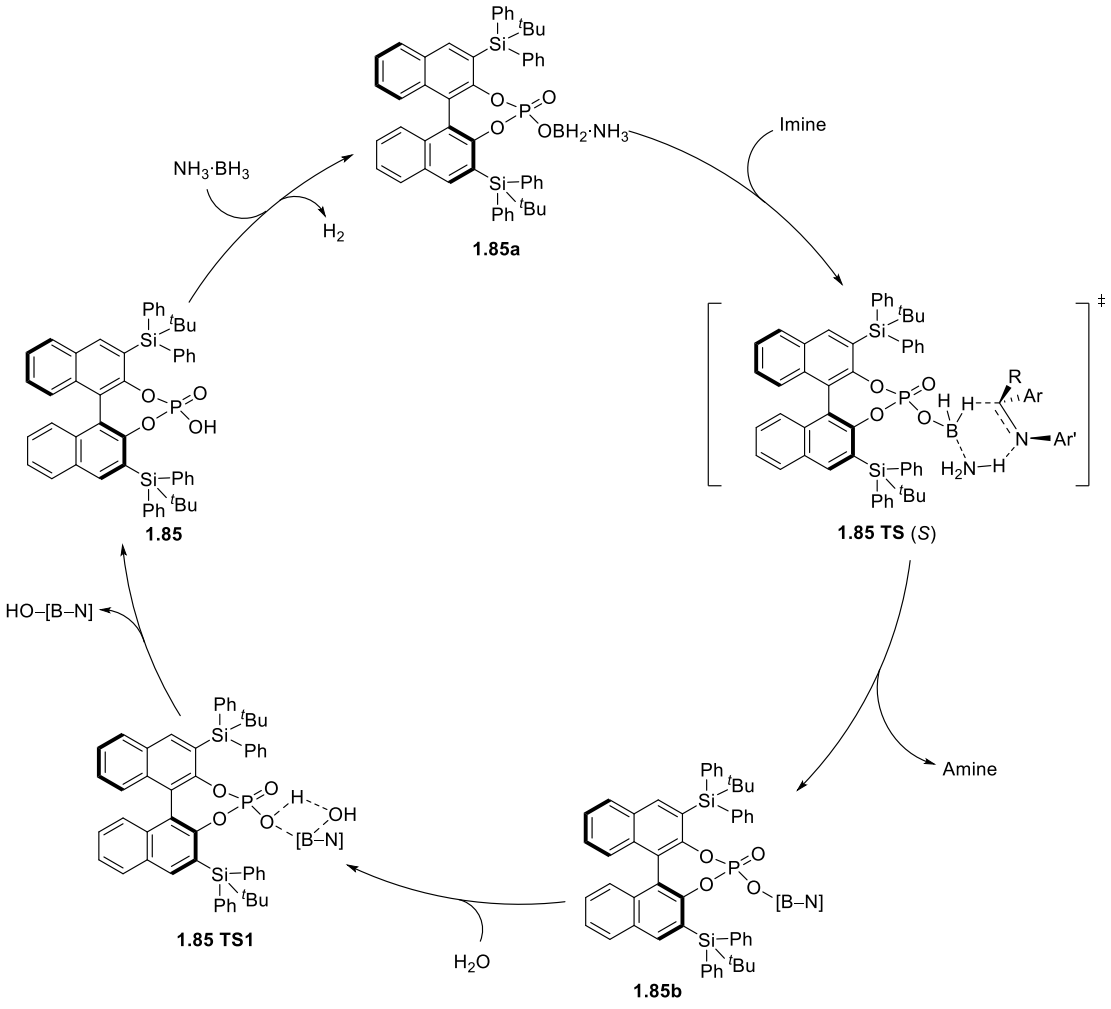
1.4.1 Acid mediated dehydrogenation of amine-boranes

In 2007, Brønsted acids such as HCl, HOTf and $[H(OEt_2)_2][B\{3,5\text{-}(CF_3)_2C_6H_3\}_4]$ were found by Baker to undergo a hydrogen evolution reaction with ammonia-borane to afford the boronium cation $NH_3BH_2^+$, which then initiates the dehydrogenation of ammonia-borane.[171]

Even in the absence of a catalyst, imines can be hydrogenated by ammonia-borane at elevated temperatures,[172] however in 2018, Du reported the use of chiral phosphoric acids in asymmetric hydrogenation of imines.[173] With 2.5 mol% of catalyst **1.85**, imine **1.83** could be hydrogenated to corresponding amine **1.84**, with 94% conversion and 93% ee (Scheme 1.29). The authors proposed a mechanism, in which the acid **1.85** first reacts with ammonia-borane to give dihydrogen gas and **1.85a**. Compound **1.85a** can further react with a molecule of the imine to generate an amine and **1.85b** through a six-membered ring transition state **1.85 TS-(*S*)**. Another four-membered ring transition state **1.85 TS1** was proposed during the hydrolysis of **1.85b** with water to regenerate the catalyst **1.85** (Scheme 1.30).

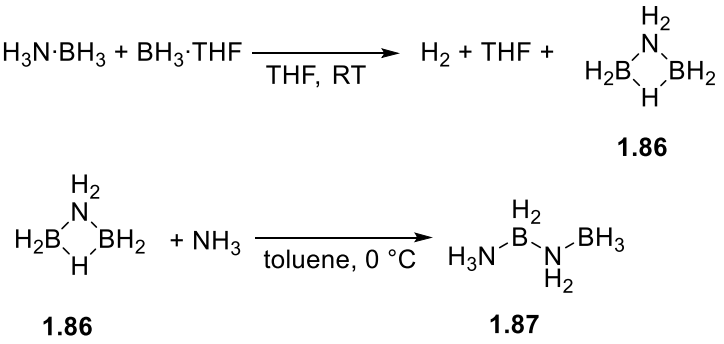


Scheme 1.29: Catalytic transfer hydrogenation of imines using catalyst **1.85**.[173]



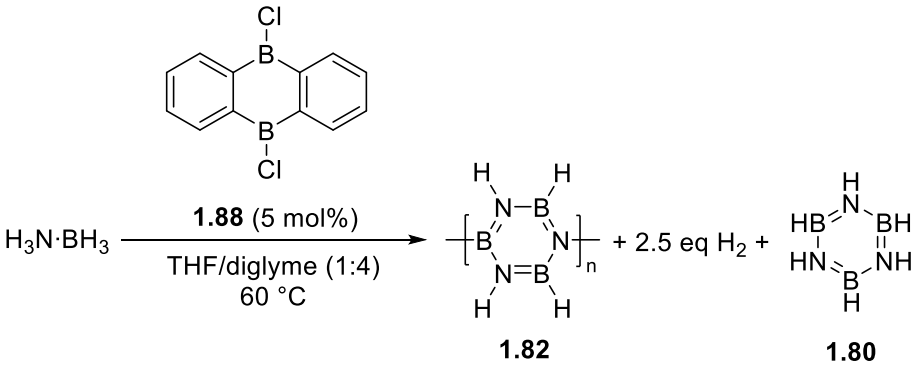
Scheme 1.30: Proposed catalytic cycle for transfer hydrogenation of imines using catalyst **1.85**.[173]

One of the simplest Lewis acids that can prompt the dehydrogenation of ammonia-borane is BH_3·THF, which was reported by Shore and co-workers in 2010.[174] At room temperature, ammonia-borane reacts with BH_3·THF to liberate one equivalent of hydrogen gas and give aminodiborane **1.86**. Aminodiborane **1.86** can further react with ammonia gas to give the inorganic butane analogue, **1.87** (Scheme 1.31).



Scheme 1.31: THF adduct of borane in ammonia-borane dehydrogenation.[174]

In 2015, Wegner compared the catalysis performance of several different Lewis acids (9,10-dichlorodiboraanthracene **1.88**, BCl_3, $BPhCl_2$, BPh_2Cl and tris(pentafluorophenyl)borane BCF) in the dehydrogenation of ammonia-borane (Table 1.3). Amongst these, compound **1.88** was the most efficient catalyst, operating at a relatively low catalyst loading of 5 mol%. It was found that this compound could controllably release 2.36 equivalents of dihydrogen at 60 °C (Scheme 1.32).[175] It is worth noting that catalyst **1.88** can be used multiple times, even after 15 cycles, and that no obvious decrease of reactivity was observed.



Scheme 1.32: Catalytic dehydrogenation of ammonia-borane by Lewis acid **1.88**.[175]

Table 1.3: Lewis acid catalysed dehydrogenation of ammonia-borane.[175]

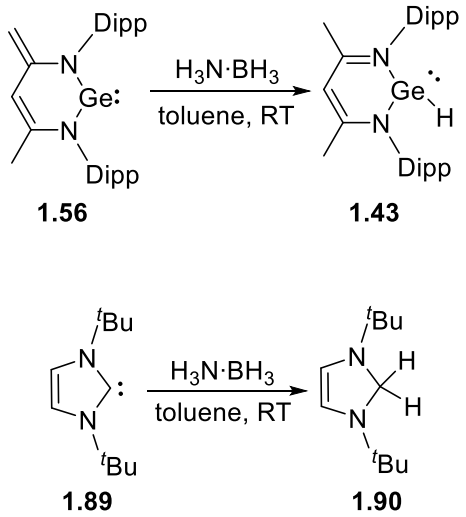
Entry	Catalyst (mol%)	T (°C)[a]	T (h)	H_2 (eq)[b]
1	**1.88** (5)	60	4	2.36
2	BCl_3 (10)	60	24	1.85
3	$BPhCl_2$ (10)	60	10	2.07
4	BPh_2Cl (10)	60	14	2.11
5	BCF (5)	60	24	0.68

[a] The reactions were performed in THF/diglyme (1:4) at 60 °C in a Schlenk tube. The starting material ammonia-borane was used as a powder. [b] The amount of H_2 was measured by displacing water from an inverted burette.

1.4.2 Base mediated dehydrogenation of amine-boranes

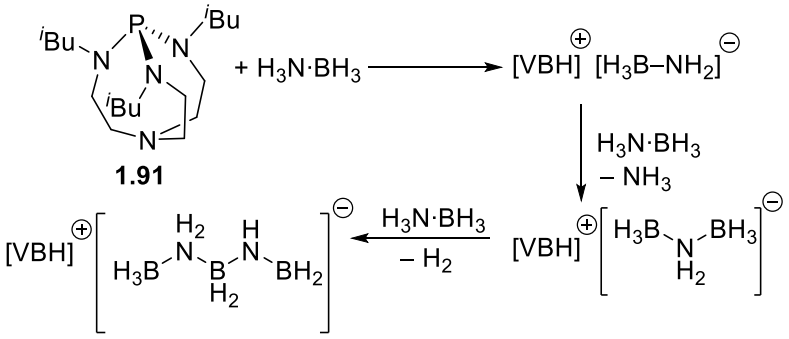
In Section 1.4.1, the application of Brønsted and Lewis acids in the stochiometric/catalytic dehydrogenation of ammonia-borane was discussed. Several research groups have found that bases can also be used for the dehydrogenation of ammonia-borane.

The use of complex **1.57** in small molecule activation reactions was reviewed in Section 1.3.3.[119,124–128] In 2009, Roesky showed its activity in the dehydrogenation of ammonia-borane. The reaction of **1.56** with ammonia-borane resulted in the formation of the germanium hydride **1.43** (Scheme 1.33).[176] The hydrogenation of 1,3-di-*tert*-butylimidazol-2-ylidene **1.89** by ammonia-borane to give **1.90** has also been documented.



Scheme 1.33: Complexes **1.56** and **1.85** and their reactivity towards ammonia-borane.[176]

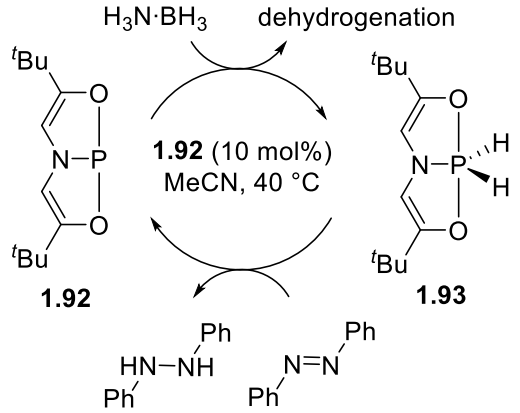
The phosphoric acid **1.85** was explored in ammonia-borane dehydrogenation (Section 1.4.1). Similarly the anionic polymerisation of ammonia-borane initiated by Verkade's base (2,8,9-tri-*iso*-butyl-2,5,8,9-tetraaza-1-phosphabicyclo[3.3.3]undecane) **1.91** was reported by Radosevich in 2011 (Scheme 1.34).[177]



Scheme 1.34: Complex **1.91** in amine-borane activation.[177]

Geometrically constrained trivalent phosphorus complex **1.92** was first reported by Arduengo in 1984,[178] but it was not until 2012, that the role of **1.92** in ammonia-borane dehydrogenation was explored by Radosevich.[179] Adopting a planar structure, complex **1.92** can formally cycle between phosphorus(III) and phosphorus(V), and can thus act as a catalyst in transfer hydrogenation reactions. When reacted with ammonia-

borane at 40 °C, phosphorus complex **1.92** converts to dihydridophosphorane **1.93**, which can hydrogenate azobenzene to give diphenylhydrazine and regenerate **1.92** (Scheme 1.35).

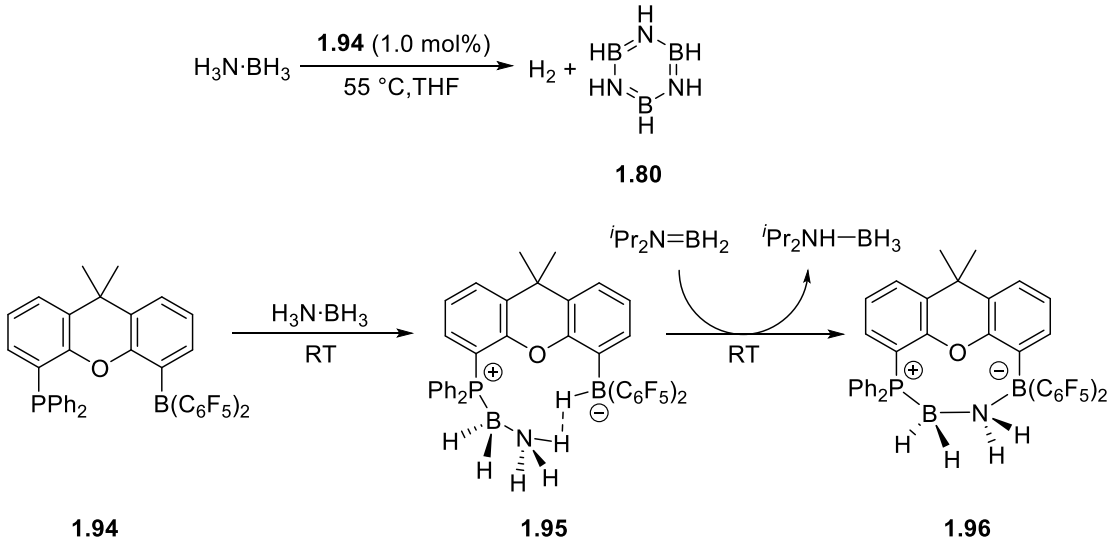


Scheme 1.35: Dehydrogenation pathway of ammonia-borane with catalyst **1.92**.[179]

1.4.3 Frustrated Lewis pair mediated dehydrogenation of amine-boranes

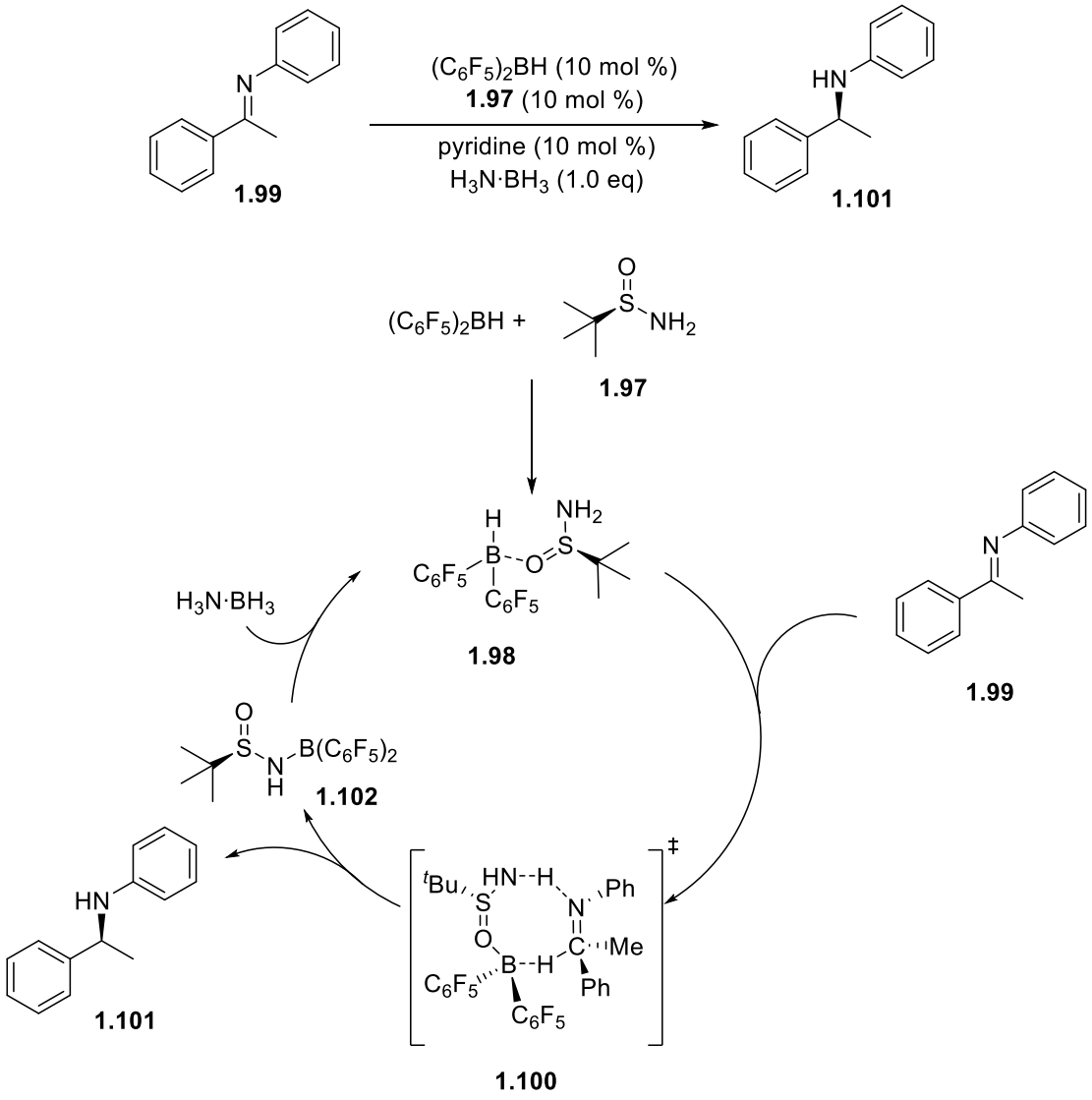
The utility of FLPs in small molecule activation has been demonstrated by Stephan and many other researchers, and FLP type dehydrogenation mechanisms are well known.[150,180–183]

In 2016, Aldridge and co-workers reported the catalytic dehydrogenation of ammonia-borane at 55 °C, with 1 mol% of catalyst **1.94**, to give **1.80** (Scheme 1.36). Stochiometric reaction of **1.94** with ammonia-borane at room temperature was found to afford an adduct **1.95**, which could further hydrogenate the hydrogen acceptor $^{i}Pr_2N{=}BH_2$ and give the aminoborane adduct **1.96** (Scheme 1.36).[184]



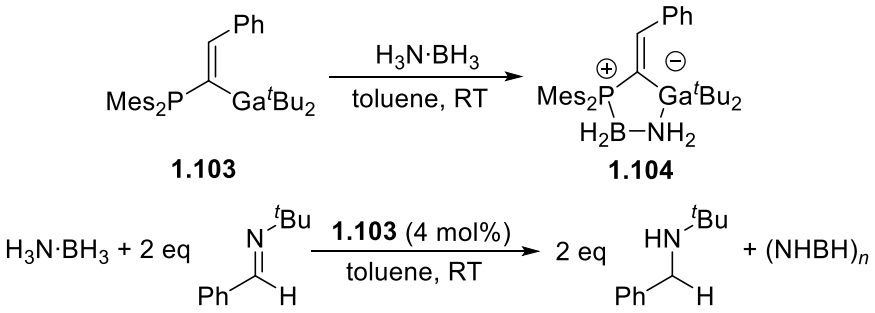
Scheme 1.36: Complex **1.94** in ammonia-borane activation.[184]

A combination of FLP-type catalysis with chiral *tert*-butylsulfinamide **1.97** and Piers' borane ($HB(C_6F_5)_2$) was reported by Du for the catalytic transfer hydrogenation of imines in 2016 (Scheme 1.37).[185] Employing 10 mol% of $HB(C_6F_5)_2$, (E)-*N*,1-diphenylethan-1-imine **1.99** can be hydrogenated by ammonia-borane at room temperature with 67% conversion. The conversion drops to 17% when 10 mol% of pyridine was added. The authors reasoned that pyridine can trap free $HB(C_6F_5)_2$ and inhibit racemic product formation. A viable reaction pathway was proposed, with adduct **1.98** being formed in situ, and then interacting with the imine through an eight-membered ring transition state **1.100**. This regenerates the catalyst **1.98** via the reaction of ammonia-borane with **1.102**.



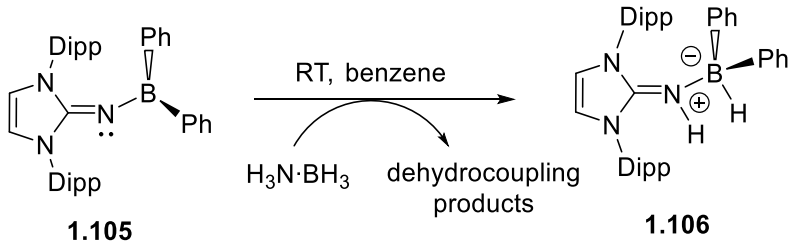
Scheme 1.37: A proposed mechanism for catalytic hydrogenation of imine by $HB(C_6F_5)_2$ and **1.97**.[185]

The gallium/phosphorus frustrated Lewis pair **1.103** was reported by Uhl in 2018, and shown to activate ammonia-borane to give **1.104**. Employing 4 mol% of **1.103**, imines can be hydrogenated to the corresponding amines, with dehydrogenated polymeric B−N compounds obtained as side products (Scheme 1.38).[186]



Scheme 1.38: Catalytic hydrogenation of imines with **1.103**.[186]

On a related note, the N-heterocyclic imine supported frustrated Lewis pair **1.105** was reported by Rivard and co-workers in 2016 (Scheme 1.39). The structure of **1.105** is interesting in its own right, as it contains a Lewis acidic boron centre and a basic nitrogen in the same molecule and can thus be considered an FLP. This compound was found to dehydrogenate ammonia-borane to give complex **1.106**.[187]



Scheme 1.39: Complex **1.105** in ammonia-borane activation.[187]

Different examples of the dehydrogenation of ammonia-borane using a variety of main group element compounds are summarised above. These can be broadly categorised as acid (Brønsted and Lewis acid), base and FLP mediated. The aforementioned studies have shown that the metal-free activation of ammonia-borane at ambient temperature is feasible and have the potential to meet the needs of the hydrogen economy in the future.

1.5 Project aims and summary

This chapter has summarised three main areas of active research in main group chemistry, all of which are of relevance to the work contained in this thesis. In Section 1.2, binary hydrides of the group 13 elements were discussed, with a specific focus on synthetic pathways for the synthesis of gallium hydrides. In Section 1.3, examples of main group elements in small molecule activation reactions were summarised, paying particular attention to catalytic hydroboration. In Section 1.4, the dehydrogenation of ammonia-borane was described, with acids, bases and FLPs as initiators for this transformation.

Gallium hydride complexes remain under-explored, and good ligand systems that are able to stabilise them for further characterisation are needed. The tridentate pincer ligand *N*,*N*-bis(3,5-di-*tert*-butyl-2-phenoxy)amine ($[ON(H)O]^{2-}$) was explored by Siu-Kwan Lo and Cory Smith in the Goicoechea group and shown to be compatible with the group 13 elements.[188,189] In this project, this ligand is used to increase the diversity of gallium complexes available and to develop a methodology for the synthesis of novel gallium hydrides. The ultimate goal is to develop suitable main group catalysts for the hydrogenation of unsaturated substrates, and as a start, the use of these compounds as hydroboration catalysts was explored.

In Chapter Two, novel pincer stabilised gallium halide complexes are reported, and their application as precursors in salt metathesis reactions is explored. Two types of novel gallium hydrides were synthesised using different synthetic pathways. The potential use of gallium hydrides in small molecule activation (such as aldehydes, ketones) is discussed as well.

In Chapter Three, gallium complexes are used as catalysts for the catalytic hydroboration of unsaturated substrates such as aldehydes, ketones, carbon dioxide, isocyanates and imines. A mechanism for catalytic hydroboration of ketones is proposed. The hydroboration of isocyanates and imines with these gallium catalysts is also explored (the first time this has been carried out to date).

In addition to our work exploring hydroboration reactions, the idea of developing novel borane reagents was appealing. The ($[ON(H)O]^{2-}$) ligand opens up possibilities for the ligand to cooperatively react in dehydrogenation reactions with boranes.

In Chapter Four, transelementation reactions between boron complexes and pincer-stabilised gallium complexes is explored. A series of boron complexes was synthesised, which demonstrates the stabilising effect of the ($[ON(H)O]^{2-}$) ligand. Later the metal-free dehydrogenation reactivity of a novel amine-borane is described.

In Chapter Five, the synthesis of pincer stabilised boron halides is reported and their reactivity towards bases is documented. A novel boron bromide complex has been found to activate C−O bond of ethers to give borate esters, which dehydrobrominate in the presence of a base to give cyclic products with N−B−O moieties.

1.6 References

[1] A. D. McNaught, A. Wilkinson, *IUPAC. Compendium of Chemical Terminology, 2nd Ed. (the "Gold Book")*, Blackwell Scientific Publications, Oxford, **1997**.

[2] A. Biffis, P. Centomo, A. Del Zotto, M. Zecca, *Chem. Rev.* **2018**, *118*, 2249–2295.

[3] W.-W. Chen, M.-H. Xu, *Org. Biomol. Chem.* **2017**, *15*, 1029–1050.

[4] M. Iglesias, L. A. Oro, *Chem. Soc. Rev.* **2018**, *47*, 2772–2808.

[5] D. L. Anderson, *J. Geophys. Res.* **1983**, *88*, 41–52.

[6] D. A. Kring, *28th Lunar* and *Planetary Science Conference* **1997**, 1–2.

[7] P. P. Power, *Nature* **2010**, *463*, 171–177.

[8] G. H. Spikes, J. C. Fettinger, P. P. Power, *J. Am. Chem. Soc.* **2005**, *127*, 12232–12233.

[9] P. J. Karol, R. C. Barber, B. M. Sherrill, E. Vardaci, T. Yamazaki, *Pure Appl. Chem.* **2016**, *88*, 139–153.

[10] R. Eichler, *J. Phys.: Conf. Ser.* **2013**, *420*, 12003.

[11] S. Itsuno, in *Boron Reagents Synth.*, American Chemical Society, **2016**, pp. 241–274.

[12] A. E. Finholt, A. C. Bond, H. I. Schlesinger, *J. Am. Chem. Soc.* **1947**, *69*, 1199–1203.

[13] B. Vest, K. Klinkhammer, C. Thierfelder, M. Lein, P. Schwerdtfeger, *Inorg. Chem.* **2009**, *48*, 7953–7961.

[14] E. Wiberg, *Pure appl. Chem.* **1977**, *49*, 691–700.

[15] A. Stock, *Hydrides of Boron and Silicon.*, Cornell University Press, **1933**.

[16] N. N. Greenwood, *Chem. Soc. Rev.* **1992**, *21*, 49–57.

[17] A. B. Burg, H. I. Schlesinger, *J. Am. Chem. Soc.* **1937**, *59*, 780–787.

[18] L. Andrews, X. Wang, *Science* **2003**, *299*, 2049–2052.

[19] J. W. Turley, H. W. Rinn, *Inorg. Chem.* **1969**, *8*, 18–22.

[20] F. M. Brower, N. E. Matzek, P. F. Reigler, H. W. Rinn, C. B. Roberts, D. L. Schmidt, J. A. Snover, K. Terada, *J. Am. Chem. Soc.* **1976**, *98*, 2450–2453.

[21] C. Jones, *Chem. Commun.* **2001**, 2293–2298.

[22] X. Wang, L. Andrews, *J. Phys. Chem. A* **2004**, *108*, 3396–3402.

[23] A. J. Downs, M. J. Goode, C. R. Pulham, *J. Am. Chem. Soc.* **1989**, *111*, 1936–1937.

[24] C. R. Pulham, A. J. Downs, M. J. Goode, D. W. H. Rankin, H. E. Robertson, *J. Am. Chem. Soc.* **1991**, *113*, 5149–5162.

[25] A. Storr, V. G. Wiebe, *Can. J. Chem.* **1969**, *47*, 673–679.

[26] S. Marchant, C. Y. Tang, A. J. Downs, T. M. Greene, H.-J. Himmel, S. Parsons, *Dalton Trans.* **2005**, 3281–3290.

[27] J. L. Atwood, S. G. Bott, C. Jones, C. L. Raston, *Inorg. Chem.* **1991**, *30*, 4868–4870.

[28] T. Bauer, S. Schulz, M. Nieger, U. Kessler, *Organometallics* **2003**, *22*, 3134–3142.

[29] D. Pugh, P. Marchand, I. P. Parkin, C. J. Carmalt, *Inorg. Chem.* **2012**, *51*, 6385–6395.

[30] B. Luo, B. E. Kucera, W. L. Gladfelter, *J. Chem. Soc., Dalton Trans.* **2006**, 4491–4498.

[31] D. Rudolf, G. Storch, E. Kaifer, H. J. Himmel, *Eur. J. Inorg. Chem.* **2012**, 2368–2372.

[32] J. A. Jegier, W. L. Gladfelter, *Coord. Chem. Rev.* **2000**, *206–207*, 631–650.

[33] P. Zanella, G. Rossetto, N. Brianese, F. Ossola, M. Porchia, J. Williams, *Chem. Mater.* **1991**, *3*, 225–242.

[34] S. J. Pearton, C. R. Abernathy, M. E. Overberg, G. T. Thaler, A. H. Onstine, B. P. Gila, F. Ren, B. Lou, J. Kim, *Mater. Today* **2002**, *5*, 24–31.

[35] N. N. Greenwood, E. J. F. Ross, A. Storr, *J. Chem. Soc. A* **1966**, 706–711.

[36] C. Y. Tang, A. R. Cowley, A. J. Downs, S. Marchant, S. Parsons, *Eur. J. Inorg. Chem.* **2008**, 737–744.

[37] C. Y. Tang, R. A. Coxall, A. J. Downs, T. M. Greene, S. Parsons, *J. Chem. Soc., Dalton Trans.* **2001**, *2*, 2141–2147.

[38] A. K. Swarnakar, M. J. Ferguson, R. McDonald, E. Rivard, *Dalton Trans.* **2017**, *46*, 1406–1412.

[39] C. Y. Tang, A. J. Downs, T. M. Greene, S. Marchant, S. Parsons, *Inorg. Chem.* **2005**, *44*, 7143–7150.

[40] A. H. Cowley, F. P. Gabbai, D. A. Atwood, C. J. Carrano, L. M. Mokry, M. R. Bond, *J. Am. Chem. Soc.* **1994**, *116*, 1559–1560.

[41] V. G. Sokolov, T. S. Koptseva, M. V. Moskalev, N. L. Bazyakina, A. V. Piskunov, A. V. Cherkasov, I. L. Fedushkin, *Inorg. Chem.* **2017**, *56*, 13401–13410.

[42] A. R. Cowley, A. J. Downs, H.-J. Himmel, S. Marchant, S. Parsons, J. A. Yeoman, *Dalton Trans.* **2005**, 1591–1597.

[43] J. A. B. Abdalla, I. M. Riddlestone, J. Turner, P. A. Kaufman, R. Tirfoin, N. Phillips, S. Aldridge, *Chem. Eur. J.* **2014**, *20*, 17624–17634.

[44] D. Pugh, L. G. Bloor, I. P. Parkin, C. J. Carmalt, *Chem. Eur. J.* **2012**, *18*, 6079–6087.

[45] S. N. König, G. Gerstberger, C. Schädle, C. Maichle-Mössmer, E. Herdtweck, R. Anwander, *Main Group Met. Chem.* **2013**, *36*, 169–180.

[46] L. Grocholl, S. A. Cullison, J. Wang, D. C. Swenson, E. G. Gillan, *Inorg. Chem.* **2002**, *41*, 2920–2926.

[47] A. Seifert, D. Scheid, G. Linti, T. Zessin, *Chem. Eur. J.* **2009**, *15*, 12114–12120.

[48] J. A. B. Abdalla, I. M. Riddlestone, R. Tirfoin, S. Aldridge, *Angew. Chem., Int. Ed.* **2015**, *54*, 5098–5102.

[49] E. Bernabé-Pablo, V. Jancik, M. Moya-Cabrera, *Inorg. Chem.* **2013**, *52*, 6944–6950.

[50] K. Burgess, M. J. Ohlmeyer, *Chem. Rev.* **1991**, *91*, 1179–1191.

[51] E. R. Burkhardt, K. Matos, *Chem. Rev.* **2006**, *106*, 2617–2650.

[52] N. Miyaura, K. Yamada, A. Suzuki, *Tetrahedron Lett.* **1979**, *20*, 3437–3440.

[53] N. Miyaura, A. Suzuki, *Chem. Rev.* **1995**, *95*, 2457–2483.

[54] D. M. T. Chan, K. L. Monaco, R.-P. Wang, M. P. Winters, *Tetrahedron Lett.* **1998**, *39*, 2933–2936.

[55] D. A. Evans, J. L. Katz, T. R. West, *Tetrahedron Lett.* **1998**, *39*, 2937–2940.

[56] P. Y. S. Lam, C. G. Clark, S. Saubern, J. Adams, M. P. Winters, D. M. T. Chan, A. Combs, *Tetrahedron Lett.* **1998**, *39*, 2941–2944.

[57] L. S. Liebeskind, J. Srogl, *J. Am. Chem. Soc.* **2000**, *122*, 11260–11261.

[58] N. A. Weires, E. L. Baker, N. K. Garg, *Nat. Chem.* **2016**, *8*, 75–79.

[59] J. C. Vantourout, H. N. Miras, A. Isidro-Llobet, S. Sproules, A. J. B. Watson, *J. Am. Chem. Soc.* **2017**, *139*, 4769–4779.

[60] H. C. Brown, H. I. Schlesinger, A. B. Burg, *J. Am. Chem. Soc.* **1939**, *61*, 673–680.

[61] H. I. Schlesinger, H. C. Brown, B. Abraham, A. C. Bond, N. Davidson, A. E. Finholt, J. R. Gilbreath, H. Hoekstra, L. Horvitz, E. K. Hyde, et al., *J. Am. Chem. Soc.* **1953**, *75*, 186–190.

[62] H. C. Brown, B. C. S. Rao, *J. Am. Chem. Soc.* **1956**, *78*, 5694–5695.

[63] D. G. Hall, in *Boronic Acids: Preparation, Applications in Organic Synthesis and Medicine*, John Wiley & Sons, Ltd, **2006**, p. 414.

[64] H. C. Brown, S. K. Gupta, *J. Am. Chem. Soc.* **1971**, *93*, 1816–1818.

[65] C. E. Tucker, J. Davidson, P. Knochel, *J. Org. Chem.* **1992**, *57*, 3482–3485.

[66] H. C. Brown, S. K. Gupta, *J. Am. Chem. Soc.* **1972**, *94*, 4370–4371.

[67] H. C. Brown, S. K. Gupta, *J. Am. Chem. Soc.* **1975**, *97*, 5249–5255.

[68] H. Kono, K. Ito, Y. Nagai, *Chem. Lett.* **1975**, *4*, 1095–1096.

[69] D. Männig, H. Nöth, *Angew. Chem., Int. Ed.* **1985**, *24*, 878–879.

[70] D. A. Evans, G. C. Fu, B. A. Anderson, *J. Am. Chem. Soc.* **1992**, *114*, 6679–6685.

[71] K. Burgess, W. A. Van der Donk, S. A. Westcott, T. B. Marder, R. T. Baker, J. C. Calabrese, *J. Am. Chem. Soc.* **1992**, *114*, 9350–9359.

[72] S. A. Westcott, H. P. Blom, T. B. Marder, R. T. Baker, J. C. Calabrese, *Inorg. Chem.* **1993**, *32*, 2175–2182.

[73] A. D. Bage, T. A. Hunt, S. P. Thomas, *Org. Lett.* **2020**, *22*, 4107–4112.

[74] E. Jeong, J. Heo, S. Park, S. Chang, *Chem. Eur. J.* **2019**, *25*, 6320–6325.

[75] C. C. Chong, R. Kinjo, *ACS Catal.* **2015**, *5*, 3238–3259.

[76] M. Ephritikhine, *Chem. Rev.* **1997**, *97*, 2193–2242.

[77] S. P. Green, C. Jones, A. Stasch, *Angew. Chem., Int. Ed.* **2008**, *47*, 9079–9083.

[78] S. Harder, J. Brettar, *Angew. Chem., Int. Ed.* **2006**, *45*, 3474–3478.

[79] H. D. Kaesz, R. B. Saillant, *Chem. Rev.* **1972**, *72*, 231–281.

[80] S. Aldridge, A. J. Downs, *Chem. Rev.* **2001**, *101*, 3305–3366.

[81] S. Harder, *Chem. Commun.* **2012**, *48*, 11165–11177.

[82] C. Weetman, S. Inoue, *ChemCatChem* **2018**, *10*, 4213–4228.

[83] J. Spielmann, S. Harder, *Chem. Eur. J.* **2007**, *13*, 8928–8938.

[84] S. Harder, J. Spielmann, *J. Organomet. Chem.* **2012**, *698*, 7–14.

[85] M. Arrowsmith, T. J. Hadlington, M. S. Hill, G. Kociok-Köhn, *Chem. Commun.* **2012**, *48*, 4567–4569.

[86] M. Arrowsmith, M. S. Hill, G. Kociok-Köhn, *Chem. Eur. J.* **2013**, *19*, 2776–2783.

[87] C. Weetman, M. S. Hill, M. F. Mahon, *Chem. Eur. J.* **2016**, *22*, 7158–7162.

[88] C. Weetman, M. D. Anker, M. Arrowsmith, M. S. Hill, G. Kociok-Köhn, D. J. Liptrot, M. F. Mahon, *Chem. Sci.* **2016**, *7*, 628–641.

[89] C. Weetman, M. S. Hill, M. F. Mahon, *Chem. Commun.* **2015**, *51*, 14477–14480.

[90] M. Arrowsmith, M. S. Hill, T. Hadlington, G. Kociok-Köhn, C. Weetman, *Organometallics* **2011**, *30*, 5556–5559.

[91] Y. Yang, M. D. Anker, J. Fang, M. F. Mahon, L. Maron, C. Weetman, M. S. Hill, *Chem. Sci.*

2017, *8*, 3529–3537.

[92] M. D. Anker, M. Arrowsmith, P. Bellham, M. S. Hill, G. Kociok-Köhn, D. J. Liptrot, M. F. Mahon, C. Weetman, *Chem. Sci.* **2014**, *5*, 2826–2830.

[93] L. Garcia, C. Dinoi, M. F. Mahon, L. Maron, M. S. Hill, *Chem. Sci.* **2019**, *10*, 8108–8118.

[94] D. Mukherjee, S. Shirase, T. P. Spaniol, K. Mashima, J. Okuda, *Chem. Commun.* **2016**, *52*, 13155–13158.

[95] Z. Yang, M. Zhong, X. Ma, S. De, C. Anusha, P. Parameswaran, H. W. Roesky, *Angew. Chem., Int. Ed.* **2015**, *54*, 10225–10229.

[96] Z. Yang, M. Zhong, X. Ma, K. Nijesh, S. De, P. Parameswaran, H. W. Roesky, *J. Am. Chem. Soc.* **2016**, *138*, 2548–2551.

[97] W. Liu, Y. Ding, D. Jin, Q. Shen, B. Yan, X. Ma, Z. Yang, *Green Chem.* **2019**, *21*, 3812–3815.

[98] D. Franz, S. Inoue, *Chem. Eur. J.* **2014**, *20*, 10645–10649.

[99] D. Franz, L. Sirtl, A. Pöthig, S. Inoue, *Z. Anorg. Allg. Chem.* **2016**, *642*, 1245–1250.

[100] Q. Liu, L. Wu, R. Jackstell, M. Beller, *Nat. Commun.* **2015**, *6*, 5933.

[101] D. Franz, C. Jandl, C. Stark, S. Inoue, *ChemCatChem* **2019**, *11*, 5275–5281.

[102] A. Ford, S. Woodward, *Angew. Chem., Int. Ed.* **1999**, *38*, 335–336.

[103] A. J. Blake, A. Cunningham, A. Ford, S. J. Teat, S. Woodward, *Chem. Eur. J.* **2000**, *6*, 3586–3594.

[104] L. Liu, S.-K. Lo, C. Smith, J. M. Goicoechea, *Chem. Eur. J.* **2021**, *27*, 17379–17385.

[105] Y. Ding, H. Hao, H. W. Roesky, M. Noltemeyer, H.-G. Schmidt, *Organometallics* **2001**, *20*, 4806–4811.

[106] L. W. Pineda, V. Jancik, K. Starke, R. B. Oswald, H. W. Roesky, *Angew. Chem., Int. Ed.* **2006**, *45*, 2602–2605.

[107] A. Jana, D. Ghoshal, H. W. Roesky, I. Objartel, G. Schwab, D. Stalke, *J. Am. Chem. Soc.* **2009**, *131*, 1288–1293.

[108] A. Jana, H. W. Roesky, C. Schulzke, *Dalton Trans.* **2010**, *39*, 132–138.

[109] N. Takagi, S. Sakaki, *J. Am. Chem. Soc.* **2013**, *135*, 8955–8965.

[110] T. J. Hadlington, M. Hermann, G. Frenking, C. Jones, *J. Am. Chem. Soc.* **2014**, *136*, 3028–3031.

[111] T. J. Hadlington, C. E. Kefalidis, L. Maron, C. Jones, *ACS Catal.* **2017**, *7*, 1853–1859.

[112] D. W. Stephan, *Acc. Chem. Res.* **2015**, *48*, 306–316.

[113] S. Freitag, K. M. Krebs, J. Henning, J. Hirdler, H. Schubert, L. Wesemann, *Organometallics* **2013**, *32*, 6785–6791.

[114] S. Freitag, J. Henning, H. Schubert, L. Wesemann, *Angew. Chem., Int. Ed.* **2013**, *52*, 5640–5643.

[115] K. M. Krebs, J. Wiederkehr, J. Schneider, H. Schubert, K. Eichele, L. Wesemann, *Angew. Chem., Int. Ed.* **2015**, *54*, 5502–5506.

[116] J. Schneider, K. M. Krebs, S. Freitag, K. Eichele, H. Schubert, L. Wesemann, *Chem. Eur. J.* **2016**, *22*, 9812–9826.

[117] J. Schneider, C. P. Sindlinger, S. M. Freitag, H. Schubert, L. Wesemann, *Angew. Chem., Int. Ed.* **2017**, *56*, 333–337.

[118] J.-J. Maudrich, F. Diab, S. Weiß, M. Zweigart, K. Eichele, H. Schubert, R. Müller, M. Kaupp, L. Wesemann, *Chem. Eur. J.* **2021**, *27*, 4691–4699.

[119] Y. Wu, C. Shan, Y. Sun, P. Chen, J. Ying, J. Zhu, L. Liu, Y. Zhao, *Chem. Commun.* **2016**, *52*, 13799–13802.

[120] M. K. Sharma, M. Ansari, P. Mahawar, G. Rajaraman, S. Nagendran, *Dalton Trans.* **2019**, *48*, 664–672.

[121] S. Sinhababu, D. Singh, M. K. Sharma, R. K. Siwatch, P. Mahawar, S. Nagendran, *Dalton Trans.* **2019**, *48*, 4094–4100.

[122] R. Dasgupta, S. Das, S. Hiwase, S. K. Pati, S. Khan, *Organometallics* **2019**, *38*, 1429–1435.

[123] V. Nesterov, R. Baierl, F. Hanusch, A. E. Ferao, S. Inoue, *J. Am. Chem. Soc.* **2019**, *141*, 14576–14580.

[124] M. Driess, S. Yao, M. Brym, C. van Wüllen, *Angew. Chem., Int. Ed.* **2006**, *45*, 4349–4352.

[125] S. Yao, C. van Wüllen, M. Driess, *Chem. Commun.* **2008**, 5393–5395.

[126] A. Jana, I. Objartel, H. W. Roesky, D. Stalke, *Inorg. Chem.* **2009**, *48*, 798–800.

[127] A. Jana, B. Nekoueishahraki, H. W. Roesky, C. Schulzke, *Organometallics* **2009**, *28*, 3763–3766.

[128] Y. Wu, L. L. Liu, J. Su, K. Yan, J. Zhu, Y. Zhao, *Chem. Commun.* **2016**, *52*, 1582–1585.

[129] C. C. Chong, H. Hirao, R. Kinjo, *Angew. Chem., Int. Ed.* **2015**, *54*, 190–194.

[130] D. Gudat, A. Haghverdi, M. Nieger, *Angew. Chem., Int. Ed.* **2000**, *39*, 3084–3086.

[131] S. Burck, D. Gudat, M. Nieger, W.-W. Du Mont, *J. Am. Chem. Soc.* **2006**, *128*, 3946–3955.

[132] M. R. Adams, C.-H. Tien, B. S. N. Huchenski, M. J. Ferguson, A. W. H. Speed, *Angew. Chem., Int. Ed.* **2017**, *56*, 6268–6271.

[133] C. C. Chong, R. Kinjo, *Angew. Chem., Int. Ed.* **2015**, *54*, 12116–12120.

[134] T. Lundrigan, C.-H. Tien, K. N. Robertson, A. W. H. Speed, *Chem. Commun.* **2020**, *56*, 8027–8030.

[135] B. Rao, C. C. Chong, R. Kinjo, *J. Am. Chem. Soc.* **2018**, *140*, 652–656.

[136] T. Lundrigan, E. N. Welsh, T. Hynes, C.-H. Tien, M. R. Adams, K. R. Roy, K. N. Robertson, A. W. H. Speed, *J. Am. Chem. Soc.* **2019**, *141*, 14083–14088.

[137] D. M. C. Ould, R. L. Melen, *Chem. Eur. J.* **2018**, *24*, 15201–15204.

[138] T. T. P. Tran, D. M. C. Ould, L. C. Wilkins, D. S. Wright, R. L. Melen, J. M. Rawson, *CrystEngComm* **2017**, *19*, 4696–4699.

[139] D. M. C. Ould, A. C. Rigby, L. C. Wilkins, S. J. Adams, J. A. Platts, S. J. A. Pope, E. Richards, R. L. Melen, *Organometallics* **2018**, *37*, 712–719.

[140] A. Rossin, M. Peruzzini, *Chem. Rev.* **2016**, *116*, 8848–8872.

[141] F. H. Stephens, V. Pons, R. Tom Baker, *Dalton Trans.* **2007**, 2613–2626.

[142] G. Moussa, R. Moury, U. B. Demirci, T. Şener, P. Miele, *Int. J. Energy Res.* **2013**, *37*, 825–842.

[143] M. G. Hu, R. A. Geanangel, W. W. Wendlandt, *Thermochim. Acta* **1978**, *23*, 249–255.

[144] V. Sit, R. A. Geanangel, W. W. Wendlandt, *Thermochim. Acta* **1987**, *113*, 379–382.

[145] X. Zhang, L. Kam, T. J. Williams, *Dalton Trans.* **2016**, *45*, 7672–7677.

[146] F. Baitalow, J. Baumann, G. Wolf, K. Jaenicke-Rößler, G. Leitner, *Thermochim. Acta* **2002**, *391*, 159–168.

[147] F. Baitalow, G. Wolf, J.-P. E. Grolier, F. Dan, S. L. Randzio, *Thermochim. Acta* **2006**, *445*, 121–125.

[148] R. Schellenberg, J. Kriehme, G. Wolf, *Thermochim. Acta* **2007**, *457*, 103–108.

[149] M. S. Hill, G. Kociok-Köhn, T. P. Robinson, *Chem. Commun.* **2010**, *46*, 7587–7589.

[150] A. M. Chapman, M. F. Haddow, D. F. Wass, *J. Am. Chem. Soc.* **2011**, *133*, 18463–18478.

[151] P. A. Lummis, R. McDonald, M. J. Ferguson, E. Rivard, *Dalton Trans.* **2015**, *44*, 7009–7020.

[152] K. A. Erickson, J. P. W. Stelmach, N. T. Mucha, R. Waterman, *Organometallics* **2015**, *34*, 4693–4699.

[153] D. Pun, E. Lobkovsky, P. J. Chirik, *Chem. Commun.* **2007**, 3297–3299.

[154] Y. Jiang, H. Berke, *Chem. Commun.* **2007**, 3571–3573.

[155] J. R. Vance, A. Scha, A. P. M. Robertson, K. Lee, J. Turner, G. R. Whittell, I. Manners, *J. Am.*

Chem. Soc. **2014**, *136*, 3048–3064.

[156] A. Glüer, M. Förster, V. R. Celinski, J. Schmedt Auf Der Günne, M. C. Holthausen, S. Schneider, *ACS Catal.* **2015**, *5*, 7214–7217.

[157] J. R. Vance, A. Schäfer, A. P. M. Robertson, K. Lee, J. Turner, G. R. Whittell, I. Manners, *J. Am. Chem. Soc.* **2014**, *136*, 3048–3064.

[158] B. L. Conley, T. J. Williams, *Chem. Commun.* **2010**, *46*, 4815–4817.

[159] M. Käß, A. Friedrich, M. Drees, S. Schneider, *Angew. Chem., Int. Ed.* **2009**, *48*, 905–907.

[160] A. Friedrich, M. Drees, S. Schneider, *Chem. Eur. J.* **2009**, *15*, 10339–10342.

[161] A. Y. Timoshkin, H. F. Schaefer, *J. Am. Chem. Soc.* **2003**, *125*, 9998–10011.

[162] A. N. Marziale, A. Friedrich, I. Klopsch, M. Drees, V. R. Celinski, J. Schmedt Auf Der Günne, S. Schneider, *J. Am. Chem. Soc.* **2013**, *135*, 13342–13355.

[163] M. J. Sgro, D. W. Stephan, *Dalton Trans.* **2013**, *42*, 10460–10472.

[164] A. Rossin, A. Rossi, M. Peruzzini, F. Zanobini, *ChemPlusChem* **2014**, *79*, 1316–1325.

[165] G. Alcaraz, L. Vendier, E. Clot, S. Sabo-Etienne, *Angew. Chem., Int. Ed.* **2010**, *49*, 918–920.

[166] M. A. Esteruelas, F. J. Fernández-Alvarez, A. M. López, M. Mora, E. Oñate, *J. Am. Chem. Soc.* **2010**, *132*, 5600–5601.

[167] C. Bianchini, G. Giambastiani, A. Rossin, *Chemtracts* **2007**, *20*, 273–276.

[168] H. C. Johnson, A. P. M. Robertson, A. B. Chaplin, L. J. Sewell, A. L. Thompson, M. F. Haddow, I. Manners, A. S. Weller, *J. Am. Chem. Soc.* **2011**, *133*, 11076–11079.

[169] B. L. Dietrich, K. I. Goldberg, D. M. Heinekey, T. Autrey, J. C. Linehan, *Inorg. Chem.* **2008**, *47*, 8583–8585.

[170] C. Y. Tang, N. Phillips, M. J. Kelly, S. Aldridge, *Chem. Commun.* **2012**, *48*, 11999–12001.

[171] F. H. Stephens, R. T. Baker, M. H. Matus, D. J. Grant, D. A. Dixon, *Angew. Chem., Int. Ed.* **2007**, *46*, 746–749.

[172] X. Yang, L. Zhao, T. Fox, Z.-X. Wang, H. Berke, *Angew. Chem., Int. Ed.* **2010**, *49*, 2058–2062.

[173] Q. Zhou, W. Meng, J. Yang, H. Du, *Angew. Chem., Int. Ed.* **2018**, *57*, 12111–12115.

[174] X. Chen, J.-C. Zhao, S. G. Shore, *J. Am. Chem. Soc.* **2010**, *132*, 10658–10659.

[175] Z. Lu, L. Schweighauser, H. Hausmann, H. A. Wegner, *Angew. Chem., Int. Ed.* **2015**, *54*, 15556–15559.

[176] A. Jana, C. Schulzke, H. W. Roesky, *J. Am. Chem. Soc.* **2009**, *131*, 4600–4601.

[177] W. C. Ewing, A. Marchione, D. W. Himmelberger, P. J. Carroll, L. G. Sneddon, *J. Am. Chem. Soc.* **2011**, *133*, 17093–17099.

[178] S. A. Culley, A. J. Arduengo, *J. Am. Chem. Soc.* **1984**, *106*, 1164–1165.

[179] N. L. Dunn, M. Ha, A. T. Radosevich, *J. Am. Chem. Soc.* **2012**, *134*, 11330–11333.

[180] S. Li, G. Li, W. Meng, H. Du, *J. Am. Chem. Soc.* **2016**, *138*, 12956–12962.

[181] D. H. A. Boom, E. J. J. de Boed, E. Nicolas, M. Nieger, A. W. Ehlers, A. R. Jupp, J. C. Slootweg, *Z. Anorg. Allg. Chem.* **2020**, *646*, 586–592.

[182] Z. Mo, A. Rit, J. Campos, E. L. Kolychev, S. Aldridge, *J. Am. Chem. Soc.* **2016**, *138*, 3306–3309.

[183] C. Appelt, J. C. Slootweg, K. Lammertsma, W. Uhl, *Angew. Chem., Int. Ed.* **2013**, *52*, 4256–4259.

[184] Z. Mo, A. Rit, J. Campos, E. L. Kolychev, S. Aldridge, *J. Am. Chem. Soc.* **2016**, *138*, 3306–3309.

[185] S. Li, G. Li, W. Meng, H. Du, *J. Am. Chem. Soc.* **2016**, *138*, 12956–12962.

[186] J. Possart, W. Uhl, *Organometallics* **2018**, *37*, 1314–1323.

[187] M. W. Lui, N. R. Paisley, R. McDonald, M. J. Ferguson, E. Rivard, *Chem. Eur. J.* **2016**, *22*, 2134–2145.

[188] S.-K. Lo, *Geometry Constrained Main-Group Compounds for the Activation of Small Molecules*, Thesis (D.Phil.) − University of Oxford, 2018, (Department of Inorganic Chemistry), Oxford, **2018**.

[189] C. D. Smith, *Synthesis and Reactivity of Geometrically Constrained Gallium(III) Complexes*, Thesis (M.Chem) − University of Oxford, (Department of Chemistry), Oxford, **2017**.

Chapter Two

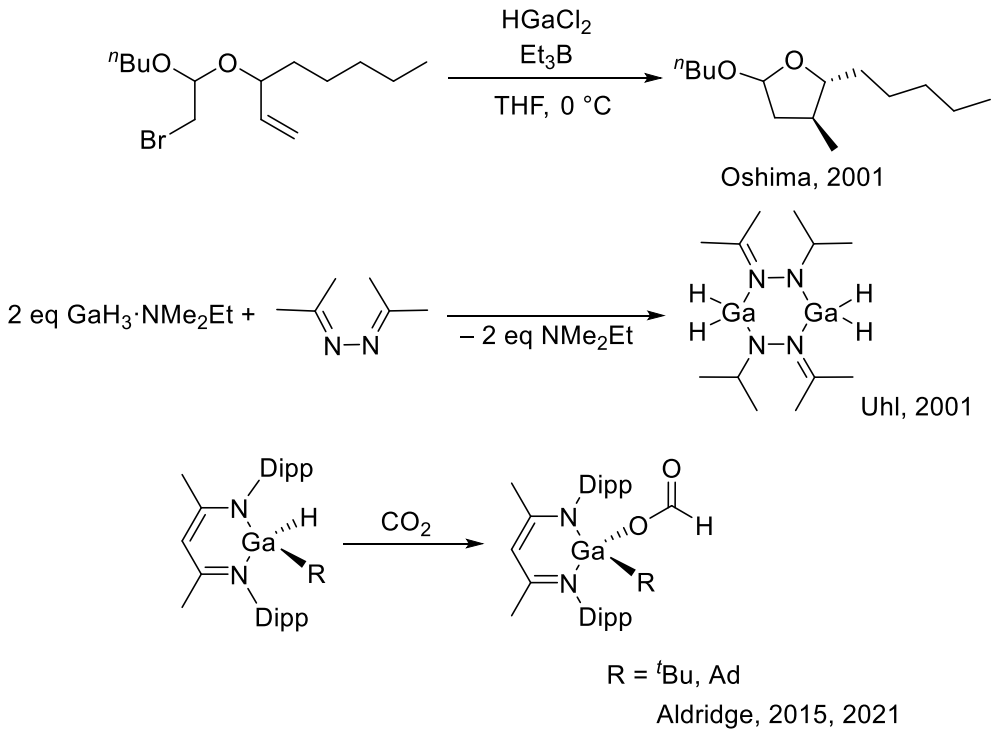
Synthesis of novel pincer-ligated gallium complexes and their use in the hydrogallation of small molecule substrates

---

2.1 Introduction and objectives

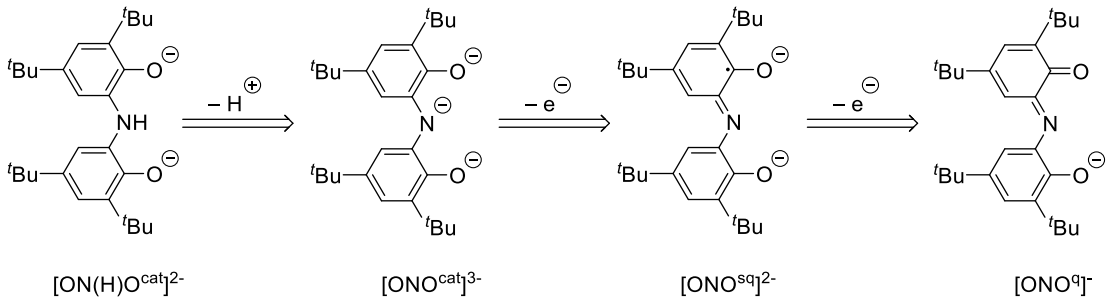
In the previous chapter, synthetic pathways for the preparation of gallium hydride complexes were reported. The use of such compounds in small molecule activation reactions has not been extensively explored, and most of the research carried out to date is centred on simple gallanes such as Ga_2H_6,[1] $HGaCl_2$,[2–6] HGa^tBu_2.[7] Gallium hydrides have been found to react with aldehydes,[8] ketones,[2] and alkenes,[1–3] and alkynes.[3,5,9–12] In 2001, Oshima and co-workers reported the use of $HGaCl_2$ as a radical mediator for the radical cyclization of halo acetals,[13] while the same year, Uhl and co-workers reported on the reaction of C=N double bonds with $GaH_3{\cdot}NMe_2Et$.[14] The activation of carbon dioxide was documented by Aldridge, with β-diketiminato supported gallium hydride complexes.[15,16] Carbon dioxide inserts into the Ga–H bond of (^{Dipp}Nacnac)Ga(^{t}Bu)(H) to afford the formate complex [(^{Dipp}Nacnac)Ga(^{t}Bu){κ^1-OC(O)H}], which can subsequently react with pinacol borane at 60 °C to regenerate the gallium hydride complex (Scheme 2.1).[15] To date, there are a limited number of examples of gallium hydrides being used for the activation of unsaturated C=E (E = C, O, N) bonds, therefore there are opportunities in this field for exploration.[13,15–17]

The use of gallium hydrides in catalytic hydroboration reactions was discussed in the Chapter One.[15,18,19] Catalytic reactions facilitated by gallium hydrides are rare, which is in part related to the unstable nature of these compounds. In view of this, the tridentate pincer ligand *N*,*N*-bis(3,5-di-*tert*-butyl-2-phenoxy)amine ($[ON(H)O]^{2-}$) was used for the stabilisation of reactive gallium hydrides, in order to allow the exploration of the stepwise activation of small molecules in solution.[20]



Scheme 2.1: Selected examples of gallium hydrides and their reactivity.[13,15–17]

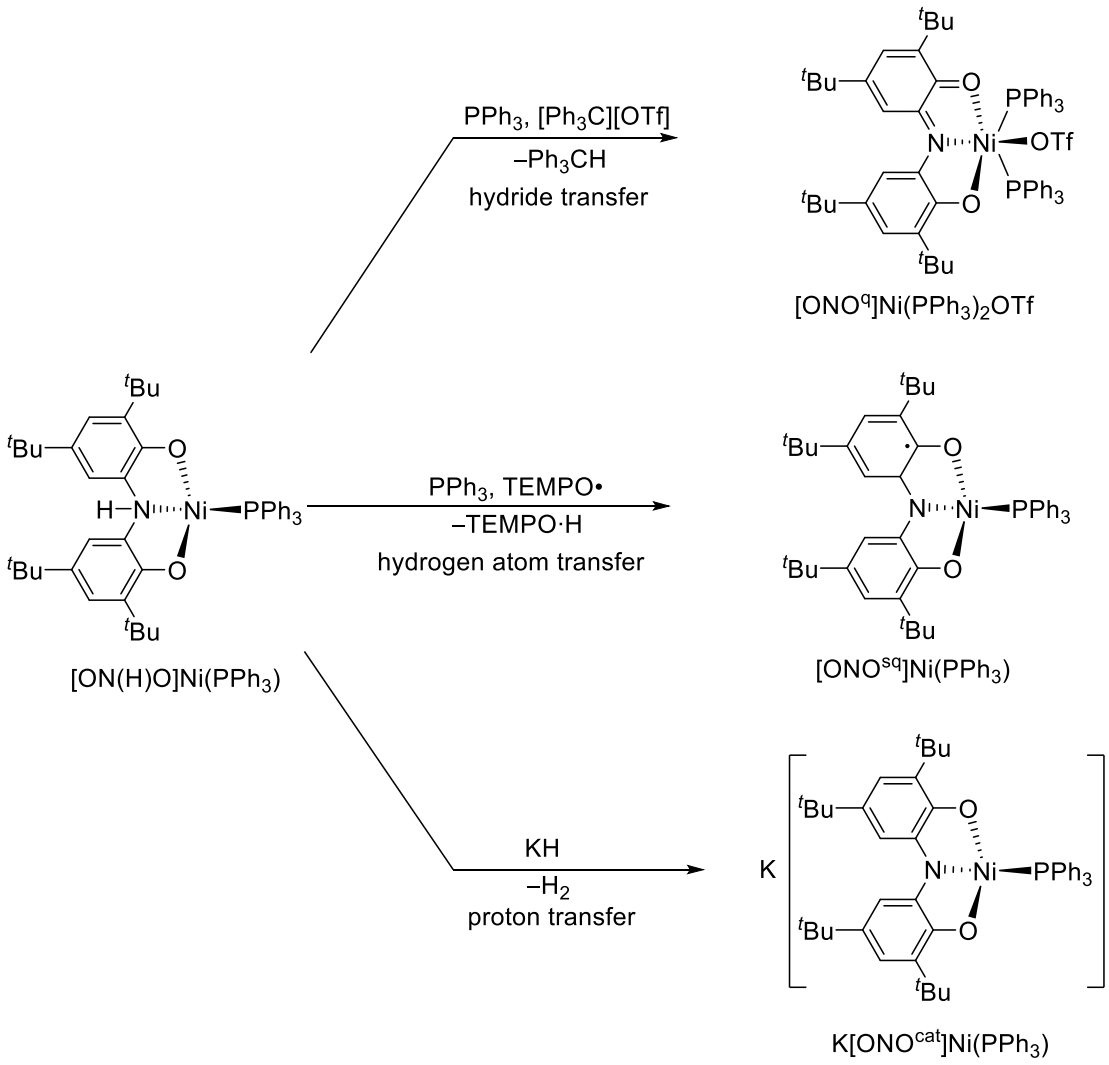
The $[ON(H)O]^{2-}$ is a known redox-active ligand, which has multiple protonation sites and oxidation states. The trianionic $[ONO]^{3-}$ ligand has been shown to act as the catecholate $[ONO^{cat}]^{3-}$, semiquinonato $[ONO^{sq}]^{2-}$ and quinonato $[ONO^{q}]^{-}$ ligand (Scheme 2.2).[21,22]



Scheme 2.2: Different oxidation states of the *N*,*N*-bis(3,5-di-*tert*-butyl-2-phenoxy)amide ligand, including catecholate $[ONO^{cat}]^{3-}$, semiquinonato $[ONO^{sq}]^{2-}$, and quinonato $[ONO^{q}]^{-}$ forms.[21,22]

A recent communication in 2021 demonstrated that the monoprotonated form of this ligand, $[ON(H)O]^{2-}$, can potentially act as a (1) proton, (2) hydrogen atom, or (3)

hydride donor (Scheme 2.3).[23] This multifunctional ligand serves not only to stabilise the metal centre, but it can also be involved in redox chemistry or metal-ligand cooperative reactions. This ligand was thus recognised to be interesting in the context of main-group hydride compounds.



Scheme 2.3: Potential application of the $[ON(H)O]^{2-}$ ligand as a proton, hydride, or hydrogen atom donor.[23]

The $[ON(H)O]^{2-}$ platform has previously been used by Heyduk for the synthesis of aluminium complexes [ON(H)O]Al(Cl)(Et_2O) and [ON(H)O]Al(Br)(THF), via the reaction of $[ON(H)O]M_2$ (M = K, Li) with AlX_3 (X = Cl, Br), respectively.[22] It has

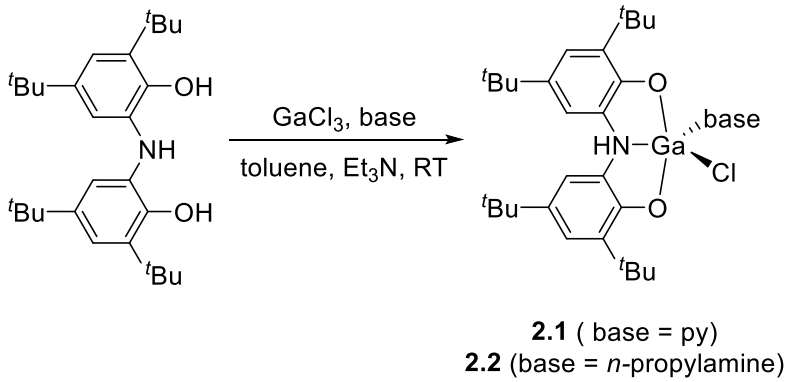
also been used to stabilise other group 13 elements such as boron and gallium, though the resulting compounds were moisture- and air-sensitive, and hence, were not fully characterised.[24]

Inspired by this research, the application of $[ON(H)O^{cat}]^{2-}$ for the synthesis of novel gallium compounds was carried out by previous Goicoechea group members.[20,25] They synthesised a base stabilised gallium chloride complex [ON(H)O]Ga(py)Cl and used it as a precursor for the synthesis of gallium monohydride [ON(H)O]Ga(H)THF·1.5BH_3:py. Preliminary reactivity studies showed that reactions with benzaldehyde and isobutyraldehyde resulted in the dimeric gallium alkoxide complexes $\{[ON(H)O]Ga(OR)\}_2$ (R = CH_2Ph, CH_2CHMe_2). The complex $\{[ON(H)O]Ga(OCH_2Ph)\}_2$ was shown to be an effective catalyst for the hydroboration of aldehydes with pinacol borane as part of preliminary reactivity studies. Unfortunately, both of these two gallium alkoxide complexes are not ideal catalysts. The first gallium alkoxide dimer $\{[ON(H)O]Ga(OCH_2Ph)\}_2$ has poor solubility in benzene, which precluded the preparation of stock solutions with a catalyst concentration greater than 1.0×10^{-3} mol L^{-1}, while the second gallium alkoxide dimer $\{[ON(H)O]Ga(OCH_2CHMe_2)\}_2$ could not be purified from the borane−pyridine adduct introduced from the precursor. The borane−pyridine residue in solution prevents the study of this species in catalytic transformations.[26]

In view of this, different gallium alkoxide complexes were explored, with a particular focus on complexes with good solubility in benzene, and gallium hydride complexes that can be crystallised without any impurities.

2.2 Synthesis of $[ON(H)O]^{2-}$ stabilised gallium chloride complexes

In this section, the synthesis of novel gallium chloride complexes supported by the $[ON(H)O]^{2-}$ ligand is described.



Scheme 2.4: Synthesis of **2.1** and **2.2**.

The reaction of *N*,*N*-bis(3,5-di-*tert*-butyl-2-phenol)amine [H_3(ONO)], $GaCl_3$ and two equivalents of triethylamine in the presence of a base (pyridine or *n*-propylamine) quantitatively affords a single product (Scheme 2.4) as evidenced by a new single ligand environment in their ^{1}H NMR spectra. These compounds exhibit two resonances for the aromatic protons of the ligand backbone (**2.1**: 7.41, 7.22 ppm; **2.2**: 7.39, 7.14 ppm), two signals for the inequivalent *tert*-butyl groups (**2.1**: 1.53, 1.38 ppm; **2.2**: 1.55, 1.36 ppm) and a broad resonance arising from the proton corresponding to the secondary amine of the ligand backbone (**2.1**: 4.61; **2.2**: 4.42 ppm). Single crystal X-ray crystallography unequivocally confirmed the structures of **2.1** and **2.2** (Figure 2.1 and 2.2).

The parameter τ_5 (or τ) was originally proposed by Addison et al. to determine if the centre of a five-coordinate complex is trigonal bipyramidal or square pyramidal.[27] The closer τ_5 is to 1, the more the geometry approaches that of an ideal trigonal bipyramid.

The formula for τ_5 is:

$$\tau_5 = \frac{\beta - \alpha}{60°}$$

where: α and β and are the two greatest valence angles of the coordination centre, and β > α. The X-ray structures reveal that the gallium centres adopt a distorted trigonal bipyramidal shape (**2.1**: τ_5 = 0.76; **2.2**: τ_5 = 0.78), with N1 and N2 in the apical positions.

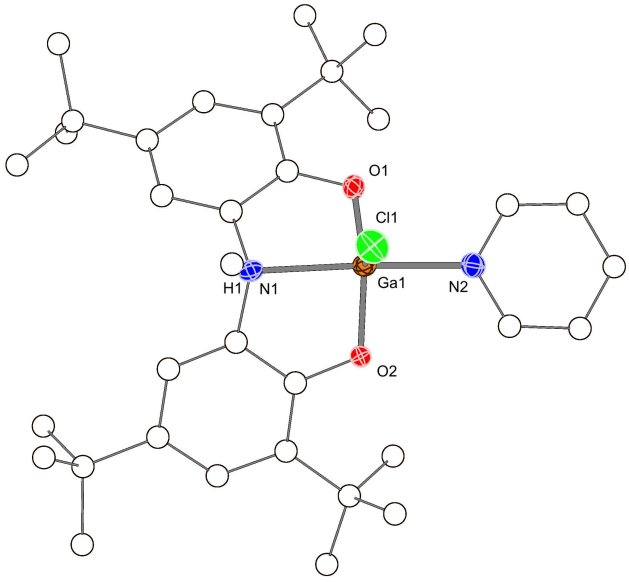


Figure 2.1: Single crystal X-ray structure of **2.1**. Anisotropic displacement ellipsoids set at 50% probability. Hydrogen atoms (with the exception of H1) have been omitted for clarity. All carbon atoms are pictured as spheres of arbitrary radius. Selected interatomic distances [Å] and angles [°]: Ga1–O1 1.8456(9), Ga1–O2 1.8461(9), Ga1–N1 2.1418(11), Ga1–N2 2.0803(11), Ga1–Cl1 2.2073(4); O1-Ga1-O2 122.34(4), O1-Ga1-N2 88.59(4), O2-Ga1-N2 90.15(4), O1-Ga1-N1 84.72(4), O2-Ga1-N1 85.10(4), N2-Ga1-N1 168.03(4), O1-Ga1-Cl1 120.25(3), O2-Ga1-Cl1 117.16(3), N2-Ga1-Cl1 96.35(3), N1-Ga1-Cl1 95.59(3). Symmetry operation ′: 1–*x*, 2–*y* –*z*.

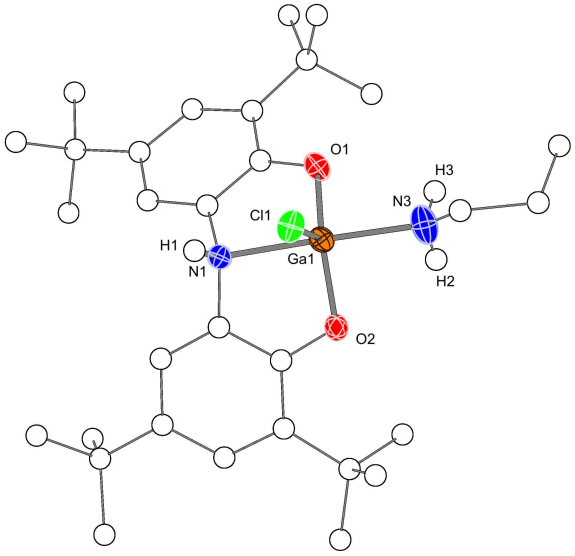


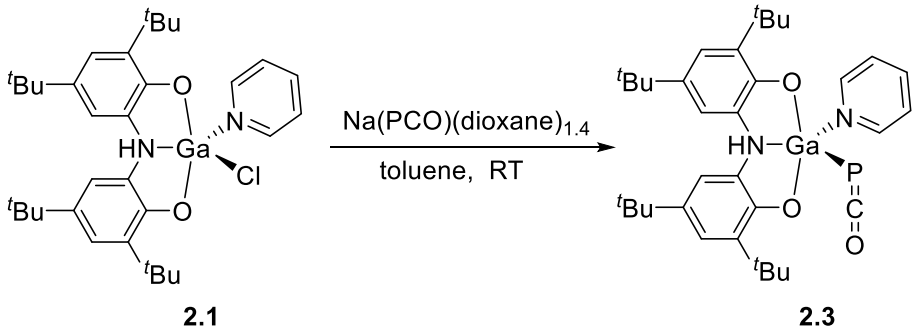
Figure 2.2: Single crystal X-ray structure of **2.2**. Anisotropic displacement ellipsoids set at 50% probability. Hydrogen atoms (with the exception of H1, H2 and H3) have been omitted for clarity. All carbon atoms are pictured as spheres of arbitrary radius. Selected interatomic distances [Å] and angles [°]: Ga1–O1 1.8585(18), Ga1–O2 1.8597(17), Ga1–N1 2.142(2), Ga1–N2 2.044(2), Ga1–Cl1 2.2066(6); O1-Ga1-O2 121.78(9), O1-Ga1-N3 90.08(11), O2-Ga1-N3 90.71(11), O1-Ga1-N1 83.93(8), O2-Ga1-N1 84.36(8), N3-Ga1-N1 168.69(10), O1-Ga1-Cl1 119.72(6), O2-Ga1-Cl1 117.64(6), N3-Ga1-Cl1 98.60(9), N1-Ga1-Cl1 92.69(6).

2.3 Synthesis of gallium phosphaketene complex 2.3

With the ligand stabilised gallium chloride complex **2.1** in hand, simple salt metathesis reactions were explored, to exchange the chloride ion for other pseudohalides. The 2-phosphaethynolate anion, P≡C−O$^-$, is a heavier analogue of cyanate (N≡C−O$^-$). The history of this ion dates back to the early 1990s, when it was first reported by Becker.[28] In recent years it has found an application as a useful phosphorus source after the large scale preparation of [Na(dioxane)$_x$](PCO) (x = 1−3) was reported.[29,30] Salt metathesis reactions of [Na(dioxane)$_x$](PCO) with metal halides were used to incorporate this ion into the coordination sphere of group 13 elements such as boron,[31,32] aluminium,[33]

and gallium.[33,34] With this in mind, the reactivity of **2.1** towards [Na(dioxane)$_x$](PCO) was tested. The resulting product would bear either a phosphorus-bonded, Ga−P=C=O, or oxygen-bonded, Ga−O−C≡P, phosphaethynolate moiety. These species can be distinguished by characteristic $^{31}P\{^1H\}$ NMR and $^{13}C\{^1H\}$ NMR resonances.

Reaction of **2.1** and sodium phosphaethynolate, [Na(dioxane)$_{1.4}$](PCO), in toluene quantitatively affords a yellow solid **2.3** as the product (Scheme 2.5).



2.1 **2.3**

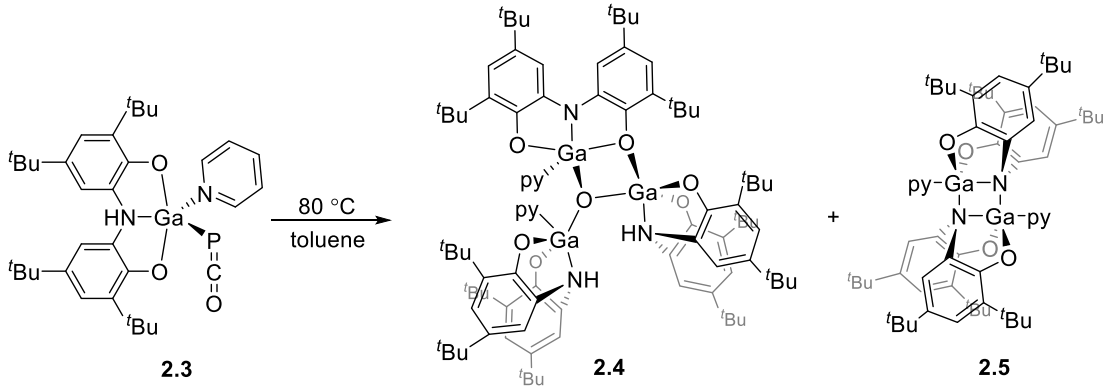
Scheme 2.5: Synthesis of **2.3**.

The $^{31}P\{^1H\}$ NMR spectrum of **2.3** reveals a singlet resonance at −374.0 ppm, which is in the same range as a salen ligand stabilised gallium phosphaketene complex reported by Grützmacher (−376.9 ppm).[33] The successful formation of a Ga−P=C=O complex was further demonstrated by the appearance of a new resonance in the $^{13}C\{^1H\}$ NMR spectrum at 182.56 ppm, which occurs as a doublet ($^1J_{C-P}$ = 94.7 Hz). This is comparable to the values reported by Grützmacher for (salen)Ga−P=C=O ($^{13}C\{^1H\}$: 182.5 ppm; $^1J_{C-P}$ = 88.2 Hz).[33] The ^1H NMR resonances for the aromatic protons of the ligand backbone do not differ from **2.1** (**2.1**: 7.41, 7.22 ppm; **2.3**: 7.40, 7.28 ppm). The ^1H NMR spectrum also reveals two signals for **2.3** at 1.54, 1.38 ppm for the *tert*-butyl groups and a broad resonance at 4.29 ppm of the secondary amine of the ligand backbone. DFT calculations at the 6-311+g(d,p)/PBE1PBE1 level of theory predict a ^{31}P NMR chemical shift at −364.0 ppm, which matches the experimental value. Despite

these successful results, a single-crystal X-ray structure for compound **2.3** has not been obtained.

2.4 Reactivity of the gallium phosphaethynolate complex

The thermal stability of **2.3** was tested to see whether it would undergo thermal decarbonylation. On heating **2.3** at 80 °C overnight in a toluene solution, the colour of the solution changed from yellow to orange (Scheme 2.6). This was accompanied by the formation of pale-yellow crystals. It is worth noting that from an NMR tube scale test reaction in C_6D_6, the formation of phosphine (PH_3) was observed in ^{31}P NMR spectrum, as a distinctive quartet signal at −242.0 ppm ($^1J_{P–H}$ = 187.8 Hz).



Scheme 2.6: Synthesis of **2.4** and **2.5**.

After separation of the precipitate (**2.5**; pale-yellow crystals) from the solution, the solution was dried to afford an orange solid, **2.4**. Recrystallisation of the orange solid from a concentrated toluene/pentane solution gave orange single crystals suitable for XRD characterisation (Figure 2.3). The structure of 2.4 reveals that three gallium-containing units, [ONO^{cat}]Ga(py), [ON(H)O]Ga and [ON(H)O]Ga(py) are linked through a trivalent oxygen centre. The bond length Ga3−N3 (1.8703(15) Å) in the [ONO^{cat}]Ga(py) unit is shorter than the Ga1−N1 bond (2.1484(15) Å) in the

[ON(H)O]Ga unit, and the Ga2−N2 (2.1588(15) Å) length in the [ON(H)O]Ga(py) unit, as the latter two bonds are dative bond interactions. The sum of the bond angles (°) Ga1-O7-Ga2 128.97(7), Ga1-O7-Ga3 102.39(6) and Ga2-O7-Ga3 127.44(7) is 358.8 degrees, which indicates the three gallium atoms are very close to coplanarity with the centre oxygen atom O7.

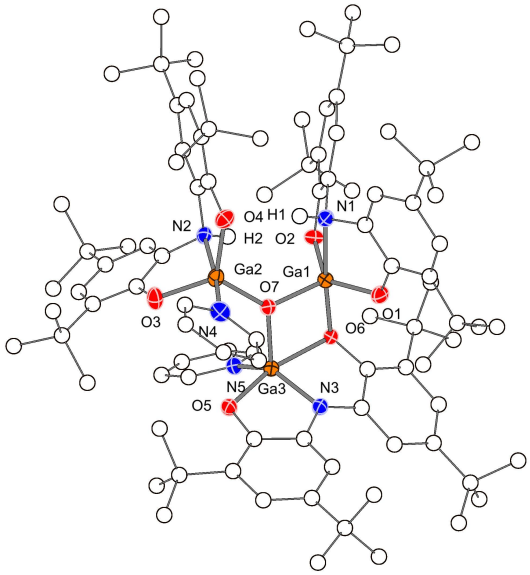


Figure 2.3: Single crystal X-ray structure of **2.4**. Anisotropic displacement ellipsoids set at 50% probability. Hydrogen atoms (with the exception of H1 and H2) have been omitted for clarity. All carbon atoms are pictured as spheres of arbitrary radius. Selected interatomic distances [Å] and angles [°]: Ga1–O1 1.8469(13), Ga1–O2 1.8651(13), Ga1–O6 1.9631(12), Ga1–O7 1.8931(12), Ga2–O3 1.8527(14), Ga2–O4 1.8716(13), Ga2–O7 1.8515(12), Ga3–O5 1.9058(13), Ga3–O6 2.1534(12), Ga3–O7 1.8780(12), Ga1–N1 2.1484(15), Ga2–N2 2.1588(15), Ga2–N4 2.0520 (17), Ga3–N3 1.8703(15), Ga3–N5 1.9994 (16); O1-Ga1-O2 131.49 (6), O1-Ga1-O6 92.24(5), O1-Ga1-O7 118.51(6), O2-Ga1-O6 97.05(5), O2-Ga1-O7 109.71(6), O6-Ga1-O7 84.88(5), O1-Ga1-N1 83.76 (6), O2-Ga1-N1 84.24 (6), O6-Ga1-N1 175.56 (6), O7-Ga1-N1 98.70 (6), O3-Ga2-O4 118.99(6), O3-Ga2-N2 83.63(6), O3-Ga2-N4 93.46(6), O4-Ga2-N2 83.80(6), O4-Ga2-N4 90.99(6), O7-Ga2-N2 92.51(6), O7-Ga2-N4 95.51(6), O7-Ga2-O3 121.86(6), O7-Ga2-O4 118.14(6), N3-Ga3-O5 87.30(6), N3-Ga3-N5 133.98(7), N3-Ga3-O6 79.35(6), N3-Ga3-O7 116.48(6), O5-Ga3-O7 107.72(6), O6-Ga3-O7 80.11(5), N5-Ga3-O5 97.95(6), O5-Ga3-O6 166.55(5), N5-Ga3-O7 105.34(6), Ga1-O7-Ga2 128.97(7), Ga1-O7-Ga3 102.39(6), Ga2-O7-Ga3 127.44(7).

The ^{1}H NMR spectrum of **2.4** in C_6D_6 exhibits six resonances for the aromatic protons of the ligand backbone [7.43 (two resonances overlapped), 7.35, 7.27, 7.09, 7.04 ppm], six signals for the inequivalent *tert*-butyl groups (1.84, 1.62, 1.56, 1.25, 1.23 and 1.17 ppm), which further supports the molecular structure of **2.4** as determined by X-ray diffraction. Compound **2.4** has good solubility in non-polar solvents such as hexane, benzene, toluene, which is in contrast to the poor solubility of complex **2.5** in both polar and non-polar solvents. This enabled us to separate these two compounds.

The ^{1}H NMR spectrum of **2.5** in $CDCl_3$ shows two doublet signals for the aromatic protons of the ligand backbone (6.89, 6.78 ppm), coordinated pyridine (9.11, 8.19, 7.70 ppm), and *tert*-butyl resonances (1.17, 1.16 ppm). No resonance was observed for the amine of the ligand backbone.

Single crystal X-ray crystallographic analysis reveals that **2.5** is a five-coordinate distorted trigonal bipyramidal gallium complex, with an *N*,*N*-bis(3,5-di-*tert*-butyl-2-phenoxy)amide ligand and a coordinated pyridine (Figure 2.4). This species forms a dimer through dative N−Ga bond interactions between two [ONO]Ga(py) units.

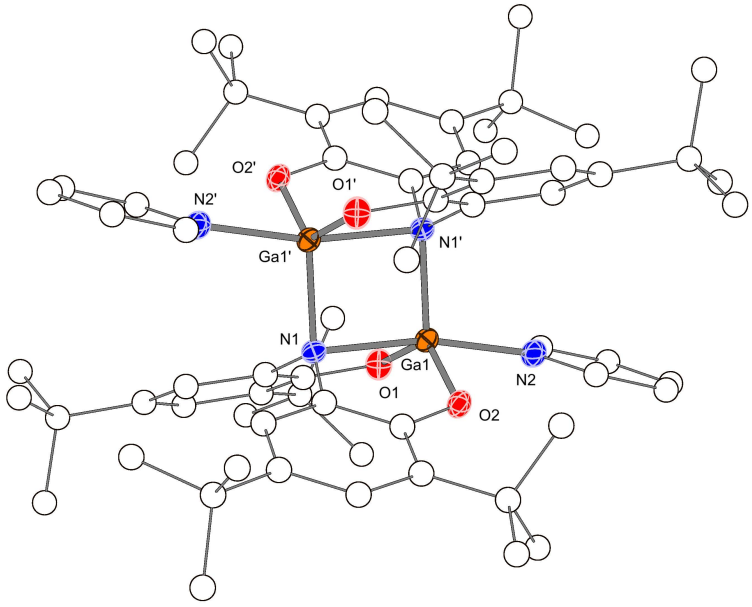
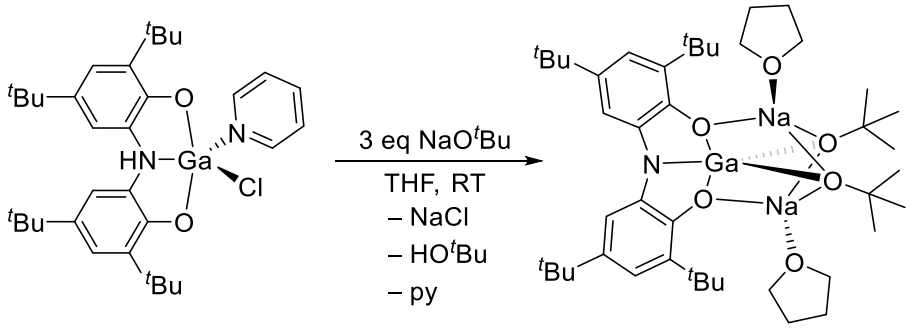


Figure 2.4: Single crystal X-ray structure of **2.5**. Anisotropic displacement ellipsoids set at 50% probability. Hydrogen atoms have been omitted for clarity. All carbon atoms are pictured as spheres of arbitrary radius. Selected interatomic distances [Å] and angles [°]: Ga1–O1 1.8454(11), Ga1–O2 1.8470(11), Ga1–N1[1] 1.9592(12), Ga1–N2 2.0819(13), Ga1–N1 2.1334(12); O1-Ga1-O2 130.05(5), O1-Ga1-N1[1] 113.63(5), O2-Ga1-N1[1] 114.77(5), O1-Ga1-N2 90.83(5), O2-Ga1-N2 89.08(5), O1-Ga1-N1 85.17(5), O2-Ga1-N1 84.99(5), N1[1]-Ga1-N1 87.84(5), N2-Ga1-N1 168.14(5).

2.5 Salt metathesis reactions of 2.3

Following the successful synthesis of gallium phosphaethynolate complex **2.3**, other salt metathesis reactions of **2.1** were explored.

In an attempt to synthesise gallium alkoxide complexes, commercially available metal alkoxides were used for salt metathesis reactions. The reaction of **2.1** and an excess of sodium *tert*-butoxide in THF solution, affords complex **2.6** as yellow solid (Scheme 2.7).



2.1 **2.6**

Scheme 2.7: Synthesis of **2.6**.

X-ray quality yellow crystals were obtained from a concentrated pentane solution at room temperature (Figure 2.5). Single crystal X-ray crystallography analysis confirms that **2.6** is a trimetallic gallium-ate complex with a geometrically constrained amide ligand backbone, in which the gallium is coplanar with the $[ONO^{cat}]^{3-}$ ligand. The two sodium atoms in **2.6** adopt distorted tetrahedral geometries and are coordinated by the oxygen atoms of the $[ONO^{cat}]^{3-}$ and alkoxide ligands, and THF. The gallium atom adopts a distorted trigonal bipyramidal structure, with the O1-Ga1-O2 bond angle of 166.37(13)°, deviating by 13.67° from the value expected for an ideal trigonal bipyramid. As a strong base, NaO^{t}Bu has deprotonated the proton of the ligand backbone to give $[ONO^{cat}]^{3-}$. This is accompanied by a shortening of the Ga1−N1 bond length (1.878(4)Å), compared to the dative Ga1−N1 bond in **2.1** (2.142(1)Å). The ^{1}H NMR spectrum of **2.6** reveals resonances attributed to the aromatic protons of the ligand backbone at 8.38, 7.13 ppm; two resonances for the *tert*-butyl groups of the ligand at 1.74, 1.67 ppm; and a singlet resonance from the *tert*-butoxide ions at 1.00 ppm. Two further resonances for the coordinated THF molecules are observed at 3.41 and 1.32 ppm, which differ from those of free THF (3.57, 1.40 ppm).

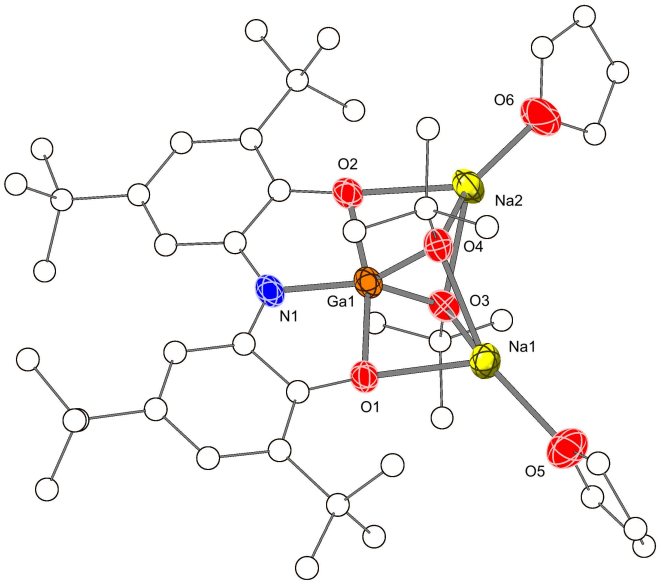
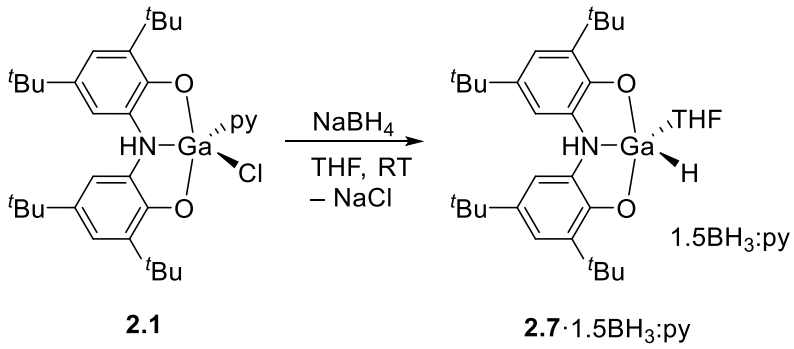


Figure 2.5: Single crystal X-ray structure of **2.6**. Anisotropic displacement ellipsoids set at 50% probability. Hydrogen atoms have been omitted for clarity. All carbon atoms are pictured as spheres of arbitrary radius. Selected interatomic distances [Å] and angles [°]: Ga1–O1 1.983(3), Ga1–O2 1.986(3), Ga1–N1 1.878(4), Ga1–O3 1.893(3), Na1–O1 2.300(4), Na1–O3 2.387(4); O1-Ga1-O2 166.37(13), O1-Ga1-N1 82.90(15), O1-Ga1-O3 94.24(13), O3-Ga1-N1 139.65(17), O2-Ga1-N1 83.66(16), O3-Ga1-O4 85.23(13), Ga1-O1-Na1 81.53(12), Ga1-O3-Na1 81.09(12), Na1-O3-Na2 105.46(15), O1-Na1-O5 124.39(16), O3-Na1-O5 137.52(15).

Evidently, alkali metal alkoxide compounds are too basic to retain the NH proton of the ligand backbone, therefore an alternative pathway to gallium alkoxide complexes is needed.

As mentioned earlier, previous members of the Goicoechea group have shown that reaction of **2.1** with excess $NaBH_4$ in THF at room temperature affords a novel gallium hydride (**2.7**·1.5BH_3:py) in which the nitrogen atom on the ligand backbone remains protonated (Scheme 2.8).[20,25] This product was purified by recrystallisation from a toluene/pentane mixture. The ^{1}H NMR spectrum of this compound reveals two sets of resonances for the aromatic and *tert*-butyl protons (ArH: 7.35, 7.20 ppm; ^{t}Bu: 1.59, 1.35 ppm) and a broad resonance for the amine proton at 4.01 ppm. In addition, a broad

resonance corresponding to the Ga−H is observed at 5.67 ppm. The Ga1−H1 bond is 1.55 (4) Å, and the hydrogen atom was observable in the crystallographic Fourier difference map (Figure 2.6). These data are comparable to Aldridge's gallium hydride (^{Dipp}Nacnac)Ga(^{t}Bu)(H), which has a Ga−H resonance at 5.44 ppm in the ^{1}H NMR spectrum and a Ga−H bond length of ~1.49 Å (no estimated standard deviation available).



Scheme 2.8: Synthesis of **2.7**·1.5BH_3:py.[20,25,35]

The ^{1}H NMR spectrum of **2.7**·1.5BH_3:py also indicates the presence of the borane-pyridine adduct, exhibiting a 1:1:1:1 intensity quartet at 3.49 ppm ($^{1}J_{B-H}$ = 99 Hz), while the ^{11}B NMR spectrum reveals a multiplet at –10.7 ppm, which collapses to a singlet upon proton decoupling. This adduct is also present in the single crystal X-ray structure of **2.7**·1.5BH_3:py which reveals 1.5 equivalents of BH_3:py in the asymmetric unit. It was shown that the hydridic hydrogen atom on BH_3 is interacting with the protic N−H on the ligand backbone of **2.7** with a distance of 2.002(4) Å (Figure 2.6). Despite repeated recrystallisation attempts we were unable to separate BH_3:py from the gallium hydride **2.7**. From the short B−H···H−N interaction observed in the crystal structure, it is possible that this interaction is preventing separation.

Compound **2.7** is an interesting species as it contains a hydridic Ga−H bond in close proximity to an acidic N−H bond in the ligand backbone. Related amine gallane compounds are scarce due to their propensity to eliminate dihydrogen, although a number of examples have been isolated and structurally characterised.[36–42]

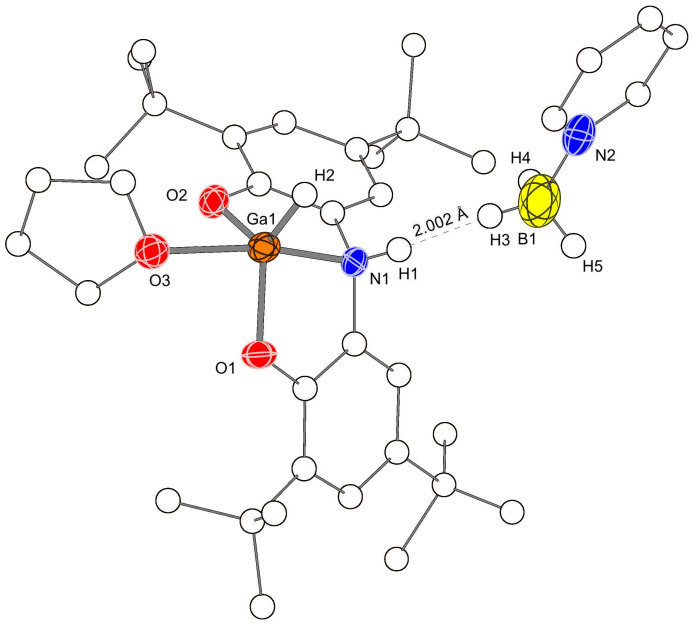
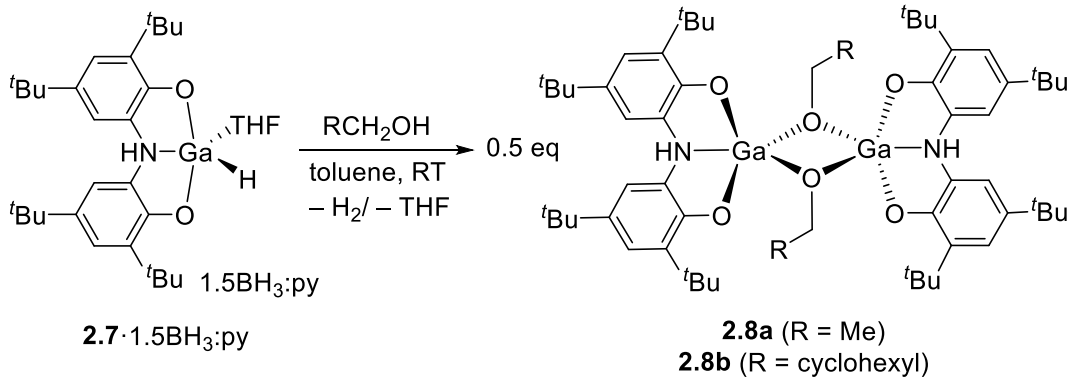


Figure 2.6: Single crystal X-ray structure of **2.7**·1.5BH_3:py. Anisotropic displacement ellipsoids set at 50% probability. Hydrogen atoms (with the exception of H1, H2, H3, H4 and H5) have been omitted for clarity. All carbon atoms are pictured as spheres of arbitrary radius. Selected interatomic distances [Å] and angles [°]: Ga1–O1 1.853(2), Ga1–O2 1.870(2), Ga1–O3 2.145(2), Ga1–N1 2.151(3), O1-Ga1-O2 121.24(10), O1-Ga1-N1 85.05(8), O1-Ga1-O2 113.37(10), O1-Ga1-O3 86.30(10), O2-Ga1-O3 86.37(9), O1-Ga1-N1 84.59(10), O2-Ga1-N1 83.27(9), O3-Ga1-N1 162.21(9).

2.6 Dehydrocoupling of 2.7 and alcohols

In Section 2.5, the reaction of **2.1** with NaO^tBu was shown to give a trimetallic complex **2.6** instead of a dimeric gallium alkoxide. This prompted us to explore whether the reaction of alcohols with **2.7** could be a new strategy for the synthesis of gallium alkoxide complexes.



Scheme 2.9: Reaction of **2.7**·1.5BH_3:py with alcohols to afford **2.8a** and **2.8b**.

Reaction of **2.7**·1.5BH_3:py with ethanol and cyclohexylmethanol afforded dimeric gallium alkoxide compounds **2.8a** and **2.8b**, respectively (Scheme 2.9). The ^{1}H NMR spectra of these compounds do not differ greatly from **2.1** and reveal the characteristic broad resonance corresponding to the amine backbone of the *N*,*N*-bis(3,5-di-*tert*-butyl-2-phenoxy)amine ligand at 5.05 and 4.97 ppm for **2.8a** and **2.8b** in $CDCl_3$, respectively. The ^{1}H NMR spectra also show two doublet signals for ligand backbone (**2.8a**: 7.56, 7.22 ppm; **2.8b**: 7.52, 7.21 ppm), *tert*-butyl groups (**2.8a**: 1.68−1.25 ppm; **2.8b**: 1.39, 1.33 ppm), and a resonance arising from the methylene group of the alkoxide (**2.8a**: 4.11 ppm; **2.8b**: 3.82 ppm). The use of ethanol plays a pivotal role here, as it effectively dissolves the unreacted pyridine-borane (and reacts with the borane slowly affording a borate ester).[43] This allowed us to obtain the product without any impurities. Complex **2.8a** has good solubility in benzene, toluene and chloroform, and poor solubility in ethanol, hexane and pentane. The solubility of **2.8a** makes it feasible for us to prepare a high concentration solution of **2.8a** in C_6D_6 as a stock solution for further catalysis studies (see Chapter Three).

Both samples were characterised by single crystal X-ray crystallographic analysis, confirming dimeric structures bridged by two μ_2-OCH_2R ligands. The crystal structures

of **2.8a** and **2.8b** are shown in Figures 2.7 and 2.8. The gallium (III) centres in both are five-coordinate with distorted pentagonal bipyramidal geometries (**2.8a**: $\tau_5 = 0.96$, **2.8b**: $\tau_5 = 0.84$) with N1 and O3 occupying the apical positions. The Ga1−O3′ (1.878(2) Å) bond length is shorter than that of Ga1−O3 (1.960(2) Å), presumably due to the fact that the second gallium−oxygen bond is a dative interaction rather than a σ-bond.

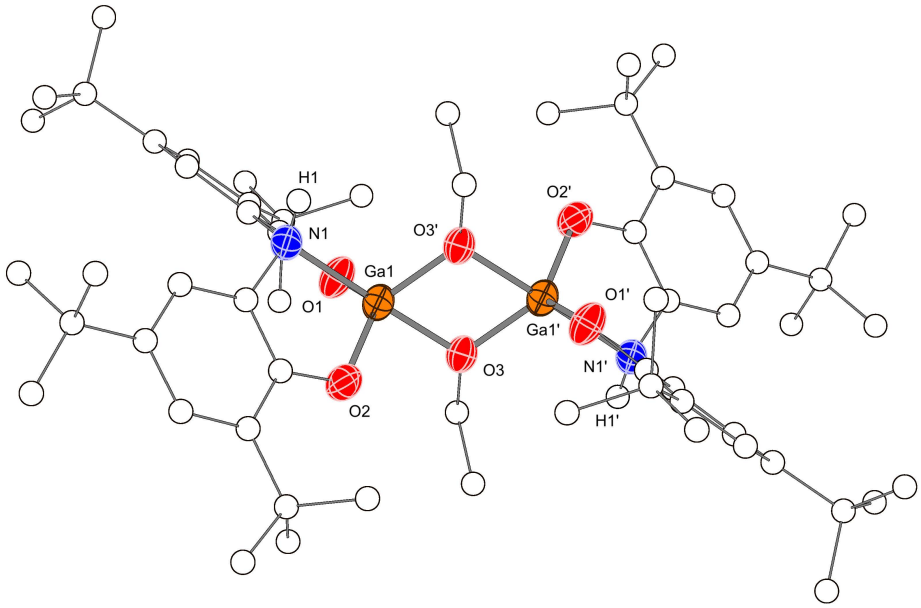


Figure 2.7: Single crystal X-ray structure of **2.8a**. Anisotropic displacement ellipsoids set at 50% probability. Hydrogen atoms (with the exception of H1 and H1′) have been omitted for clarity. All carbon atoms are pictured as spheres of arbitrary radius. Selected interatomic distances [Å] and angles [°]: Ga1–O1 1.838(2), Ga1–O2 1.836(2), Ga1–N1 2.149(2), Ga1–O3 1.960(2), Ga1–O3′ 1.878(2); O1-Ga1-O2 121.24(10), O1-Ga1-N1 85.05(8), O1-Ga1-O3 94.43(8), O1-Ga1-O3′ 117.99(9), O2-Ga1-N1 85.20(8), O2-Ga1-O3 96.15(8), O2-Ga1-O3′ 120.76(9), N1-Ga1-O3 178.63(7), N1-Ga1-O3′ 100.89(8), O3-Ga1-O3′ 78.22(8). Symmetry operation ′: 1–*x*, 2–*y* –*z*.

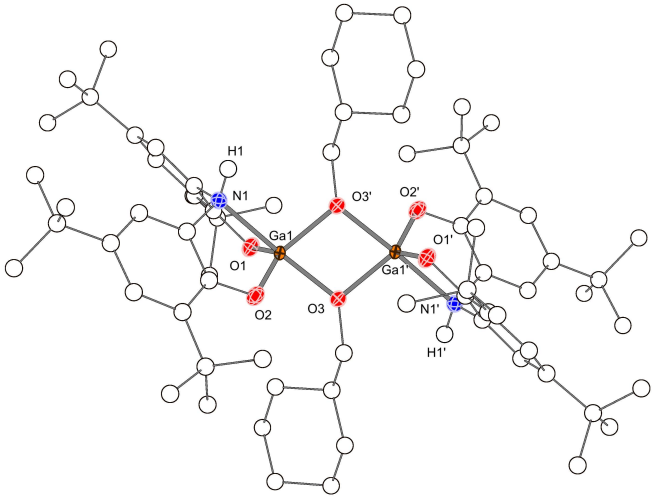


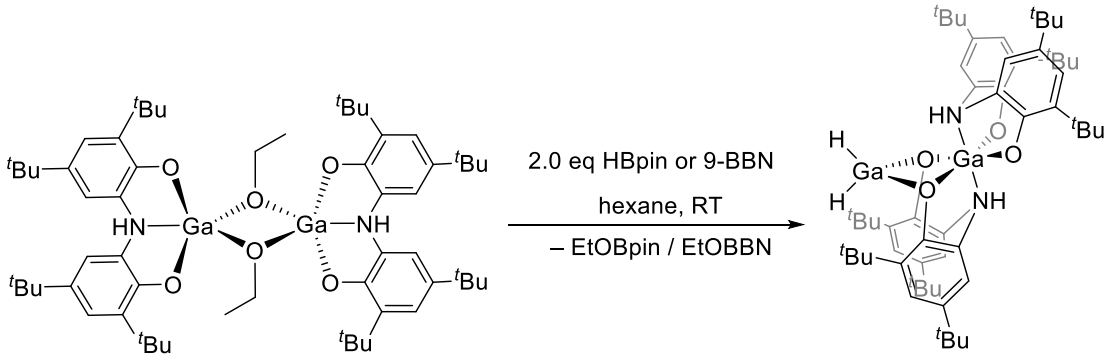
Figure 2.8: Single crystal X-ray structure of **2.8b**. Anisotropic displacement ellipsoids set at 50% probability. Hydrogen atoms (with the exception of H1 and H1′) have been omitted for clarity. All carbon atoms are pictured as spheres of arbitrary radius. Selected interatomic distances [Å] and angles [°]: Ga1–O1 1.8417(14), Ga1–O2 1.8466(14), Ga1–O3 1.9006(13), Ga1–O3′ 1.9612(13), Ga1–N1 2.1366(16); O1-Ga1-O2 125.64(6), O1-Ga1-O3 110.83(6), O2-Ga1-O3 123.40(6), O1-Ga1-O3′ 98.24(6), O2-Ga1-O3′ 94.69(6), O3-Ga1-O3′ 79.69(6), O1-Ga1-N1 85.30(6), O2-Ga1-N1 84.65(6), O3-Ga1-N1 97.38(6), O3′ -Ga1-N1 176.02(6), O1-Ga1-Ga1′ 108.83(4), O2-Ga1-Ga1′ 114.01(4), O3-Ga1-Ga1′ 40.60(4), O3′ -Ga1-Ga1′ 39.09(4), N1-Ga1-Ga1′ 137.92(5). Symmetry operation ′: 1–*x*, 2–*y* –*z*.

2.7 Reaction of 2.8a with boranes

In Chapter One, a documented synthetic strategy for gallium−hydride bond formation was reported. Aldridge and co-workers suggested that reaction of a gallium formate complex with pinacol borane could give a gallium hydride as the product.[15] This led us to explore whether Ga−O/B−H σ-bond metathesis could be used as a general approach for gallium−hydride bond formation. With the alkoxide-bridged dimer **2.8a** in hand, we decided to explore its reactivity towards boranes.

Stoichiometric reactions of **2.8a** with two equivalents of HBpin or one equivalent of the 9-borabicyclo[3.3.1]nonane (9-BBN) dimer in C_6D_6 were monitored by ^{1}H NMR

spectroscopy (Scheme 2.10), which suggested full consumption of **2.8a** within 5 minutes when employing HBpin (or 24 hours when using 9-BBN dimer). Both reactions give rise to the same product, **2.9**.



2.8a **2.9**

Scheme 2.10: Synthesis of **2.9**.

Recrystallisation of **2.9** from toluene at −30 °C afforded crystals suitable for a single-crystal X-ray diffraction. The analysis confirms that, in the solid state, compound **2.9** consists of two gallium atoms linked by two μ_2-O bridging atoms, with one (Ga1) in a tetrahedral geometry and one (Ga2) in a distorted octahedral shape (Figure 2.9). The Ga1−H1 (1.49(4) Å) and Ga1−H2 (1.48(3) Å) bond distances are similar to the gallium−hydride bond in **2.7**·1.5BH_3:py (Ga−H 1.55(4) Å)and (^{Dipp}Nacnac)Ga(^{t}Bu)(H) (Ga−H ca. 1.49 Å).[15]

The formation of this unique structure is most likely due to the absence of a basic donor in the solution, and we will discuss the monomerization of **2.9** with bases in Section 2.10. This is also a rare case of an isolable gallium dihydride complex. Other related examples of gallium dihydrides with amine ligand backbones such as $[H_2Ga(NH_2R)_2]Cl$ (R = Me, ^{i}Pr, ^{t}Bu, ^{s}Bu), were previously reported by Downs in 2005.[37]

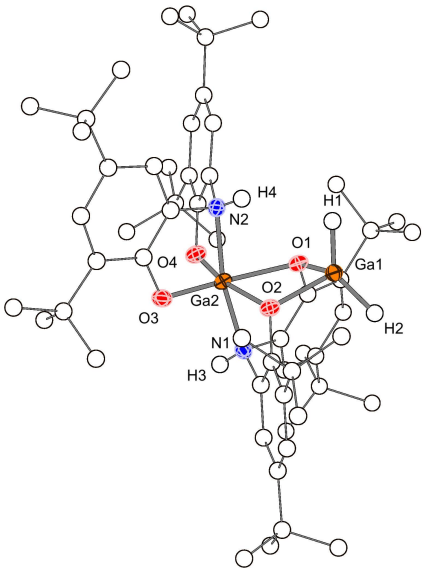


Figure 2.9: Single crystal X-ray structure of **2.9**. Anisotropic displacement ellipsoids set at 50% probability. Hydrogen atoms (with the exception of H1, H2, H3, H4) have been omitted for clarity. All carbon atoms are pictured as spheres of arbitrary radius. Selected interatomic distances [Å] and angles [°]: Ga1–O1 1.9278(19), Ga1–O2 1.951(2), Ga2–O3 1.872(2), Ga2–O4 1.883(2), Ga2–N1 2.045(2), Ga2–N2 2.053(2), Ga2–O2 2.0852(19), Ga2–O1 2.1311(19); O1-Ga1-O2 84.88(8), O3-Ga2-O4 101.22(9), O3-Ga2-N1 102.18(9), O4-Ga2-N1 95.63(9), O3-Ga2-N2 87.97(9), O4-Ga2-N2 86.35(9), N1-Ga2-N2 169.02(10), O3-Ga2-O2 92.02(8), O4-Ga2-O2 166.76(8), N1-Ga2-O2 81.71(9), N2-Ga2-O2 93.89(9), O3-Ga2-O1 168.18(8), O4-Ga2-O1 90.04(8), N1-Ga2-O1 80.06(9), N2-Ga2-O1 89.16(8), O2-Ga2-O1 76.73(7).

The solution behavior of compound **2.9** is intriguing, as a compositionally pure sample of **2.9** was found to have four possible isomers by ^{1}H NMR spectroscopy in C_6D_6 (Figure 2.10). The spectrum reveals four sets of resonances for the amine proton of the ligand backbone [4.02 (**I**), 4.56 (**III**), 4.67 (**III**), 4.70 (**IV**), 4.82 (**II**) and 5.11 (**II**) ppm] as well as GaH resonances at 5.55 (**I**), 5.80 (**III**), 5.86 (**II**), 5.90 (**III**), 5.94 (**II**), 6.50 (**IV**), 6.62 (**IV**) ppm.

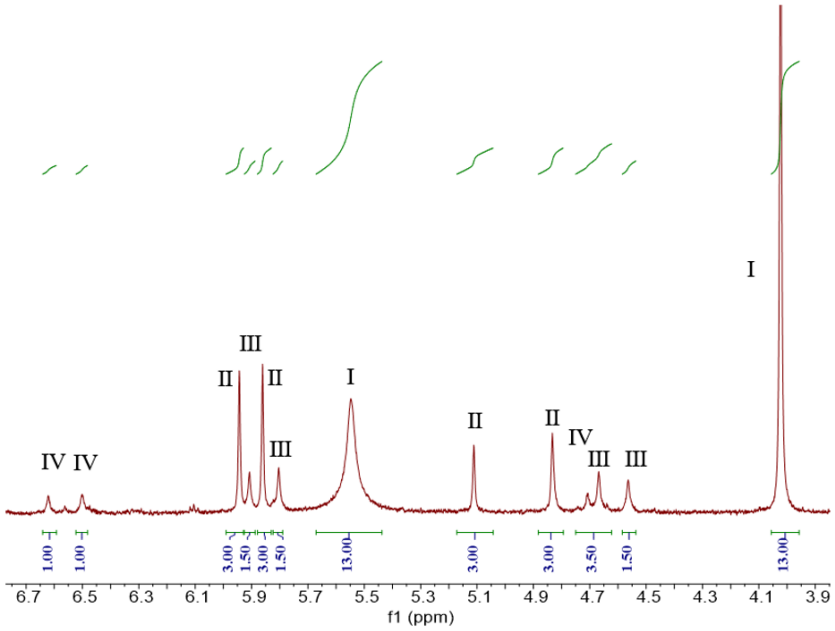


Figure 2.10: Excerpt from the ^{1}H NMR spectrum of complex **2.9** in C_6D_6.

Several attempts were made to recrystallise other isomers from solution, however, only the structure shown in Figure 2.9 could be acquired.

2.8 Application of NMR techniques in the characterisation of 2.9

NOESY NMR experiments (Nuclear Overhauser Effect Spectroscopy) are used to show through-space interactions within a molecule, and they are frequently used to detect chemical or conformational exchange.[44] In an attempt to clarify the structures of the isomers of **2.9** in solution, one-dimensional ^{1}H NOESY and two-dimensional ^{1}H–^{1}H NOESY experiments were carried out on a C_6D_6 solution of the compound.

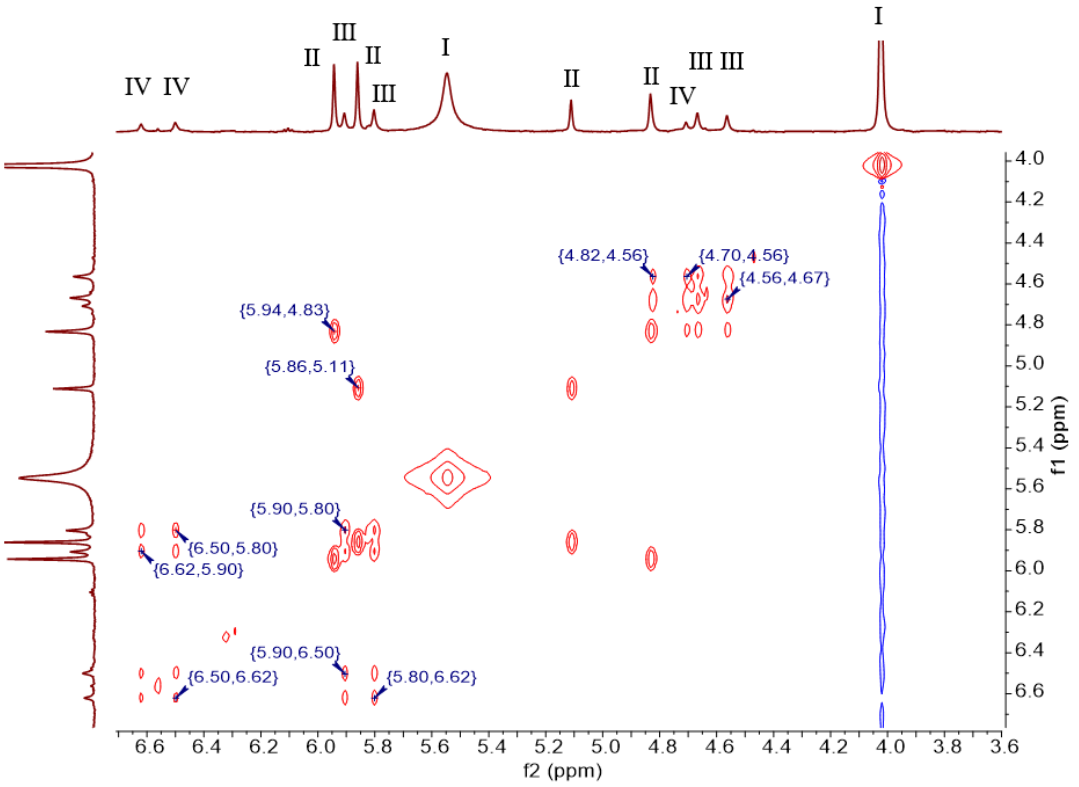


Figure 2.11: 2D NOESY of **2.9** in C_6D_6.

The exchanging peaks shown above (Figure 2.11) are listed in Table 2.1.

Table 2.1: Exchanging peaks and assignment of 2D NOESY of **2.9** in C_6D_6.

Entry	f2 (ppm)	Isomer	f1 (ppm)	Isomer
1	6.62	IV	6.50	IV
2	6.62	IV	5.90	III
3	6.50	IV	5.80	III
4	5.94	II	4.83	II
5	5.90	III	5.80	III
6	5.90	III	6.50	IV
7	5.86	II	5.11	II
8	5.80	III	6.62	IV
9	4.82	II	4.67	III
10	4.82	II	4.56	II
11	4.70	IV	4.67	III
12	4.70	IV	4.56	II
13	4.56	III	4.67	III

Irradiation of the NH resonance corresponding to **2.9**$_{\mathbf{I}}$ at 4.02 ppm with a mixing time of 0.1s, shows that the NH peak is exchanging with NH peaks of **2.9**$_{\mathbf{II}}$ and **2.9**$_{\mathbf{III}}$ at 4.82

(**II**) and 4.56 and 4.67 (**III**), respectively (Figure 2.12). The NH resonance of **2.9$_{I}$** at 4.02 ppm has NOE signals with ArH peaks of **2.9$_{I}$** at 7.03 ppm and *tert*-butyl peaks at 1.30 and 1.58 ppm.

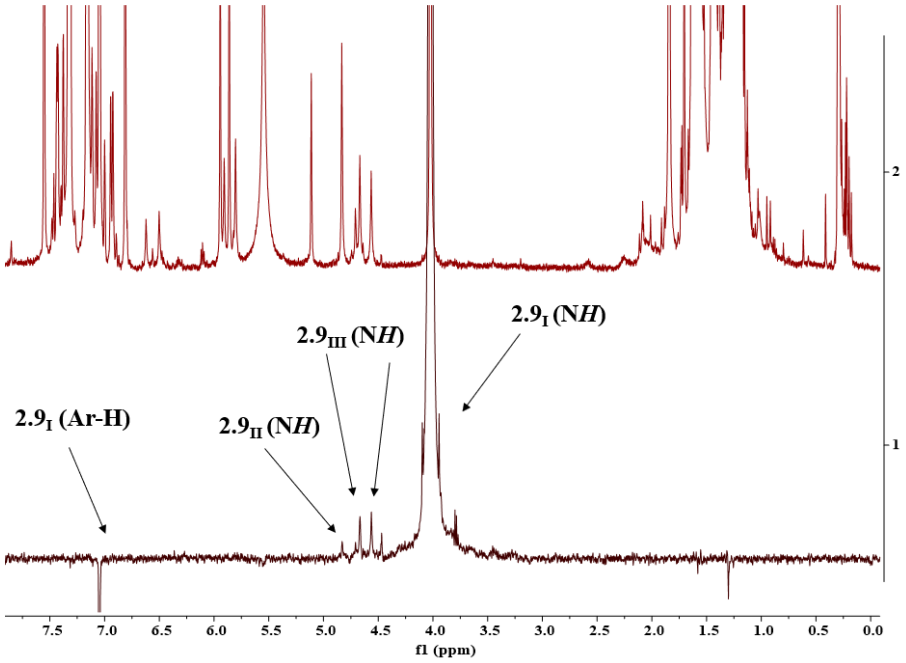


Figure 2.12: One-dimensional selective gradient NOESY of **2.9** in C_6D_6.

The ^{1}H NMR spectrum of **2.9$_{I}$** is largely similar to the monomeric gallium hydride **2.7**, with two aromatic resonances for the ligand backbone (7.32, 7.05 ppm), a broad peak for the gallium hydride (5.55 ppm), a signal attributed to N−H (4.02 ppm), and two inequivalent *tert*-butyl signals (1.58, 1.30 ppm). The ^{13}C{H} NMR spectrum is in agreement with the ^{1}H NMR spectrum: the main species **2.9$_{I}$** has six different resonances (155.59, 138.96, 138.57, 131.25, 123.50 and 118.76 ppm), which account for a highly symmetrical ligand backbone, and four *tert*-butyl peaks (35.72, 34.36, 31,84 and 29.54 ppm). It is worth noting that some resonances attributed to the minor products are also observed, but could not be properly assigned due to their low intensity.

Variable-temperature NMR studies of **2.9** were carried out in toluene-d_8, because it has a wider liquid-phase temperature range (−95 to 110.6 °C) under atmospheric pressure (Figures 2.13−2.14).

This variable-temperature NMR study indicates that the ratio of compound **2.9$_{\mathrm{I}}$** to other isomers increases when the temperature is gradually increased above 298 K, and that it is reversible once the solution is cooled back to room temperature (i.e. the other isomers appear in the same ratio as observed previously).

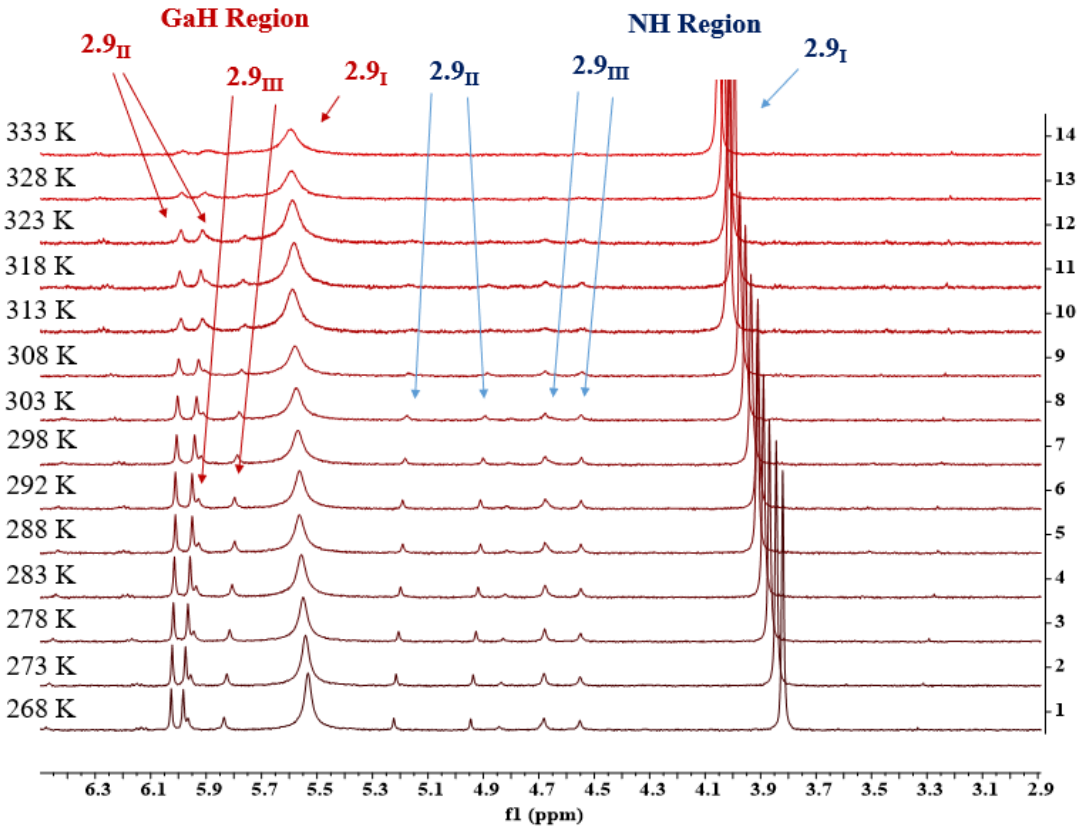


Figure 2.13: Variable-temperature NMR spectra for **2.9** (268K−333K).

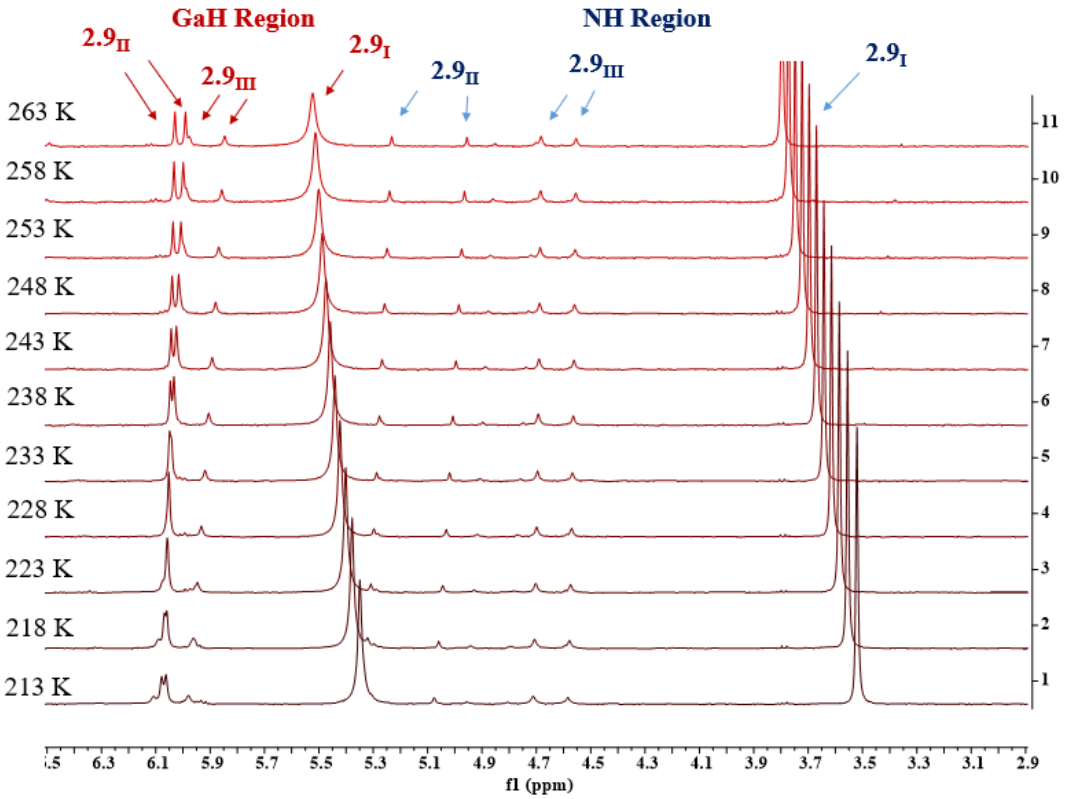


Figure 2.14: Variable-temperature NMR studies of **2.9** (213K−263K).

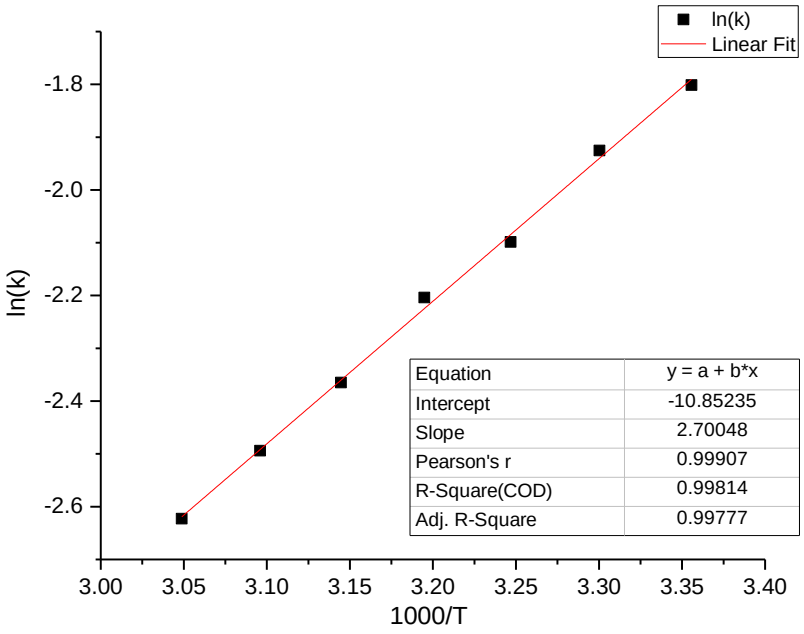


Figure 2.15: Van't Hoff plot of equilibrium between isomers **2.9$_{I}$** and **2.9$_{II}$**.

For the two most intense isomers, **2.9$_{I}$** and **2.9$_{II}$**, we were able to plot a Van't Hoff plot (Figure 2.15) for the equilibrium between them, and were able to extract the following thermodynamic parameters:

$$\Delta H = -R \times \text{slope} = -8.314 J \cdot K^{-1} \cdot mol^{-1} \times (2700) = -22.45\ kJ \cdot mol^{-1}$$

$$\Delta S = R \times \text{intercept} = 8.314 J \cdot K^{-1} \cdot mol^{-1} \times (-10.86) = -90.29\ J \cdot K^{-1} \cdot mol^{-1}$$

This illustrates that the isomers are exchanging in solution. Given the complexity of the NMR spectra recorded for this mixture of isomers, we are unable to unequivocally determine the structures of the isomers in solution. We believe that **2.9$_{I}$** is monomeric, as the NMR data for this compound are in good agreement with related complexes. It seems reasonable that one of the other isomers is a dimeric form of the complex in line with the structure determined by single crystal X-ray diffraction. The identity/structure of the other isomers remains unknown, although we can be certain that they all have the same empirical formula as reaction with donor solvents gives rise to a single compound (see Section 2.10).

Diffusion-ordered spectroscopy (DOSY) is a well-established two-dimensional NMR method to determine diffusion coefficients, which are related to the hydrodynamic radii of compounds.[45,46] As previous NMR experiments suggested an equilibrium between monomeric and dimeric gallium hydrides, we sought to use DOSY to investigate the aggregation states. The SEGWE (Stokes-Einstein Gierer-Wirtz Estimation) equation was used for the calculation of molecular weights.[45,46]

Solution diffusion-ordered spectroscopy (DOSY) (Figure 2.16) of a C_6D_6 solution of **2.9** allows for the observation of two isomers with different diffusion coefficients, $7.8 \cdot 10^{-10} \cdot m^2 \cdot s^{-1}$ (isomer **2.9$_{I}$**; with *tert*-butyl signals at 1.54 and 1.30 ppm) and

$5.8 \cdot 10^{-10} \cdot m^2 \cdot s^{-1}$ (isomer **2.9$_{II}$**; with *tert*-butyl signals at 1.32, 1.25 and 1.24 ppm). The concentrations of other isomers are relatively low and exhibit poor signal to noise ratios, so they could not be detected.

Calculations suggest that at 298.2 K the spectra with a diffusion coefficient of $7.8 \cdot 10^{-10} \cdot m^2 \cdot s^{-1}$ corresponds to a compound with a molecular weight of 445 $g \cdot mol^{-1}$ and a hydrodynamic radius of $6.6 \cdot 10^{-10} \cdot m$, while the spectra with a diffusion coefficient of $5.8 \cdot 10^{-10} \cdot m^2 \cdot s^{-1}$ corresponds to a predicted molecular weight of 846 $g \cdot mol^{-1}$ and a hydrodynamic radius of $8.1 \cdot 10^{-10} \cdot m$. These results suggest that the molecular weight of **2.9$_{II}$** is roughly twice that of **2.9$_{I}$**.

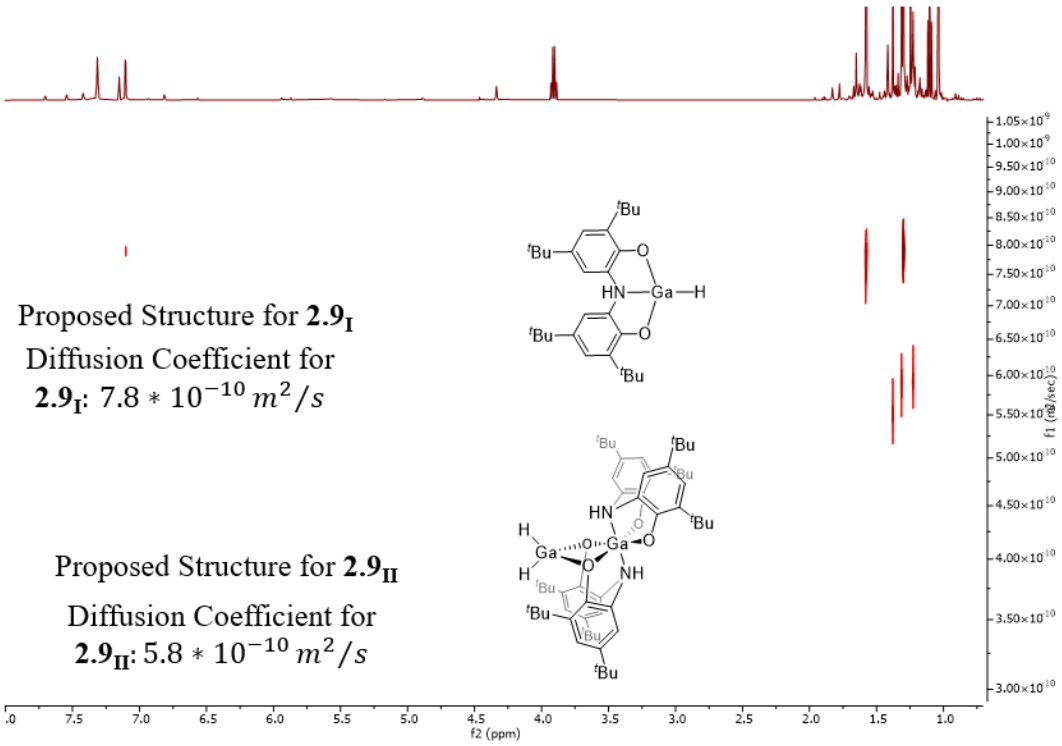


Figure 2.16: DOSY NMR spectrum of **2.9** in C_6D_6.

For comparison, the DOSY NMR spectrum of **2.8a** (Figure 2.17) reveals a diffusion coefficient of $5.8 \cdot 10^{-10} \cdot m^2 \cdot s^{-1}$ which is comparable to the diffusion coefficient for **2.9$_{II}$**. Taking this into consideration, we postulate that species **2.9$_{II}$** is a dimer as suggested

by single-crystal X-ray diffraction, whereas **2.9I** is presumed to be a monomeric gallium hydride.

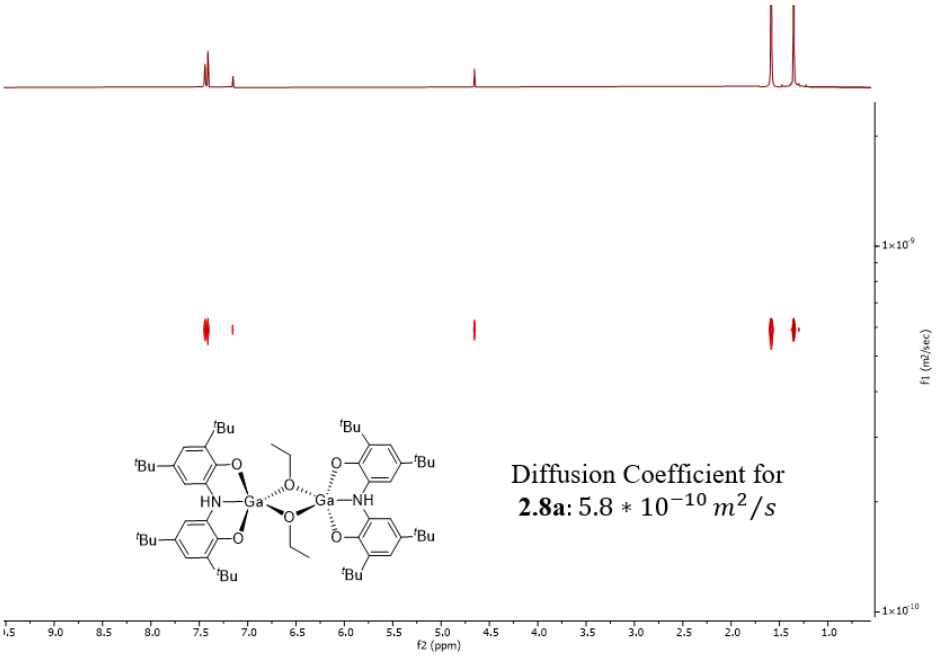
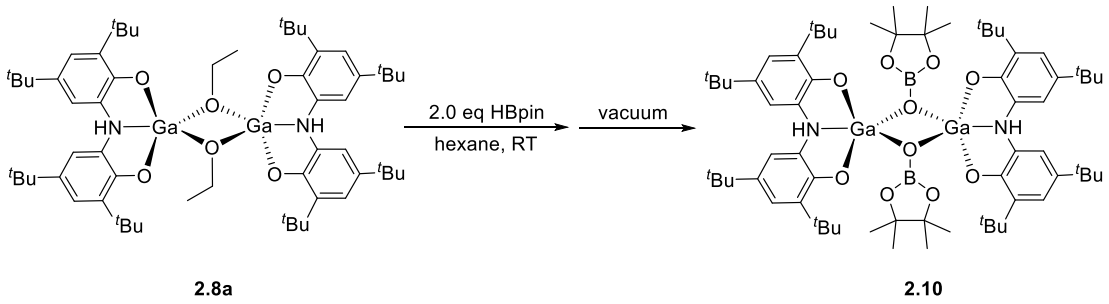


Figure 2.17: DOSY NMR spectrum of **2.8a** in C_6D_6.

2.9 A boryloxy-bridged side-product formed during the synthesis of 2.9

During the synthesis of compound **2.9**, an unexpected product **2.10** was observed and fully characterised. When two equivalents of pinacol borane were added to a hexane solution of **2.8a**, the formation of complex **2.9** was observed. However, if the toluene solvent was removed under a dynamic vacuum, the resulting solid could be recrystallised from toluene affording **2.10** as colourless crystals (Scheme 2.11).



Scheme 2.11: Formation of **2.10**.

In order to shed on light on the mechanism of this reaction, a C_6D_6 solution of **2.9** and EtOBpin was heated at 60 °C overnight, however, no formation of **2.10** could be observed by NMR spectroscopy. Hence, we have no viable hypothesis on how this complex is formed. The composition of complex **2.10** was established by elemental analysis (CHN), NMR spectroscopy and single crystal X-ray diffraction (Figure 2.18).

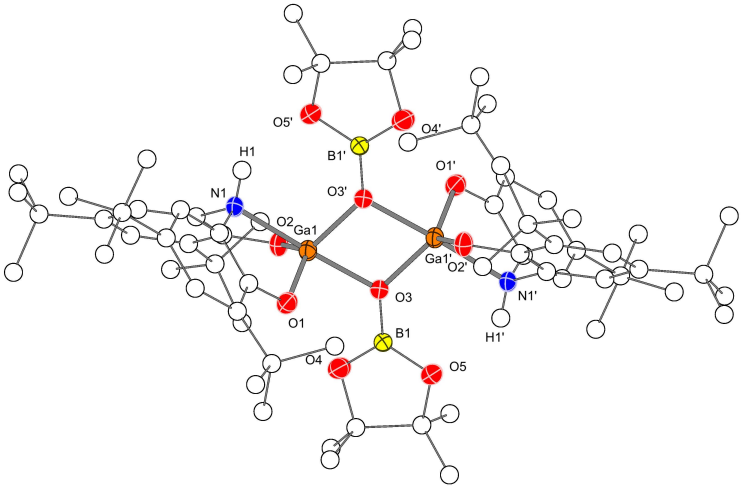
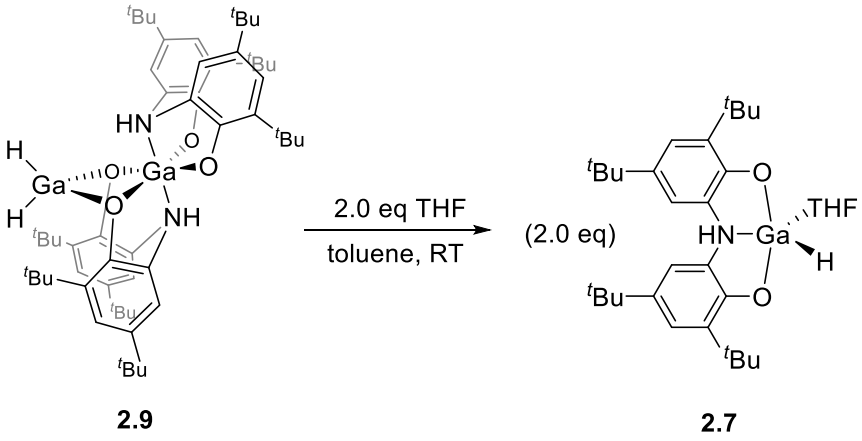


Figure 2.18: Single crystal X-ray structure of **2.10**. Anisotropic displacement ellipsoids set at 50% probability. Hydrogen atoms (with the exception of H1 and H1′) have been omitted for clarity. All carbon atoms are pictured as spheres of arbitrary radius. Selected interatomic distances [Å] and angles [°]: Ga1–O1 1.848(2), Ga1–O2 1.839(2), Ga1–O3 1.910(2), Ga1–$O3^1$ 1.9811(19), Ga1–N1 2.104(2); O2-Ga1-O1 126.78(10), O2-Ga1-O3 121.44(9), O1-Ga1-O3 111.73(9), O2-Ga1-$O3^1$ 97.59(9), O1-Ga1-$O3^1$ 94.76(8), O3-Ga1-$O3^1$ 78.32(8), O2-Ga1-N1 85.58(9), O1-Ga1-N1 84.83(9), O3-Ga1-N1 98.40(9), $O3^1$-Ga1-N1 176.29(9).

The ^{1}H NMR spectrum of **2.10** in $CDCl_3$ is similar to that of **2.8a**, with resonances for the aromatic region of ligand backbone (7.51, 7.19 ppm), a broad peak assigned to the amine (6.36 ppm), two overlapping resonances arising from the *tert*-butyl groups (1.34 ppm), and a singlet for the methyl groups of the two μ_2-OBpin bridges (1.09 ppm). The existence of μ_2-OBpin group is further supported by ^{11}B{H} NMR spectroscopy which reveals a broad peak at 22.5 ppm. The ^{13}C{H} NMR spectrum reveals resonances of the μ_2-OBpin moiety at 83.54 (for O*C*$(CH_3)_2$) and 24.44 ppm (for OC(*C*$H_3)_2$). It is worth noting that when using 9-BBN dimer as the borane, this type of reactivity was not observed.

2.10 Monomerisation of 2.9 to 2.7 using a coordinating solvent

Addition of a stochiometric amount of THF can break up the gallium dihydride complex **2.9** to afford product **2.7** (Scheme 2.12). The ^{1}H NMR spectrum of **2.7** reveals a single ligand environment (ArH: 7.35, 7.15 ppm; NH: 3.92 ppm; *tert*-butyl: 1.59, 1.35 ppm), and a broad gallium hydride resonance (5.65 ppm). This is very similar to what we observed for **2.7**·1.5BH_3:py. This compound was assigned as the THF adduct of the gallium hydride complex **2.7** and its structure was confirmed by single crystal X-ray diffraction (Figure 2.19).



Scheme 2.12: Synthesis of complex **2.7**.

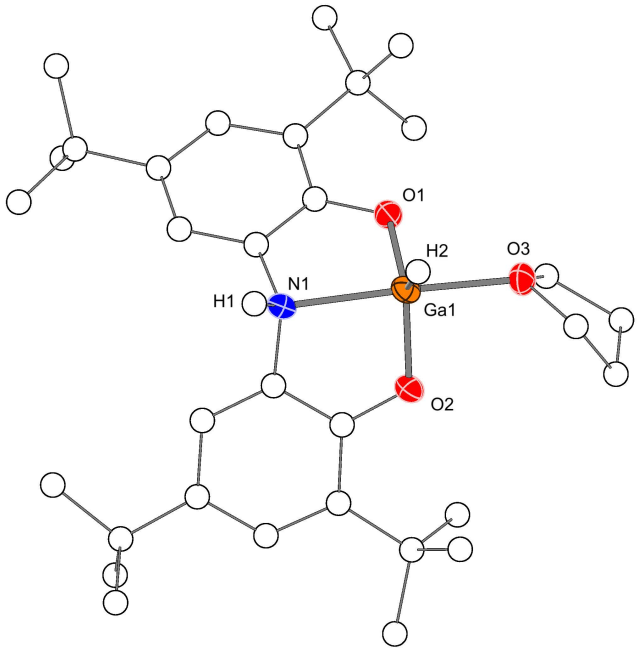
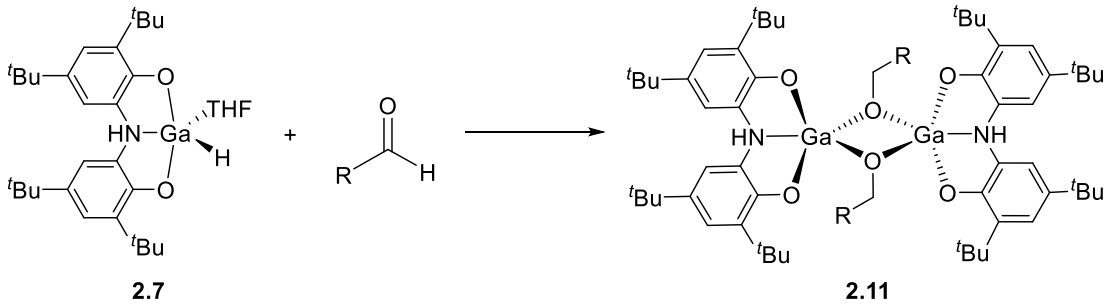


Figure 2.19: Single crystal X-ray structure of **2.7**. Anisotropic displacement ellipsoids set at 50% probability. Hydrogen atoms (with the exception of H1 and H2) have been omitted for clarity. All carbon atoms are pictured as spheres of arbitrary radius. Selected interatomic distances [Å] and angles [°]: Ga1−O1 1.857(2), Ga1−O2 1.865(2), Ga1−O3 2.111(2), Ga1−N1 2.191(2); O1-Ga1-O2 113.54(9), O1-Ga1-O3 85.54(9), O2-Ga1-O3 87.35(9), O1-Ga1-N1 83.10(9), O2-Ga1-N1 83.35(9), O3-Ga1-N1 161.03(9).

2.11 Hydrogallation of aldehydes by complexes 2.7 and 2.9



2.7 **2.11**

Aldehydes
2.11a: R = C_6H_5
2.11b: R = ^{i}Pr
2.11c: R = 4-$OMeC_6H_4$
2.11d: R = 4-BrC_6H_4
2.11e: R = Mes

Scheme 2.13: Synthesis of compounds **2.11a**−**2.11e** $[Ga(ON(H)O)(OCH_2R)]_2$.

Having identified two kinds of novel gallium hydride, **2.7** and **2.9**, we wanted to investigate their reactivity towards substrates, specifically aldehydes and ketones. A 1:1 stoichiometric reaction of benzaldehyde and **2.7** at room temperature in C_6D_6 showed complete consumption of **2.7** over 12 hours (Scheme 2.13), as evidenced by the disappearance of the Ga−H resonance in the ^{1}H NMR spectrum at 5.65 ppm. Single crystals were obtained from the reaction mixture and single-crystal X-ray analysis confirmed the formation of gallium alkoxide complex **2.11a** (Figure 2.20).[20,25] The ^{1}H NMR spectrum of **2.11a** reveals the aromatic resonances attributed to ligand backbone at 7.11 and 7.01 ppm, as well as resonances for the amine at 3.93 ppm and *tert*-butyl protons at 1.39 and 1.27 ppm.

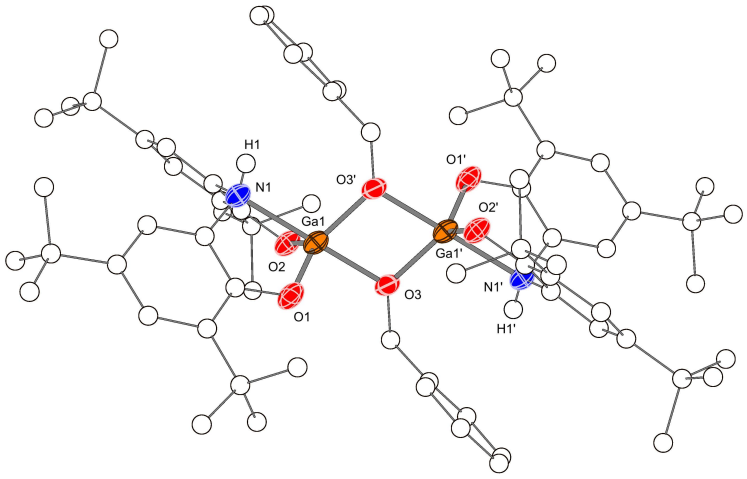


Figure 2.20: Single crystal X-ray structure of **2.11a**. Anisotropic displacement ellipsoids set at 50% probability. Hydrogen atoms (with the exception of H1 and H1′) have been omitted for clarity. All carbon atoms are pictured as spheres of arbitrary radius. Selected interatomic distances [Å] and angles [°]: Ga1−O2 1.835(2), Ga1−O1 1.842(2), Ga1−O3 1.874(2), Ga1−O3′ 1.959(2), Ga1−N1 2.132(3); O2-Ga1-O1 121.63(10), O2-Ga1-O3 119.38(9), O1-Ga1-O3 118.96(10), O2-Ga1-O3′ 95.51(9), O1-Ga1-O3′ 94.60(9), O3-Ga1-O3′ 77.70(9), O2-Ga1-N1 84.90(9), O1-Ga1-N1 85.50(10), O3-Ga1-N1 101.77(9), O3′-Ga1-N1 179.44(10).

Inspired by the reactivity of gallium hydride **2.7** with benzaldehyde, we wanted to extend this reactivity to other aldehydes, thus, stoichiometric reactions of **2.7** with other aldehyde, including isobutyraldehyde, 4-methoxybenzaldehyde, 4-bromobenzaldehyde and 2,4,6-trimethylbenzaldehyde were carried out (Scheme 2.13). In these reactions, insertion of the aldehyde carbonyl into the Ga−H bond of **2.7** was observed, and confirmed by single-crystal X-ray diffraction (see Figures 2.21−2.24).

The ^{1}H NMR spectra of **2.11b**−**2.11d** reveal the aromatic protons of the ligand backbone at (**2.11b**: 7.53, 7.21 ppm; **2.11c**: 7.14, 7.08 ppm; **2.11d**: 7.20, 7.15 ppm; **2.11e**: 7.10, 6.97 ppm), a resonance for the amine group of the ligand (**2.11b**: 5.01 ppm; **2.11c**: 4.00 ppm; **2.11d**: 4.02 ppm), and two resonances for the *tert*-butyl protons (**2.11b**:

1.38, 1.33 ppm; **2.11c**: 1.39, 1.27 ppm; **2.11d**: 1.40, 1.32 ppm; **2.11e**: 1.39, 1.31 ppm). These data are listed in Table 2.2. These results clearly indicate facile addition of Ga–H over the carbonyl in aldehydes and show that **2.7** has a good tolerance for non-aromatic aldehydes, as well as aldehydes with halo- and methoxy-substituents. It is worth-noting that the reaction of **2.9** with these aldehydes affords the same products.

Table 2.2: Selected ^{1}H NMR resonances of complexes **2.11a−e**.

	Ar1 (ppm)	Ar2 (ppm)	NH (ppm)	*tert*-butyl (ppm)	*tert*-butyl (ppm)
2.11a	7.11	7.01	3.93	1.39	1.27
2.11b	7.53	7.21	5.01	1.38	1.33
2.11c	7.14	7.08	4.00	1.39	1.27
2.11d	7.20	7.15	4.02	1.40	1.32
2.11e	7.10	6.97	n/a	1.39	1.31

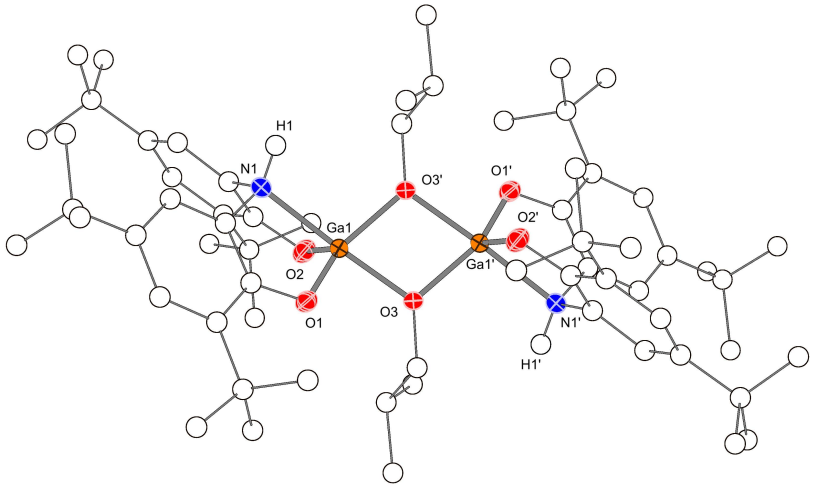


Figure 2.21: Single crystal X-ray structure of **2.11b**. Anisotropic displacement ellipsoids set at 50% probability. Hydrogen atoms (with the exception of H1 and H1′) have been omitted for clarity. All carbon atoms are pictured as spheres of arbitrary radius. Selected interatomic distances [Å] and angles [°]: Ga1−O2 1.8396(19), Ga1−O1 1.8445(19), Ga1−O3 1.8847(18), Ga1−O3′ 1.9634(18), Ga1−N1 2.152(2); O2-Ga1-O1 117.84(9), O2-Ga1-O3 115.96(9), O1-Ga1-O3 126.20(9), O2-Ga1-O3′ 99.50(8), O1-Ga1-O3′ 93.88(8), O3-Ga1-O3′ 77.68(8), O2-Ga1-N1 85.33(8), O1-Ga1-N1 84.96(8), O3-Ga1-N1 99.06(8), O3′-Ga1-N1 174.99(8), Ga1-O3-Ga1′ 102.32(8).

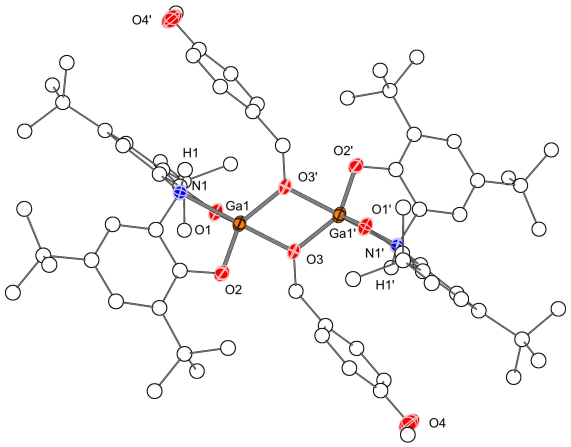


Figure 2.22: Single crystal X-ray structure of **2.11c**. Anisotropic displacement ellipsoids set at 50% probability. Hydrogen atoms (with the exception of H1 and H1′) have been omitted for clarity. All carbon atoms are pictured as spheres of arbitrary radius. Selected interatomic distances [Å] and angles [°]: Ga1–O1 1.8397(10), Ga1–O2 1.8459(10), Ga1–O3 1.8813(10), Ga1–O3′ 1.9666(9), Ga1–N1 2.1308(11); O1-Ga1-O2 121.16(5), O1-Ga1-O3 120.50(4), O2-Ga1-O3 118.27(4), O1-Ga1-O3′ 94.77(4), O2-Ga1-O3′ 95.08(4), O3-Ga1-O3′ 77.31(4), O1-Ga1-N1 85.10(4), O2-Ga1-N1 85.59(4), O3-Ga1-N1 102.14(4), O3′-Ga1-N1 179.28(4), Ga1-O3-Ga1′ 102.69(4).

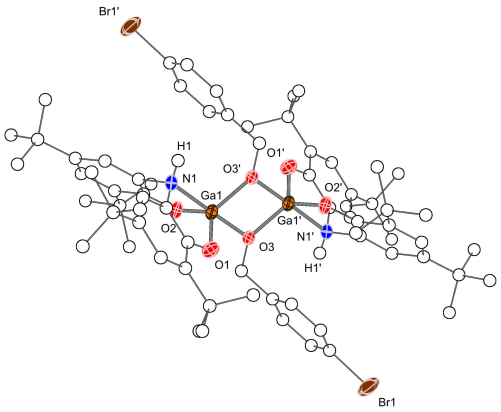


Figure 2.23: Single crystal X-ray structure of **2.11d**. Anisotropic displacement ellipsoids set at 50% probability. Hydrogen atoms (with the exception of H1 and H1′) have been omitted for clarity. All carbon atoms are pictured as spheres of arbitrary radius. Selected interatomic distances [Å] and angles [°]: Ga1-O2 1.8324(12), Ga1-O1 1.8409(13), Ga1-O3 1.8775(12), Ga1-O3′ 1.9603(11), Ga1-N1 2.1211(13); O2-Ga1-O1 121.19(6), O2-Ga1-O3 118.26(6), O1-Ga1-O3 120.40(6), O2-Ga1-O3′ 93.99(5), O1-Ga1-O3′ 94.95(5), O3-Ga1-O3′ 76.99(5), O2-Ga1-N1 86.18(5), O1-Ga1-N1 85.76(6), O3-Ga1-N1 102.11(5), O31-Ga1-N1 179.06(6).

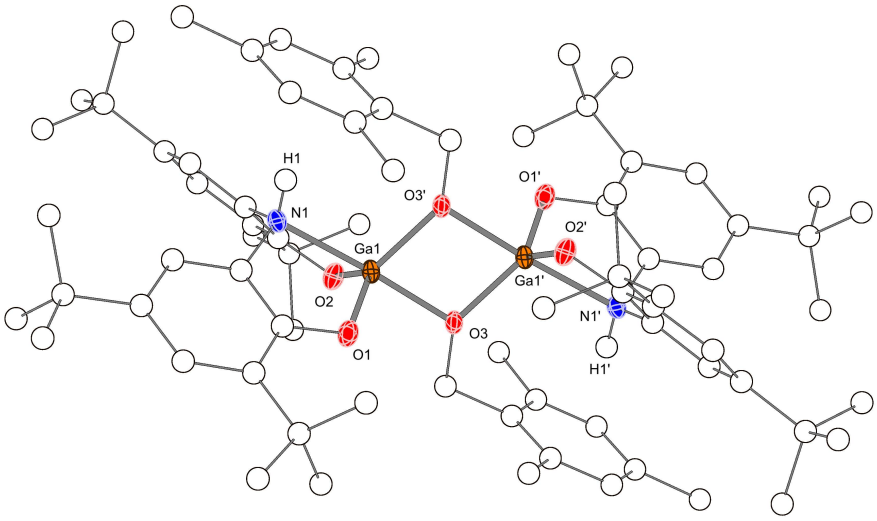


Figure 2.24: Single crystal X-ray structure of **2.11e**. Anisotropic displacement ellipsoids set at 50% probability. Hydrogen atoms (with the exception of H1 and H1′) have been omitted for clarity. All carbon atoms are pictured as spheres of arbitrary radius. Selected interatomic distances [Å] and angles [°]: Ga1–O1 1.8486(16), Ga1–O2 1.8609(16), Ga1–O3 1.8836(16), Ga1–O3′ 1.9684(15), Ga1–N1 2.1131(19); O1-Ga1-O2 122.96(8), O1-Ga1-O3 119.01(7), O2-Ga1-O3 117.78(7), O1-Ga1-O3′ 94.00(7), O2-Ga1-O3′ 92.93(7), O3-Ga1-O3′ 77.59(7), O1-Ga1-N1 85.64(7), O2-Ga1-N1 84.15(7), O3-Ga1-N1 105.86(7), O3′-Ga1-N1 176.24(7), Ga1-O3-Ga1′ 102.41(7).

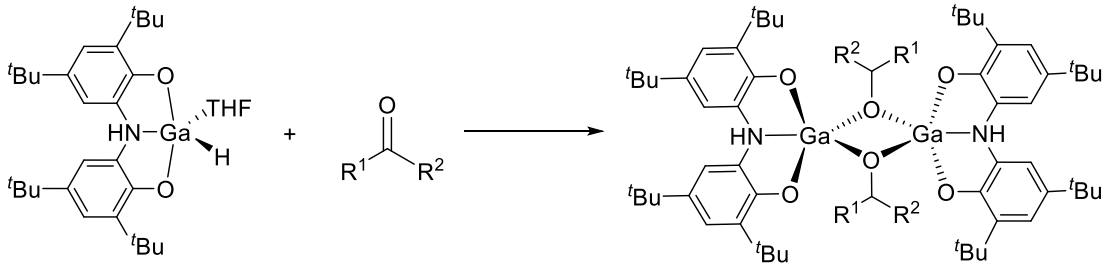
Selected bond lengths and bond angles for complexes **2.11a**−**e** are listed in Table 2.3. The complexes all have similar bond lengths, with Ga1−N1 bond around 2.11−2.16 Å, Ga1−O3 bond around 1.87−1.89 Å, and Ga1−O3′ bond around 1.95−1.97 Å. The gallium centres all adopt trigonal bipyramidal shapes, with τ_5 value between 0.81−0.97, of which **2.11b** is the most distorted, which is related the steric effect of the alkoxide substituents.

Table 2.3: Selected bond lengths and bond angles of complexes **2.11a**–**e**.

	Ga1–N1 (Å)	Ga1–O3 (Å)	Ga1–O3′ (Å)
2.11a	2.132(3)	1.874(2)	1.959(2)
2.11b	2.152(2)	1.8847(18)	1.9634(18)
2.11c	2.1308(11)	1.8813(10)	1.9666(9)
2.11d	2.1211(13)	1.8775(12)	1.9603(11)
2.11e	2.1131(19)	1.8836(16)	1.9684(15)

	N1-Ga1-O3 (°)	O1-Ga1-O2 (°)	O1-Ga1-O3 (°)	τ_5
2.11a	179.44(10)	121.63(10)	118.96(10)	0.96
2.11b	174.99(8)	117.84(9)	126.20(9)	0.81
2.11c	179.28(4)	121.16(5)	120.50(4)	0.97
2.11d	179.06(6)	121.19(6)	120.40(6)	0.96
2.11e	176.24(7)	122.96(8)	119.01(7)	0.89

2.12 Hydrogallation of ketones by complexes 2.7 and 2.9



2.7 + ketone → **2.12** $[Ga(ON(H)O)(OC(H)(R^1)R^2)]_2$

Ketones
2.12a: $R^1 = C_6H_5$, $R^2 = C_6H_5$
2.12b: R^1 = Me, R^2 = Me
2.12c: R^1 = 4-OMe-C_6H_4, R^2 = Me
2.12d: R^1 = 4-BrC_6H_4, R^2 = Me
2.12e: R = 2-indanyl
2.12f: R^1 = 4-$NO_2C_6H_4$, R^2 = Me

Scheme 2.14: Synthesis of compounds **2.12a**–**2.12f** $[Ga(ON(H)O)(OC(H)(R^1)R^2)]_2$.

With this reactivity in hand, we speculated that gallium hydride complexes **2.7** and **2.9** could also activate other carbonyl substrates, for example ketones. A series of stoichiometric reactions between **2.7** and **2.9** and six different ketones were undertaken, all of which afforded dimeric gallium alkoxide complexes, similar to the aforementioned reactions with aldehydes (Scheme 2.14). The gallium alkoxide species

2.12a−**2.12f** were isolated and fully characterised, and their structures were confirmed by single-crystal X-ray diffraction (Figures 2.25−2.29). The ^{1}H NMR spectra of **2.12a**−**2.12f** reveal resonances for the aromatic protons of the ligand backbone at (**2.12a**: 7.06, 6.86 ppm; **2.12b**: 7.59, 7.23 ppm; **2.12c**: 7.14, 7.13, 7.12, 7.03 ppm; **2.12d**: 7.16, 7.15, 7.14, 7.13, 7.07, 7.06 ppm, **2.12e**: 7.17−7.06, 6.85 ppm; **2.12f**: 7.15, 7.09−6.95 ppm), a broad resonance for the amine proton (**2.12a**: 3.75 ppm; **2.12b**: 5.02 ppm; **2.12c**: 4.03, 3.96 ppm; **2.12d**: 3.92, 3.86 ppm, **2.12e**: 3.66 ppm; **2.12f**: 3.96, 3.94ppm) and two resonances for the *tert*-butyl protons (**2.12a**: 1.22, 1.19 ppm; **2.12b**: 1,40, 1.34 ppm; **2.12c**: 1.41, 1.27 ppm; **2.12d**: 1.46−1.21 ppm, **2.12e**: 1.39, 1.29 ppm; **2.12f**: 1.39, 1.22 ppm) in $CDCl_3$, as Table 2.4. The single-crystal X-ray structures of all these compounds are presented below and are in line with the other alkoxide-bridged compounds reported in this thesis thus far.

Table 2.4: Selected ^{1}H NMR resonances of complexes **2.12a**−**f**.

	Ar1 (ppm)	Ar2 (ppm)	NH (ppm)	*tert*-butyl (ppm)	*tert*-butyl (ppm)
2.12a	7.06	6.86	3.75	1.22	1.19
2.12b	7.59	7.23	5.02	1.40	1.34
2.12c	7.14−7.12	7.03	4.03, 3.96	1.41	1.27
2.12d	7.16−7.13	7.07−7.06	3.92, 3.86	1.46−1.21	
2.12e	7.17−7.06	6.85	3.66	1.39	1.29
2.12f	7.15	7.09−6.95	3.96, 3.94	1.39	1.22

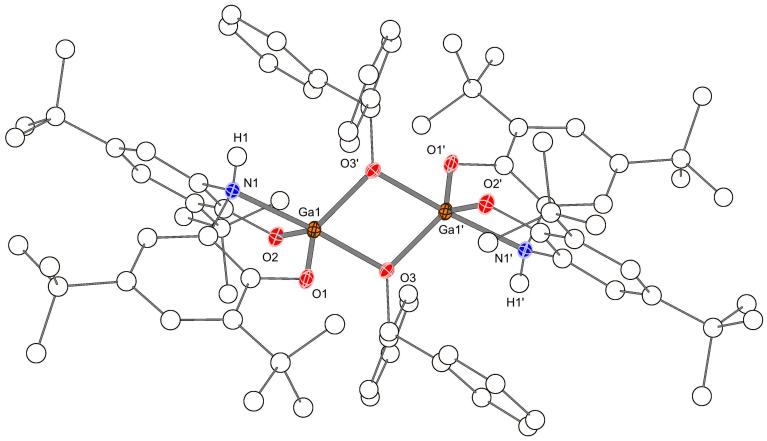


Figure 2.25: Single crystal X-ray structure of **2.12a**. Anisotropic displacement ellipsoids set at 50% probability. Hydrogen atoms (with the exception of H1 and H1′) have been omitted for clarity. All carbon atoms are pictured as spheres of arbitrary radius. Selected interatomic distances [Å] and angles [°]: Ga1–O2 1.8431(14), Ga1–O1 1.8610(14), Ga1–O3 1.8899(14), Ga1–O3′ 1.9700(14), Ga1–N1 2.1164(17); O2-Ga1-O1 128.07(7), O2-Ga1-O3 121.18(6), O1-Ga1-O3 110.63(6), O2-Ga1-O3′ 94.73(6), O1-Ga1-O3′ 92.60(6), O3-Ga1-O3′ 77.89(6), O2-Ga1-N1 84.65(6), O1-Ga1-N1 85.06(6), O3-Ga1-N1 105.43(6), O3′-Ga1-N1 176.45(6), Ga1-O3-Ga1′ -102.12(6).

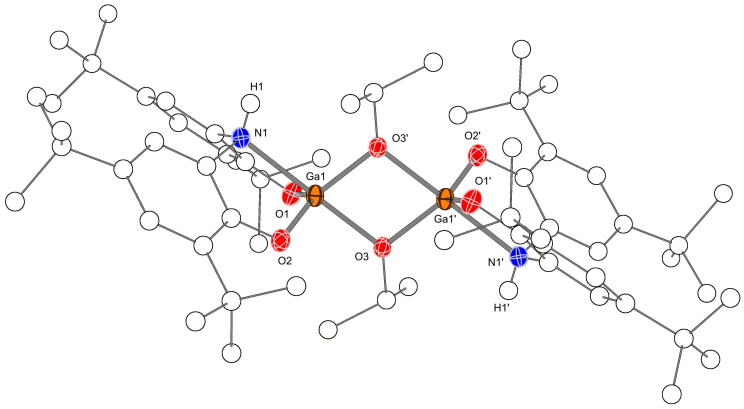


Figure 2.26: Single crystal X-ray structure of **2.12b**. Anisotropic displacement ellipsoids set at 50% probability. Hydrogen atoms (with the exception of H1 and H1′) have been omitted for clarity. All carbon atoms are pictured as spheres of arbitrary radius. Selected interatomic distances [Å] and angles [°]: Ga1–O2 1.8423(10), Ga1–O1 1.8431(10), Ga1–O3 1.8834(10), Ga1–O3′ 1.9738(10), Ga1–N1 2.1720(12); O2-Ga1-O1 125.50(5), O2-Ga1-O3 116.60(5), O1-Ga1-O3 117.88(5), O2-Ga1-O3′ 96.55(4), O1-Ga1-O3′ 95.77(4), O3-Ga1-O3′ 78.18(5), O2-Ga1-N1 84.17(5), O1-Ga1-N1 83.96(5),O3-Ga1-N1 101.33(5), O3′ -Ga1-N1 179.26(5), Ga1-O3-Ga1′ 101.82(5).

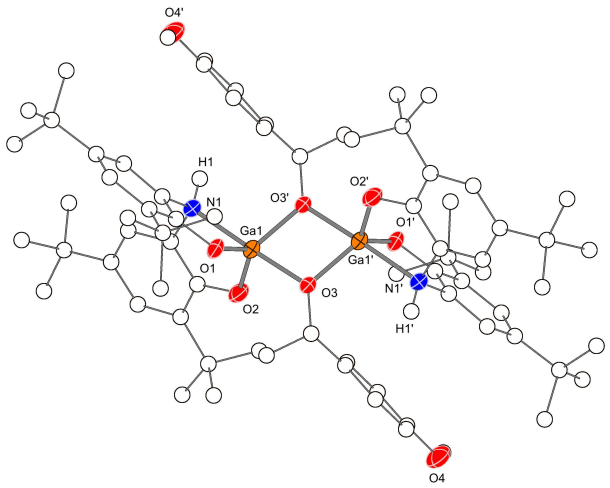


Figure 2.27: Single crystal X-ray structure of **2.12c**. Anisotropic displacement ellipsoids set at 50% probability. Hydrogen atoms (with the exception of H1 and H1′) have been omitted for clarity. All carbon atoms are pictured as spheres of arbitrary radius. Selected interatomic distances [Å] and angles [°]: Ga1–O1 1.843(2), Ga1–O2 1.850(2), Ga1–O3 1.8826(19), Ga1–O3′ 1.9684(19), Ga1–N1 2.141(2); O1-Ga1-O2 121.64(9), O1-Ga1-O3 120.19(9), O2-Ga1-O3 118.17(10), O1-Ga1-O3′ 97.01(9), O2-Ga1-O3′ 95.32(9), O3-Ga1-O3′ 77.22(9), O1-Ga1-N1 84.66(9), O2-Ga1-N1 84.95(9), O3-Ga1-N1 100.74(9), O3′-Ga1-N1 177.82(8), Ga1-O3-Ga1′ 102.78(9).

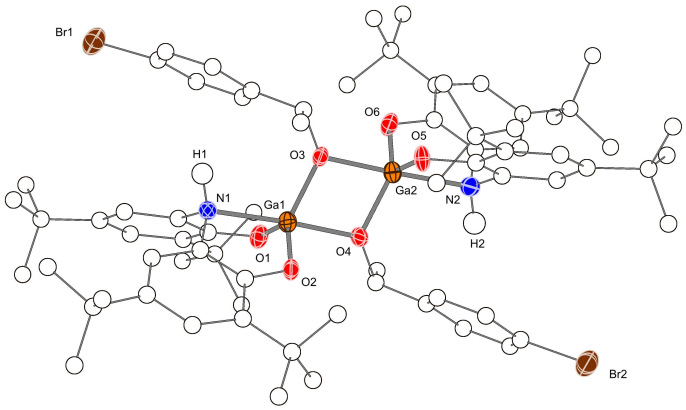


Figure 2.28: Single crystal X-ray structure of **2.12d**. Anisotropic displacement ellipsoids set at 50% probability. Hydrogen atoms (with the exception of H1 and H2) have been omitted for clarity. All carbon atoms are pictured as spheres of arbitrary radius. Selected interatomic distances [Å] and angles [°]: Ga1–O2 1.819(7), Ga1–O1 1.823(8), Ga1–O3 1.876(7), Ga1–O4 1.977(7), Ga1–N1 2.144(8), Ga2-O5 1.838(7), Ga2-O6 1.842(8), Ga2-O4 1.874(7), Ga2-O3 1.976(7), Ga2-N2 2.134(9); O2-Ga1-O1 123.6(4), O2-Ga1-O3 118.1(3), O1-Ga1-O3 118.1(3), O2-Ga1-O4 93.0(3), O1-Ga1-O4 93.9(3), O3-Ga1-O4 77.9(3), O2-Ga1-N1 85.0(3), O1-Ga1-N1 84.9(3), O3-Ga1-N1 105.3(3), O4-Ga1-N1 176.7(3).

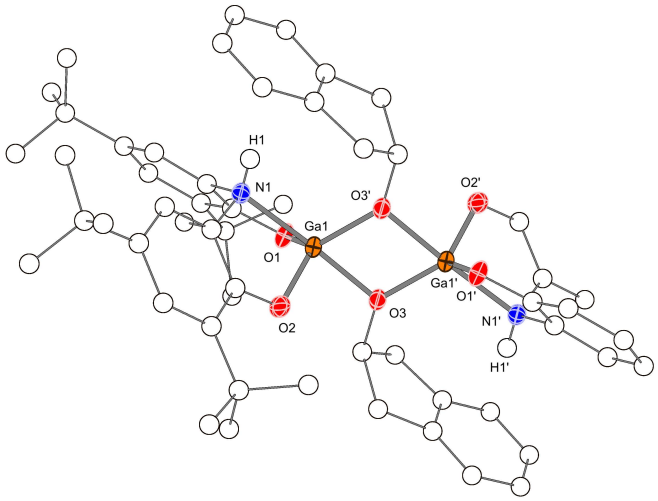


Figure 2.29: Single crystal X-ray structure of **2.12e**. Anisotropic displacement ellipsoids set at 50% probability. Hydrogen atoms (with the exception of H1 and H1′) have been omitted for clarity. All carbon atoms are pictured as spheres of arbitrary radius. Selected interatomic distances [Å] and angles [°]: Ga1–O2 1.8413(17), Ga1–O1 1.8464(16), Ga1–O3 1.8814(15), Ga1–O3′ 1.9660(15), Ga1–N1 2.1147(18); O2-Ga1-O1 118.54(8), O2-Ga1-O3 116.55(7), O1-Ga1-O3 124.54(8), O2-Ga1-O3′ 92.32(7), O1-Ga1-O3′ 93.57(7), O3-Ga1-O3′ 78.24(7), O2-Ga1-N1 85.55(7), O1-Ga1-N1 86.03(7), O3-Ga1-N1 104.18(7), O3′-Ga1-N1 177.31(7).

Selected bond lengths and bond angles for complexes **2.12a**−**e** are listed in Table 2.5. Similar to complexes **2.11a**−**e**, those complexes all have similar bond lengths, with Ga1−N1 bonds around 2.11−2.18 Å, Ga1−O3 bonds around 1.87−1.89 Å and Ga1−O3′ bonds around 1.96−1.98 Å. The gallium centres all adopt trigonal bipyramidal shapes, with τ_5 value between 0.81−0.94, of which **2.12a** is the most distorted due to the steric effect of the bridging alkoxide groups.

Table 2.5: Selected bond lengths and bond angles of complexes **2.12a−e**

	Ga1–N1(Å)	Ga1–O3(Å)	Ga1–O3′(Å)
2.12a	2.1164(17)	1.8899(14)	1.9700(14)
2.12b	2.1720(12)	1.8834(10)	1.9738(10)
2.12c	2.141(2)	1.8826(19)	1.9684(19)
2.12d	2.144(8)	1.876(7)	1.977(7)
2.12e	2.1147(18)	1.8814(15)	1.9660(15)

	N1-Ga1-O3(°)	O1-Ga1-O2(°)	O1-Ga1-O3(°)	τ
2.12a	176.45(6)	128.07(7)	110.63(6)	0.81
2.12b	179.26(5)	125.50(5)	117.88(5)	0.90
2.12c	177.82(8)	121.64(9)	120.19(9)	0.94
2.12d	176.7(3)	123.6(4)	118.1(3)	0.89
2.12e	177.31(7)	118.54(8)	124.54(8)	0.88

To summarise, we have isolated two novel gallium hydride complexes, **2.7** and **2.9,** stabilised by the *N*,*N*-bis(3,5-di-*tert*-butyl-2-phenoxy)amine ligand $[ON(H)O^{cat}]^{2-}$. These species afford novel bimetallic bis-alkoxide gallium complexes through a Ga−H/C=O insertion reaction (hydrogallation) with aldehydes and ketones. Similar 1,2-hydrogallation reactivity has not yet been observed for other unsaturated substrates such as alkenes, alkynes and carbon dioxide, and we are still working on investigating whether other types of unsaturated bond could be activated.

2.13 Conclusions

In this chapter, we have demonstrated the synthesis of two base-stabilised gallium chloride complexes, **2.1** and **2.2**, and have investigated their reactivity in salt metathesis reactions. The reaction of $[Na(dioxane)_{1.4}](PCO)$ with **2.1** quantitatively affords a ligand stabilised gallium phosphaethynolate complexes **2.3**, which converts to a mixture of **2.4** and **2.5** upon thermolysis. The reaction of **2.1** and NaO^{t}Bu in THF solution afford a geometrically constrained gallium sodium trimetallic complex **2.6**, while the reaction of **2.1** and $NaBH_4$ affords the amine-stabilised gallium hydride

complex **2.7**·1.5BH_3:py. This gallium monohydride is reactive towards alcohols, such as ethanol and cyclohexylmethanol, affording dimeric gallium alkoxide complexes **2.8a** and **2.8b**. Upon the addition of HBpin or 9-BBN dimer, **2.8a** can be converted to a unique bimetallic gallium dihydride complex **2.9**, which can be monomerised by employing a simple base, such as THF, to give **2.7**. We have also shown the hydrogallation reactivity of **2.7** towards a wide scope of aldehydes and ketones, which go through a C=O/Ga−H bond metathesis process to generate bimetallic gallium alkoxide complexes (**2.11a**−**2.11e** and **2.12a**−**2.12f**).

In the future, we will extend the scope of unsaturated substrates to see if compounds **2.7** and **2.9** can be used for the hydrogallation of other, less polar, substrates. Given the aforementioned reactivity, we have also explored the reactivity of the gallium ethoxide complex **2.8a**, and the gallium hydrides **2.7** and **2.9** in catalytic hydroboration reactions. These results are described in the following chapter.

2.14 References

[1] C. R. Pulham, A. J. Downs, M. J. Goode, D. W. H. Rankin, H. E. Robertson, *J. Am. Chem. Soc.* **1991**, *113*, 5149–5162.

[2] H. Schmidbaur, H. F. Klein, *Angew. Chem., Int. Ed.* **1966**, *5*, 312–312.

[3] J. Ohshita, H. Schmidbaur, *J. Organomet. Chem.* **1993**, *453*, 7–12.

[4] S. Nogai, H. Schmidbaur, *Inorg. Chem.* **2002**, *41*, 4770–4774.

[5] W. Uhl, *Coord. Chem. Rev.* **2008**, *252*, 1540–1563.

[6] W. Uhl, H. R. Bock, M. Claesener, M. Layh, I. Tiesmeyer, E.-U. Würthwein, *Chem. Eur. J.* **2008**, *14*, 11557–11564.

[7] W. Uhl, F. Hengesbach, J. Isermann, M. Soleimani, L. Schürmann, A. Hepp, M. Layh, *Z. Anorg. Allg. Chem.* **2019**, *645*, 1205–1214.

[8] V. G. Sokolov, T. S. Koptseva, M. V. Moskalev, N. L. Bazyakina, A. V. Piskunov, A. V. Cherkasov, I. L. Fedushkin, *Inorg. Chem.* **2017**, *56*, 13401–13410.

[9] W. Uhl, H. R. Bock, F. Breher, M. Claesener, S. Haddadpour, B. Jasper, A. Hepp, *Organometallics* **2007**, *26*, 2363–2369.

[10] W. Uhl, M. Claesener, *Inorg. Chem.* **2008**, *47*, 729–735.

[11] W. Uhl, A. Hentschel, D. Kovert, J. Kösters, M. Layh, *Eur. J. Inorg. Chem.* **2015**, *2015*, 2486–2496.

[12] J.-H. Lamm, J. Horstmann, J. H. Nissen, J.-H. Weddeling, B. Neumann, H.-G. Stammler, N. W. Mitzel, *Eur. J. Inorg. Chem.* **2014**, *2014*, 4294–4301.

[13] S. Mikami, K. Fujita, T. Nakamura, H. Yorimitsu, H. Shinokubo, S. Matsubara, K. Oshima, *Org. Lett.* **2001**, *3*, 1853–1855.

[14] W. Uhl, J. Molter, B. Neumüller, *J. Organomet. Chem.* **2001**, *634*, 193–197.

[15] J. A. B. Abdalla, I. M. Riddlestone, R. Tirfoin, S. Aldridge, *Angew. Chem., Int. Ed.* **2015**, *54*, 5098–5102.

[16] A. Caise, J. Hicks, M. Ángeles Fuentes, J. M. Goicoechea, S. Aldridge, *Chem. Eur. J.* **2021**, *27*, 2138–2148.

[17] W. Uhl, J. Molter, B. Neumüller, *J. Organomet. Chem.* **2001**, *634*, 193–197.

[18] A. Ford, S. Woodward, *Angew. Chem., Int. Ed.* **1999**, *38*, 335–336.

[19] A. J. Blake, A. Cunningham, A. Ford, S. J. Teat, S. Woodward, *Chem. Eur. J.* **2000**, *6*, 3586–

3594.

[20] S.-K. Lo, *Geometry Constrained Main-Group Compounds for the Activation of Small Molecules*, Thesis (D.Phil.) − University of Oxford, 2018, (Department of Inorganic Chemistry), Oxford, **2018**.

[21] A. Y. Girgis, A. L. Balch, *Inorg. Chem.* **1975**, *14*, 2724–2727.

[22] G. Szigethy, A. F. Heyduk, *Dalton Trans.* **2012**, *41*, 8144–8152.

[23] B. J. Charette, J. W. Ziller, A. F. Heyduk, *Inorg. Chem.* **2021**, *60*, 5367–5375.

[24] C. Camacho-Camacho, G. Merino, F. J. Martínez-Martínez, H. Nöth, R. Contreras, *Eur. J. Inorg. Chem.* **1999**, 1021–1027.

[25] C. D. Smith, *Synthesis and Reactivity of Geometrically Constrained Gallium(III) Complexes*, Thesis (M.Chem) − University of Oxford, (Department of Chemistry), Oxford, **2017**.

[26] A. D. Bage, T. A. Hunt, S. P. Thomas, *Org. Lett.* **2020**, *22*, 4107–4112.

[27] A. W. Addison, T. N. Rao, J. Reedijk, J. van Rijn, G. C. Verschoor, *J. Chem. Soc., Dalt. Trans.* **1984**, 1349–1356.

[28] G. Becker, W. Schwarz, N. Seidler, M. Westerhausen, *Z. Anorg. Allg. Chem.* **1992**, *612*, 72–82.

[29] F. F. Puschmann, D. Stein, D. Heift, C. Hendriksen, Z. A. Gal, H. F. Grützmacher, H. Grützmacher, *Angew. Chem., Int. Ed.* **2011**, *50*, 8420–8423.

[30] A. R. Jupp, J. M. Goicoechea, *Angew. Chem., Int. Ed.* **2013**, *52*, 10064–10067.

[31] D. W. N. Wilson, A. Hinz, J. M. Goicoechea, *Angew. Chem., Int. Ed.* **2018**, *57*, 2188–2193.

[32] S. Hagspiel, F. Fantuzzi, R. D. Dewhurst, A. Gärtner, F. Lindl, A. Lamprecht, H. Braunschweig, *Angew. Chem., Int. Ed.* **2021**, *60*, 13666–13670.

[33] Y. Mei, J. E. Borger, D. J. Wu, H. Grützmacher, *Dalton Trans.* **2019**, *48*, 4370–4374.

[34] D. W. N. Wilson, W. K. Myers, J. M. Goicoechea, *Dalton Trans.* **2020**, *49*, 15249–15255.

[35] L. Liu, S.-K. Lo, C. Smith, J. M. Goicoechea, *Chem. Eur. J.* **2021**, *27*, 17379–17385.

[36] C. Y. Tang, R. A. Coxall, A. J. Downs, T. M. Greene, S. Parsons, *J. Chem. Soc., Dalton Trans.* **2001**, *2*, 2141–2147.

[37] C. Y. Tang, A. J. Downs, T. M. Greene, S. Marchant, S. Parsons, *Inorg. Chem.* **2005**, *44*, 7143–7150.

[38] S. Marchant, C. Y. Tang, A. J. Downs, T. M. Greene, H.-J. Himmel, S. Parsons, *Dalton Trans.* **2005**, 3281–3290.

[39] C. Y. Tang, A. R. Cowley, A. J. Downs, S. Marchant, S. Parsons, *Eur. J. Inorg. Chem.* **2008**, 737–744.

[40] N. N. Greenwood, E. J. F. Ross, A. Storr, *J. Chem. Soc. A* **1966**, 706–711.

[41] A. K. Swarnakar, M. J. Ferguson, R. McDonald, E. Rivard, *Dalton Trans.* **2017**, *46*, 1406–1412.

[42] A. H. Cowley, F. P. Gabbai, D. A. Atwood, C. J. Carrano, L. M. Mokry, M. R. Bond, *J. Am. Chem. Soc.* **1994**, *116*, 1559–1560.

[43] H. Dong, H. Berke, *J. Organomet. Chem.* **2011**, *696*, 1803–1808.

[44] T. D. W. Claridge, *High-Resolution NMR Techniques in Organic Chemistry*, Elsevier Science, **2016**.

[45] R. Evans, Z. Deng, A. K. Rogerson, A. S. McLachlan, J. J. Richards, M. Nilsson, G. A. Morris, *Angew. Chem., Int. Ed.* **2013**, *52*, 3199–3202.

[46] R. Evans, G. Dal Poggetto, M. Nilsson, G. A. Morris, *Anal. Chem.* **2018**, *90*, 3987–3994.

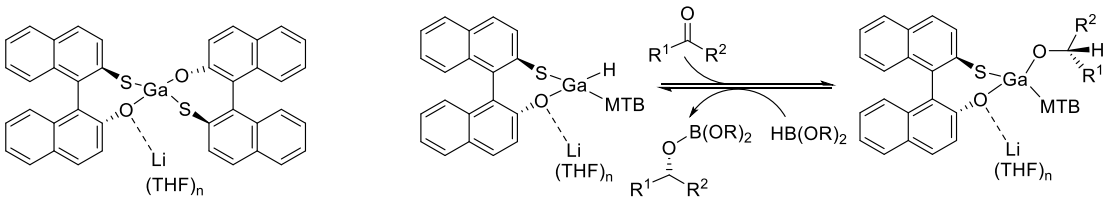
Chapter Three

Gallium hydride catalysts for the hydroboration of unsaturated substrates

3.1 Introduction and objectives

Main group hydrides are promising candidates for the functionalisation of substrates with unsaturated bond. Due to their weak and highly polarised $^{\delta+}M-H^{\delta-}$ bonds, main group hydrides can readily undergo 1,2-hydrometallation reactions with unsaturated substrates.[1] This makes them attractive compounds for hydride transfer reactions such as hydroboration, hydrosilylation and hydrogenation.[2–5] A number reports have documented the functionalisation of unsaturated substrates containing C=E bonds (E = C, N, O) by main group complexes containing elements such as magnesium,[6–13] calcium,[13–15] aluminium,[16–26] germanium and tin.[27–31] By contrast, only a handful of examples of gallium compounds in catalytic hydroboration have been reported (see also Chapter One).[32–34]

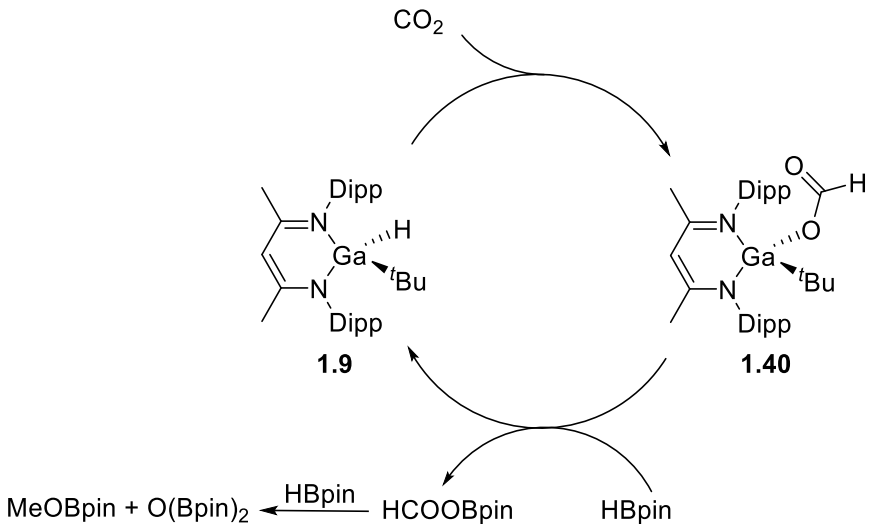
Woodward and co-workers have shown that $LiGaH_4$ in combination with monothiobinaphthol (MTB) or $MTBH_2$ ligands is active for the asymmetric hydroboration of ketones as shown in Scheme 3.1 (see also Chapter One, Section 1.3.1).[33,34]



Scheme 3.1: Catalyst **1.37** and proposed working model for hydroboration.[33,34]

In 2015, Aldridge and co-workers prepared a (^{Dipp}Nacnac)Ga(H)(^{t}Bu) complex, which could facilitate the hydroboration of carbon dioxide (Scheme 3.2).[32] The mechanism for this reaction is similar to that proposed by Woodward.[33,34] The carbonyl first inserts

into the Ga−H bond to form gallium formate, which can regenerate the gallium hydride through a Ga−O/B−H metathesis reaction with a borane (see also Chapter One, Section 1.3.1).



Scheme 3.2: Gallium hydride **1.9** and proposed mechanism for hydroboration of CO_2.[32]

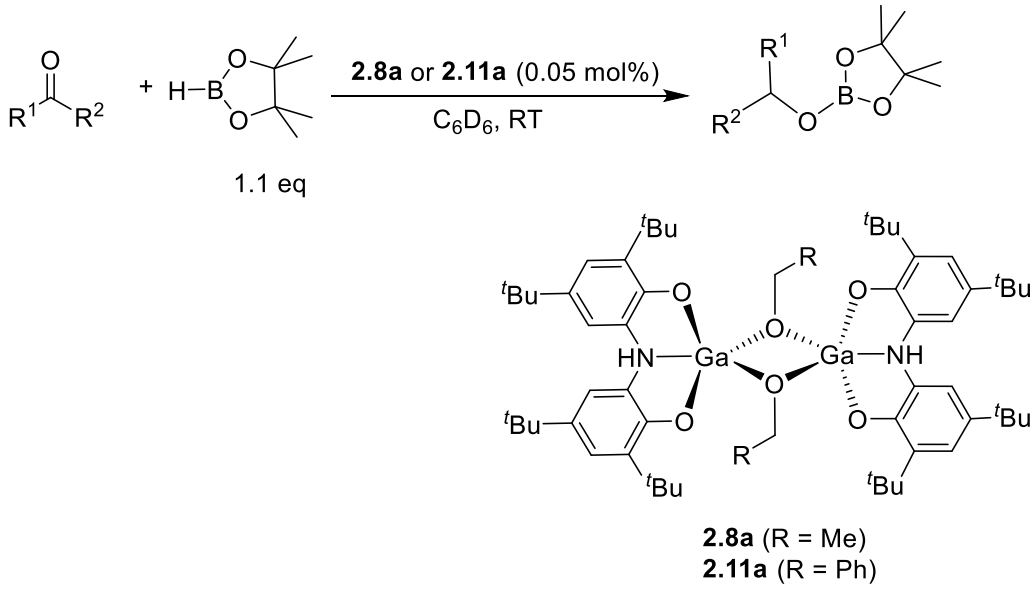
In this chapter, we will discuss the use of the novel gallium complexes introduced in the previous chapter as catalysts in the hydroboration of different substrates including aldehydes, ketones, carbon dioxide, isocyanates and imines.

3.2 Gallium catalysed hydroboration of aldehydes

3.2.1 Catalytic hydroboration of aldehydes

As demonstrated in Chapter Two, isolable gallium hydrides can be generated by reacting HBpin and gallium alkoxides such as **2.8a** or **2.11a**. We reasoned that such gallium alkoxides could be used as pre-catalysts in a number of transformations.[35,36] Firstly, we explored the catalytic hydroboration of aldehydes using **2.8a** and **2.11a** (0.05 mol%) as pre-catalysts (Scheme 3.3).

Reactions were conducted using a stock solution of **2.8a** or **2.11a** in C_6D_6 and hexamethylcyclotrisiloxane (HMCTS) as an internal standard (Scheme 3.3). The aldehyde, HBpin (1.1 equivalents) and the stock solution of **2.8a** were added at room temperature and the reaction was monitored using ^{1}H NMR spectroscopy.

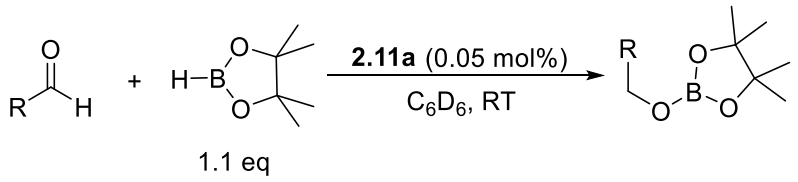


Scheme 3.3: Catalytic hydroboration of aldehydes and ketones.

A preliminary reaction was conducted by adding 1.1 equivalents of HBpin to a mixture of benzaldehyde and a stock solution of C_6D_6 with 0.05 mol% catalyst **2.11a**. The formation of the corresponding borylated ester $PhCH_2OBpin$ was confirmed by observation of a ^{11}B NMR resonance at 22.8 ppm, and a characteristic ^{1}H NMR resonance for methylene moiety ($PhCH_2OBpin$) at 5.05 ppm.[8] The hydroboration of benzaldehyde reached completion after 7 hours, as shown in Table 3.1 (Entry 1).

Under the same conditions, the catalytic hydroboration of *para*-substituted benzaldehydes (methoxy-, bromo-, fluoro-, methyl-), mesitylaldehyde and isobutyraldehyde was monitored until completion by ^{1}H NMR spectroscopy, as shown in Table 3.1 and Figure 3.1.

Table 3.1: Catalytic hydroboration of aldehydes.



Entry	Aldehyde	Catalyst loading (%)	Time (h)	NMR yield (%)
1	Benzaldehyde	0.05	7	>99
2	4-Methoxybenzaldehyde	0.05	3.5	>99
3	4-Bromobenzaldehyde	0.05	12	>99
4	4-Fluorobenzaldehyde	0.05	1	>99
5	4-Methylbenzaldehyde	0.05	1	>99
6	Mesitaldehyde	0.05	2	>99
7	Isobutyraldehyde	0.05	1.5	>99

Reagents: 0.5 mmol aldehyde, 0.55 mmol HBpin. Reactions were performed at room temperature. ^{1}H NMR yields relative to internal standard HMCTS.

Reaction conditions: to a stock solution (500 μL C_6D_6, with 0.00025 mmol **2.11a**) in an NMR tube with J. Young NMR valve, was added neat aldehyde (ca. 0.5 mmol), then neat HBpin (80 μL, 0.55 mmol). The reaction was monitored by NMR spectroscopy until completion. All reagents were degassed and stored under an inert atmosphere as received.

Table 3.1 suggests the rates for hydroboration of *para*-substituted benzaldehydes fall in the order of R = F, Me > MeO > H > Br. On basis of this, it is difficult to draw a trend based on the electronic effect on the R substituents. The reaction rates of more sterically hindered mesitylaldehyde and isobutyraldehyde are slightly slower than 4-fluorobenzaldehyde and 4-methylbenzaldehyde but faster than 4-methoxybenzaldehyde, so the steric effect is not a significant factor. It is likely that the reaction process is complicated, affected by several factors, such as substrate purity, or that different reaction mechanisms are operative (these will be discussed in the coming sections).

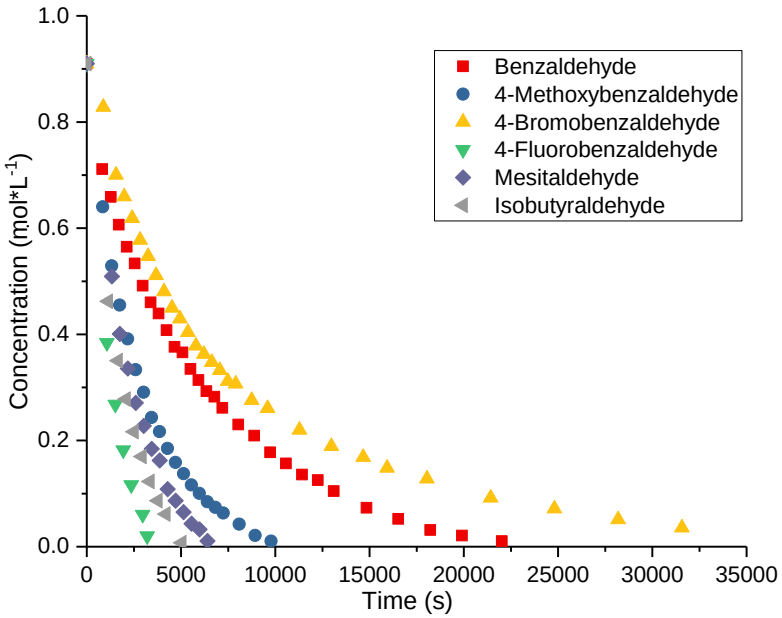


Figure 3.1: Concentration plots of aldehydes based on the relative integration to internal standard HMCTS in C_6D_6. To a stock solution (500 µL, with 0.00025 mmol **2.11a**), the neat aldehyde (ca. 0.50 mmol) was added, then neat HBpin (80 µL, 0.55 mmol). The volume of solution is approximated to 550 µL.

The turnover number (TON) for the catalytic hydroboration of aldehydes was determined to be about 2000, while the turnover frequency (TOF) was around 286 – 2000 h^{-1}. For the hydroboration of substituted benzaldehydes, the TOF of the tin hydride catalyst **1.48** developed by Jones was around 17−67 h^{-1}, while the analogous germanium system **1.47** showed a TOF of about 450−800 h^{-1}.[30] Our pre-catalyst **2.11a** has a comparable performance to this latter compound.

3.2.2 Control experiments for the hydroboration of aldehydes

In an effort to benchmark the results described in the previous section, we also explored the uncatalysed hydroboration of benzaldehyde.

Marks has previously reported that the reaction of benzaldehyde with HBpin in the absence of a catalyst reaches 11% conversion in the first hour,[37] which is in sharp contrast to a report by Hill, who observed only 2% conversion within first two hours.[38] A plausible explanation for these different reaction rates is that the precursors employed varied in purity. It is well-established that aldehydes can be oxidised by exposure to air.[39]

The oxidation of aldehydes to their corresponding carboxylic acids was first documented in 1832 by Liebig,[39] although it was not until more recently that Hutchings and co-workers reported a radical mechanism for the auto-oxidation of aldehydes (Figure 3.2).[40] They suggested that aldehydes could be oxidised through a radical mechanism and generate carbon-centred benzoyl radicals, PhCO·, and benzoylperoxy radicals, PhC(O)−OO·. Given these observations, it is important to understand whether radical species can affect the hydroboration rates of aldehydes.[41,42]

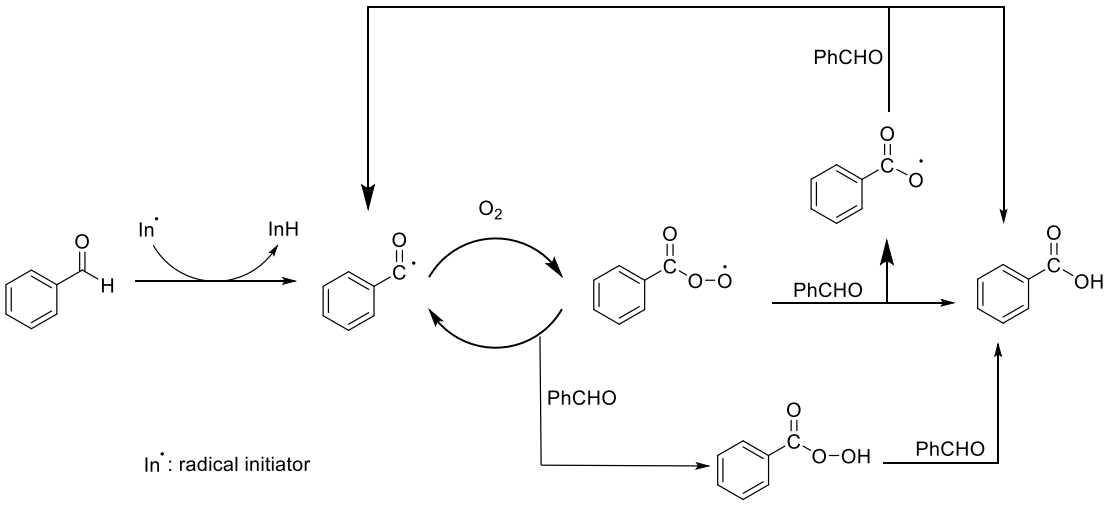


Figure 3.2: Proposed mechanism for auto-oxidation of benzaldehyde.[40]

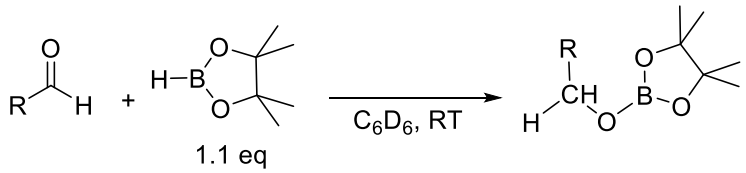
It is worth noting at this stage that Jin and Xue have shown that carboxylic acids can act as catalysts in hydroboration reactions,[43,44] hence aldehyde purity may play an important role in the overall rate of hydroboration

To investigate this, we explored the reactivity of two different batches of benzaldehyde toward HBpin. Batch **a** had been exposed to air for two years while the batch **b** was degassed as soon as it was received from the supplier. Without adding the catalyst, the reaction of HBpin with benzaldehyde from batch **a** (Table 3.2, Entry 1) reached completion and converted to $PhCH_2OBpin$ within 16 hours, while the batch **b** (Table 3.2, Entry 2) only showed 16% conversion after 42 hours. From the different reactivity observed, we can conclude that oxidised benzaldehyde (as benzoic acid or radicals) may be acting as a masked catalyst.

Similar reactivity was also observed for *para*-functionalised benzaldehydes. A batch of 4-methoxybenzaldehyde that had been exposed to air reached 36% conversion in 22 hours on reaction with HBpin, while 19% conversion was recorded for the less oxidised batch on the same time scale (Table 3.2; Entries 3−4). For the reaction of HBpin and 4-bromobenzaldehyde, 91% conversion was recorded within 25 hours for a batch exposed to air, while a fresh batch reached less than 2% conversion on the same time scale (Table 3.2; Entries 5−6).

In general, the reaction of air-exposed substrates (Table 3.2, Entries 1, 3, 5) are faster than samples that were degassed and stored under an inert atmosphere (Table 3.2, Entry 2, 4, 6), which suggests that aldehydes with a greater concentration of oxidised components react faster with HBpin. These results support the argument that presence of trace amount of carboxylic acid or radicals could facilitate the hydroboration of aldehydes.

Table 3.2: Comparison for different batches of aldehydes in hydroboration without catalyst.



Entry	Aldehyde	Catalyst loading (mol%)	Time (h)	NMR yield (%)
1	Benzaldehyde[a]	0	24	>99
2	Benzaldehyde[b]	0	42	16
3	4-Methoxybenzaldehyde[a]	0	22	36
4	4-Methoxybenzaldehyde[b]	0	42	19
5	4-Bromobenzaldehyde[a]	0	25	91
6	4-Bromobenzaldehyde[b]	0	42	<2.0

Reagents: 0.5 mmol aldehyde and 0.55 mmol HBpin. Reactions were performed at room temperature, ^{1}H NMR yields relative to internal standard HMCTS. [a]sample stored in air for two years, [b]sample degassed once received from supplier.

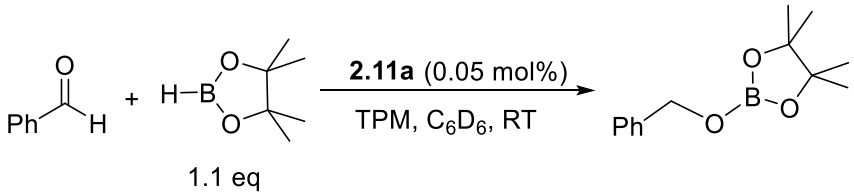
Reaction conditions: C_6D_6 (500 μL) in an NMR tube with J. Young NMR valve, was added neat aldehyde (ca. 0.5 mmol), then neat HBpin (80 μL, 0.55 mmol). The reaction was monitored by NMR spectroscopy until completion.

In order to rule out the effect of radicals in these catalytic runs a radical inhibitor was used to intercept acylperoxy radicals.[40] As HBpin is reactive towards unsaturated bonds and hydroxyl groups, the relatively inert triphenylmethane (TPM, 10 mol%) inhibitor was selected.

The results for the catalytic hydroboration of benzaldehyde without a radical inhibitor were compared to a batch with 10 mol% TPM. The reaction of the oxidised batch of benzaldehyde (Table 3.3: Entry 2) takes 71 mins to 99% conversion after the addition of TPM, in contrast to 5 mins without the radical inhibitor (Table 3.3: Entry 1). The reaction of the fresh batch of benzaldehyde (Table 3.3: Entry 4) takes 630 mins to reach 99% conversion after the addition of TPM, in contrast to 426 mins without adding TPM (Table 3.3: Entry 3). The addition of TPM slows the reaction rate in both cases, which supports the possibility that a tandem radical reaction pathway can take place in these systems. However, even after addition of TPM, the oxidised batch of benzaldehyde still

reacts significantly faster with HBpin than the degassed batch stored under an inert atmosphere. This suggests that other reactions mechanisms are possibly operative.

Table 3.3: Hydroboration of benzaldehyde with TPM.



Entry	Catalyst loading (mol%)	TPM loading (mol%)	Time (min)	NMR yield (%)
1[a]	0.05	0	5	>99
2[a]	0.05	10	71	>99
3[b]	0.05	0	426	>99
4[b]	0.05	10	630	>99

Reagents: 0.5 mmol aldehyde and 0.55 mmol HBpin. Reactions were performed at room temperature, ^{1}H NMR yields relative to internal standard HMCTS. [a]sample stored in air for two years, [b]sample degassed once received from supplier.

Reaction conditions: To a stock solution (500 μL C_6D_6, with 0.00025 mmol **2.11a**) in an NMR tube with J. Young NMR valve, was added neat aldehyde (ca. 0.5 mmol), then neat HBpin (80 μL, 0.55 mmol). The reaction was monitored by NMR spectroscopy until completion.

To conclude, reaction rates for the hydroboration of aldehydes heavily depend on the purity of the feedstocks. Aldehydes can form radicals once stored in air, and the radical trap TPM can significantly inhibit a radical mechanism which accelerates the rate with which aldehydes react with HBpin. However, aldehydes can also be oxidised in air to form carboxylic acids, which are also known as hydroboration catalysts. These competing reaction pathways highlight the difficulty associated with investigating the catalytic hydroboration of aldehydes. Hence, we moved our attention to substrates with increased stability towards oxidation, namely ketones.

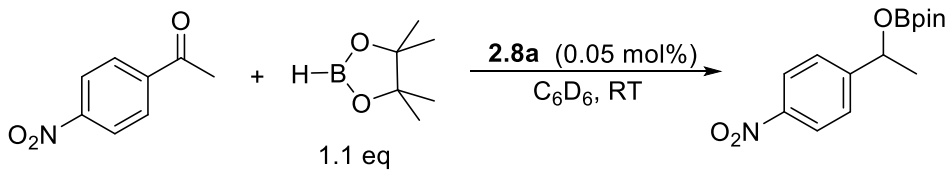
3.3 Gallium catalysed hydroboration of ketones

In Chapter one, the application of main group catalysts in hydroboration reactions was discussed. Of the catalysts discussed, it was noted that the gallium catalyst **2.11a** was

found to be active towards the hydroboration of aldehydes as well as more stable substrates, such as ketones. This prompted us to explore the use of our gallium alkoxide compounds as pre-catalysts for ketone reduction.

3.3.1 Catalytic hydroboration of ketones

A preliminary study was performed using one equivalent of 4′-nitroacetophenone, 1.1 equivalents of HBpin and 0.05 mol% pre-catalyst of **2.8a** in C_6D_6 solution at room temperature (Scheme 3.4).



Scheme 3.4: Catalytic hydroboration of 4′-nitroacetophenone.

The reaction was monitored by ^{1}H NMR spectroscopy for consumption of 4′-nitroacetophenone and formation of the borate ester. After 10 hours, nearly full conversion of 4′-nitroacetophenone to the corresponding borate ester $CH_3C(H)(OBpin)C_6H_4NO_2$ was recorded (Figure 3.3).

A concentration plot of HBpin, 4′-nitroacetophenone and the borate ester was generated (Figure 3.4). From inspection of this figure, it appears that the catalytic run reached 50% conversion around 3 hours, and 99% conversion around 9 hours. The reaction rate was roughly consistent during the first 10% conversion, and gradually decreased when the concentration of reactants decreased.

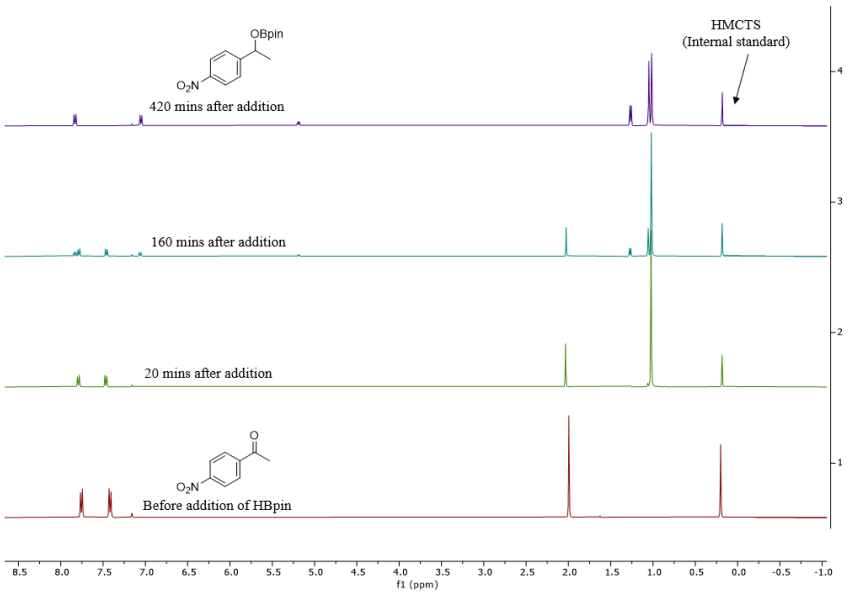


Figure 3.3: Monitoring the hydroboration of 4′-nitroacetophenone with HBpin in C_6D_6. The signals at 2.00, 7.42 and 7.76 ppm correspond to 4′-nitroacetophenone, the resonances at 1.27, 5.19, 7.05 and 7.83 ppm correspond to the hydroborated product. HMCTS was used as an internal standard (resonance at 0.18 ppm).

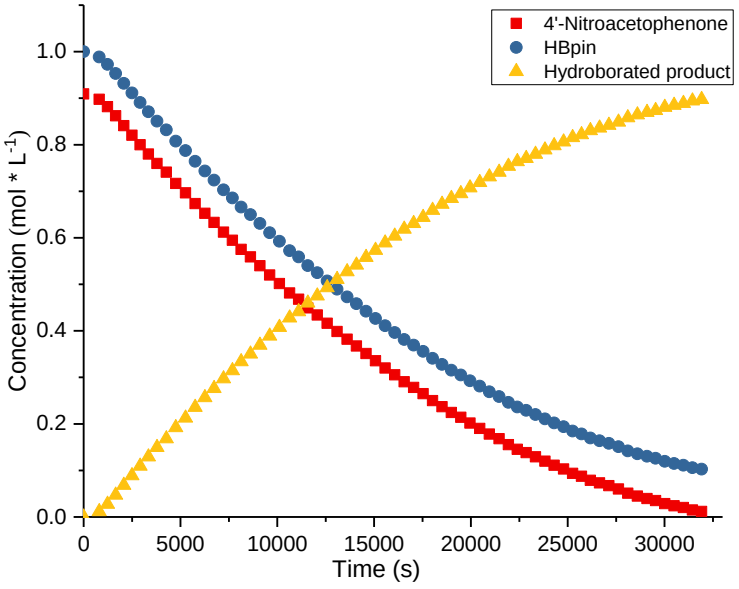
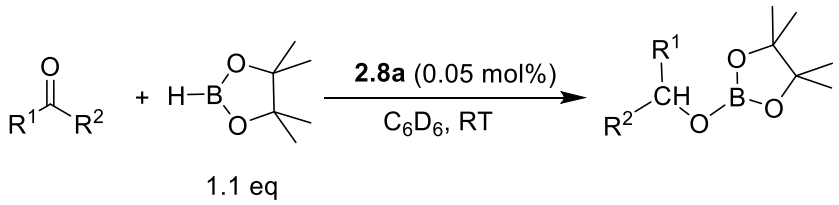


Figure 3.4: Concentration plots based of the hydroboration of 4′-nitroacetophenone with HBpin in C_6D_6. To a stock solution (500 µL C_6D_6, with 0.00025 mmol **2.8a**), neat 4′-nitroacetophenone (ca. 0.5 mmol) was added, followed by HBpin (80 µL, 0.55 mmol).

The scope of ketone substrates was extended to examine the functional group tolerance of catalyst **2.8a**. Ketones were stirred with 1.1 equivalents of HBpin in an anhydrous C_6D_6 solution containing 0.05 mol% **2.8a** for 10 hours. This afforded nearly quantitative amounts of the corresponding borate esters (Table 3.4). These results suggest catalyst **2.8a** has good tolerance towards functional groups, such as halogens (X = Cl, Br, I), nitro and methoxy groups.

Table 3.4: Scope of gallium-catalysed hydroboration of ketones.



Entry	R^1	R^2	Catalyst loading (mol%)	NMR Yield (%)
1	4-NO_2-C_6H_4	Me	0.05	99
2	C_6H_5	Me	0.05	99
3	4-OMe-C_6H_4	Me	0.05	92
4	4-Br-C_6H_4	Me	0.05	99
5	4-Cl-C_6H_4	Me	0.05	99
6	4-I-C_6H_4	Me	0.05	98

Reagents: 0.5 mmol ketone and 0.55 mmol HBpin. Reactions were performed at room temperature for ten hours. ^{1}H NMR yields relative to internal standard HMCTS.

Reaction conditions: to a stock solution (500 μL C_6D_6, with 0.00025 mmol **2.8a**) in an NMR tube with J. Young NMR valve, was added neat ketone (ca. 0.5 mmol), then neat HBpin (80 μL, 0.55 mmol). The reaction was monitored by NMR spectroscopy until completion. All reagents were degassed and stored under inert atmosphere as received.

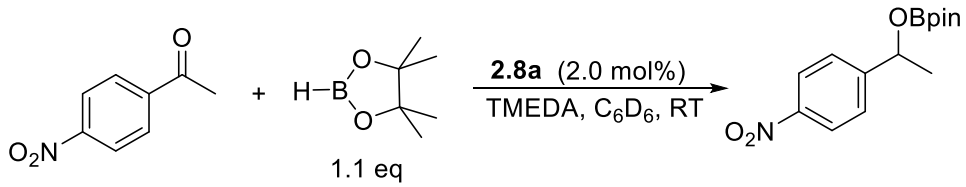
Complex **2.8a** acts as a pre-catalyst for the catalytic hydroboration of ketones even at low catalyst loadings (0.05 mol%). It is important to clarify that without the presence of catalyst, the reaction of ketones and HBpin is much slower. Control experiments of ketones with HBpin in the absence of **2.8a** were carried out and revealed less than 1% conversion in the first 24 hours.

3.3.2 Inhibition of ketone hydroboration by tetramethylethylenediamine (TMEDA)

Nucleophiles, such as NaOH, ^{t}BuOK and NaH, have previously been reported by Wu et al. as catalysts for the hydroboration of aldehydes, ketones, alkenes and alkynes.[45] However, more recently, Thomas and co-workers proposed that the nucleophile could induce the decomposition of HBpin to afford BH_3 and B_2pin_3, and that BH_3 is in fact the catalytically active species in these hydroboration reactions.[46] In order to rule out the role of BH_3 in our catalytic runs, tetramethylethylenediamine (TMEDA) was added to the reaction mixture, as it can bind to BH_3 and inhibit its role in catalysis.[47]

In a typical experiment, a C_6D_6 solution with 2.0 mol% catalyst **2.8a**, 20 mol% TMEDA and 1.1 equivalents of HBpin was reacted with 4′-nitroacetophenone. The reaction was monitored by ^{1}H NMR spectroscopy, which indicated that in the presence of TMEDA the conversion in the first one hour decreases from 99% to 62% (Table 3.5).

Table 3.5: TMEDA experiment for gallium-catalysed hydroboration of 4′-nitroacetophenone.



Entry	Ketone	Catalyst loading (mol%)	Time (h)	NMR Yield (%)
1	4′-Nitroacetophenone	2.0	1	99
2[a]	4′-Nitroacetophenone	2.0	1	62

Reagents: 0.5 mmol 4′-nitroacetophenone and 0.55 mmol HBpin. Reactions performed at room temperature. ^{1}H NMR yields relative to internal standard HMCTS. [a]With 0.1 mmol TMEDA.

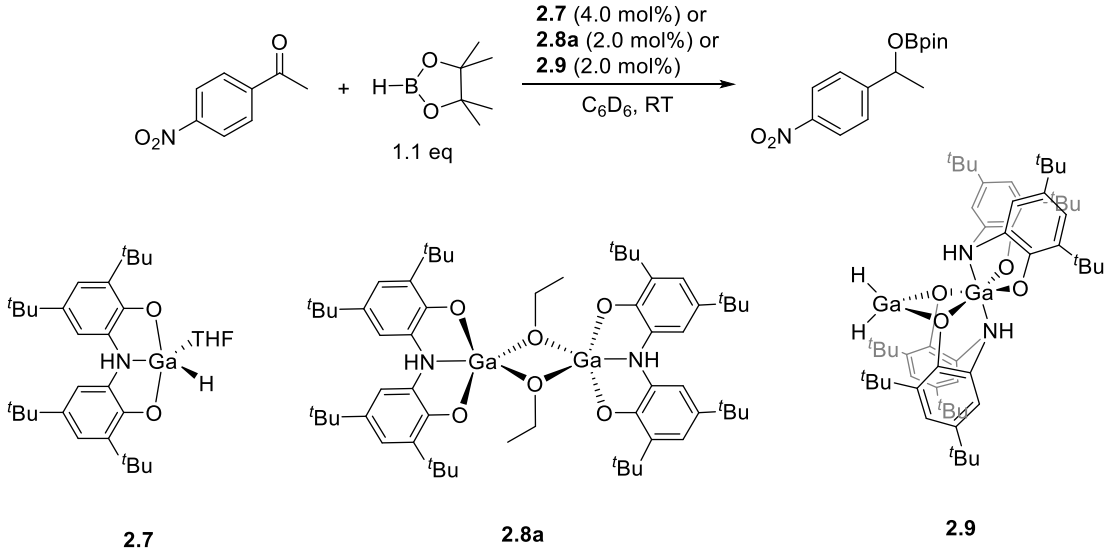
Reaction conditions: to a stock solution (500 μL C_6D_6, with 0.01 mmol **2.8a**) in an NMR tube with J. Young NMR valve, was added neat 4′-nitroacetophenone (ca. 0.5 mmol), then neat HBpin (80 μL, 0.55 mmol). All reagents were degassed and stored under an inert atmosphere as received.

Although the conversion decreased in the presence of TMEDA, 62% conversion of the 4′-nitroacetophenone (in the first one hour) still supports the role of a gallium complex

as the ‘true’ hydroboration catalyst. We believe that the decreased activity observed in the presence of TMEDA is due to the fact that it can bind to the active gallium catalyst, and affect the reactivity.

3.3.3 Monitoring of hydroboration of 4′-nitroacetophenone with different catalysts

As described in earlier sections, we have shown that compound **2.8a** can act as a pre-catalyst for the hydroboration of aldehydes and ketones. From Chapter Two, we know that the reaction of HBpin with **2.8a** affords gallium dihydride complex **2.9**, and complex **2.9** can give rise to a monomeric gallium hydride (**2.7**) when reacted with tetrahydrofuran. It is likely that during catalysis our pre-catalyst first reacts with the borane to generate a gallium hydride intermediate. To support this argument, three different gallium complexes **2.7**, **2.8a** and **2.9** were studied under the same catalytic conditions and monitored by ^{1}H NMR spectroscopy (Scheme 3.5).



Scheme 3.5: Catalytic hydroboration of 4′-nitroacetophenone by three different catalysts.

The reactions are monitored by ^{1}H NMR until the reaction was completed (all the 4′-nitroacetophenone consumed). Concentration plots were made based on the integration of the reactant (4′-nitroacetophenone) and product (the corresponding borate ester) relative to HMCTS, as shown in Figure 3.5. The three plots are largely identical, which suggests under catalytic conditions a similar mechanism is operable involving the same catalytically active species.

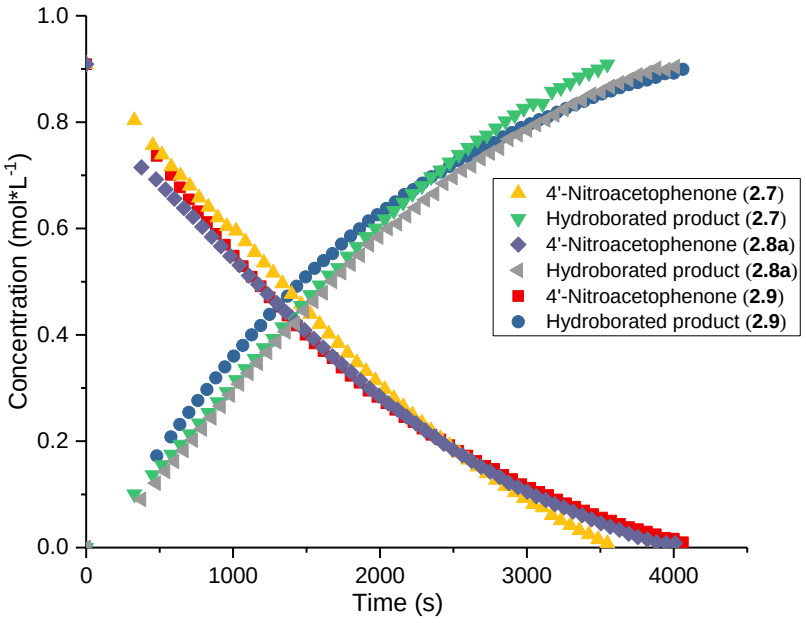


Figure 3.5: Concentration plots based on integration of the hydroboration of 4′-nitroacetophenone with HBpin in C_6D_6.

Intermediates A−C were detected by ^{1}H NMR spectroscopy during the reactions, and their resonances are listed in Table 3.6 (Entry 5−7). For comparison, the ^{1}H NMR chemical shifts of **2.7**, **2.7**·1.5BH_3:py, **2.8a**, **2.9I** and **2.12e** are also listed in Table 3.6.

On basis of the ^{1}H NMR spectra, we can conclude that intermediates A−C are largely similar, and we reasoned that they are monomeric gallium hydrides. In all likelihood,

this is that the catalytically active species present when different pre-catalysts **2.7**, **2.8a** or **2.9** are used.

Table 3.6: ^{1}H NMR chemical shift of gallium complexes and intermediates

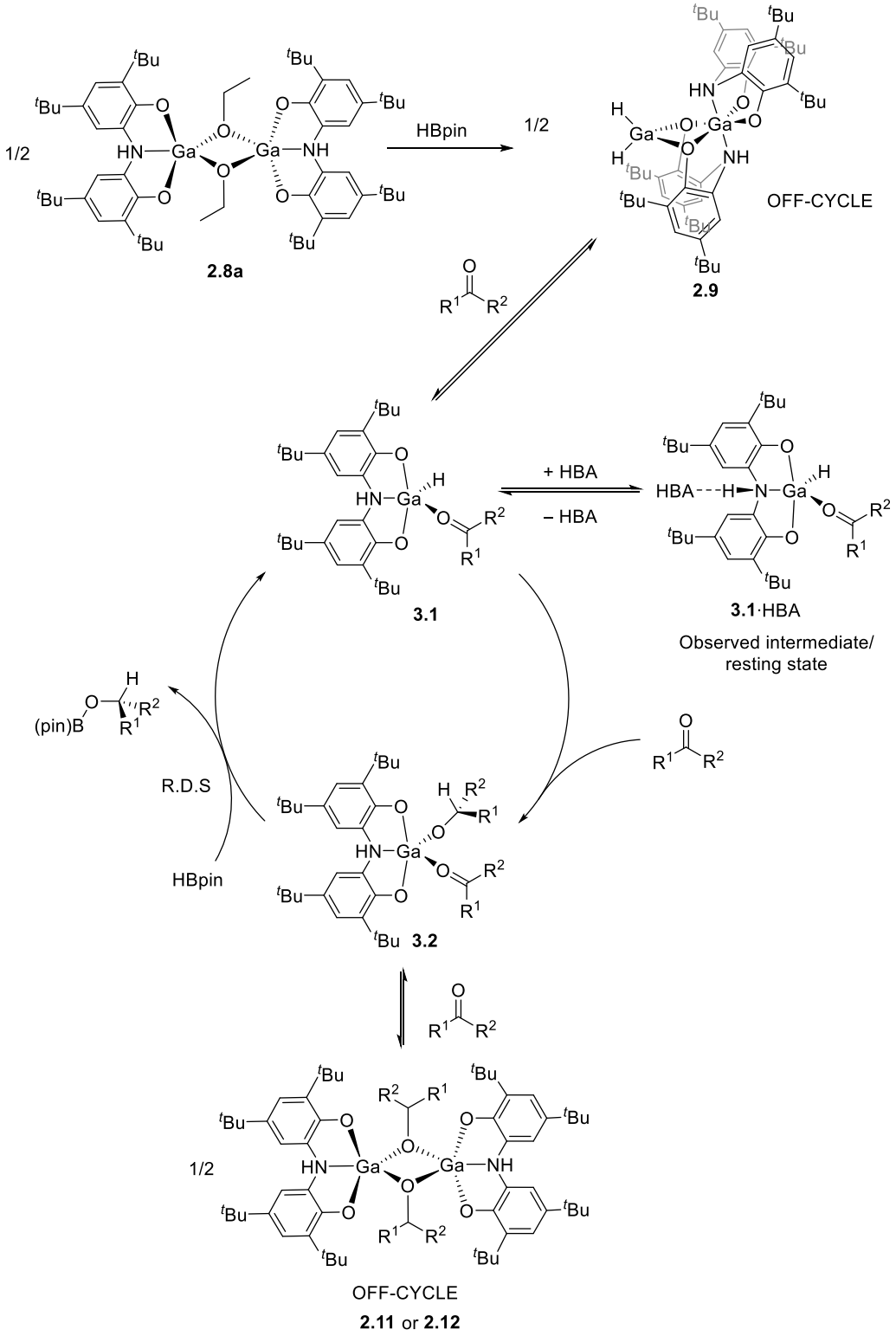
		^{1}H NMR chemical shift in C_6D_6 solution					
Entry	Compound	Ga−H (ppm)	N−H (ppm)	ArH (ppm)		*tert*-butyl (ppm)	
1	**2.7**	5.65	3.92	7.35	7.15	1.59	1.35
2	**2.7**·1.5BH_3:py	5.67	4.01	7.35	7.20	1.59	1.35
3	**2.8a**	N/A	4.70	7.46	7.42	1.40−1.29	
4	**2.9$_I$**	5.55	4.02	7.32	7.05	1.58	1.30
5	Proposed Intermediate A[a]	5.65	5.12	7.39	7.29	1.52	1.31
6	Proposed Intermediate B[b]	5.76	5.68	7.40	7.29	1.51	1.30
7	Proposed Intermediate C[c]	5.75	5.84	7.42	7.30	1.51	1.30
8	**2.12e**	N/A	3.90	7.86, 7.42	7.36, 7.26	1.58, 1.55	1.33, 1.28

Intermediate A, B, C are monitored by ^{1}H NMR spectroscopy through the process of hydroboration of 4′-nitroacetophenone using different catalysts. [a] Using catalyst **2.7**, [b] Using catalyst **2.8a**, [c] Using catalyst **2.9**.

3.3.4 A simplified proposed mechanism for the hydroboration of aldehydes and ketones

A simplified mechanistic model for gallium catalysed hydroboration (using **2.8a** as catalyst) was proposed involving: (i) the reaction of HBpin with **2.8a** to generate the gallium dihydride **2.9**, (ii) monomerisation of **2.9** to a base-stabilised gallium monohydride species **3.1** in the presence of a nucleophile, (iii) insertion of the C=O bond into the Ga−H bond of **3.1** to form gallium alkoxide complexes **3.2**, (iv) σ-metathesis of the Ga−O bond with HBpin to regenerate **3.1** and liberate the borate ester (Scheme 3.6). It is worth noting that **2.9** and **2.11** (or **2.12**) are all off-cycle species. Stochiometric reactions indicate that the reactions of **2.9** with ketones and the reaction of **2.12** with HBpin are slow, so these species are unlikely to be the active catalysts. Instead, a monomeric gallium hydride species is observed as the resting state during catalysis (Table 3.6, Entry 5−7). A downfield-shifted ^{1}H NMR resonance attributed to the amine ligand backbone suggests that the amine-proton on **3.1** is interacting with

hydrogen bonding acceptor (HBA). Thus, the structure for the observed intermediate is proposed as **3.1**·HBA.



Scheme 3.6: Proposed mechanism for hydroboration of aldehydes and ketones.

Several attempts were made to isolate intermediate **3.1** or **3.2** (Scheme 3.6), for example, by reacting **2.9** with 1 equivalent of ketone, or reacting **2.8a** with 1 equivalent of HBpin. However, the reaction of **2.8a** with 1 equivalent of HBpin only gives 0.5 equivalents of **2.9** (with the other half of an equivalent of **2.8a** remaining unreacted). When reacting **2.9** with 1 equivalent of ketone, only 50% of **2.9** converts to the corresponding stable bis(alkoxide) bridged gallium complex **2.12**. In the future, some extremely bulky ketones could be used to see if a monohydride can be isolated.

3.3.5 Kinetic studies for the hydroboration of ketones

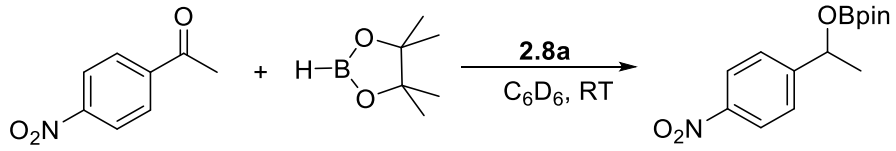
In 2016, Burés proposed a graphical method (variable time normalization analysis) to determine the average kinetic order of reactants for catalytic reactions by directly comparing the concentration profiles.[48,49] Using this method, the kinetic concentration effect of each substrate is removed. Employing the correct macroscopic reaction orders α, β, γ, the graphical representation of the concentration of product vs. the normalized time-axis will show overlaid straight lines with the slope corresponding to k_{obs}. As it employs the entire reaction trace and is a multi-point comparison, this method is fast and easy to use, requiring fewer experiments.

In the case of our particular system (Table 3.7), the kinetic orders α (for the concentration of ketone), β (for the concentration of HBpin), γ (for the concentration of catalyst) in the hydroboration can be written as an equation (1).

$$[\mathrm{P}] = k_{obs} \int [Ketone]^{\alpha} \times [HBpin]^{\beta} \times [Ga]^{\gamma} dt \quad (1)$$

For the kinetic study, four experiments with a matrix of different concentrations of ketone, HBpin and **2.8a** were undertaken (as listed in Table 3.7). The reactions were monitored by ^{1}H NMR spectroscopy.

Table 3.7: Reaction conditions for kinetic studies.



Experiment	4′-nitroacetophenone (mol·L^{-1})	HBpin (mol·L^{-1})	2.8a (mol·L^{-1})
A	0.910	1.0	0.000454
B	0.455	1.0	0.000454
C	0.455	0.8	0.000454
D	0.455	1.0	0.000363

By adjusting individual reaction orders in the profile, a pseudo-zero order in concentration of ketone, and first order in catalyst and HBpin was determined (Figure 3.6, first set of reaction orders). A better fit was obtained by adjusting the order of ketone to 0.1 (second set of reaction order).

$$\text{First set of reaction orders } [P] = k_{obs1} \int [Ketone]^0 \times [HBpin]^1 \times [Ga]^1 dt$$

$$\text{Second set of reaction orders } [P] = k_{obs2} \int [Ketone]^{0.1} \times [HBpin]^1 \times [Ga]^1 dt$$

In a combination of the proposed mechanism and kinetic studies, the reaction of **3.2** with HBpin is the rate determining step, while the insertion of ketone into gallium-hydride of **3.1** to form **3.2** is a fast step (Scheme 3.6). With this result in hand, we are going to use the simulation studies to acquire possible reaction rates for each step.

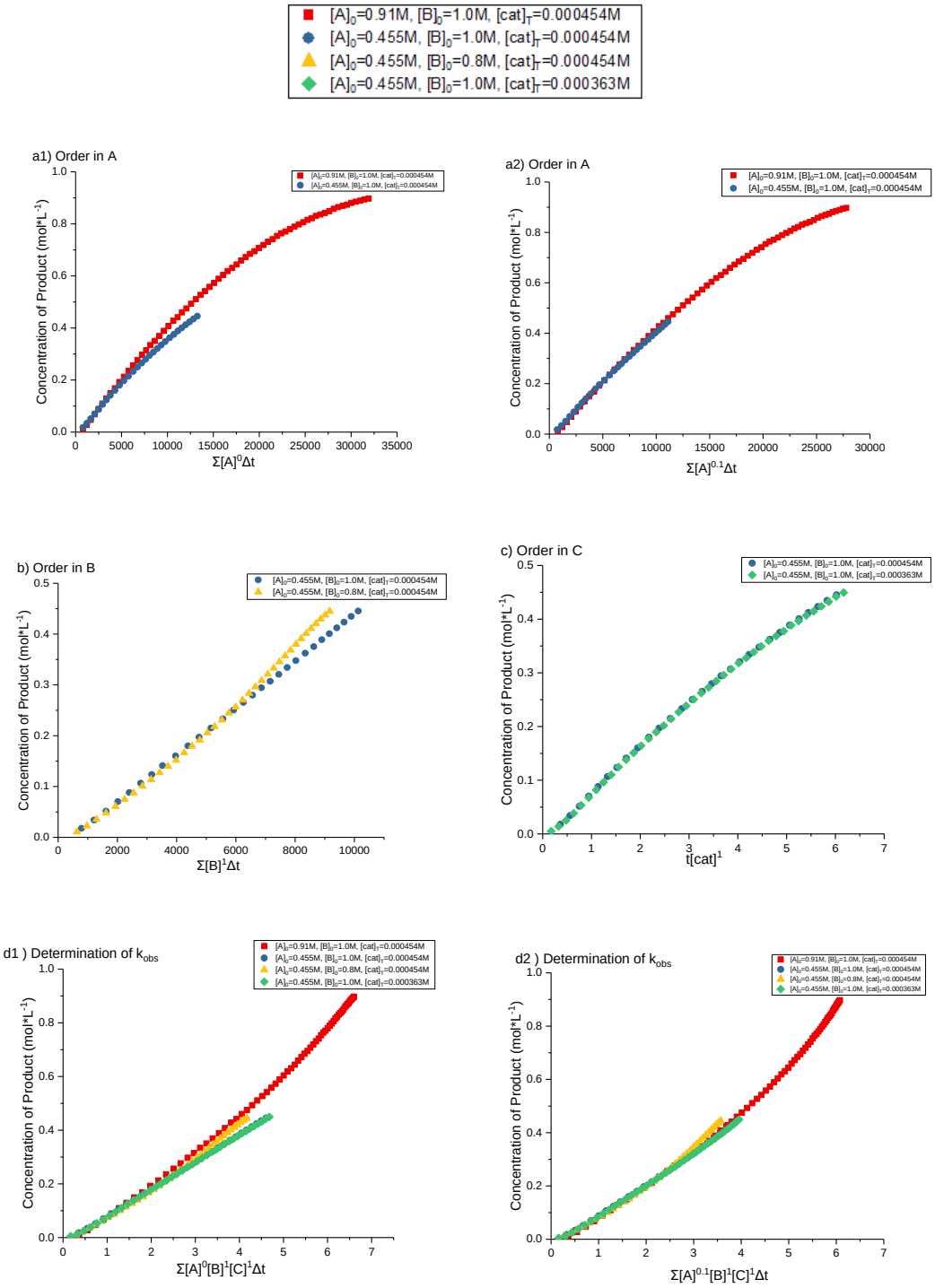


Figure 3.6: Variable time normalization analysis of the kinetic profiles, a1, b, c and d1 are order obtained with the method, while a2 and d2 are mathematical representations of the experimental values. [A] = concentration of 4′-nitroacetophenone, [B] = concentration of HBpin, $[cat]_T$ = concentration of pre-catalyst **2.8a**. Concentration were recorded via the ^{1}H NMR spectra integration of the product relative to an internal standard. For accurate integration, d1 has been changed to 35s.

3.3.6 Simulation studies for the hydroboration of ketones

A mathematical fit of the data presented in Figure 3.5 using COPASI (Complex Pathway Simulator) was used to determine viable rates for the mechanistic model described in Section 3.3.4, as Figure 3.7 and Figure 3.8.[48,49]

In a typical experiment a C_6D_6 (500 μL) solution containing 4′-nitroacetophenone (0.5 mmol), complex **2.7** (0.02 mmol, 4.0 mol%) and HMCTS (0.05 mmol) was reacted with HBpin (0.05 mmol).

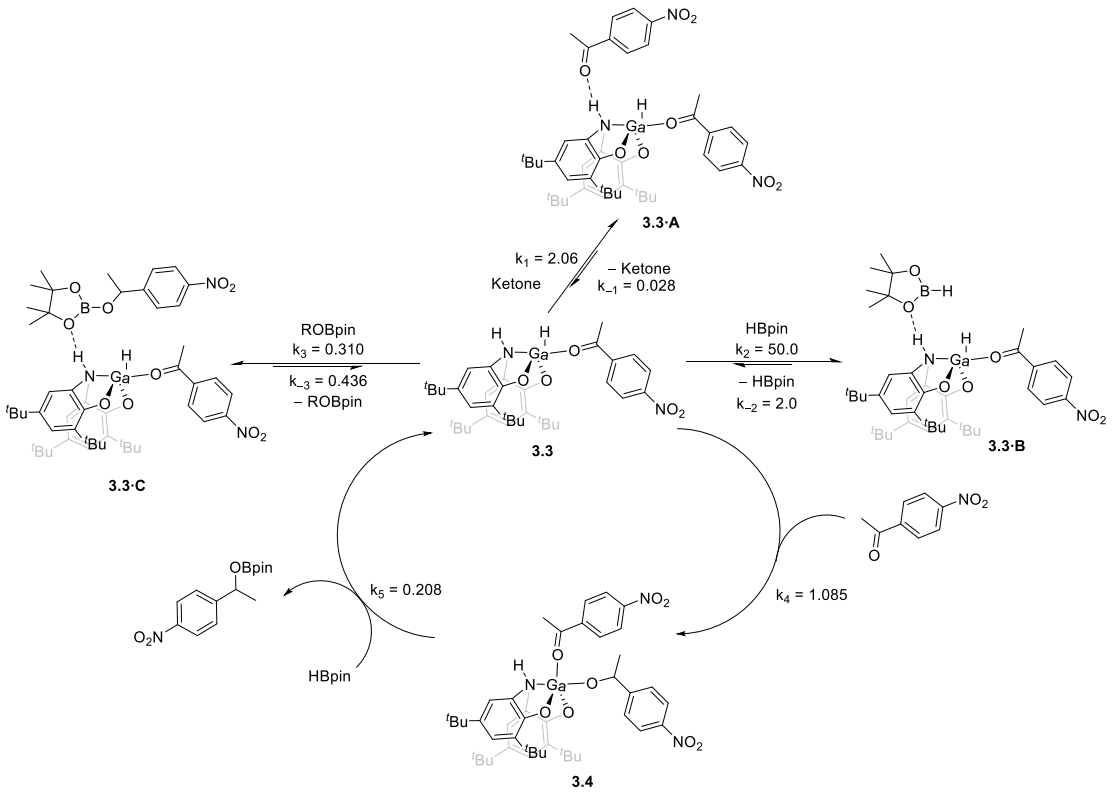


Figure 3.7: Proposed working model with kinetic constants based on simulation studies for hydroboration of ketone (4′-nitroacetophenone) derived from a COPASI fit.

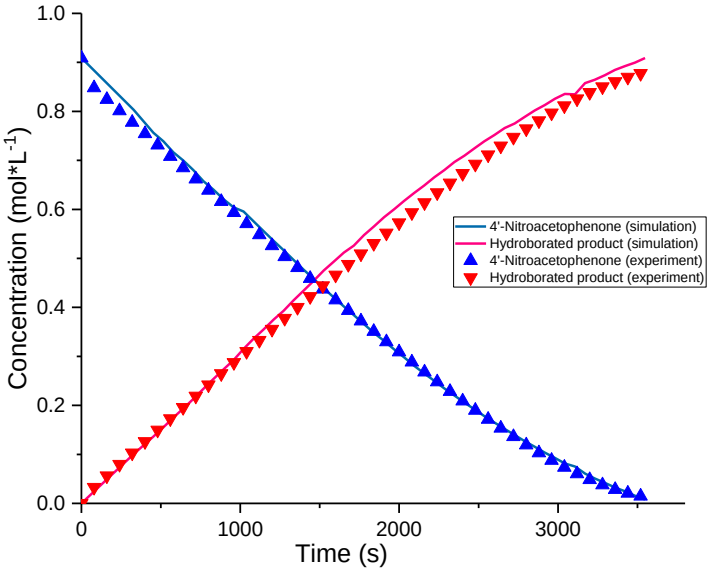


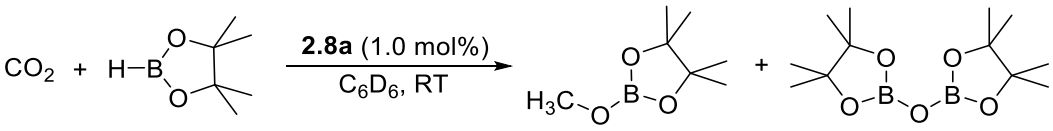
Figure 3.8: Concentration plots for hydroboration of 4′-nitroacetophenone based on experimental results and simulation by COPASI.

The simulation studies (Figure 3.7) suggest that the reaction of HBpin with **3.4** is the rate determining step in the catalytic cycle, with a reaction rate constant k_5 as 0.208 ($mL \cdot mmol^{-1} \cdot s^{-1}$), while the carbonyl insertion step has a rate constant k_4 as 1.085 ($mL \cdot mmol^{-1} \cdot s^{-1}$), which matches the experimental finding of the observed rate law as $k[HBpin]^1[ketone]^0[catalyst]^1$ based on experiments. Besides, complex **3.3** is likely to be in solution equilibria with hydrogen bond acceptors such as HBpin and 4′-nitroacetophenone as **3.3**·HBA.

3.4 Catalytic hydroboration of carbon dioxide

Given that we demonstrated hydroboration of ketones, we decided to expand these reactivities to the catalytic reduction of CO_2.

The hydroboration of CO_2 was attempted with **2.8a** (1.0 mol%), using one equivalent of HBpin and 2 bar of CO_2 (excess) at room temperature in C_6D_6, and the reaction was monitored by ^1H NMR spectroscopy (Scheme 3.7).



Scheme 3.7: Catalytic hydroboration of carbon dioxide.

In accordance with literature reported chemical shifts, the formation of MeOBpin is supported by the presence of singlet resonances at 1.04 and 3.50 ppm (Figure 3.9) in the ^1H NMR spectrum, and a resonance at 22.7 ppm (Figure 3.10) in the ^{11}B NMR spectrum.[32] Another product, $O(Bpin)_2$ was observed as a singlet resonance at 1.01 ppm in the ^1H NMR spectrum, and at 21.8 ppm in the ^{11}B NMR spectrum as well as two resonances at 24.67 and 82.94 ppm in the $^{13}C\{H\}$ NMR spectrum. The reaction reached full conversion within 38 hours, which gives a turnover frequency of 2.6 h^{-1}.

To summarise, catalyst **2.8a** (1.0 mol%) has been successfully employed in the catalytic hydroboration of carbon dioxide to a methanol equivalent. It is the first time that a gallium catalyst has been found to catalyse this transformation at room temperature. The reaction gave an overall turnover frequency (TOF) of 2.6 h^{-1} at room temperature, which outperformed Aldridge's gallium catalyst (2.4 h^{-1}, at 60 °C).[32] The performance of catalyst **2.8a** is comparable to Jones' germanium catalyst (TOF = 2.1 h^{-1}), yet somewhat slower than the analogous tin system (TOF = 14.5 h^{-1}), both of which operated at room temperature.[27,32]

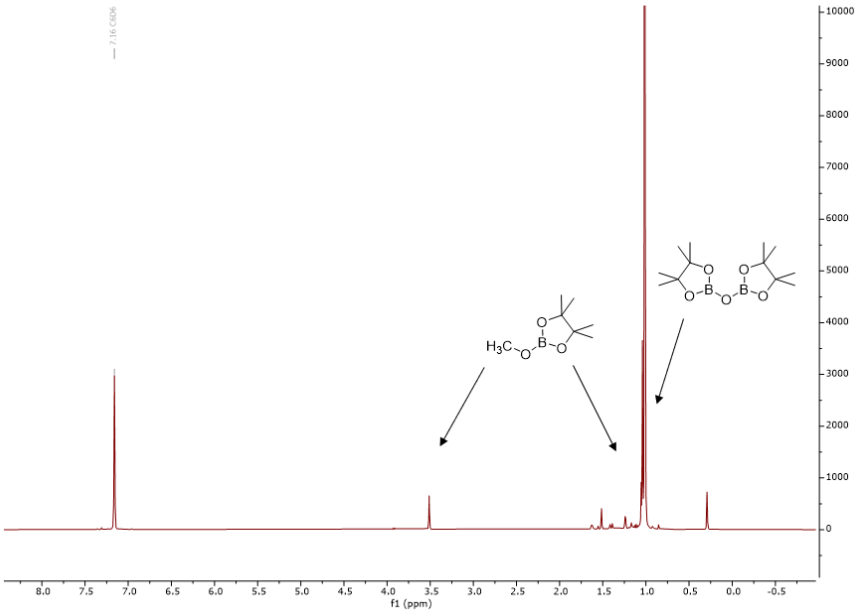


Figure 3.9: ^{1}H NMR spectrum of the hydroboration product of carbon dioxide. Singlet resonances at 1.04 and 3.50 ppm correspond to CH_3OBpin, the resonance at 1.01 ppm corresponds to $O(Bpin)_2$.

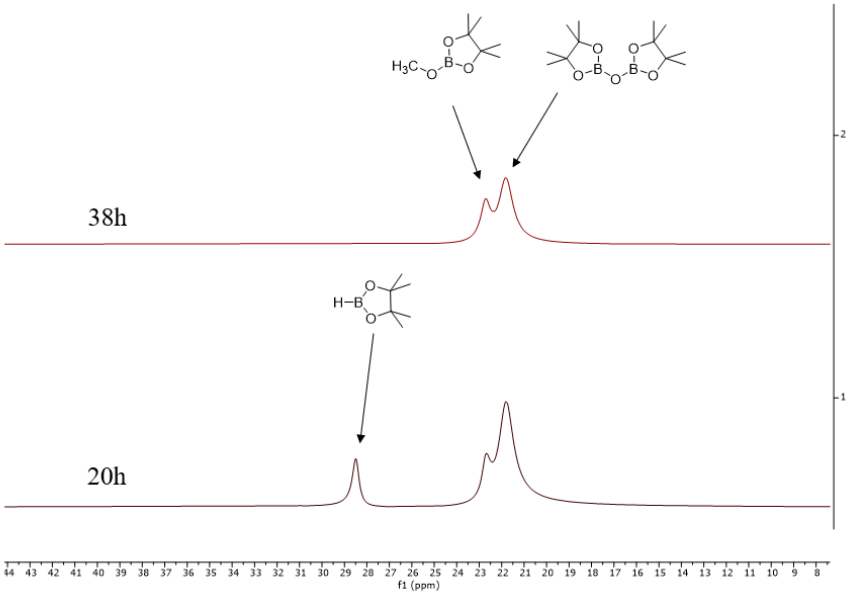
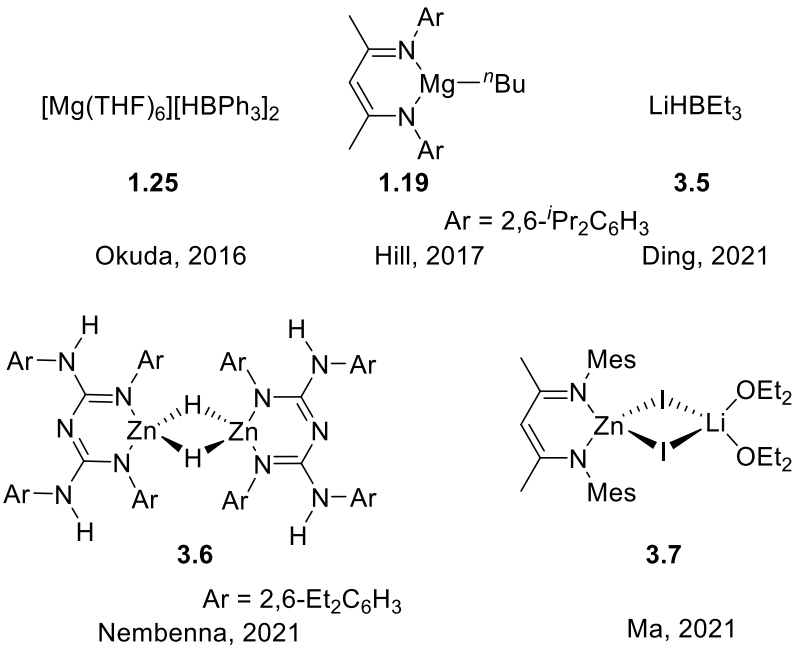


Figure 3.10: Stacked $^{11}B\{^{1}H\}$ NMR spectra for the hydroboration of carbon dioxide at 20 h and 38 h. Conditions: Neat HBpin (0.093 mmol) was added to a stock solution of C_6D_6 (0.5 mL) with **2.8a** (0.00093 mmol) under 2 bar CO_2 at room temperature. The resonance at 22.7 ppm corresponds to CH_3OBpin, while that at 21.8 ppm corresponds to $O(Bpin)_2$.

3.5 Catalytic hydroboration of isocyanates

In contrast to the relatively large number of studies focused on the catalytic hydroboration of aldehydes and ketones using main group hydrides, examples of catalytic hydroboration of other substrates, such as isocyanates, are scarce.

To the best of our knowledge, only a handful of examples of the catalytic hydroboration of isocyanates have been reported (Scheme 3.8). The first example was reported by Okuda in 2016, who demonstrated that the magnesium catalyst $[Mg(THF)_6][HBPh_3]_2$ **1.25** could be used for the hydroboration of ^{t}BuNCO, although only one substrate was studied and the operation mechanism is unclear.[50] In 2017, Hill and coworkers demonstrated the use of (^{Dipp}Nacnac)Mg(^{t}Bu), **1.19**, in the catalytic hydroboration of isocyanates, which is the first systematic study of this transformation.[6] In 2021, Ding, Nembenna and Ma developed lithium (**3.5**), zinc (**3.6**), and bimetallic lithium-zinc (**3.7**) catalysts for the hydroboration of isocyanates.[51–53]

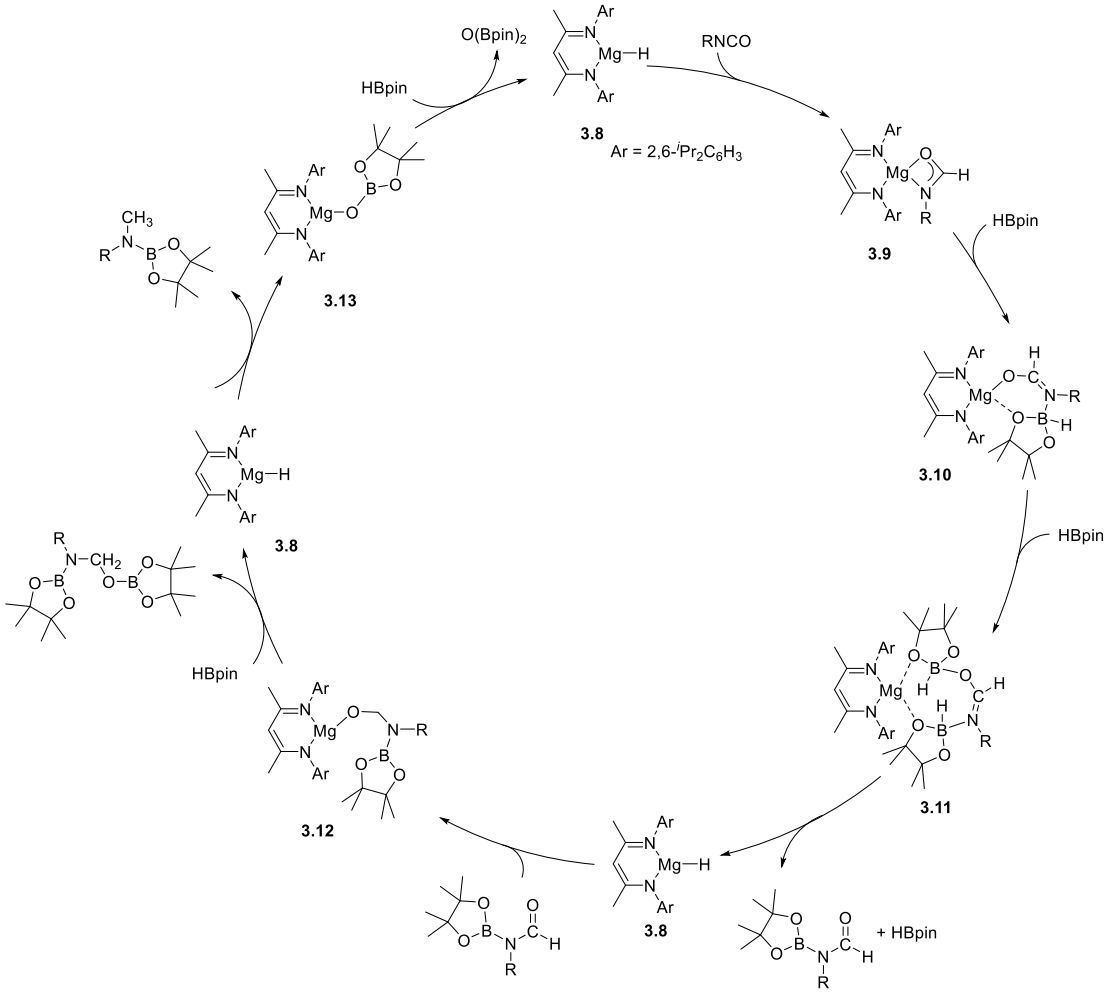


Scheme 3.8: Reported catalysts for the catalytic hydroboration of isocyanates.[6,50–53]

A mechanistic study on the activity of (^{Dipp}Nacnac)Mg(^{n}Bu) (**1.19**, 5−10 mol%) was performed by Hill and co-workers (Scheme 3.9).[6] The magnesium hydride **3.8** (^{Dipp}Nacnac)Mg(H) was first generated by reaction of (^{Dipp}Nacnac)Mg(^{n}Bu) with HBpin. Subsequent reaction of **3.8** with RNCO affords a magnesium formamidate species **3.9**. The reaction of **3.9** with HBpin affords **3.10** as the product, which could further react with HBpin to regenerate magnesium hydride, **3.8**, and generate an *N*-borylated formamidine, RN(Bpin)CH(O) as a product. Compound RN(Bpin)CH(O) is not stable under the catalytic conditions and continues to reach with magnesium hydride **3.8** to give two other products, *N*-,*O*-bis(boryl)hemiaminal, RN(Bpin)CH_2O-Bpin and *N*-borylated methylamine, MeN(R)Bpin.[6] The limitation of this system is that it requires relatively high temperatures (60 °C) for the activation of *N*-aliphatic isocyanates (to give MeN(R)Bpin). Aromatic isocyantes, such as DippNCO and MesNCO, can be selectively hydroborated to RN(Bpin)CH_2OBpin at room temperature.

In 2021, Nembenna and co-workers reported a zinc hydride catalyst **3.6** which can selectively hydroborate isocyanates (at 2 mol% loading) to *N*-borylated formamides, RN(Bpin)CH(O) at room temperature. At elevated temperatures, 70 °C, the substrates can be fully hydroborated to *N*-borylated methylamine, MeN(R)Bpin.[52]

Despite these advances, the room temperature hydroboration of isocyanates to *N*-borylated methylamines with low catalyst loadings remains a challenge. As complex **2.8a** was shown to act as a catalyst for the hydroboration of carbonyls, we decided to explore its activity in the catalytic reduction of isocyanates.

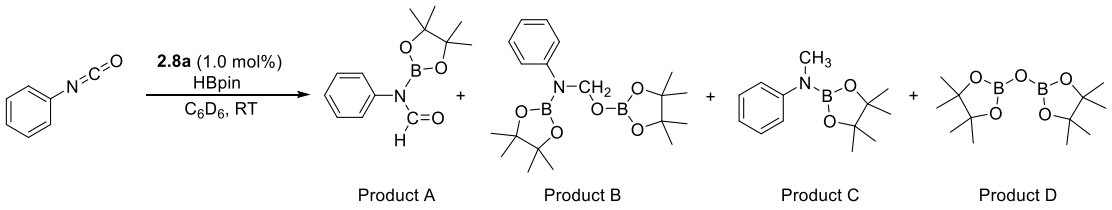


Scheme 3.9: Proposed mechanism for the magnesium catalysed hydroboration of isocyanates.[6]

3.5.1 Catalytic hydroboration of isocyanates

In principle, the hydroboration of phenyl isocyanate can afford four products: PhN(Bpin)CH(O) (product A), PhN(Bpin)CH_2OBpin (product B), MeN(Ph)Bpin (product C) and O(Bpin)$_2$ (product D) (Scheme 3.10). With the aim of establishing whether **2.8a** could selectively catalyse the hydroboration of isocyanates, the reaction of phenyl isocyanate (PhNCO) and one equivalent of HBpin was carried at room temperature with **2.8a** (1 mol%). After 16 hours, the identifiable products in the ^{1}H NMR spectrum were PhN(Bpin)HC(O) (35%), PhN(Bpin)CH_2OBpin (13%) and MeN(Ph)Bpin (13%). No selectivity was observed in this case.[54] To the mixture,

another equivalent of HBpin was added and the reaction was monitored for a further 16 hours, which revealed the presence of PhN(Bpin)CH(O) (7%), PhN(Bpin)CH_2OBpin (26%) and MeN(Ph)Bpin (47%). This suggests an accumulation of PhN(Bpin)CH_2OBpin, indicating that all three products are all stable intermediates under catalytic conditions (as Scheme 3.10).



Scheme 3.10: Gallium catalysed hydroboration of phenyl isocyanate.

This multiple-step process was monitored by solution phase ^{1}H NMR spectroscopy (Figure 3.11). A concentration plot of the different products as a function of time was generated by determining the relative concentrations of phenyl isocyanate and the products (A−C) against internal standard HMCTS, as shown in Figure 3.12. The plot suggests that products A−C were generated almost simultaneously. Phenyl isocyanate was fully consumed within 14 h, the concentration of product A reached a maximum after approximately 6 h and was fully consumed after 14 h. Product B reached highest concentration after approximately 8 h, then gradually decreased and converted to product C.

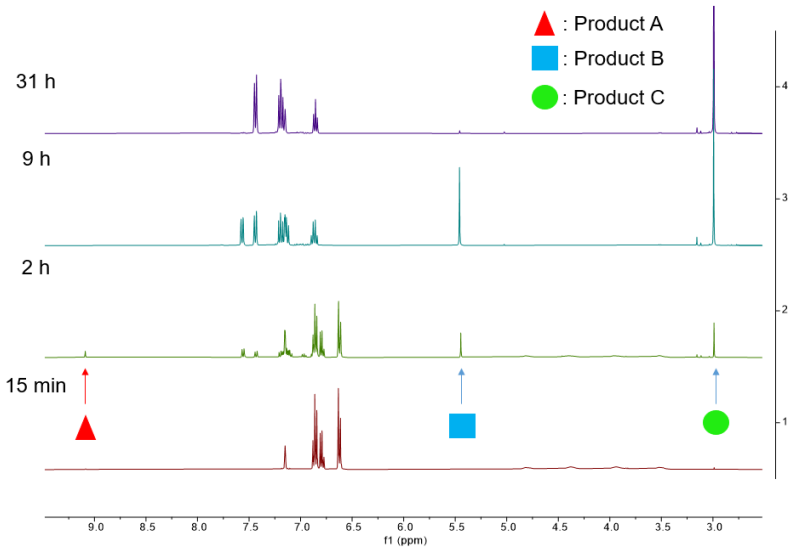


Figure 3.11: Stacked ^{1}H NMR spectra of the reaction between PhNCO and HBpin in the presence of **2.8a** (1 mol%) after 15 mins, 2 h, 9 h and 31 h. Reaction conditions: 0.2 mmol of phenyl isocyanate and 0.05 mmol of HMCTS were added to 0.62 mmol of HBpin in 0.5 mL C_6D_6, to give a solution with rougly 0.34 mol·L^{-1} of phenyl isocyanate. The resonances at 6.62, 6.80 and 6.86 ppm correspond to phenyl isocyanate, the resonance at 9.15 ppm corresponds to product A, the resonance at 5.49 ppm corresponds to product B, the resonance at 3.00 ppm corresponds to the product C. The internal standard HMCTS was observed at 0.18 ppm.

Following these initial results, other isocyanate substrates were trialed. In the presence of catalyst **2.8a** (1.0 mol%), the reaction of MesNCO with 2 equivalents of HBpin afforded 0.66 equivalents of MeN(Mes)Bpin within 24 hours, while only trace amounts (<1%) of MesN(Bpin)CH(O) and MesN(Bpin)CH_2OBpin could be observed. This suggests that the reaction of MesN(Bpin)CH(O) and MesN(Bpin)CH_2OBpin with HBpin is much faster than the reaction of MesNCO with HBpin. This is in contrast with the results observed by Hill and Nembenna, as analogous reactions stopped at RN(Bpin)CH(O) and RN(Bpin)CH_2OBpin.[52,54]

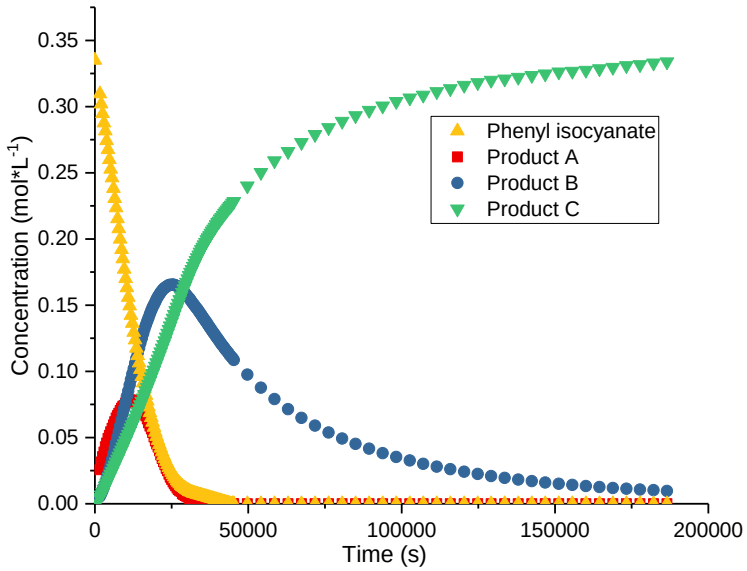


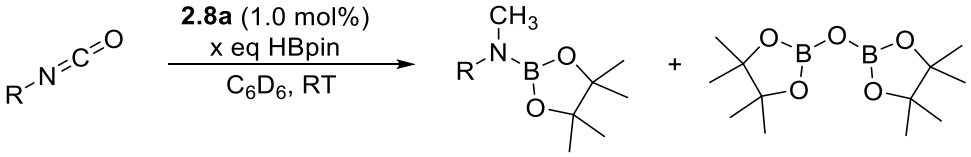
Figure 3.12: Concentration plots over time of the hydroboration of phenyl isocyanate with HBpin in C_6D_6. Reaction conditions: 0.2 mmol of phenyl isocyanate and 0.05 mmol of HMCTS were added to 0.62 mmol of HBpin (90 µL) in 0.5 mL C_6D_6, to give a solution with rougly 0.34 mol·L^{-1} of phenyl isocyanate. Concentrations were monitored via relative integration to the internal standard HMCTS.

In the presence of catalyst **2.8a** (1.0 mol%), the reaction of aliphatic CyNCO with HBpin affords CyN(Bpin)CH(O) and MeN(Cy)Bpin, while no CyN(Bpin)CH_2OBpin was observed during the reaction process. For the allyl isocyanate, only MeN($CH_2CH{=}CH_2$)Bpin was obtained, although trace amount of ($CH_2{=}CHCH_2$)N(Bpin)CH(O) was detected in the ^{1}H NMR spectra through the process.

As the aforementioned hydroboration did not afford isolable stable intermediates, the investigation was targeted at obtaining the final hydroborated product MeN(R)Bpin (Table 3.8). In the presence of **2.8a** (1.0 mol%), at room temperature, RNCO (R = allyl, $C_6H_5CH_2$, 4-acetylC_6H_4, and 2-$CF_3C_6H_4$) could be hydroborated to MeN(R)Bpin (almost quantitatively) within 24 hours. While it takes 48 hours for other isocyanates, such as RNCO (R = C_6H_5, Mes, 4-MeC_6H_4 and 4-BrC_6H_4) to reach completion. The

catalytic hydroboration of CyNCO is much slower, with only 68% conversion to MeN(Cy)Bpin within 168 hours, which is related to steric effects.

Table 3.8: Scope of gallium-catalysed hydroboration of isocyanates.



Entry	R	HBpin (equiv)	Reaction time (h)	NMR Yield (%)
1	C_6H_5	3.1	48	98
2	CH_2=$CHCH_2$	3.1	24	98
3	Cy	3.1	168	68
4	$C_6H_5CH_2$	3.1	24	99
5	4-AcetylC_6H_4	4.1	24	99
6	Mes	3.1	48	98
7	4-MeC_6H_4	3.1	48	99
8	4-BrC_6H_4	3.1	48	97
9	2-CF_3-C_6H_4	3.1	24	99

Reagents: 0.2 mmol isocyanate and x equivalent HBpin. Reactions performed at room temperature. ^{1}H NMR yields relative to internal standard HMCTS.

Reaction conditions: to a stock solution (500 μL C_6D_6, with 0.002 mmol **2.8a**) in an NMR tube with J. Young NMR valve, was added neat isocyanate (ca. 0.2 mmol), then neat HBpin. All reagents were degassed and stored under an inert atmosphere as received

It is worth noting that a control reaction between HBpin (3.1 equivalents) with phenyl isocyanate was performed at room temperature in the absence of catalyst, and no hydroborated product was observed after 48 hours.

As a brief summary, complex **2.8a** has been shown to act as an efficient catalyst for the catalytic hydroboration of isocyanates. The most noteworthy observation is that certain isocyanates can be hydroborated to give *N*-borylated methylamines at room temperature. The typical TOF for the hydroboration of aryl-substituted isocyanates is around 2.08−4.16 h^{-1} at room temperature (with catalyst **2.8a**), which is significantly faster than the β-diketiminato magnesium catalyst developed by Hill (with TOF about

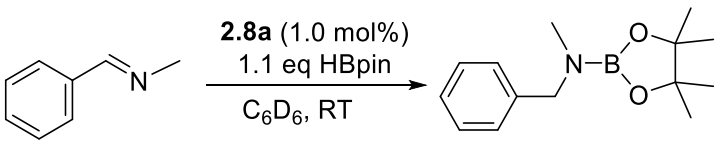
0.0042 h^{-1} at 60 °C).[54] Mechanistic studies on the activity of **2.8a** are currently ongoing.

3.6 Hydroboration of imines

Amines are ubiquitous in nature, and important components of biomolecules, such as proteins and nucleic acids. Amines also play important roles in the synthesis of dyes, rubbers and pharmaceuticals.[55,56] One synthetic method for the preparation of amines is through the hydroboration of imines. The hydroboration of imines by HBpin are operative at elevated temperature (60 or 80 °C) without the presence of a catalyst, but no reaction was observed at room temperature.[57–59]

The catalytic hydroboration of imines using main group hydrides has been previously reported by Hill and Okuda (see Chapter One), but to the best of our knowledge, there are no examples of gallium catalysts that can facilitate this process.[12,50] This prompted us to explore the use of **2.8a** as a catalyst for imine hydroboration.

A preliminary experiment was carried out (Scheme 3.11), between 0.1 mmol of *N*-benzylidenemethylamine and 0.11 mmol HBpin in the presence of HMCTS as an internal standard (0.05 mmol). The reaction was monitored by ^{1}H NMR spectroscopy until completion (Figures 3.13−3.14), and the product was identified by chemical shifts at 2.54 (*N*-Me) and 4.10 ppm (*N*-CH_2). The *N*-benzylidenemethylamine was fully converted to the hydroborated product within 4 h, giving a turnover frequency of approximately 25 h^{-1}.



Scheme 3.11: Hydroboration of *N*-benzylidenemethylamine.

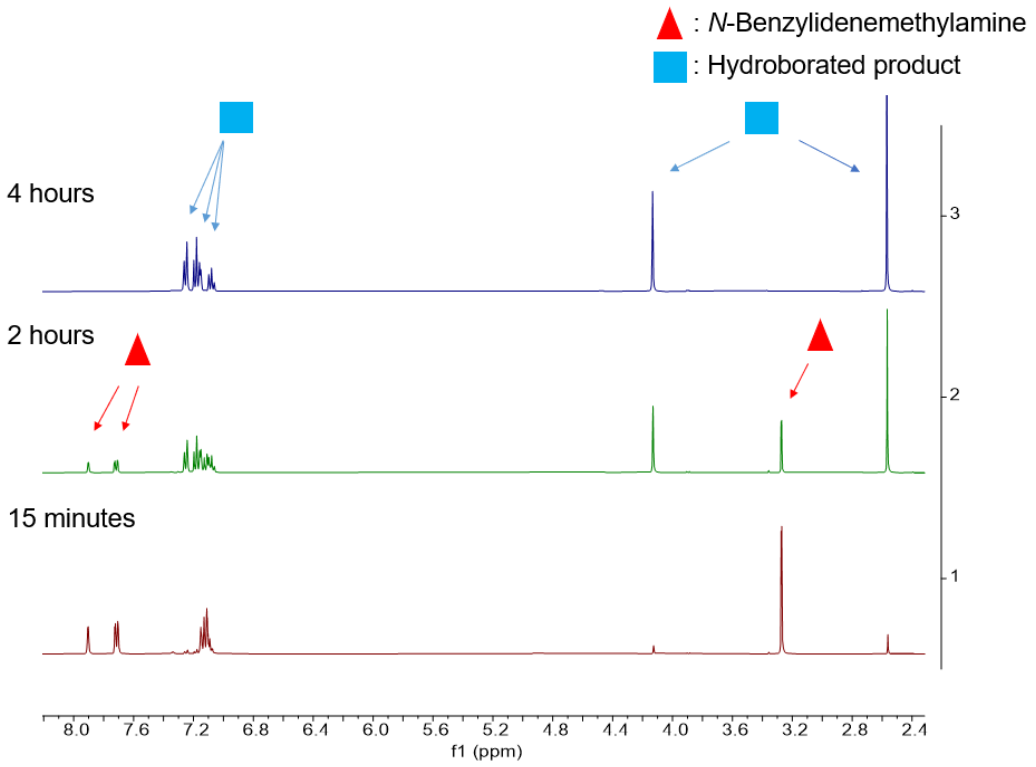


Figure 3.13: Stacked ^{1}H NMR spectra after the reaction starts for 15 minutes, 2 hours and 4 hours. Reaction conditions: *N*-benzylidenemethylamine (0.1 mmol) and HMCTS (0.05 mmol) were added with HBpin (0.11 mmol, 16 μL) in C_6D_6 (0.5 mL) to give a solution with rougly 0.20 mol·L^{-1} of *N*-benzylidenemethylamine. The resonances at 3.26, 7.71 and 7.90 ppm correspond to the *N*-benzylidenemethylamine, the resonances at 2.54, 4.10, 7.06, 7.15 and 7.23 ppm correspond to the hydroborated product.

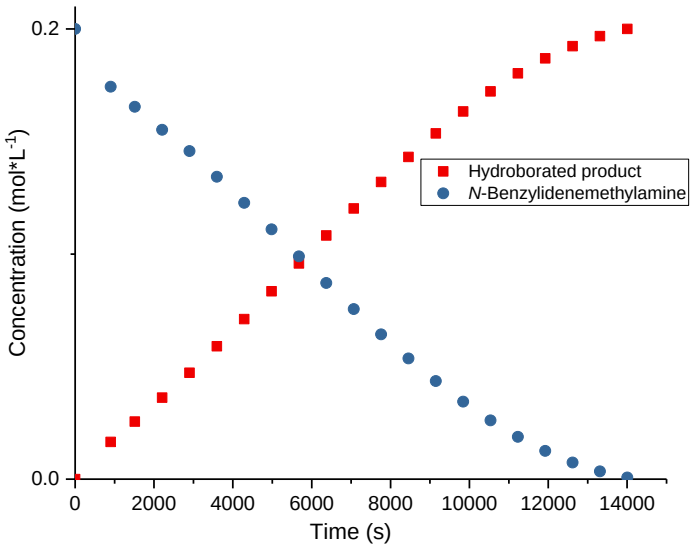
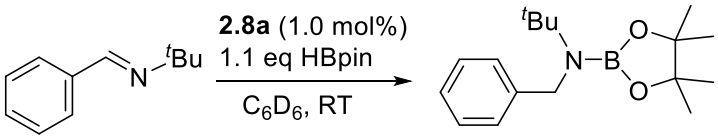


Figure 3.14: Concentration plots for the hydroboration of *N*-benzylidenemethylamine with HBpin in C_6D_6.

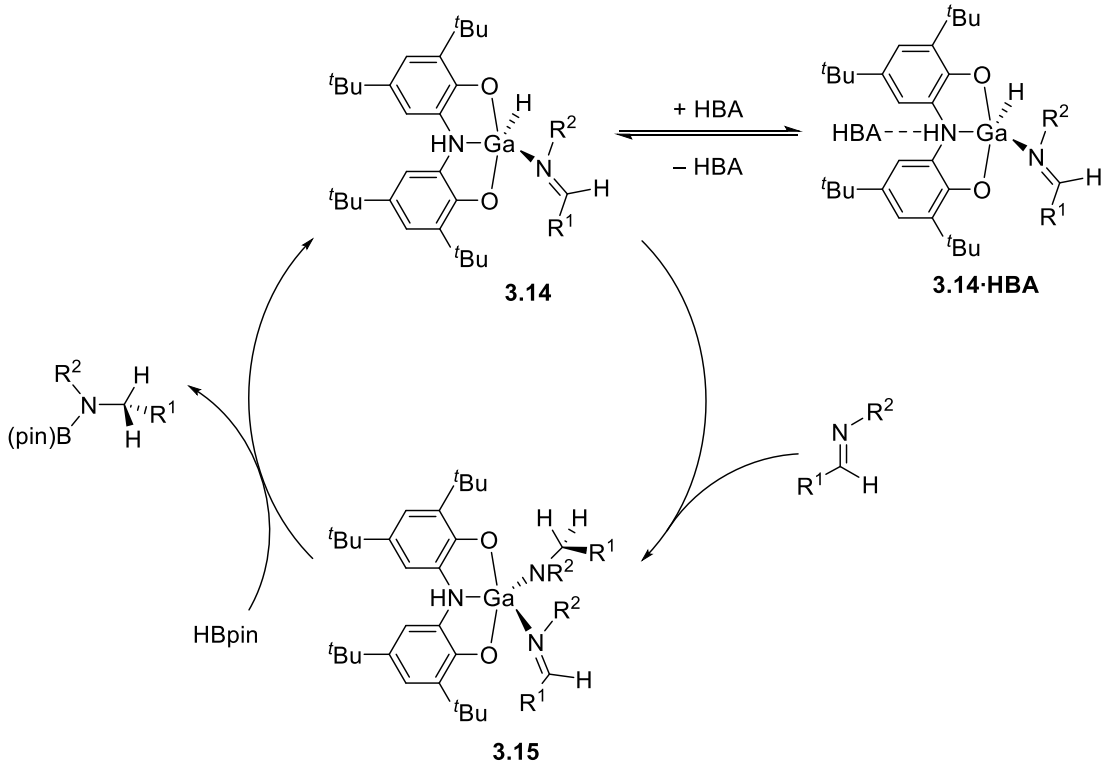
The substrate scope was extended to the more sterically demanding *N*-benzylidene-*tert*-butylamine, which Hill has previously identified as a challenging substrate for hydroboration (requiring 10 mol% of **1.19**, 70 °C, 3 d, 42% conversion, TOF = 0.058 h^{-1}).[12] Employing 1 mol% of catalyst **2.8a** at room temperature, *N*-benzylidene-*tert*-butylamine can be hydroborated (Scheme 3.12), with 99% conversion within 2 days. This gives an observed TOF of 2.08 h^{-1}, which is a significant increase in activity for this transformation.



Scheme 3.12: Hydroboration of *N*-benzylidene-*tert*-butylamine.

We believe that a similar mechanism (see Scheme 3.13) to that observed for ketone hydroboration is operative in this process. Accordingly, an imine-coordinated gallium

monohydride **3.14**, is in equilibrium with the hydrogen bonded adduct **3.14**·HBA. During the hydroboration of *N*-benzylidenemethylamine, an intermediate (presumably **3.14**·HBA) was detected by the in situ ^{1}H NMR spectroscopy, with a characteristic gallium-hydride resonance at 5.57 ppm. This chemical shift agrees with the observed intermediate in the hydroboration of ketones (Table 3.6). The gallium monohydride **3.14** can further react with an imine through C=N bond insertion into the Ga−H bond to give an amine coordinated gallium complex **3.15**. The hydroborated amine product $CH_2(R^1)N(R^2)Bpin$ is generated through B−H/Ga−N bond metathesis from HBpin and **3.15**, whilst gallium monohydride **3.14** is regenerated.



Scheme 3.13: Proposed mechanism for the hydroboration imines.

Thus far, we have shown that pre-catalyst **2.8a** is active in the catalytic hydroboration of imines. Due to time constraints a full substrate scope could not be explored.

3.7 Summary and perspective

In this chapter we have explored the use of gallium hydrides in the catalytic hydroboration of a number of substrates. Using catalyst **2.8a** (0.05 mol%), the catalytic hydroboration of aldehydes reached a TOF around 166−2000 h^{-1}, and the hydroboration of ketones reached a TOF around 200 h^{-1}. The TMEDA test for the ketone hydroboration ruled out the possibility that **2.8a** only acts as a precursor for BH_3 generation. A mechanism for the carbonyl hydroboration has been proposed, and is in line with the kinetic and simulation studies.

With **2.8a** (1.0 mol%), carbon dioxide could be catalytically hydroborated to the methanol equivalent MeOBpin and $O(Bpin)_2$ at room temperature, with a relatively high TOF of 2.63 h^{-1}. The TOF for the catalytic hydroboration (with 1.0 mol% **2.8a**) of isocyanates to give *N*-borylated methylamine at room temperature is around 2.08−4.16 h^{-1}. The mechanisms for the catalytic hydroboration of carbon dioxide and isocyanates are yet to be determined.

Regarding the catalytic hydroboration of imines (with 1.0 mol% **2.8a**), the TOF for the hydroboration of *N*-benzylidenemethylamine is around 25.7 h^{-1}, while a bulkier substrate *N*-benzylidene-*tert*-butylamine has a TOF of 2.08 h^{-1}. In general, **2.8a** is an efficient catalyst for catalytic hydroboration with good stability. However, this type of catalyst still has some limitations. The catalyst reacts with boranes (such as HBpin, BCF) at high temperatures (60 °C) through a transelementation process (which will be discussed in Chapter Four). Although **2.8a** can facilitate the hydroboration of alkenes (such as 1-hexene) at 60 °C, severe decomposition of the catalyst (via transelementation) prevents it from acting as a stable catalyst for the catalytic hydroboration of alkenes. In

the future, the use of other more stable borane substrates instead of HBpin for these transformations is worth exploring.

3.8 References

[1] S. Harder, *Chem. Commun.* **2012**, *48*, 11165–11177.

[2] C. C. Chong, R. Kinjo, *ACS Catal.* **2015**, *5*, 3238–3259.

[3] M. S. Hill, D. J. Liptrot, C. Weetman, *Chem. Soc. Rev.* **2016**, *45*, 972–988.

[4] L. C. Wilkins, R. L. Melen, *Coord. Chem. Rev.* **2016**, *324*, 123–139.

[5] M. L. Shegavi, S. K. Bose, *Catal. Sci. Technol.* **2019**, *9*, 3307–3336.

[6] Y. Yang, M. D. Anker, J. Fang, M. F. Mahon, L. Maron, C. Weetman, M. S. Hill, *Chem. Sci.* **2017**, *8*, 3529–3537.

[7] C. Weetman, M. S. Hill, M. F. Mahon, *Chem. Eur. J.* **2016**, *22*, 7158–7162.

[8] M. Arrowsmith, T. J. Hadlington, M. S. Hill, G. Kociok-Köhn, *Chem. Commun.* **2012**, *48*, 4567–4569.

[9] C. Weetman, M. D. Anker, M. Arrowsmith, M. S. Hill, G. Kociok-Köhn, D. J. Liptrot, M. F. Mahon, *Chem. Sci.* **2016**, *7*, 628–641.

[10] C. Weetman, M. S. Hill, M. F. Mahon, *Chem. Commun.* **2015**, *51*, 14477–14480.

[11] M. Arrowsmith, M. S. Hill, T. Hadlington, G. Kociok-Köhn, C. Weetman, *Organometallics* **2011**, *30*, 5556–5559.

[12] M. Arrowsmith, M. S. Hill, G. Kociok-Köhn, *Chem. Eur. J.* **2013**, *19*, 2776–2783.

[13] M. D. Anker, M. Arrowsmith, P. Bellham, M. S. Hill, G. Kociok-Köhn, D. J. Liptrot, M. F. Mahon, C. Weetman, *Chem. Sci.* **2014**, *5*, 2826–2830.

[14] S. Harder, J. Spielmann, *J. Organomet. Chem.* **2012**, *698*, 7–14.

[15] S. Yadav, S. Pahar, S. S. Sen, *Chem. Commun.* **2017**, *53*, 4562–4564.

[16] D. Franz, C. Jandl, C. Stark, S. Inoue, *ChemCatChem* **2019**, *11*, 5275–5281.

[17] A. Bismuto, M. J. Cowley, S. P. Thomas, *ACS Catal.* **2018**, *8*, 2001–2005.

[18] D. Franz, L. Sirtl, A. Pöthig, S. Inoue, *Z. Anorg. Allg. Chem.* **2016**, *642*, 1245–1250.

[19] Q. Shen, X. Ma, W. Li, W. Liu, Y. Ding, Z. Yang, H. W. Roesky, *Chem. Eur. J.* **2019**, *25*, 11918–11923.

[20] W. Liu, Y. Ding, D. Jin, Q. Shen, B. Yan, X. Ma, Z. Yang, *Green Chem.* **2019**, *21*, 3812–3815.

[21] V. K. Jakhar, M. K. Barman, S. Nembenna, *Org. Lett.* **2016**, *18*, 4710–4713.

[22] A. J. Woodside, M. A. Smith, T. M. Herb, B. C. Manor, P. J. Carroll, P. R. Rablen, C. R. Graves, *Organometallics* **2019**, *38*, 1017–1020.

[23] N. Sarkar, S. Bera, S. Nembenna, *J. Org. Chem.* **2020**, *85*, 4999–5009.

[24] T. Peddarao, N. Sarkar, S. Nembenna, *Inorg. Chem.* **2020**, *59*, 4693–4702.

[25] Z. Yang, M. Zhong, X. Ma, K. Nijesh, S. De, P. Parameswaran, H. W. Roesky, *J. Am. Chem. Soc.* **2016**, *138*, 2548–2551.

[26] Z. Yang, M. Zhong, X. Ma, S. De, C. Anusha, P. Parameswaran, H. W. Roesky, *Angew. Chem., Int. Ed.* **2015**, *54*, 10225–10229.

[27] T. J. Hadlington, C. E. Kefalidis, L. Maron, C. Jones, *ACS Catal.* **2017**, *7*, 1853–1859.

[28] V. Nesterov, R. Baierl, F. Hanusch, A. E. Ferao, S. Inoue, *J. Am. Chem. Soc.* **2019**, *141*, 14576–14580.

[29] Y. Wu, C. Shan, Y. Sun, P. Chen, J. Ying, J. Zhu, L. Liu, Y. Zhao, *Chem. Commun.* **2016**, *52*, 13799–13802.

[30] T. J. Hadlington, M. Hermann, G. Frenking, C. Jones, *J. Am. Chem. Soc.* **2014**, *136*, 3028–3031.

[31] J. Schneider, C. P. Sindlinger, S. M. Freitag, H. Schubert, L. Wesemann, *Angew. Chem., Int. Ed.* **2017**, *56*, 333–337.

[32] J. A. B. Abdalla, I. M. Riddlestone, R. Tirfoin, S. Aldridge, *Angew. Chem., Int. Ed.* **2015**, *54*, 5098–5102.

[33] A. Ford, S. Woodward, *Angew. Chem., Int. Ed.* **1999**, *38*, 335–336.

[34] A. J. Blake, A. Cunningham, A. Ford, S. J. Teat, S. Woodward, *Chem. Eur. J.* **2000**, *6*, 3586–3594.

[35] C. D. Smith, *Synthesis and Reactivity of Geometrically Constrained Gallium(III) Complexes*, Thesis (M.Chem) − University of Oxford, (Department of Chemistry), Oxford, **2017**.

[36] S.-K. Lo, *Geometry Constrained Main-Group Compounds for the Activation of Small Molecules*, Thesis (D.Phil.) − University of Oxford, 2018, (Department of Inorganic Chemistry), Oxford, **2018**.

[37] V. L. Weidner, C. J. Barger, M. Delferro, T. L. Lohr, T. J. Marks, *ACS Catal.* **2017**, *7*, 1244–1247.

[38] M. Arrowsmith, T. J. Hadlington, M. S. Hill, G. Kociok-Köhn, *Chem. Commun.* **2012**, *48*, 4567–4569.

[39] W. P. Jorissen, P. A. A. van der Beek, *Recl. Trav. Chim. Pays-Bas* **1930**, *49*, 138–141.

[40] M. Sankar, E. Nowicka, E. Carter, D. M. Murphy, D. W. Knight, D. Bethell, G. J. Hutchings, *Nat.*

Commun. **2014**, *5*, 3332–3337.

[41] J. Qi, F.-L. Zhang, J.-K. Jin, Q. Zhao, B. Li, L.-X. Liu, Y.-F. Wang, *Angew. Chem., Int. Ed.* **2020**, *59*, 12876–12884.

[42] Y. Liu, J.-L. Li, X.-G. Liu, J.-Q. Wu, Z.-S. Huang, Q. Li, H. Wang, *Org. Lett.* **2021**, *23*, 1891–1897.

[43] H. E. Ho, N. Asao, Y. Yamamoto, T. Jin, *Org. Lett.* **2014**, *16*, 4670–4673.

[44] X. Xu, D. Yan, Z. Zhu, Z. Kang, Y. Yao, Q. Shen, M. Xue, *ACS Omega* **2019**, *4*, 6775–6783.

[45] Y. Wu, C. Shan, J. Ying, J. Su, J. Zhu, L. L. Liu, Y. Zhao, *Green Chem.* **2017**, *19*, 4169–4175.

[46] A. D. Bage, T. A. Hunt, S. P. Thomas, *Org. Lett.* **2020**, *22*, 4107–4112.

[47] A. R. Gatti, T. Wartik, *Inorg. Chem.* **1966**, *5*, 329–330.

[48] J. Burés, *Angew. Chem., Int. Ed.* **2016**, *55*, 2028–2031.

[49] J. Burés, *Angew. Chem., Int. Ed.* **2016**, *55*, 16084–16087.

[50] D. Mukherjee, S. Shirase, T. P. Spaniol, K. Mashima, J. Okuda, *Chem. Commun.* **2016**, *52*, 13155–13158.

[51] Z. Du, B. Behera, A. Kumar, Y. Ding, *J. Organomet. Chem.* **2021**, *950*, 121982.

[52] R. K. Sahoo, N. Sarkar, S. Nembenna, *Angew. Chem., Int. Ed.* **2021**, *60*, 11991–12000.

[53] S. Z. Qian Xiao Zewei Chen, Weiwei Yao, Jing Zheng, Mengtao Ma, *Chinese J. Org. Chem.* **2021**, *41*, 357–363.

[54] Y. Yang, M. D. Anker, J. Fang, M. F. Mahon, L. Maron, C. Weetman, M. S. Hill, *Chem. Sci.* **2017**, *8*, 3529–3537.

[55] N. Fleury-Brégeot, V. de la Fuente, S. Castillón, C. Claver, *ChemCatChem* **2010**, *2*, 1346–1371.

[56] S. D. Roughley, A. M. Jordan, *J. Med. Chem.* **2011**, *54*, 3451–3479.

[57] V. K. Pandey, S. N. R. Donthireddy, A. Rit, *Chem. Asian J.* **2019**, *14*, 3255–3258.

[58] A. Kaithal, B. Chatterjee, C. Gunanathan, *J. Org. Chem.* **2016**, *81*, 11153–11161.

[59] R. Arévalo, C. M. Vogels, G. A. MacNeil, L. Riera, J. Pérez, S. A. Westcott, *Dalton Trans.* **2017**, *46*, 7750–7757.

Chapter Four

Synthesis and reactivity of pincer stabilised boron complexes

4.1 Introduction and objectives

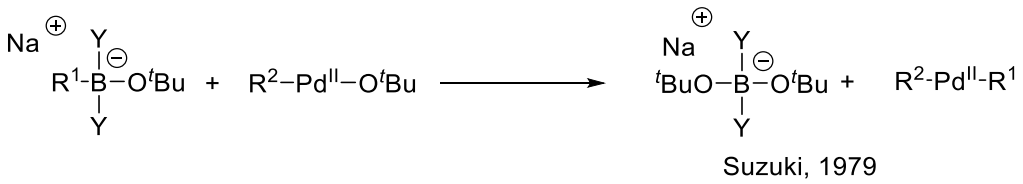
In the earlier chapters, the synthesis of gallium complexes supported by the $[ON(H)O]^{2-}$ ligand was described, as was the use of such complexes in catalytic hydroboration reactions.[1] The same ligand, $[ON(H)O]^{2-}$, has previously been used by Heyduk for the isolation of base-stabilised aluminium complexes.[2] The first attempt at the synthesis of a $[ON(H)O]^{2-}$ stabilised boron complex was reported by Contreras and co-workers by transelementation of a zinc precursor with the $BCl_3{\cdot}SMe_2$, although the compound was never structurally authenticated.[3] Given our previous work with gallium, we decided to explore the reactivity of $[H_3(ONO)]$ towards a series of boron compounds for the synthesis of novel boron complexes of this interesting pincer ligand.

As part of the emerging hydrogen economy, the development of materials for the storage of hydrogen is critical. Hydrogen-rich compounds containing B−N building blocks have attracted considerable interest in recent decades as potential hydrogen storage materials.[4] Specifically, amine-borane adducts with both protic (N−H) and hydridic hydrogens (B−H) are especially of high interest as they fulfil the conditions of an ideal hydrogen storage material.[5] Amine-borane adducts are usually stable at room temperature, and contain a high gravimetric hydrogen storage capacity. They have been shown to release hydrogen under relatively mild conditions with the aid of a catalyst.[6] One explanation is that the different polarity of the E−H bonds enables the formation of dihydrogen bonding (DHB) $N{-}H^{\delta+}\cdots H^{\delta-}{-}B$ within the molecule, facilitating the dehydrogenation process.[5] In most reported cases of amine-borane dehydrogenation, a transition metal catalyst is needed (examples include Y,[7] Zr,[8–12] Re,[13] Fe,[14–16] Ru,[17–24] Os,[25] and Ir),[26–29] however, some FLP type dehydrogenation mechanisms are also known (see Chapter One).[8,30–35]

In this chapter, transelementation reactions between the gallium complexes described previously and boranes will be discussed. This is followed by the targeted formation of boron complexes of the $[ON(H)O]^{2-}$ ligand. A novel amine-borane system has been developed which exhibits unusual dehydrogenation reactivity. Finally, the reactivity of a novel amine-borane complex in the hydroboration of aldehydes and ketones will also be discussed.

4.2 Transelementation reactions and the formation of borane complexes of $[ON(H)O]^{2-}$

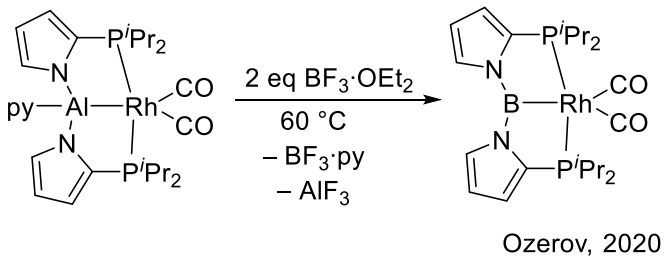
Transmetalation and transelementation reactions play an important role in in organic synthesis.[36,37] One of the most famous applications of boron-metal transelementation is the Suzuki reaction, where a boronic acid is cross-coupled with an organohalide.[38,39] Regarding the mechanism, it is widely thought that the ligand (R^1) on the boronate species exchanges with the *tert*-butoxide on the palladium catalyst through a transelementation process (Scheme 4.1).[38,39]



Scheme 4.1: Proposed transelementation process in the Suzuki reaction.[38]

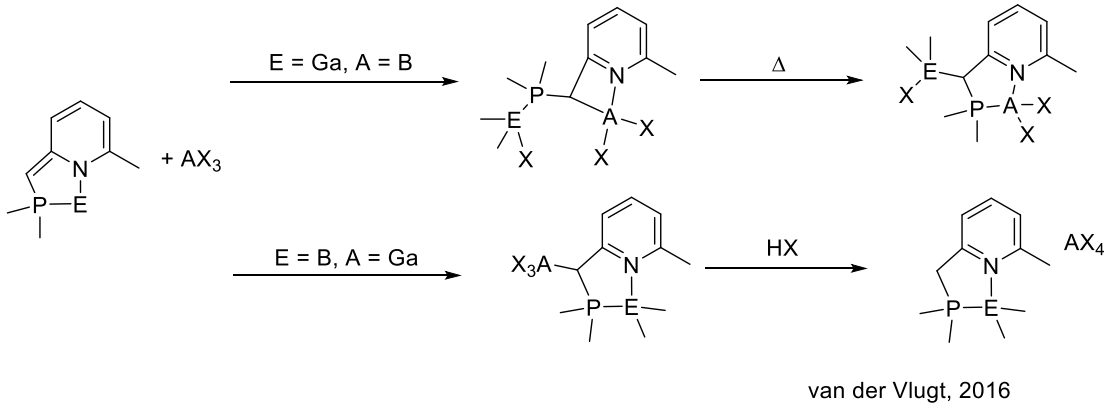
A well-established transelementation process involving two group 13 elements was reported recently by Ozerov and co-workers (Scheme 4.2).[37] Instead of removing the pyridine coordinated to the aluminium centre of the ligand backbone (to afford BF_3·py), the use of BF_3·Et_2O was shown to exchange the aluminium atom of the ligand with boron (Scheme 4.2). The authors postulated this unexpected reactivity may be due to

the fact that the transelementation product is more thermodynamically favoured. This reaction gives a single product in 60% yield. The same reactivity was not observed when using BCF (tris(pentafluorophenyl)borane) as a reagent.



Scheme 4.2: An example of Al/B transelementation.[37]

Examples of Ga/B transelementation are rare. Zhu and co-workers have previously suggested that transelementation may take place in the reaction of boronic acids with benzaldehyde facilitated by $GaMe_3$.[40] In 2016, van der Vlugt and co-workers reported the transelementation of boron and gallium in the reaction of a series of (phosphinomethyl)pyridine supported complexes (Scheme 4.3).[41] Barry and co-workers have also shown that gallium complexes of the 2-^{t}Bu$_2$P(C$_6$H$_4$)EH (E = O, S) ligand can exchange ligands with BCF when heating together in toluene under reflux.[42]

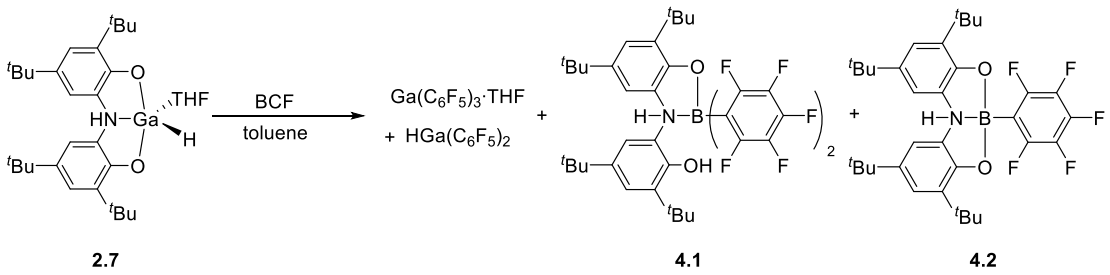


Scheme 4.3: Examples of B/Ga transelementation reported by van der Vlugt.[41,42]

In Chapter Two, a series of gallium complexes (including a ligand-stabilised gallium monohydride complex **2.7**) were discussed, and they were explored as catalysts for

hydroboration. During these catalytic studies, the transelementation of the gallium complexes on reaction with HBPin was observed. This reaction is investigated in greater detail here.

The reaction of **2.7** with BCF in a toluene solution afforded a series of transelementation products including [O(H)N(H)O]B(C_6F_5)$_2$ (**4.1**), [ON(H)O]B(C_6F_5) (**4.2**), Ga(C_6F_5)$_3$·THF, and HGa(C_6F_5)$_2$ (Scheme 4.4).



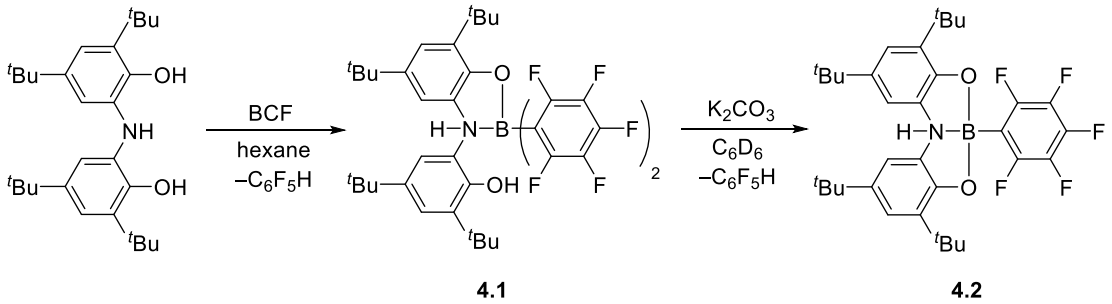
Scheme 4.4: Transelementation of **2.7** with BCF.

Crystallisation of the crude mixture from hexane afforded single crystals suitable for X-ray diffraction. These were identified as the known compound Ga(C_6F_5)$_3$·THF.[43] The ^{1}H and ^{19}F{^{1}H}NMR spectra of these crystals were consistent with literature-reported values. A minor species was identified, with three ^{19}F{^{1}H} NMR resonances at −123.63, −151.08 and −160.35 ppm and a broad ^{1}H NMR resonance 5.74 ppm corresponding to a Ga−H moiety. We believe that this species corresponds to HGa(C_6F_5)$_2$. In situ NMR studies of these reaction mixtures suggest the initial formation of **4.1** (Scheme 4.4), which completely converts to **4.2** after 4 days (NMR spectroscopic data and independent syntheses are discussed in Section 4.3).

4.3 Synthesis of boron complexes stabilised by the $[ON(H)O]^{2-}$ ligand

As complexes **4.1** and **4.2** are challenging to isolate as compositionally pure samples from the aforementioned reaction mixtures, we sought to synthesise them independently, by reacting the $[H_3(ONO)]$ directly with BCF.

A hexane solution of BCF and $[H_3(ONO)]$ was stirred at room temperature overnight to give **4.1** (Scheme 4.5). The ^{1}H NMR spectrum for the crude product in C_6D_6 revealed resonances at 7.44, 7.29, 7.10 and 6.91 ppm corresponding to the aromatic protons of the ligand backbone. This suggests asymmetric coordination of the ligand, and is supported by the presence of four inequivalent *tert*-butyl resonances at 1.70, 1,01, 0.99 and 0.94 ppm. Additional resonances corresponding to N−H and O−H environments were observed at 4.73 and 9.97 ppm, respectively. The $^{11}B\{^{1}H\}$ NMR spectrum of **4.1** reveals a single resonance at 8.6 ppm indicative of a four-coordinate boron centre, while the ^{19}F NMR spectrum revealed eight resonances for the $B(C_6F_5)_2$ moiety at −131.49, −133.38, −137.04, −155.81, −156.41 −162.68, −163.02 and −165.26 ppm (integrating in a ratio of 1:1:2:1:1:2:1:1).



Scheme 4.5: Synthesis of **4.1** and **4.2**.

Colourless crystals of **4.1** suitable for single crystal X-ray crystallography were grown from a concentrated hexane solution at room temperature. The structure of **4.1** (Figure 4.1) reveals that the boron centre adopts a distorted tetrahedral geometry bonded to a nitrogen and an oxygen atom of the ligand and two pentafluorophenyl groups. One of the fluorine atoms shows C−F···H−N hydrogen bonding with the amine-proton on the ligand backbone, with a bond distance of 2.088(33) Å.

Complex **4.1** does not undergo dearylation even at 60 °C overnight. However, the use of a base, such as K_2CO_3 can facilitate the O−H/B−C metathesis at room temperature to give **4.2** and pentafluorobenzene (HC_6F_5) as a side-product, as shown in Scheme 4.5. Formation of HC_6F_5 was observed by in situ NMR spectroscopy, revealing a characteristic ^{1}H NMR multiplet at 5.80 ppm, and three resonances in the ^{19}F NMR spectrum at −139.12, −154.10 and −162.33 ppm.

The solution ^{1}H NMR spectrum of **4.2** in C_6D_6 shows resonances attributed to a symmetrically bonded ligand backbone (ArH: 7.33, 6.98 ppm; NH: 6.12 ppm; *tert*-butyl: 1.49, 1,24 ppm). The ^{11}B{^{1}H} NMR spectrum of **4.2** reveals a single resonance at 13.0 ppm, while the ^{19}F NMR spectrum revealed three resonances at −132.83, −155.23 and −162.97 ppm.

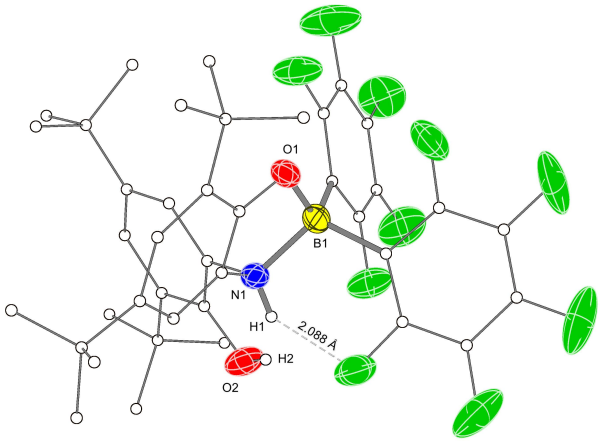
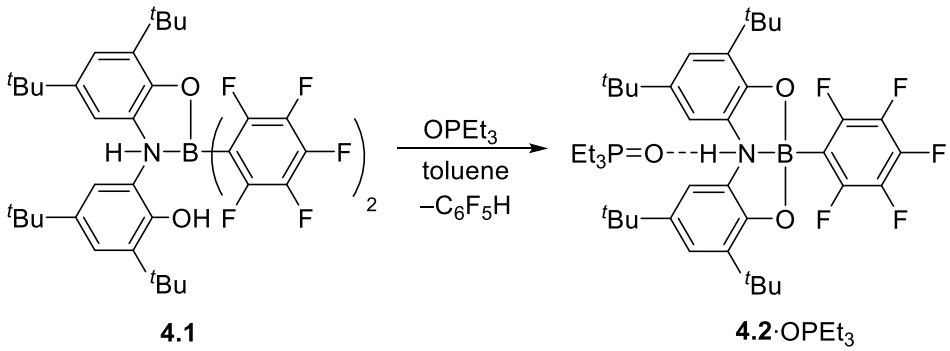


Figure 4.1: Single crystal X-ray structure of **4.1**. Anisotropic displacement ellipsoids are set at 50% probability. Hydrogen atoms have been omitted for clarity (with the exception of H1 and H2). All carbon atoms are pictured as spheres of arbitrary radius. Selected interatomic distances [Å] and angles [°]: B1–N1 1.658(4), B1–O1 1.469(4), B1–C29 1.626(4), B1–C35 1.617(5); O1-B1-N1 100.4(2), O1-B1-O2 112.2(2), O1-B1-C29 101.09(18), O1-B1-C35 114.4(2).



Scheme 4.6: Synthesis of **4.2**·$OPEt_3$.

In addition to K_2CO_3, weaker Lewis bases can also induce dearylation of **4.1**. Reaction of **4.1** and Et_3PO afforded a Et_3PO adduct of **4.2**. The ^{1}H, $^{11}B\{^{1}H\}$ and $^{19}F\{^{1}H\}$ NMR spectra of this hydrogen-bonded adduct do not differ significantly from **4.2** (see Experimental Section). The amine proton resonance in the ^{1}H NMR spectrum of **4.2**·$OPEt_3$ (at 11.85 ppm) is considerably more downfield than in the case of base-free **4.2** (at 6.12 ppm), suggesting that the N−H···O=P hydrogen bond persists in solution.

The $^{31}P\{^{1}H\}$ NMR spectrum of **4.2**·$OPEt_3$ reveals a resonance at 51.3 ppm for Et_3PO, while free $OPEt_3$ is typically observed at 45.8 ppm.

Single crystals of **4.2**·$OPEt_3$ were obtained from a hexane solution at room temperature. The structure of **4.2**·$OPEt_3$ was unambiguously characterised by single crystal X-ray diffraction (Figure 4.2). The N−H···O=P bond is 1.773(27) Å which indicates a moderately strong hydrogen bond.[44]

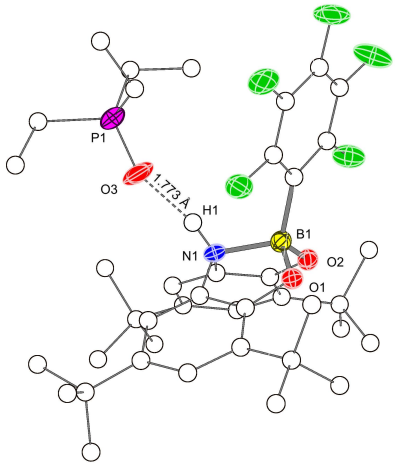
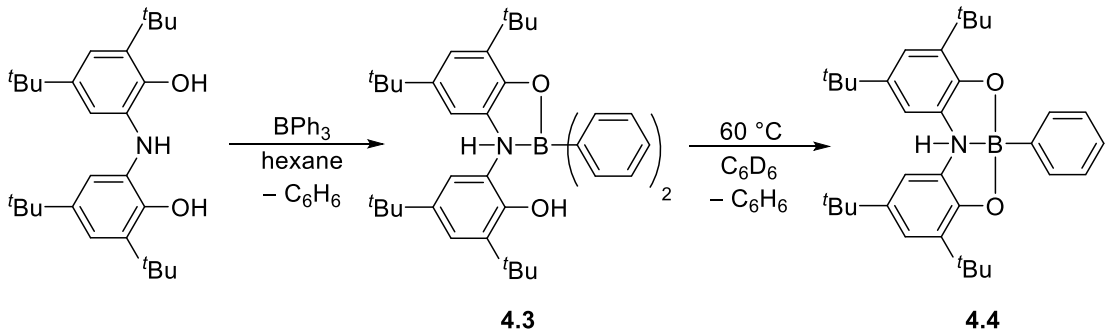


Figure 4.2: Single crystal X-ray structure of **4.2**·$OPEt_3$. Anisotropic displacement ellipsoids are set at 50% probability. Hydrogen atoms have been omitted for clarity (with the exception of H1 and H2). All carbon atoms are pictured as spheres of arbitrary radius. Selected interatomic distances [Å] and angles [°]: B1–N1 1.653(3), B1–O1 1.472(3), B1–C29 1.626(4), B1–O2 1.451(3); O1-B1-N1 102.67(19), O1-B1-O2 112.8(2), O1-B1-C29 110.1(2), O1-B1-O2 112.8(2), O2-B1-C29 114.2(2), N1-B1-C29 113.1 (2).

Given the successful synthesis of **4.1** and **4.2**, we reasoned that [H_3(ONO)] would readily react with other organoboron regents.

Triphenylborane (BPh_3) and [H_3(ONO)] were dissolved in hexane at room temperature and the mixture was stirred overnight (Scheme 4.7). On completion of the reaction, the solution was filtered and stored at −30 °C to give colourless crystals of **4.3**.



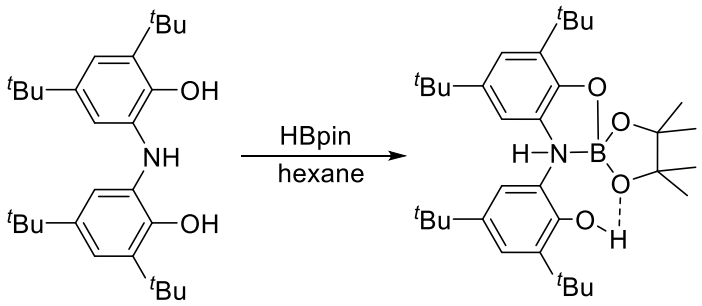
4.3 **4.4**

Scheme 4.7: Synthesis of **4.3** and **4.4**.

As with **4.1**, the solution phase ^{1}H NMR spectrum of **4.3** in C_6D_6 reveals four inequivalent aromatic proton resonances attributed to the ligand backbone at 7.46, 6.95, 6.76 and 6.45 ppm, as well as resonances arising from the *tert*-butyl groups at 1.79, 1.06, 1.05 and 1.04 ppm. Resonances were also observed for the amine proton (4.20 ppm), and phenoxy group (8.00 ppm) of the partially deprotonated ligand. Inclusion of a diphenylborane moiety was confirmed by observation of three broad resonances at 7.96, 7.20 and 7.10 ppm. The ^{11}B{^{1}H} NMR spectrum exhibits a broad resonance at 13.5 ppm which falls in the same range as other four-coordinate boron complexes. Complex **4.3** is stable in the solid state at room temperature, but in solution, it releases one equivalent of benzene through the O−H/B−Ph metathesis, and give complex **4.4** (Scheme 4.7). The dearylation of **4.3** to **4.4** requires a week to reach completion at room temperature but can be sped up by heating at 60 ℃ for 2 hours. Solution ^{1}H NMR spectroscopy of **4.4** in $CDCl_3$ displayed resonances attributed to the ligand (ArH: 7.16, 7.12 ppm; NH: 6.18 ppm; *tert*-butyl: 1.38, 1.20 ppm) and the BPh moiety (7.51, 7.20 and 7.19 ppm). The ^{11}B{^{1}H} NMR spectrum shows a resonance at 14.7 ppm. A broad resonance attributable to the carbon atom adjacent to boron centre was observed at 127.95 ppm in ^{13}C{^{1}H} NMR spectrum.

The boron substrate scope was extended to a borane with strong B−O bonds, pinacol borane (HBpin) (Scheme 4.8). Addition of HBpin to a C_6D_6 solution of [H_3(ONO)] resulted in visible gas evolution. A resonance in the ^{1}H NMR spectrum at 4.47 ppm confirmed the formation of H_2, and the clean formation of a single product [O(H)N(H)O]B(pin) (**4.5**). The ^{1}H NMR spectrum of **4.5** in C_6D_6 is similar to that of **4.1** and **4.3** with resonances attributable to a singly deprotonated [H_3(ONO)] ligand (see Experimental Section for full details). Incorporation of a Bpin moiety was confirmed be the appearance of a new resonance at 1.02 ppm. The ^{11}B{^{1}H} NMR spectrum reveals a sharp peak at 23.0 ppm and the ^{13}C NMR spectrum also supported the presence of a Bpin moiety with resonances observed at 84.10 (O*C*(CH_3)$_2$) and 24.44 ppm (OC(*C*H_3)$_2$).

The crystal structure of **4.5** (Figure 4.3) shows that the boron centre adopts a distorted tetrahedral geometry. Complex **4.5** exhibits an intramolecular hydrogen bond O−H···O−B (1.598(26) Å), which increases the stability of **4.5**. No further reactivity was observed when excess HBpin was added to a C_6D_6 solution of **4.5**.



4.5

Scheme 4.8: Synthesis of **4.5**.

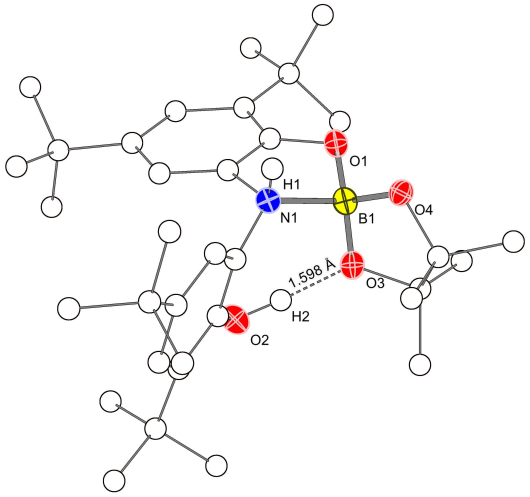


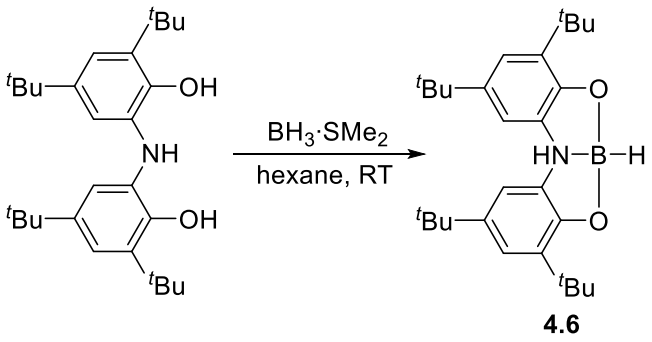
Figure 4.3: Single crystal X-ray structure of **4.5**. Anisotropic displacement ellipsoids are set at 50% probability. Hydrogen atoms have been omitted for clarity (with the exception of H1 and H2). All carbon atoms are pictured as spheres of arbitrary radius. Selected interatomic distances [Å] and angles [°]: B1–N1 1.693(2), B1–O1 1.4656(19), B1–O3 1.4243(19), B1–O4 1.4245(19); O1-B1-N1 98.71(11), O3-B1-N1 107.17(11), O3-B1-O1 116.00(12), O4-B1-N1 114.50(11), O4-B1-O1 112.73(12), O4-B1-O3 107.63(13).

So far, the reactivity of [H_3(ONO)] towards different organoboron compounds (BCF, BPh_3 and HBpin) has been described, giving rise to novel ligand-stabilised boron complexes. As [H_3(ONO)] has been found to undergo dehydrocoupling with HBpin, the reactivity of [H_3(ONO)] was also investigated with another borane, $BH_3{\cdot}SMe_2$.

4.4 Synthesis of novel amine-borane complexes as hydrogen carriers

The reaction of $BH_3{\cdot}SMe_2$ with [H_3(ONO)] in a hexane solution resulted in the formation of a white precipitate accompanied by gas evolution. The white solid was shown to be a novel amine-borane complex [ON(H)O]BH (**4.6**) while the gas was

shown to be dihydrogen by in situ solution ^{1}H NMR spectroscopy (Scheme 4.9), which displayed a singlet at 4.47 ppm. The ^{1}H NMR spectrum of **4.6** in C_6D_6 shows two resonances for the aromatic protons of the ligand backbone at 7.29 and 6.88 ppm, a resonance for the amine proton at 5.41 ppm, and a very broad signal corresponding to a B−H group around 5.3−4.4 ppm. No splitting of the B−H resonance was observed, presumably due to fast ^{11}B{^{1}H} nuclear spin relaxation. The ^{11}B{^{1}H} NMR spectrum of **4.6** shows a broad resonance at 11.8 ppm, which is consistent with a four-coordinate boron environment. Compound **4.6** is stable at room temperature as a solid under an inert atmosphere and does not decompose upon heating. While it has good solubility in THF, hot benzene and hot toluene, it is only sparingly soluble in cold benzene, toluene or chloroform.

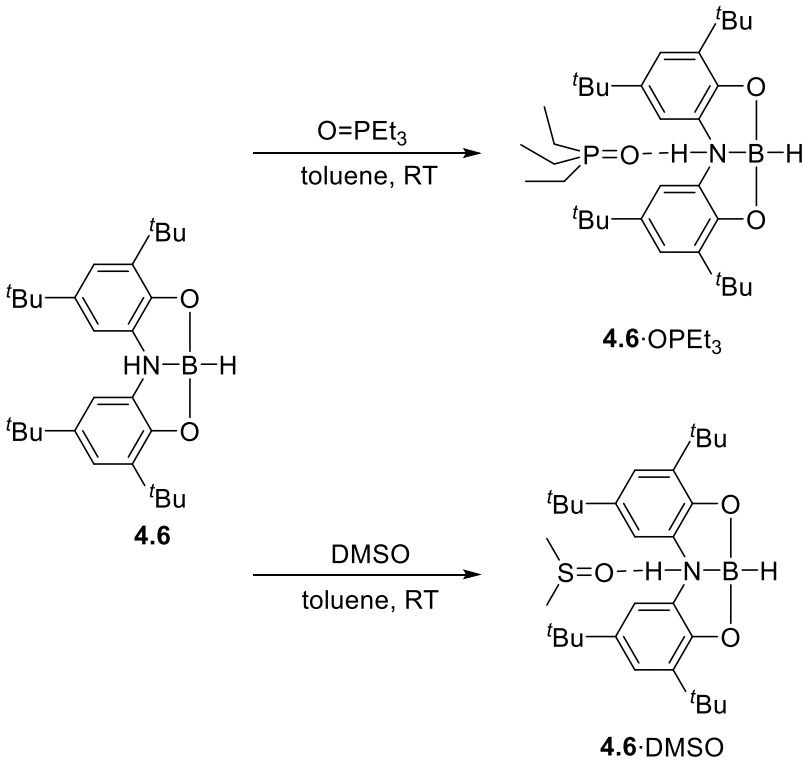


Scheme 4.9: Synthesis of **4.6**.

Single crystals of **4.6** suitable for X-ray crystallography could not be obtained despite repeated attempts, as the compound consistently forms micro-crystals. In Section 4.3 it was noted that the amine (NH) moiety of the ligand backbone interacts strongly with hydrogen bond acceptors (HBA), so the addition of a HBA, such as triethylphosphine oxide and DMSO were explored.

An equivalent of triethylphosphine oxide ($OPEt_3$) was added to a toluene solution of **4.6**, resulting in a colourless solution of **4.6**·$OPEt_3$ (Scheme 4.10). The ^{31}P{^{1}H} NMR

signal of triethylphosphine oxide shifts from 45.8 to 52.7 ppm (**4.6**·$OPEt_3$), which is in line with a weak interaction between the phosphine oxide and the protic N−H.[45] X-ray quality colourless crystals were obtained from a concentrated pentane solution. The analysis (Figure 4.4) confirms that, in the solid state, the oxygen atom on triethylphosphine oxide is interacting with the protic N−H on the ligand backbone of **4.6**·$OPEt_3$ through a strong hydrogen bond P=O···H−N with a distance of ca. 1.882(22) Å.



Scheme 4.10: Synthesis of **4.6**·$OPEt_3$ and **4.6**·DMSO.

In the same fashion, compound **4.6**·DMSO was synthesised by adding a stochiometric amount of DMSO to a toluene solution of **4.6** at room temperature, allowing for the product to be isolated as a white powder.

On addition of a HBA, the amine resonance of **4.6** in the ^1H NMR spectrum shifts downfield from 5.41 ppm and broadens (**4.6**·$OPEt_3$: 11.62 ppm; **4.6**·DMSO: 10.65

ppm). The respective $^{11}B\{^{1}H\}$ NMR spectra are largely similar, indicating the lack of interaction with the boron centre (**4.6**: 11.8 ppm; **4.6**·$OPEt_3$: 10.9 ppm; **4.6**·DMSO: 11.4 ppm).

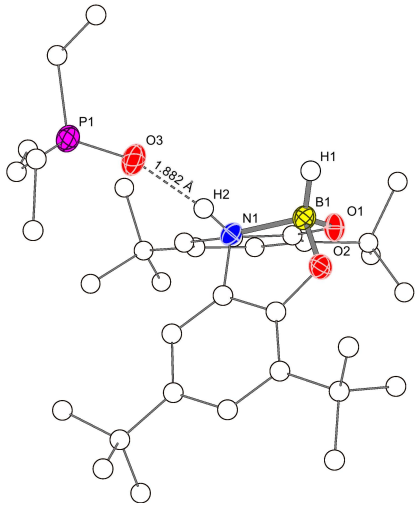


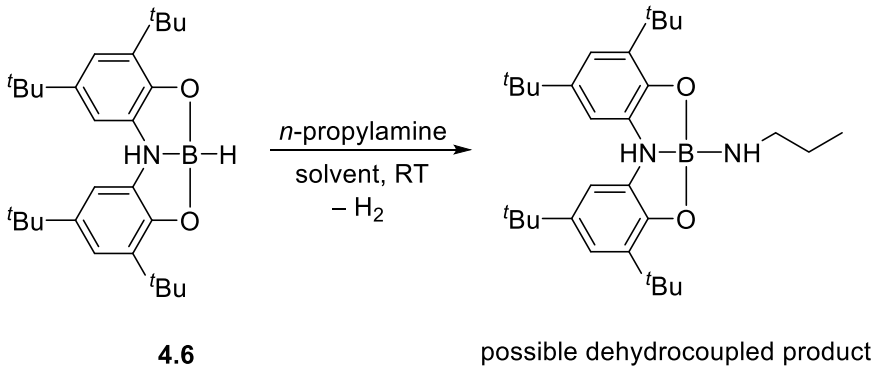
Figure 4.4: Single crystal X-ray structure of **4.6**·$OPEt_3$. Anisotropic displacement ellipsoids are set at 50% probability. Hydrogen atoms (with the exception of H1 and H2) have been omitted for clarity. All carbon atoms are pictured as spheres of arbitrary radius. Selected interatomic distances [Å] and angles [°]: B1–N1 1.655(2), B1–O1 1.4788(19), B1–O2 1.465(2), P1–O3 1.4953(12); O1-B1-N1 101.41(11), O1-B1-O2 112.44(13), O2-B1-N1 102.93(12).

To conclude, dehydrocoupling of $[H_3(ONO)]$ with HBpin and BH_3·SMe_2 is a viable route to afford novel boron complexes **4.5** and **4.6**, respectively. As **4.6** contains both N−H and B−H moieties in the same molecule, we reasoned that it could potentially dehydrogenate. This reactivity has been explored and is discussed in Section 4.5−4.6.

4.5 Dehydrogenation studies of 4.6

Boranes are known to react in dehydrocoupling reactions with amines, phosphines and alcohols.[46] Dehydrocoupling involves elimination of dihydrogen between two E−H bonds, with new E−E bond formation (Scheme 4.11). The reaction of amines with

boranes (such as HBpin, HBcat) often results in the formation of aminoboranes (R)(H)N−B(R′)$_2$,[47] however, catalysts are often needed and some side products such as B_2pin_3, B_2cat_3 are often formed at high temperatures.[46,48]

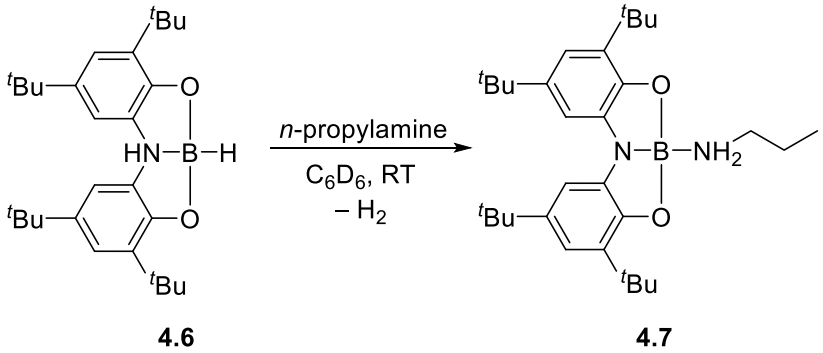


Scheme 4.11: Proposed dehydrocoupling reaction of **4.6** with *n*-propylamine.

A possible dehydrocoupling reaction between **4.6** and *n*-propylamine is shown in Scheme 4.11, in which the B−H of **4.6** and N−H of *n*-propylamine eliminate dihydrogen. However, when this reaction was carried out, a different, unexpected, product was obtained. Addition of two equivalents of *n*-propylamine to a C_6D_6 solution of **4.6** at room temperature results in visible gas evolution and formation of compound **4.7** (Scheme 4.12). A signal at 4.47 ppm in the ^{1}H NMR spectrum supports dihydrogen formation.[49] The ^{1}H NMR spectrum of the resulting product shows resonances attributed to ligand backbone (ArH: 7.62, 7.16 ppm; *tert*-butyl: 1.65, 1.46 ppm). In addition, a resonance integrating to two protons was observed at 4.28 ppm arising from an NH_2 group. The ^{11}B{^{1}H} NMR spectrum of **4.7** reveals a singlet at 14.2 ppm.

As the experiment gave a different result from what was expected, DFT computational studies at the 6-311G/PBE1PBE level (with dispersion correction gd3bj) were performed. The Gibbs free energy of **4.7** and the hypothetical dehydrocoupling product [ON(H)OB]N(H)^{n}Pr were compared, revealing that the Gibbs free energy of **4.7** is 11.18 kJ·mol^{-1} lower in energy. These computational studies are in agreement with the

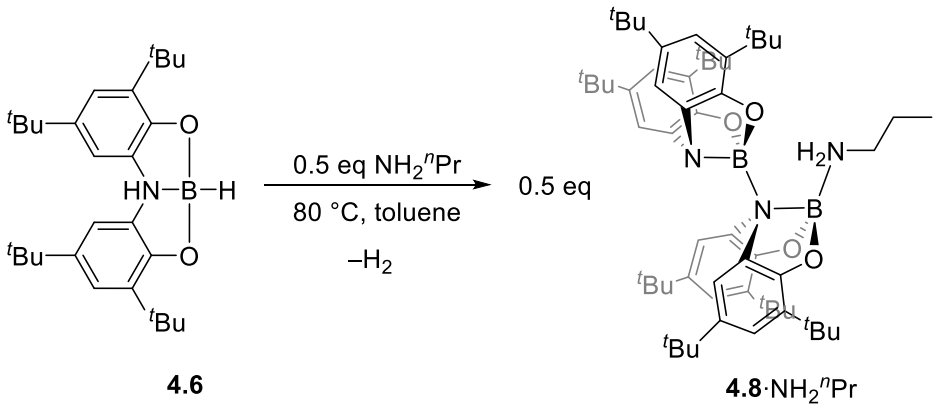
experimental findings. This dehydrogenation reactivity is related to the acidic nature of the amine-proton on the ligand backbone, where *n*-propylamine is more basic.



4.6 **4.7**

Scheme 4.12: Synthesis of **4.7**.

At room temperature, the reaction of **4.6** with *n*-propylamine results in the formation of **4.7**, however, at 80 °C, a different product was observed. The reaction of **4.6** with half an equivalent of *n*-propylamine at 80 °C results into the formation of **4.8**·$NH_2{}^n$Pr, as shown in Scheme 4.13.



4.6 **4.8**·$NH_2{}^n$Pr

Scheme 4.13: Synthesis of **4.8**·$NH_2{}^n$Pr.

Four doublet resonances in the ^{1}H NMR spectrum at 7.60, 7.31, 6.92 and 6.62 ppm account for the four different environments of the aromatic ligand protons, whilst four singlets with chemical shifts at 1.34, 1.32, 1.02 and 0.96 ppm account for the *tert*-butyl

groups. The $^{11}B\{^{1}H\}$ NMR spectrum showed two peaks at 15.9 and 12.6 ppm for the two inequivalent boron centres.

Compound **4.8**·$NH_2{}^nPr$ was characterised by single-crystal X-ray diffraction (Figure 4.5). Crystals were grown from a toluene solution at room temperature, and the resulting structure confirms the dehydrogenated amine-borane complex forms a dimer with one *n*-propylamine coordinated to the terminal boron atom.

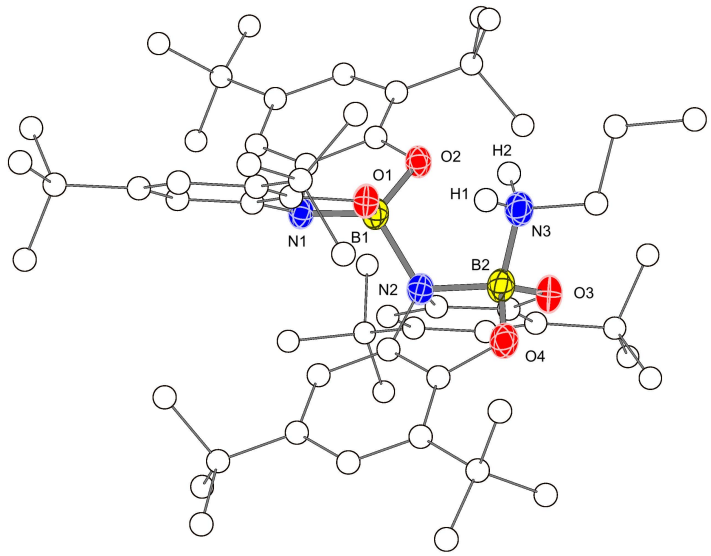


Figure 4.5: Single crystal X-ray structure of **4.8**·$NH_2{}^nPr$. Anisotropic displacement ellipsoids are set at 50% probability. Hydrogen atoms have been omitted for clarity (with the exception of H1 and H2). All carbon atoms are pictured as spheres of arbitrary radius. Selected interatomic distances [Å] and angles [°]: B1–N1 1.5161(18), B1–N2 1.6303(19), B1–O1 1.4633(18), B1–O2 1.4665(17), B2–N2 1.6175(19), B2–N3 1.587(2), B2–O3 1.4402(19), B2–O4 1.4411(18); O1-B1-N1 106.66(11), O1-B1-O2 117.53(12), O1-B1-N2 105.21(10), O2-B1-N1 106.68(11), O2-B1-N2 104.60(10), N1-B1-N2 116.66(11), N3-B2-N2 112.58(11), O3-B2-N2 106.27(11), O3-B2-N3 106.84(12), O3-B2-O4 116.93(13), O4-B2-N2 106.01(11), O4-B2-N3 108.34(12).

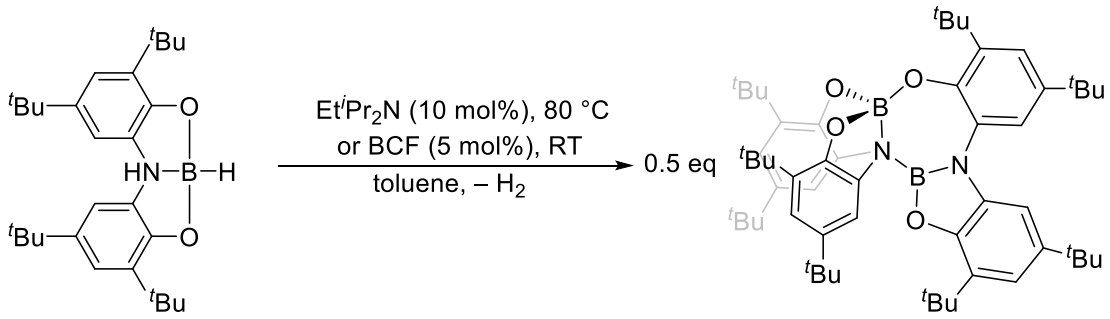
It is worth noting that **4.8**·$NH_2{}^nPr$ reacts with $NH_2{}^nPr$ affording **4.7** in the presence of extra $NH_2{}^nPr$. This is an interesting finding, as one equivalent of *n*-propylamine could,

in principle, induce the dehydrogenation of two equivalent of complex **4.6** to generate two equivalents of dihydrogen. This prompted us to explore the catalytic dehydrogenation of **4.6**.

4.6 Catalytic dehydrogenation of 4.6

In Section 4.5, the unexpected dehydrogenation reactivity of amine-borane **4.6** upon addition of a simple base such as *n*-propylamine was demonstrated. However, as *n*-propylamine is a nucleophile and can bind to the Lewis acidic boron centre, it is unable to dehydrogenate **4.6** catalytically. In view of this, non-nucleophilic bases were explored as potential catalysts for the dehydrogenation of **4.6**.

N,*N*-Diisopropylethylamine, also known as Hünig's base, is a weak nucleophile as the nitrogen atom is surrounded by bulky alkyl groups. Given the unfavourable sterics, it was examined as a potential dehydrogenation catalyst (Scheme 4.14).



4.6 **4.9**

Scheme 4.14: Synthesis of **4.9**.

At 80 °C, addition of 10 mol% of *N*,*N*-diisopropylethylamine results in catalytic dehydrogenation of **4.6** with observable gas evolution (H_2). After heating for 4 hours, the absence of N−H or B−H resonances in ^{1}H NMR spectrum suggested full conversion from **4.6** to **4.9**. The ^{1}H NMR spectrum shows eight inequivalent peaks for aromatic

protons of the ligand backbone (at 8.44, 7.74, 7.51, 7.49, 7.37, 7.21, 7.20 and 7.04 ppm); and eight singlets for *tert*-butyl groups (at 1.90, 1.65, 1.58, 1.55, 1.34; 1.23, 1.20 and 1.00 ppm), which suggests an unsymmetrical dimer. Two broad $^{11}B\{^{1}H\}$ NMR signals at 26.0 and 14.6 ppm indicate two inequivalent boron environments.

Single-crystals of **4.9** suitable for X-ray diffraction were grown from a concentrated pentane solution. As shown in Figure 4.6, the dehydrogenated B(ONO) moieties readily dimerise. The single crystal structure of **4.9** is in agreement with the solution phase NMR data.

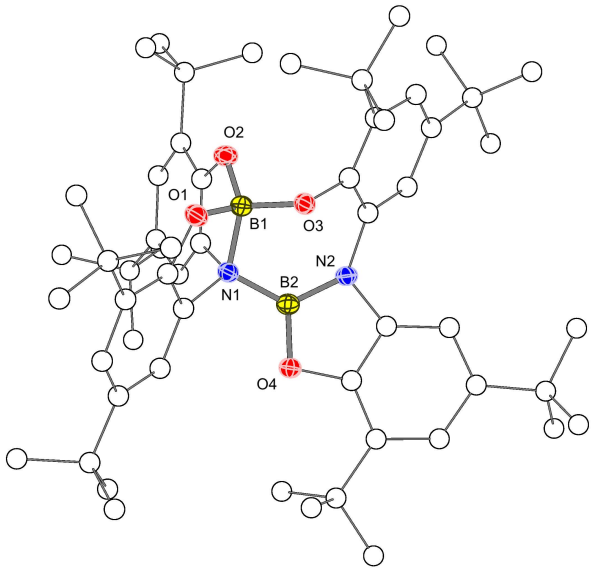


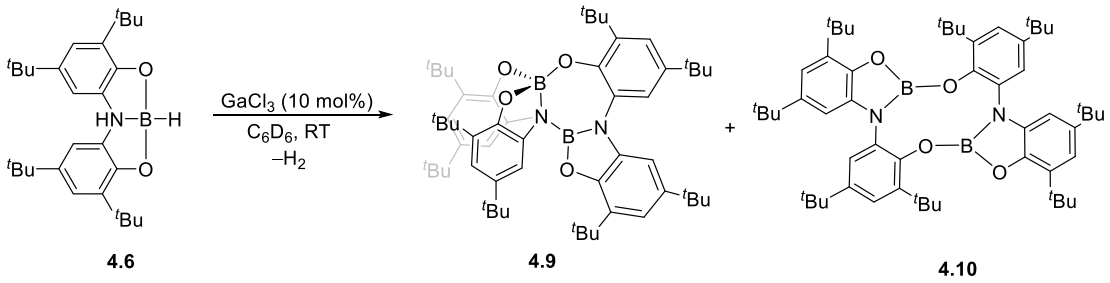
Figure 4.6: Single crystal X-ray structure of **4.9**. Anisotropic displacement ellipsoids are set at 50% probability. Hydrogen atoms have been omitted for clarity. All carbon atoms are pictured as spheres of arbitrary radius. Selected interatomic distances [Å] and angles [°]: B1–N1 1.7303(16), B1–O1 1.4391(16), B1–O2 1.4510(15), B1–O3 1.4174(16), B2–N1 1.4937(16), B2–N2 1.4105(17), B2–O4 1.3758(15); O1-B1-N1 101.57(9), O1-B1-O2 115.24(10), O2-B1-N1 101.45(9), O3-B1-N1 112.12(9), O3-B1-O1 110.74(10), O3-B1-O2 114.56(10), N2-B2-N1 127.24(11), O4-B2-N1 121.39(11), O4-B2-N2 111.29(11), B1-N1-B2 111.74(9).

Given that the use of a non-nucleophilic base in the catalytic dehydrogenation of **4.6** was successful, the catalyst scope was extended to Lewis acids, such as BCF.

At room temperature, 5 mol% BCF was added into a C_6D_6 suspension of **4.6**, resulting in a colourless solution, with hydrogen gas evolution and compound **4.9** formation as indicated by an in situ NMR spectroscopy. The ^{19}F NMR spectrum of the crude mixture contained only resonances corresponding to unreacted BCF, indicating that it is not consumed during the reaction.

Seeing as simple main-group compounds (such as $SnCl_2$) have also been used in catalytic dehydrogenation or dehydrocoupling,[46,50] we sought to check if they would induce dehydrogenation of **4.6**. For this purpose, we explored its reactivity towards $GaCl_3$.

At room temperature, addition of 10 mol% $GaCl_3$ to a suspension of **4.6** in C_6D_6 immediately evolves dihydrogen. NMR studies of the resulting solution revealed the formation of two different products, complex **4.9** and another unexpected product, believed to be a different isomer, **4.10** (Scheme 4.15).



Scheme 4.15: Synthesis of **4.9** and **4.10**.

Complex **4.10** was previously prepared by Dr Lo by heating a THF solution of $[H_3(ONO)]$ with $BH_3{\cdot}PPh_3$ at 80 °C for 14 days.[51] The solution ^1H NMR spectrum in C_6D_6 reveals four resonances for the ligand (7.19, 6.90, 1.38 and 1.15 ppm), while the

$^{11}B\{^{1}H\}$ NMR spectrum gives a single broad resonance at 19.0 ppm. Single crystals of **4.10** were grown by slow diffusion of hexane into a toluene solution of **4.10**, and reveal a dimeric boron complex (Figure 4.7).[51] The boron centres both adopt trigonal planar geometries (the sum of bond angles for B1 and B2 are 360 degrees). The N−B bond distances in **4.10** are 1.4336(18) and 1.4329(18) Å, which are significantly shorter than the (H)N−B bond of **4.6**·$OPEt_3$ (1.655(2) Å). Complex **4.10** could also be synthesised via the catalytic dehydrogenation of **4.6** in C_6D_6 using PPh_3 as a catalyst (10 mol%) at 80 °C, however, this is a slow reaction and reaches completion only after 2 weeks.

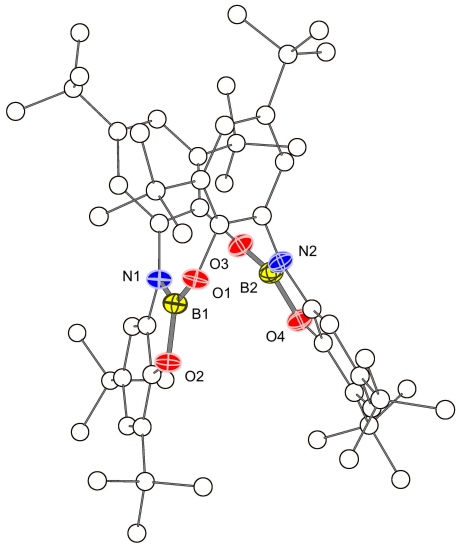


Figure 4.7: Single crystal X-ray structure of **4.10**. Anisotropic displacement ellipsoids are set at 50% probability. Hydrogen atoms have been omitted for clarity. All carbon atoms are pictured as spheres of arbitrary radius. Selected interatomic distances [Å] and angles [°]: B1–N1 1.4336(18), B1–O2 1.3890(15), B1–O3 1.3642(17), B2–N2 1.4329(18), B2–O1 1.3587(18), B2–O4 1.3876(16); O2-B1-N1 109.82(11), O3-B1-N1 131.25(12), O3-B1-O2 118.92(12), O1-B2-N3 131.98(12), O1-B2-O4 118.38(12), O4-B2-N3 109.64(11).[51]

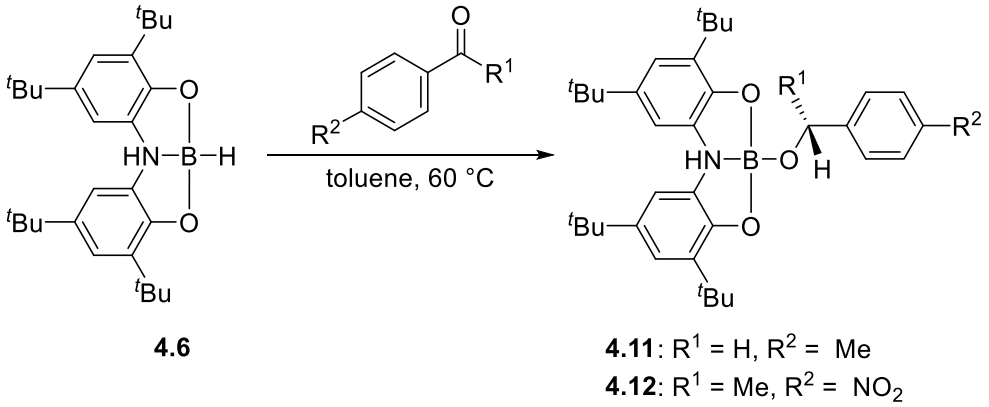
To conclude, we have shown that Lewis acids or bases can act as catalysts for the dehydrogenation of the amine-borane **4.6**. The controllable dehydrogenation reactivity provides a conceptual model for the study of hydrogen storage materials. That being

said, **4.6** has a low gravimetric density of dihydrogen (0.0046 kg H_2 per kg of **4.6**) and regeneration of **4.6** from **4.9** (or **4.10**) is not thermodynamically favoured, so this system is of limited practical utility.

4.7 Reaction of 4.6 towards unsaturated substrates

Organoboranes such as pinacolborane (HBpin) or catecholborane (HBCat) are widely used in organic synthesis. The reaction of boranes with unsaturated substrates often results in the hydroborated product, although catalysts are needed in most cases.[52] The reactivity of **4.6** towards Lewis acids and bases was demonstrated in Sections 4.5 and 4.6, and in this section, the reactivity of **4.6** towards small molecule substrates such as aldehydes and ketones is explored.

The reaction of 4-methylbenzaldehyde with **4.6** in toluene at 60 °C for 4 hours results in the hydroborated product **4.11** (Scheme 4.16). This is evidenced by the appearance of a characteristic ^{1}H NMR resonance at 5.04 ppm for the methylene group of **4.11**. The ^{1}H NMR spectrum reveals resonances attributed to the $[ON(H)O]^{2-}$ ligand backbone at 7.30 and 6.92 (Ar-H), 5.04 ppm (N−H), and 1.49 and 1.24 ppm (^{t}Bu). A singlet resonance in the $^{11}B\{^1H\}$ NMR spectrum at 13.8 ppm is consistent with a pseudo-tetrahedral boron centre. Single crystals of **4.11** were isolated by crystallisation from a pentane solution. The structure reveals the insertion of the carbonyl (C=O) from 4-methylbenzaldehyde into the B−H bond of **4.6** (Figure 4.8).



Scheme 4.16: Synthesis of **4.11** and **4.12**.

The use of catalysts is necessary for hydroboration of ketones in many cases, for example, in the reaction of HBpin with ketones, but amine-borane **4.6** can hydroborate ketones at mild temperature without the addition of a catalyst.[53] Carbonyl insertion of 4′-nitroacetophenone into the B−H bond of **4.6** is slow at room temperature as a result of the poor solubility of **4.6** in toluene, however full conversion from **4.6** to **4.12** was observed after the solution has been heated at 60 ℃ for four hours. A quartet signal at 5.18 ppm in ^{1}H NMR spectrum indicates the formation of the new C−H bond. All other resonances arising from the ligand are similar to those observed for **4.11**. The ^{11}B{^{1}H} NMR resonance observed for **4.12** (12.9 ppm) is also similar to that of **4.11** (13.8 ppm).

To summarise, in this section, amine-borane **4.6** is shown to react with an aldehyde and a ketone to give boron ester complexes **4.11** and **4.12** in the absence of a catalyst. In principle, those boron ester complexes can be hydrolysed to give the corresponding alcohols. A substrate scope for this process has not yet been fully established, and other substrates such as imines and isocyanates would also be worthy of exploration.

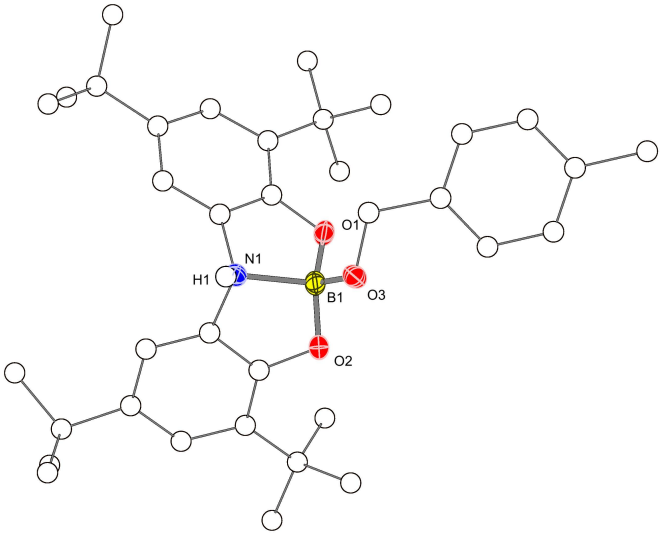


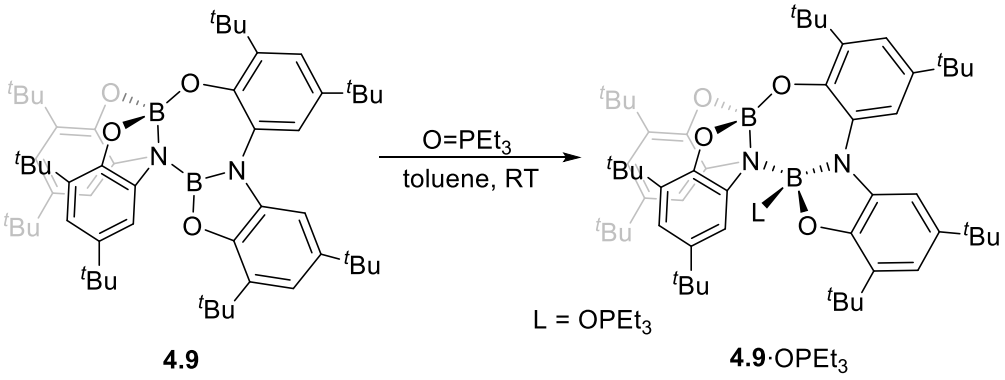
Figure 4.8: Single crystal X-ray structure of **4.11**. Anisotropic displacement ellipsoids are set at 50% probability. Hydrogen atoms (with the exception of H1) have been omitted for clarity. All carbon atoms are pictured as spheres of arbitrary radius. Selected interatomic distances [Å] and angles [°]: B1–N1 1.693(3), B1–O1 1.460(3), B1–O2 1.446(3), B1–O3 1.421(3); O1-B1-N1 101.12(15), O1-B1-O2 113.89(19), O2-B1-N1 102.71(16), O3-B1-N1 112.57(18), O3-B1-O1 114.44(18), O3-B1-O2 111.10(17).

4.8 Determination of the Lewis acidity of 4.8 and 4.9

The definition of a Lewis acid was first introduced in 1923 and has been extensively studied ever since.[54–58] According to Krossing, species with a greater Lewis acidity than SbF_5 in the gas phase are Lewis superacids, and their strength can be determined by calculating their fluoride ion affinity (FIA). More recently, Greb has defined the concept of a "soft" Lewis superacid as a species which exhibits a greater hydride ion affinity than BCF.[59] Other experimental methods for measuring Lewis acidity like the Gutmann-Beckett method (which compares the induced $^{31}P\{^{1}H\}$ NMR chemical shift of the Et_3PO adduct relative to the free phosphine oxide) or Child's method (comparing the induced ^{1}H NMR shift of the H3 proton in *trans*-crotonaldehyde on reaction with

an acid) are routinely employed.[60,61] These experimental methods are all highly system dependent, so multiple methods are often used together for a more accurate determination for Lewis acidity.[62]

As complex **4.9** has one tricoordinate boron centre (Figure 4.6), it provides a coordination site (an empty boron-based p-orbital) for nucleophiles. Triethylphosphine oxide, as an indicator of Lewis acid strength, was added to **4.9** to afford **4.9**·$OPEt_3$, as shown in Scheme 4.17.



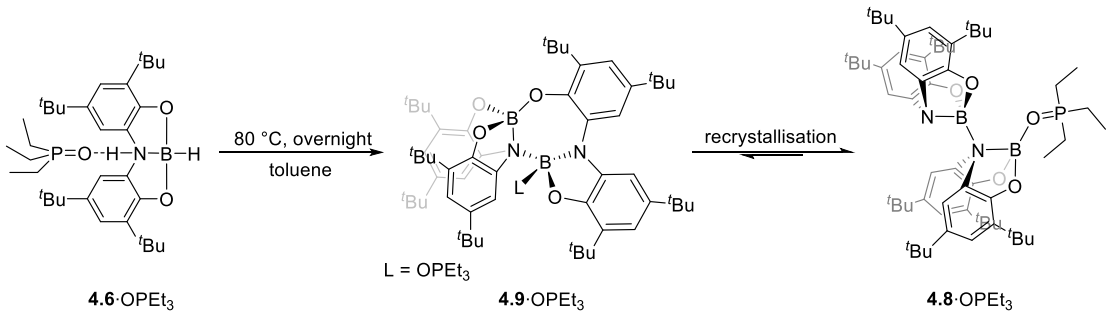
Scheme 4.17: Synthesis of **4.9**·$OPEt_3$.

In situ ^1H NMR studies indicate eight inequivalent signals for the aromatic ligand backbone of **4.9**·$OPEt_3$ (8.16, 7.72, 7.67, 7.46, 7.28, 7.22, 7.06 and 6.98 ppm), together with eight inequivalent singlets for the *tert*-butyl groups (1.98, 1.89, 1.61, 1.48, 1.40, 1.37, 1.32 and 1.13 ppm). The $^{11}B\{^1H\}$ NMR resonances at 13.8 and 8.0 ppm indicate two boron atoms with different environments.

The $^{31}P\{^1H\}$ NMR spectrum of **4.9**·$OPEt_3$ reveals a broad resonance at 73.6 ppm, which suggests **4.9** is a moderate Lewis acid. To benchmark the Lewis acidity of **4.9**, the $^{31}P\{^1H\}$ NMR chemical shift of triethylphosphine oxide adduct of BCF (75.9 ppm) and BPh_3 (71.0 ppm) were measured. This shows that **4.9** has stronger Lewis acidity than BPh_3, but weaker than BCF.

As mentioned previously, we have shown that complex **4.6** is stable in the solid state and in solution, without observable decomposition even after heating at 80 °C over a week. As the single crystal structure of **4.6**·$OPEt_3$ (Figure 4.4) suggests a strong hydrogen bonding interaction between $OPEt_3$ and the amine moiety (N−H) of ligand backbone of **4.6**, we reasoned that this would weaken the N−H bond, and that **4.6**·$OPEt_3$ is more likely to generate a molecule of dihydrogen upon heating.

Heating a C_6D_6 solution of **4.6**·$OPEt_3$ at 80 °C overnight releases H_2, as evidence by the observation of a resonance in the ^1H NMR spectrum of the mixture at 4.47 ppm. The ^1H NMR spectrum also indicates the formation of dimeric boron complex **4.9**·$OPEt_3$ (Scheme 4.18).



Scheme 4.18: Synthesis of **4.8**·$OPEt_3$ and **4.9**·$OPEt_3$.

Interestingly, recrystallisation of **4.9**·$OPEt_3$ in benzene or toluene only affords its isomer **4.8**·$OPEt_3$ (Figure 4.9). Single crystals of **4.8**·$OPEt_3$ were re-dissolved in $CDCl_3$ for NMR spectroscopic studies, and the $^{31}P\{^1H\}$ NMR spectrum revealed a signal at 80.0 ppm which was downshifted from that of **4.9**·$OPEt_3$ at 73.6 ppm. The $^{11}B\{^1H\}$ NMR spectrum of **4.8**·$OPEt_3$ showed resonances at 16.3 and 13.1 ppm, which differ from those of **4.9**·$OPEt_3$ at 13.8 and 8.0 ppm.

The molecular structure of **4.8**·$OPEt_3$ reveals that, in the solid state, two equivalents of *N*,*N*-bis(3,5-di-*tert*-butyl-2-phenoxy)amide boron form a dimer through dative bond

interactions, with one boron coordinated to a triethylphosphine oxide. The length of the B···OPh_3 interaction in **4.8**·$OPEt_3$ (1.472(3) Å) is relatively short compared to other $OPEt_3$ adducts Lewis acids such as that of 9-phosphonium-10-boratriptycene (1.503(2) Å), which corresponds to the greater Lewis acidity of **4.8**.[63]

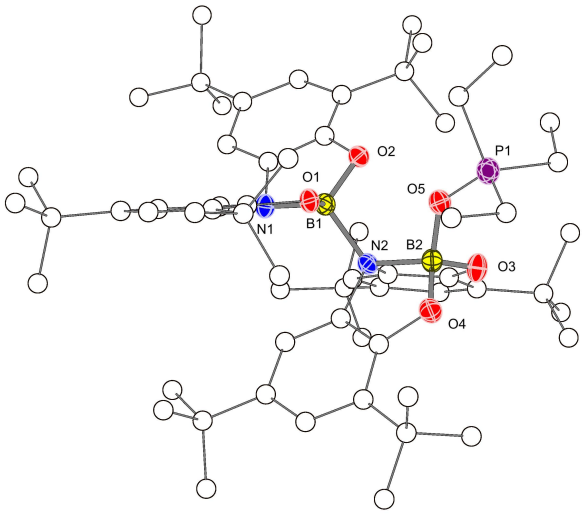
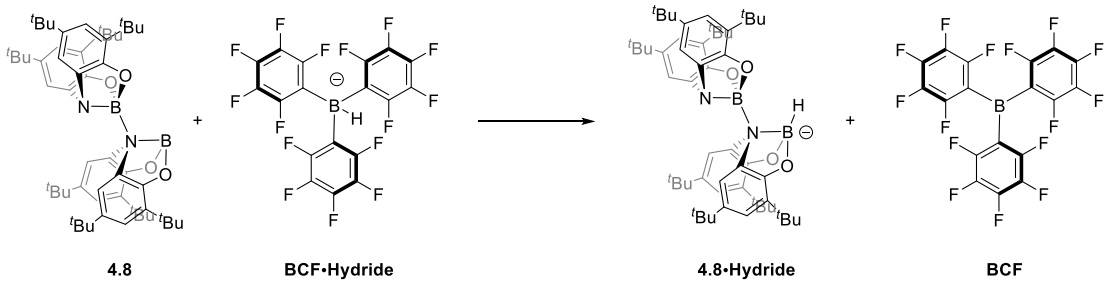


Figure 4.9: Single crystal X-ray structure of **4.8**·$OPEt_3$. Anisotropic displacement ellipsoids are set at 50% probability. Hydrogen atoms have been omitted for clarity. All carbon atoms are pictured as spheres of arbitrary radius. Selected interatomic distances [Å] and angles [°]: B1–N1 1.534(3), B1–N2 1.636(3), B1–O1 1.469(2), B1–O2 1.465(2), B2–N2 1.634(3), B2–O3 1.453(2), B2–O4 1.454(3), B2–O5 1.472(3), P1–O5 1.5271(15); O1-B1-N1 104.98(14), O1-B1-O2 121.09(16), O1-B1-N2 104.80(15), O2-B1-N1 104.93(15), O2-B1-N2 104.95(14), N1-B1-N2 116.88(16), O3-B2-N2 105.19(15), O3-B2-O4 113.87(17), O3-B2-O5 110.67(16), O4-B2-N2 105.09(15), O4-B2-O5 110.42(16), O5-B2-N2 111.37(15), B2-N2-B1 115.27(14), B2-O5-P1 137.47(13).

The observed $^{31}P\{^{1}H\}$ NMR signal at 80.0 ppm for Et_3PO in **4.8**·$OPEt_3$ (with an acceptor number AN = 86.2) is 4.1 ppm more downfield than the Et_3PO adduct of BCF at 75.9 ppm (with an acceptor number AN = 77.1), suggesting the boron centre in **4.8** is a stronger Lewis acid. The computational hydride affinity (HIA) of **4.8** in the gas phase is 22 kJ mol^{-1} greater than BCF (Scheme 4.19), which suggests that **4.8** is a soft Lewis superacid according to Greb's definition.[59]



Scheme 4.19: Calculation of hydride affinity of **4.8**.

Unfortunately, the Lewis acidity indicator $OPEt_3$ does not react with **4.10** even after heating at 80 °C for 2 days. The boron centre of **4.10** adopts a planar geometry that may receive π-electrons from the ligand, which stops the boron centre from accepting a lone pair electron from $OPEt_3$. Hence, **4.10** was not targeted for further reactivity tests.

4.9 Conclusions

In this chapter, the transelementation of gallium hydride **2.7** with BCF was described. The reactivity of $[H_3(ONO)]$ with boranes such as BPh_3, BCF, HBpin and $BH_3{\cdot}SMe_2$ was also examined. Boron complex **4.3** undergoes dearylation to give benzene and **4.4** in solution spontaneously at room temperature. Boron complex **4.1** is stable even after heating at 60 °C overnight, but the use of a base was found to facilitate the release of one equivalent of pentafluorobenzene at room temperature. The dehydrocoupling reactivity of $[H_3(ONO)]$ with HBpin to give **4.5** was established as well.

The reaction of amine-borane **4.6** with $OPEt_3$ and DMSO afforded the adducts **4.6**·$OPEt_3$ and **4.6**·DMSO respectively, through hydrogen bonding interactions. Instead of undergoing a classic dehydrocoupling reaction between an amine and a borane, addition of *n*-propylamine resulted in the dehydrogenation of **4.6**, giving a Lewis acid-base adduct **4.7** as the product.

Amine-borane complex **4.6** is stable as a solid or towards heat in the absence of a Lewis acid or base, and the synthesis is feasible on a gram scale. However, in the presence of Lewis acid, such as BCF (5 mol%), it dehydrogenates at room temperature to give the dimeric boron complex **4.9** as the product. This catalytic dehydrogenation reactivity was also found to be active in the presence of a non-nucleophilic Lewis base, e.g. $Et^{i}Pr_2N$ (10 mol%), albeit heating at 80 ℃ was needed. Interestingly, at room temperature, the use of $GaCl_3$ (10 mol%) as a catalyst in the dehydrogenation of **4.6**, resulting in the formation of two different boron complexes **4.9** and **4.10**.

The reactivity of **4.6** in carbonyl reduction was also carried at 60 ℃, **4.6** could hydroborate 4-methylbenzaldehyde and 4′-nitroacetophenone to give corresponding borate esters **4.11** and **4.12**.

Later, the Lewis acidity of boron complexes was studied. Upon the addition of a Lewis base, such as $OPEt_3$, complex **4.9** converts to an adduct of **4.9**·$OPEt_3$. Heating the adduct of **4.6**·$OPEt_3$ at 80 ℃ afforded a pair of isomers, **4.8**·$OPEt_3$ and **4.9**·$OPEt_3$, as evidenced by in situ NMR experiments, while subsequent recrystallisation only gave **4.8**·$OPEt_3$ in the solid state. Using the Gutmann–Beckett method, Lewis acidity strength was established, suggesting the order of BPh_3 < **4.9** < BCF < **4.8**, in which **4.8** is a mid-strength Lewis acid, while **4.9** is a strong Lewis acid.

4.10 References

[1] L. Liu, S.-K. Lo, C. Smith, J. M. Goicoechea, *Chem. Eur. J.* **2021**, *27*, 17379–17385.

[2] G. Szigethy, A. F. Heyduk, *Dalton Trans.* **2012**, *41*, 8144–8152.

[3] C. Camacho-Camacho, G. Merino, F. J. Martínez-Martínez, H. Nöth, R. Contreras, *Eur. J. Inorg. Chem.* **1999**, 1021–1027.

[4] A. Lale, S. Bernard, U. B. Demirci, *ChemPlusChem* **2018**, *83*, 893–903.

[5] A. Rossin, M. Peruzzini, *Chem. Rev.* **2016**, *116*, 8848–8872.

[6] S. Akbayrak, S. Özkar, *Int. J. Hydrogen Energy* **2018**, *43*, 18592–18606.

[7] M. S. Hill, G. Kociok-Köhn, T. P. Robinson, *Chem. Commun.* **2010**, *46*, 7587–7589.

[8] A. M. Chapman, M. F. Haddow, D. F. Wass, *J. Am. Chem. Soc.* **2011**, *133*, 18463–18478.

[9] E. Bernabé-Pablo, V. Jancik, M. Moya-Cabrera, *Inorg. Chem.* **2013**, *52*, 6944–6950.

[10] P. A. Lummis, R. McDonald, M. J. Ferguson, E. Rivard, *Dalton Trans.* **2015**, *44*, 7009–7020.

[11] K. A. Erickson, J. P. W. Stelmach, N. T. Mucha, R. Waterman, *Organometallics* **2015**, *34*, 4693–4699.

[12] D. Pun, E. Lobkovsky, P. J. Chirik, *Chem. Commun.* **2007**, 3297–3299.

[13] Y. Jiang, H. Berke, *Chem. Commun.* **2007**, 3571–3573.

[14] J. R. Vance, A. Scha, A. P. M. Robertson, K. Lee, J. Turner, G. R. Whittell, I. Manners, *J. Am. Chem. Soc.* **2014**, *136*, 3048–3064.

[15] A. Glüer, M. Förster, V. R. Celinski, J. Schmedt Auf Der Günne, M. C. Holthausen, S. Schneider, *ACS Catal.* **2015**, *5*, 7214–7217.

[16] J. R. Vance, A. Schäfer, A. P. M. Robertson, K. Lee, J. Turner, G. R. Whittell, I. Manners, *J. Am. Chem. Soc.* **2014**, *136*, 3048–3064.

[17] B. L. Conley, T. J. Williams, *Chem. Commun.* **2010**, *46*, 4815–4817.

[18] M. Käß, A. Friedrich, M. Drees, S. Schneider, *Angew. Chem., Int. Ed.* **2009**, *48*, 905–907.

[19] A. Friedrich, M. Drees, S. Schneider, *Chem. Eur. J.* **2009**, *15*, 10339–10342.

[20] A. Y. Timoshkin, H. F. Schaefer, *J. Am. Chem. Soc.* **2003**, *125*, 9998–10011.

[21] A. N. Marziale, A. Friedrich, I. Klopsch, M. Drees, V. R. Celinski, J. Schmedt Auf Der Günne, S. Schneider, *J. Am. Chem. Soc.* **2013**, *135*, 13342–13355.

[22] M. J. Sgro, D. W. Stephan, *Dalton Trans.* **2013**, *42*, 10460–10472.

[23] A. Rossin, A. Rossi, M. Peruzzini, F. Zanobini, *ChemPlusChem* **2014**, *79*, 1316–1325.

[24] G. Alcaraz, L. Vendier, E. Clot, S. Sabo-Etienne, *Angew. Chem., Int. Ed.* **2010**, *49*, 918–920.

[25] M. A. Esteruelas, F. J. Fernández-Alvarez, A. M. López, M. Mora, E. Oñate, *J. Am. Chem. Soc.* **2010**, *132*, 5600–5601.

[26] C. Bianchini, G. Giambastiani, A. Rossin, *Chemtracts* **2007**, *20*, 273–276.

[27] H. C. Johnson, A. P. M. Robertson, A. B. Chaplin, L. J. Sewell, A. L. Thompson, M. F. Haddow, I. Manners, A. S. Weller, *J. Am. Chem. Soc.* **2011**, *133*, 11076–11079.

[28] B. L. Dietrich, K. I. Goldberg, D. M. Heinekey, T. Autrey, J. C. Linehan, *Inorg. Chem.* **2008**, *47*, 8583–8585.

[29] C. Y. Tang, N. Phillips, M. J. Kelly, S. Aldridge, *Chem. Commun.* **2012**, *48*, 11999–12001.

[30] S. Li, G. Li, W. Meng, H. Du, *J. Am. Chem. Soc.* **2016**, *138*, 12956–12962.

[31] D. H. A. Boom, E. J. J. de Boed, E. Nicolas, M. Nieger, A. W. Ehlers, A. R. Jupp, J. C. Slootweg, *Z. Anorg. Allg. Chem.* **2020**, *646*, 586–592.

[32] Z. Mo, A. Rit, J. Campos, E. L. Kolychev, S. Aldridge, *J. Am. Chem. Soc.* **2016**, *138*, 3306–3309.

[33] D. W. Stephan, G. Erker, *Angew. Chem., Int. Ed.* **2015**, *54*, 6400–6441.

[34] D. W. Stephan, G. Erker, *Angew. Chem., Int. Ed.* **2010**, *49*, 46–76.

[35] C. Appelt, J. C. Slootweg, K. Lammertsma, W. Uhl, *Angew. Chem., Int. Ed.* **2013**, *52*, 4256–4259.

[36] H. Kurosawa Yamamoto, Akio, *Fundamentals of Molecular Catalysis*, Elsevier, Amsterdam; Boston, **2003**.

[37] Q. Lai, N. Bhuvanesh, O. V Ozerov, *J. Am. Chem. Soc.* **2020**, *142*, 20920–20923.

[38] N. Miyaura, K. Yamada, A. Suzuki, *Tetrahedron Lett.* **1979**, *20*, 3437–3440.

[39] N. Miyaura, A. Suzuki, *Chem. Rev.* **1995**, *95*, 2457–2483.

[40] X. Jia, L. Fang, A. Lin, Y. Pan, C. Zhu, *Synlett* **2009**, *3*, 495–499.

[41] M. Devillard, C. Alvarez Lamsfus, V. Vreeken, L. Maron, J. I. van der Vlugt, *Dalton Trans.* **2016**, *45*, 10989–10998.

[42] J. A. Bruggen, K. D. Feller, H. I. Schickel, N. Tuleushova, M. Zhukush, K. Lam, B. M. Barry, R. A. Kemp, *Main Group Chem.* **2017**, *16*, 307–319.

[43] A. H. Cowley, C. L. B. Macdonald, J. S. Silverman, J. D. Gorden, A. Voigt, *Chem. Commun.* **2001**, 175–176.

[44] G. Desiraju, T. Steiner, *The Weak Hydrogen Bond: In Structural Chemistry and Biology*, Oxford University Press, **2001**.

[45] S. Kharel, N. Bhuvanesh, J. A. Gladysz, J. Blümel, *Inorg. Chim. Acta* **2019**, *490*, 215–219.

[46] R. L. Melen, *Chem. Soc. Rev.* **2016**, *45*, 775–788.

[47] D. J. Liptrot, M. S. Hill, M. F. Mahon, A. S. S. Wilson, *Angew. Chem., Int. Ed.* **2015**, *54*, 13362–13365.

[48] J. D. Erickson, T. Y. Lai, D. J. Liptrot, M. M. Olmstead, P. P. Power, *Chem. Commun.* **2016**, *52*, 13656–13659.

[49] G. R. Fulmer, A. J. M. Miller, N. H. Sherden, H. E. Gottlieb, A. Nudelman, B. M. Stoltz, J. E. Bercaw, K. I. Goldberg, *Organometallics* **2010**, *29*, 2176–2179.

[50] K. A. Erickson, D. S. Wright, R. Waterman, *J. Organomet. Chem.* **2014**, *751*, 541–545.

[51] S.-K. Lo, *Geometry Constrained Main-Group Compounds for the Activation of Small Molecules*, Thesis (D.Phil.) − University of Oxford, 2018, (Department of Inorganic Chemistry), Oxford, **2018**.

[52] M. L. Shegavi, S. K. Bose, *Catal. Sci. Technol.* **2019**, *9*, 3307–3336.

[53] C. C. Chong, R. Kinjo, *ACS Catal.* **2015**, *5*, 3238–3259.

[54] G. N. Lewis, *Valence and the Structure of Atoms and Molecules*, The Chemical Catalog Company, Book Department, New York, **1923**.

[55] A. Corma, H. García, *Chem. Rev.* **2003**, *103*, 4307–4366.

[56] G. A. Olah, R. H. Schlosberg, *J. Am. Chem. Soc.* **1968**, *90*, 2726–2727.

[57] J. S. G. A.Olah, G. K. S. Prakash, Á. Molnár, *Superacid Chemistry, Second Edition*, **2009**.

[58] L. O. Müller, D. Himmel, J. Stauffer, G. Steinfeld, J. Slattery, G. Santiso-Quiñones, V. Brecht, I. Krossing, *Angew. Chem., Int. Ed.* **2008**, *47*, 7659–7663.

[59] L. Greb, *Chem. Eur. J.* **2018**, *24*, 17881–17896.

[60] U. Mayer, V. Gutmann, W. Gerger, *Monatsh. Chem.* **1975**, *106*, 1235–1257.

[61] R. F. Childs, D. L. Mulholland, A. Nixon, *Can. J. Chem.* **1982**, *60*, 809–812.

[62] P. Erdmann, L. Greb, *ChemPhysChem* **2021**, *22*, 935–943.

[63] A. Ben Saida, A. Chardon, A. Osi, N. Tumanov, J. Wouters, A. I. Adjieufack, B. Champagne, G. Berionni, *Angew. Chem., Int. Ed.* **2019**, *58*, 16889–16893.

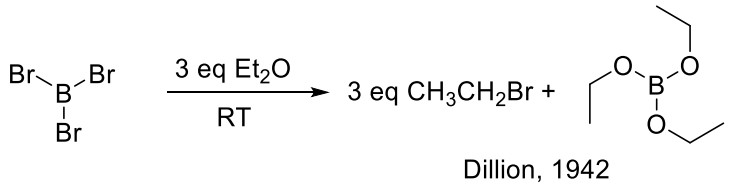
Chapter Five

Synthesis and reactivity of pincer stabilised boron halide complexes

5.1 Introduction and objectives

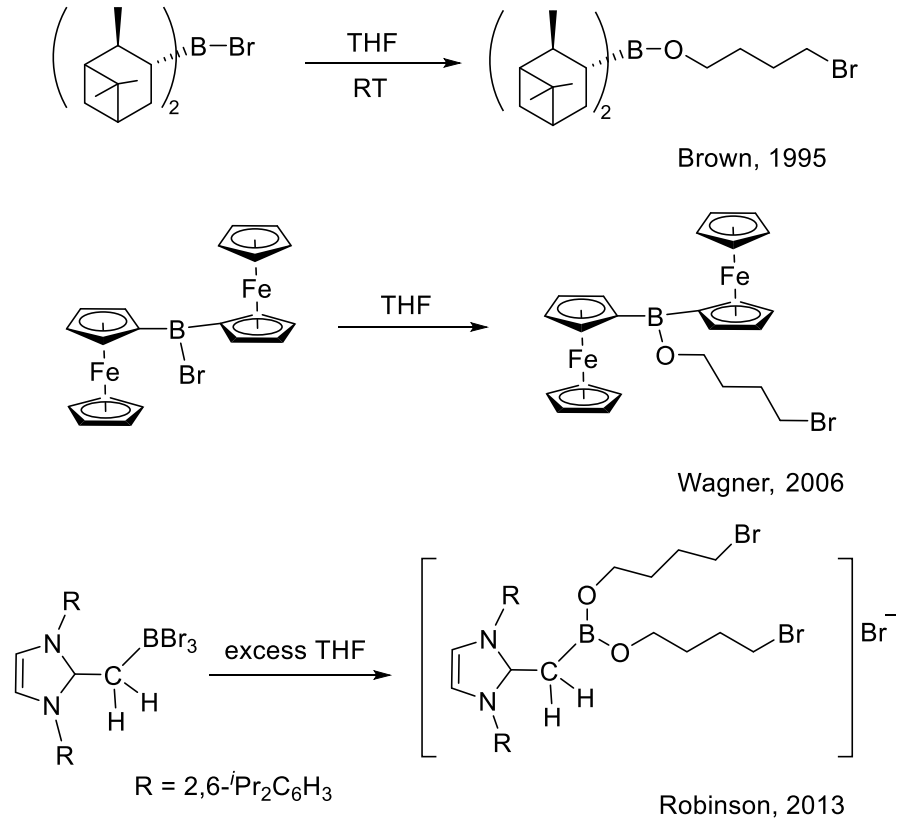
In Chapter Four, the preparation of a series of boron complexes was described, with the dehydrogenation reactivity of an amine-borane (**4.6**) complex highlighted. As mentioned in the Section 4.1, the first attempt to synthesise the [ON(H)O]BCl ($[ON(H)O]^{2-}$ = *N*,*N*-bis(3,5-di-*tert*-butyl-2-phenoxy)amide) complex was previously reported by Contreras and co-workers using transelementation, however they were unable to structurally authenticate this compound by single crystal X-ray diffraction.[1] This chapter investigates [H_3(ONO)] in boron halide stabilization, and describes the reactivity of the resulting ligand-stabilised boron halides.

Carbon−oxygen (C−O) bonds in ethers are prevalent in natural products or bio-active molecules such as lignin, ramelteon and taxol. C−O bonds are robust and difficult to activate. Methods to activate them include using strong protic acids (such as HI, HBr) at elevated temperature, transition metals or strong Lewis acids (such as BBr_3, BI_3).[2,3] The history of boron tribromide in C−O bond cleavage dates back to 1942, in which Dillion reported the C−O bond cleavage of Et_2O by BBr_3 (Scheme 5.1).[4]



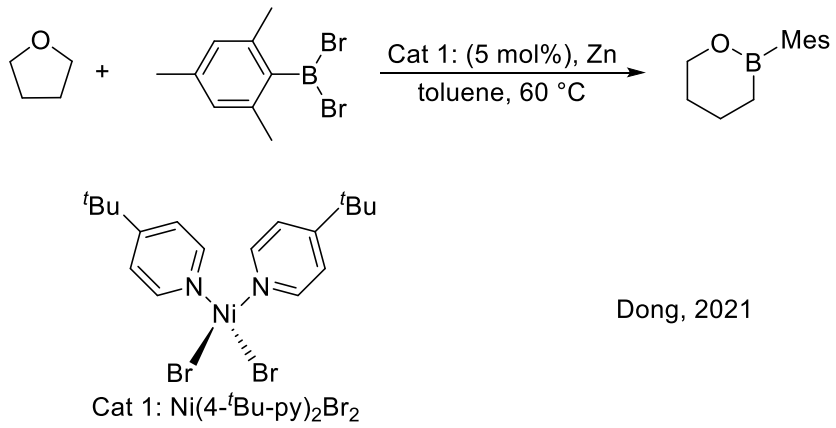
Scheme 5.1: Boron tribromide in diethyl ether activation.[4]

Other examples, such as diisopinocampheylbromoborane (IPc_2BBr), diferrocenylbromoborane (Fc_2BBr) and ylidic *N*-heterocyclic olefin-stabilised boron tribromide ($NHO{\cdot}BBr_3$) have been reported to activate the C−O bond of THF by Brown, Wagner and Robinson, respectively (Scheme 5.2).[5–9]



Scheme 5.2: Boron bromides in THF activation.[5,6,9]

Recently, Dong has demonstrated the borylation of cyclic ethers through a cleavage-then-rebound pathway, by using a nickel catalyst Ni(4-^{t}Bu-py)$_2$Br$_2$ and a zinc reductant.[10] As an example, the boron atom of MesBBr$_2$ inserted into the C−O moiety of THF to give an expanded six-membered ring (oxaborinane) bearing a B−O moiety (Scheme 5.3). This strategy is applicable to the ring expansion of a wide scope of cyclic ethers. The boron moiety in isolable oxaborinanes can be further functionalised to boronates, pyrrolidines, or even take part in one-carbon ring expansions. The exploration of C−O bond activation singular could shed light on new synthetic strategies for organic and bioactive compounds.



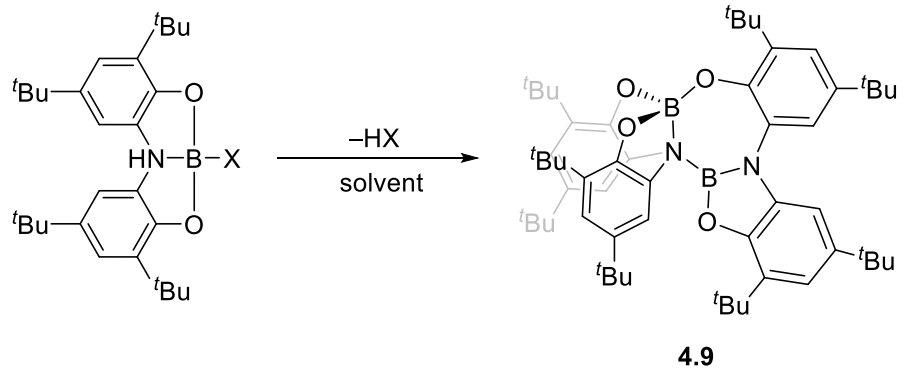
Scheme 5.3: An example of THF borylation.[10]

In this chapter, the preparation of a series of boron halide complexes supported by the $[ON(H)O]^{2-}$ ligand is first discussed, followed by the synthesis of base-stabilised boron complexes. Later we will introduce the application of a pincer-stabilised boron bromide in C−O bond cleavage and ring-closing reactivity with a base. Finally, the reactivity of boron halides in small molecule activation will also be demonstrated.

5.2 Synthesis of pincer stabilised boron halide complexes

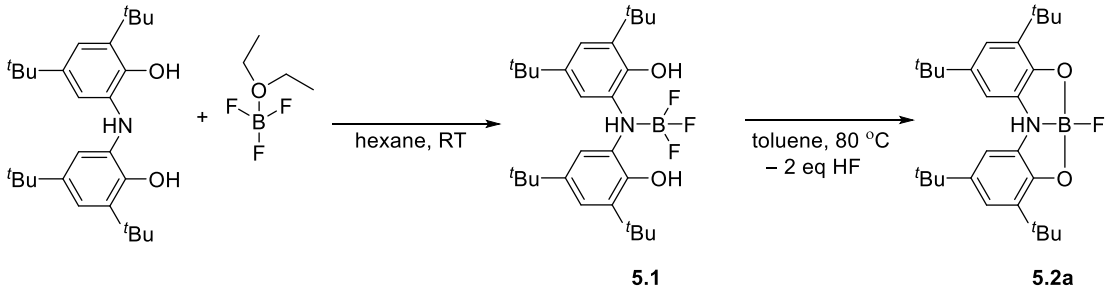
The boron halides $[(Me)N(OCH_2CH_2)_2]BX$ (X = F, Cl) bearing the tridentate ligand (O, N, O) was previously reported by Aldridge and co-workers through the reaction of $(Me_3SiOCH_2CH_2)_2NMe$ and BX_3 (X = F, Cl).[11] In view of this, we sought to synthesise novel boron complexes [ON(H)O]BX through similar synthetic protocols.

In Chapter Four, the ligand cooperative dehydrogenation reactivity of amine-borane **4.6** was demonstrated. With a similar structure, the same type of dehydrohalogenation reactivity was investigated for the ligand stabilised boron halides [ON(H)O]BX. This kind of transformation could controllably release a stoichiometric amount of hydrohalide acids (Scheme 5.4).[12,13]



Scheme 5.4: Proposed model for dehydrogenation/dehydrohalogenation of pincer stabilised boron halides.

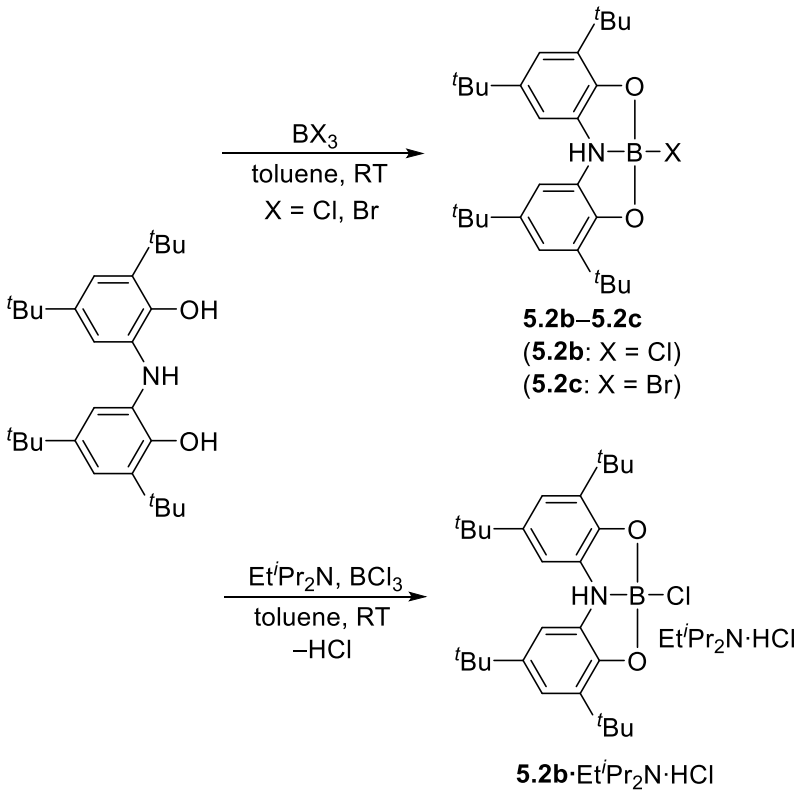
A preliminary reaction of [H_3(ONO)] with boron trifluoride diethyl etherate ($BF_3{\cdot}OEt_2$) was carried in hexane at room temperature, resulting in a white precipitate consisting of a mixture of **5.1** and **5.2a** (Scheme 5.5). Complex **5.1** has a protic hydroxy group and a four-coordinate boron trifluoride, which could possibly act as a source of HF. At room temperature, complex **5.1** has a tendency to release HF in solution and give **5.2a**, thus a compositionally pure sample of **5.1** could not be isolated. The ^{1}H NMR spectrum of **5.1** reveals two broad aromatic resonances attributed to ligand backbone at 7.92 and 7.32 ppm, with a phenol-proton signal at 10.49 ppm and an amine-proton signal at 6.93 ppm. A $^{11}B\{^{1}H\}$ NMR signal was observed at 0.1 ppm, while a $^{19}F\{^{1}H\}$ NMR signal was recorded at −145.79 ppm. As both resonances are broad, no B−F coupling was observed.



Scheme 5.5: Synthesis of **5.1** and **5.2a**.

Upon heating at 80 °C for 2 hours, complex **5.1** releases two equivalents of HF and affords **5.2a** as the sole product (Scheme 5.5). The ^{1}H NMR spectrum of **5.2a** displays two aromatic resonances attributed to the ligand backbone at 7.30 and 6.83 ppm, a resonance attributed to amine proton at 5.37 ppm, and two resonances attributed to *tert*-butyl groups at 1.47 and 1.24 ppm. The ^{11}B{^{1}H} NMR signal, at 12.2 ppm, is similar to the aforementioned four-coordinated boron complex, and ^{19}F{^{1}H} NMR spectrum reveals a signal at −144.15 ppm.

The synthesis of **5.2a** via the reaction of the protio-ligand and boron trifluoride was successful, and this general protocol was extended to the synthesis of other ligand stabilised boron halides **5.2b**, **5.2c**. The reaction of stochiometric amount of boron halides (BX_3, X = Cl, Br) with [H_3(ONO)] at room temperature directly afforded the [ON(H)O]BX (**5.2b**, **5.2c**) as white solids (Scheme 5.6).



Scheme 5.6: Synthesis of **5.2b**–**5.2c** and **5.2b** Et^{i}Pr$_2$N·HCl.

The ^{1}H NMR spectra in C_6D_6 of the [ON(H)O]BX complexes consistently show two doublet resonances for the aromatic protons of the ligand backbone (**5.2b**: 7.31, 6.76 ppm, **5.2c**: 7.30, 6.73 ppm), a broad N−H peak (**5.2b**: 6.05 ppm, **5.2c**: 6.30 ppm), and two *tert*-butyl resonances (**5.2b**: 1.44, 1.23 ppm, **5.2c**: 1.42, 1.21 ppm). The chemical shifts in the ^{11}B{^{1}H} NMR spectrum (**5.2b**: 14.7 ppm, **5.2c**: 12.4 ppm) are largely similar to that of **5.2a**.

When trying to synthesise **5.2b** in a toluene solution by reacting [H_3(ONO)] and BCl_3, in the presence of Et^{i}Pr$_2$N as the base, a different product **5.2b**·Et^{i}Pr$_2$N·HCl was formed (Scheme 5.6). ^{1}H NMR spectroscopic studies revealed a single product, with resonances attributed to the ligand (ArH: 8.00, 7.31 ppm; ^{t}Bu: 1.54, 1.29 ppm). The ^{11}B{^{1}H} NMR spectrum revealed a broad resonance at 14.9 ppm which is similar to that of **5.2b**. A broad downfield resonance at 11.44 ppm is attributed to the N−H moiety of the ligand backbone, while another downfield resonance at 12.17 ppm is from the proton of the ammonium cation (Et^{i}Pr$_2$NH^{+}). The downfield chemical shift of amine-proton of **5.2b** is due to the hydrogen bonding (Cl$^{\delta-}\cdots$H$^{\delta+}$−N, 2.10(3) Å) between N−H on ligand backbone and chlorine atom.

Subsequent crystallisation of the crude product from benzene afforded colourless single crystals, which were characterised as [ON(H)O]BCl·Et^{i}Pr$_2$N·HCl (**5.2b**·Et^{i}Pr$_2$N·HCl) by single crystal X-ray crystallography (Figure 5.1).

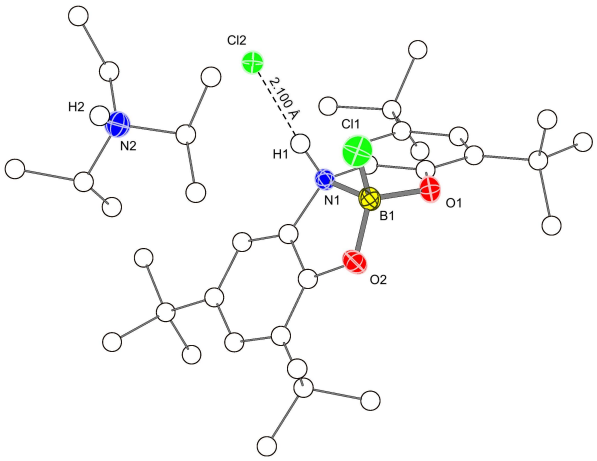


Figure 5.1: Single crystal X-ray structure of **5.2b**·Et^{i}Pr$_2$N·HCl. Anisotropic displacement ellipsoids are set at 50% probability. Hydrogen atoms (with the exception of H1 and H2) have been omitted for clarity. All carbon atoms are pictured as spheres of arbitrary radius. Selected interatomic distances [Å] and angles [°]: B1–Cl1 1.840(2), B1–N1 1.641(3), B1–O1 1.445(2), B1–O2 1.444(2); N1-B1-Cl1 112.36(14), O1-B1-Cl1 110.48(13), O1-B1-N1 104.29(14), O2-B1-Cl1 111.56(13), O2-B1-N1 103.76(14), O2-B1-O1 114.02(17).

Single crystals of **5.2c** suitable for X-ray crystallography were obtained from a concentrated benzene solution (Figure 5.2). The crystal structure of **5.2c** reveals a distorted tetrahedral boron atom. The bond length of B1−Br1 2.027(13) Å is longer than B1−Cl1 in **5.2b**·Et^{i}Pr$_2$N·HCl (1.840(2) Å), which is in line with the increased covalent radius of bromine relative to chlorine (r_{Cl} = 1.02 Å, r_{Br} = 1.20 Å, $r_{Br} - r_C$ = 0.18 Å).[14]

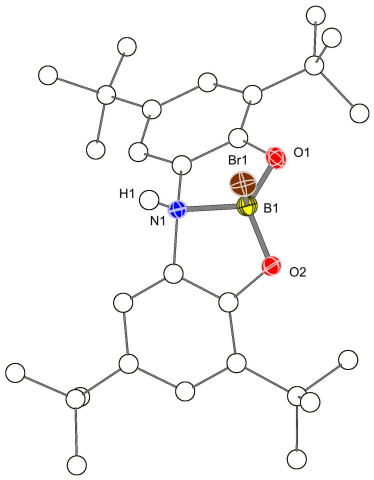


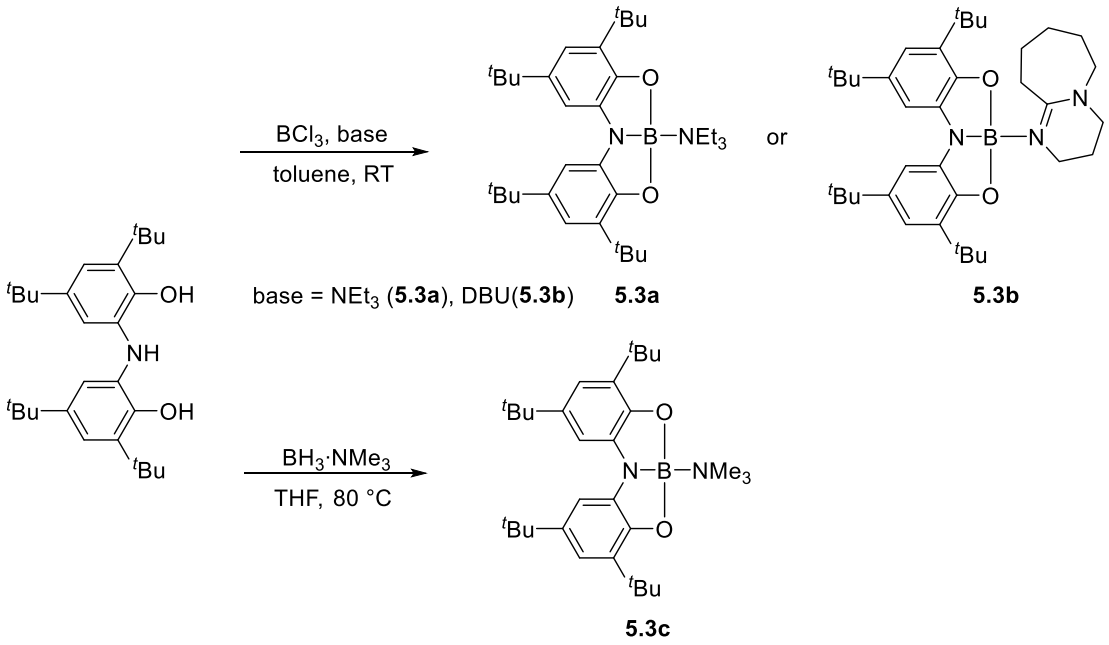
Figure 5.2: Single crystal X-ray structure of **5.2c**. Anisotropic displacement ellipsoids are set at 50% probability. Hydrogen atoms (with the exception of H1) have been omitted for clarity. All carbon atoms are pictured as spheres of arbitrary radius. Selected interatomic distances [Å] and angles [°]: B1–Br1 2.027(1), B1–N1 1.656(2), B1–O1 1.432 (2), B1–O2 1.436(2); N1-B1-Br1 110.08(8), O1-B1-N1 104.32(9), O1-B1-O2 115.40(11), O1-B1-Br1 110.84(8), O2-B1-N1 103.64(9), O1-B1-O2 115.40(11) O2-B1-Br1 111.94(8).

In summary, a series of ligand stabilised boron halides have been prepared through the reaction of BX_3 with $[H_3(ONO)]$. In the coming section, their reactivity will be further discussed.

5.3 Synthesis of Lewis base adducts of boron-halide complexes

As discussed in Chapter Four, Lewis base adducts of boron complexes can be synthesised through various pathways: (i) nucleophilic base induced dehydrogenation of amine-boranes (see, for example, the synthesis of **4.6**); or (ii) reaction of dimeric boron complexes with a Lewis base (see synthesis of **4.9**). With the novel ligand stabilised boron halides [ON(H)O]BX (**5.2b**−**5.2c**, X = Cl, Br) in hand, their application as precursors for the synthesis of boron Lewis base adducts was investigated.

The reaction of boron trichloride and [H_3(ONO)] in the presence of four equivalents of sterically unencumbered amines, such as triethylamine (NEt_3) and 1,8-diazabicyclo[5.4.0]undec-7-ene (DBU), results in base stabilised boron adducts **5.3a** and **5.3b** (**5.3a**: NEt_3, **5.3b**: DBU), as shown in Scheme 5.7. In this transformation, [H_3(ONO)] first reacts with boron trichloride in solution to generate (base-free) amine boron chloride **5.2b**, which subsequently reacts with the amine (NEt_3 or DBU) to afford ammonium hydrochloride salts and **5.3a** or **5.3b** as the final products. Direct dehydrohalogenation of **5.2b** with a base affords the same products as using boron trichloride.



Scheme 5.7: Synthesis of **5.3a**–**5.3c**.

Another strategy for Lewis base adduct synthesis is through the reaction of [H_3(ONO)] with amine-boranes, which was documented in the thesis of Dr Siu-Kwan Lo, as pictured in Scheme 5.7.[15] The reaction of one equivalent of trimethylamine-borane ($H_3B{\cdot}NMe_3$) in tetrahydrofuran with [H_3(ONO)] at 80 °C, results in the formation of **5.3c**. The ^{1}H NMR spectra of **5.3a** and **5.3c** in C_6D_6 are closely related, with two

resonances for the aromatic protons of the ligand backbone (**5.3a**: 7.63, 7.16 ppm; **5.3c**: 7.62, 7.16 ppm) and *tert*-butyl substituents (**5.3a**: 1.60, 1.43 ppm; **5.3c**: 1.59, 1.43 ppm). Their $^{11}B\{^{1}H\}$ NMR signals (**5.3a**: 16.2 ppm; **5.3c**: 15.7 ppm) are also relatively similar. The DBU boron adduct **5.3b** has poor solubility in benzene but good solubility in chloroform. The ^{1}H NMR spectrum of **5.3b** in $CDCl_3$ shows the resonances of the ligand backbone as two doublets at 7.18, 6.79 ppm, the *tert*-butyl resonances at 1.37 and 1.32 ppm, and the base (DBU) in the range of 3.53−1.32 ppm. The $^{11}B\{^{1}H\}$ NMR resonance was observed at 14.6 ppm.

Single crystals of **5.3b** suitable for XRD were grown from a benzene solution (Figure 5.3). The single crystal structure of **5.3c** was previously reported by Dr Siu-Kwan Lo in his doctoral thesis (Figure 5.4).[15] Both boron atoms of **5.3b** and **5.3c** are four-coordinate and adopt a tetrahedral geometry. The B1−N1 and B1−N2 bond distance of **5.3b** are close to that of **5.3c**.

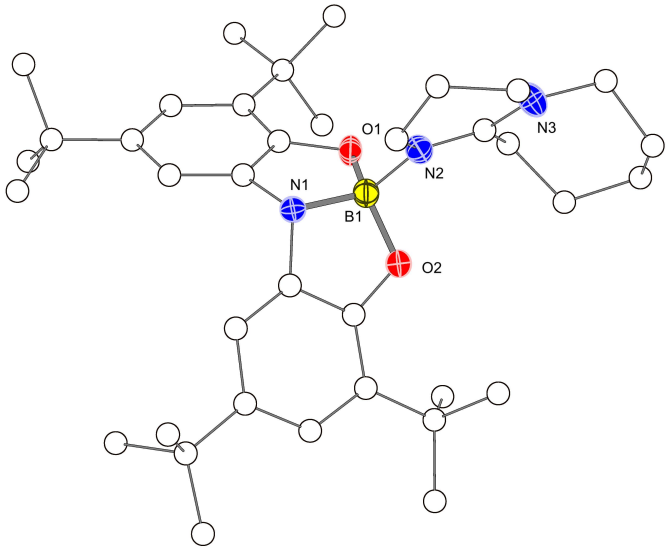


Figure 5.3: Single crystal X-ray structure of **5.3b**. Anisotropic displacement ellipsoids are set at 50% probability. Hydrogen atoms have been omitted for clarity. All carbon atoms are pictured as spheres of arbitrary radius. Selected interatomic distances [Å] and angles [°]: B1–N1 1.531(3), B1–O1 1.476(3), B1–O2 1.477(3), B1–N2 1.591(3); N1-B1-N2 114.3(2), O1-B1-N1 105.06(18), O1-B1-O2 116.2(2), O1-B1-N2 109.26(19), O2-B1-N1 105.04(19), O2-B1-N2 107.17(18).

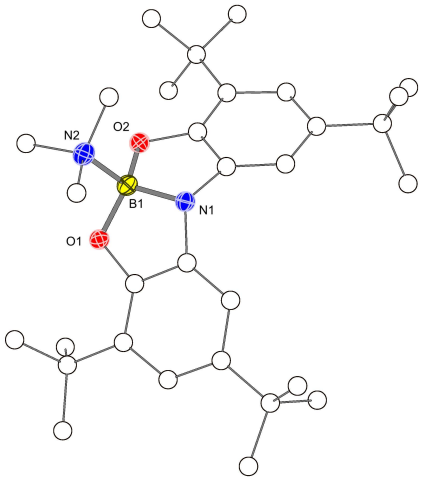
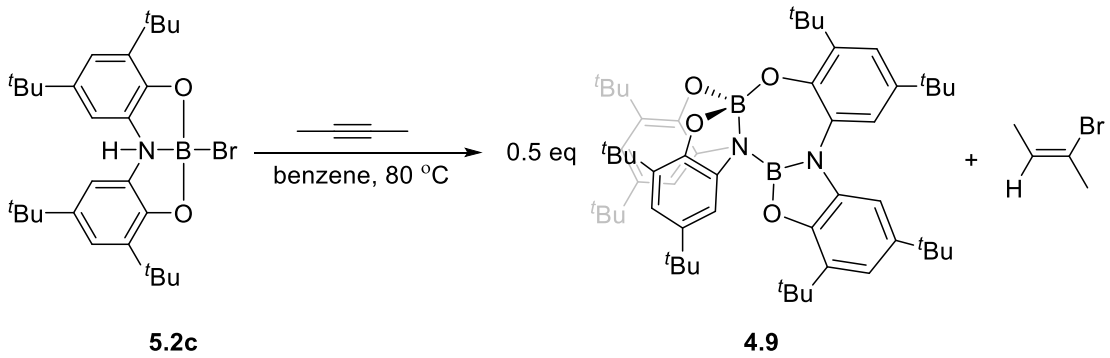


Figure 5.4: Single crystal X-ray structure of **5.3c**. Anisotropic displacement ellipsoids are set at 50% probability. Hydrogen atoms have been omitted for clarity. All carbon atoms are pictured as spheres of arbitrary radius. Selected interatomic distances [Å] and angles [°]: B1–N1 1.5133(17), B1–O1 1.4661(17), B1–O2 1.4630(17), B1–N2 1.6393(17); N1-B1-N2 112.00(10), O1-B1-N1 106.21(10), O1-B1-O2 119.31(11), O1-B1-N2 106.01(10), O2-B1-N1 106.33(11), O2-B1-N2 107.08(10).[15]

5.4 Transfer hydrobromination of 5.2c to an alkyne

As mentioned previously, we have synthesised three boron halide complexes [ON(H)O]BX (**5.2a**−**5.2c**) (Section 5.2). In an effort to understand their reactivity, we explored their thermostability. Heating the compounds in C_6D_6 solutions at 80 °C overnight demonstrated that **5.2a** and **5.2b** are both stable as determined by NMR spectroscopy, however **5.2c** gradually dehydrohalogenated to **4.9** and HBr. Even in solution, at room temperature, ^{1}H NMR spectroscopy revealed that **5.2c** would slowly dehydrohalogenate. After heating a solution of **5.2c** in C_6D_6, the solution was found to be in an equilibrium between **5.2** and **4.9** (and HBr). On equilibration, the **5.2c**:**4.9** ratio was found to be 1:1 (as determined by integration of ^{1}H NMR resonances). As this dehydrohalogenation reactivity could not reach full conversion, it was hypothesised some sort of hydrogen bromide acceptor, such as alkenes or alkynes, could react with the resulting hydrogen bromide and provide a thermodynamic driving force for complete dehydrohalogenation.[16,17]

To a benzene solution of **5.2c**, stochiometric 2-butyne was added which upon heating at 80 °C overnight, fully converted to **4.9**. The 2-butyne was hydrobrominated to *trans*-2-bromo-butene, as evidenced by a new ^{1}H NMR chemical shift at 5.22 ppm.



5.2c **4.9**

Scheme 5.8: Transfer hydrobromination of **5.2c** to 2-butyne.

The transfer hydrobromination reactivity shown as Scheme 5.8 supports the hypothesis that an HBr acceptor (such as an alkyne) could lead to a full conversion of **5.2c** to **4.9**. As the stereoselectivity is not the main target of this study, the mechanism for this selectivity was not further explored. In the future, a wider scope of substrates such as other alkynes and alkenes could be explored as potential HBr acceptors.

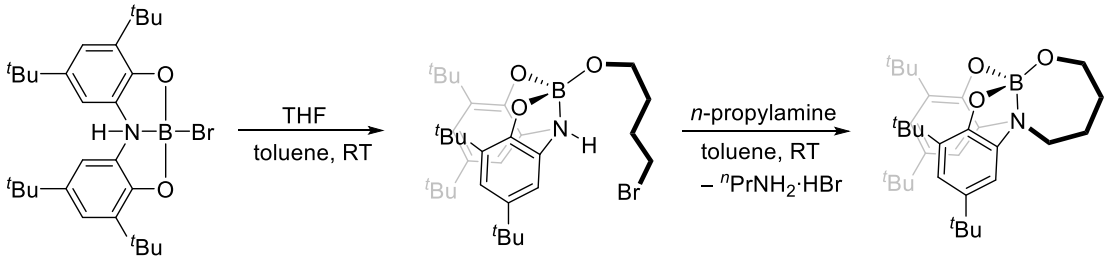
5.5 Application of 5.2c in C−O bond cleavage

In Section 5.1, some examples of boron bromide derivatives capable of C−O bond activation were discussed, with a highlight on THF (cyclic ether) ring-fission (Scheme 5.2). The preparation and reactivity (towards bases) of the pincer stabilised boron halide **5.2b** has been introduced in earlier sections and herein, the reactivity of **5.2c** towards heterocycles such as THF and dioxane will be discussed.

A preliminary reaction was performed when a stochiometric amount of THF was added to solution of **5.2c** in C_6D_6. Complex **5.2c** was fully consumed overnight at room temperature, as evidenced by NMR spectroscopy. The product was isolated as white solid.

Four new resonances (corresponding to the new product **5.4**) at 3.80 (triplet), 3.12 (triplet), 1.87 (multiplet) and 1.73 (multiplet) ppm, were assigned to a 2-bromobutoxy moiety (Scheme 5.9), which suggests that on reaction with THF, **5.2c** ring-opens the cyclic ether. The ^{1}H NMR spectrum also displayed two ligand backbone resonances as two doublets at 7.30 and 6.97 ppm, an amine resonance at 5.94 ppm, and two *tert*-butyl resonances at 1.48 and 1.26 ppm. The transformation from **5.2c** to **5.4** is an interesting process, as the four-carbon chain results from THF ring-opening, which is conceptually

similar to previously reported boron bromide complexes that are able to activate THF (Scheme 5.2).[4,5,18]

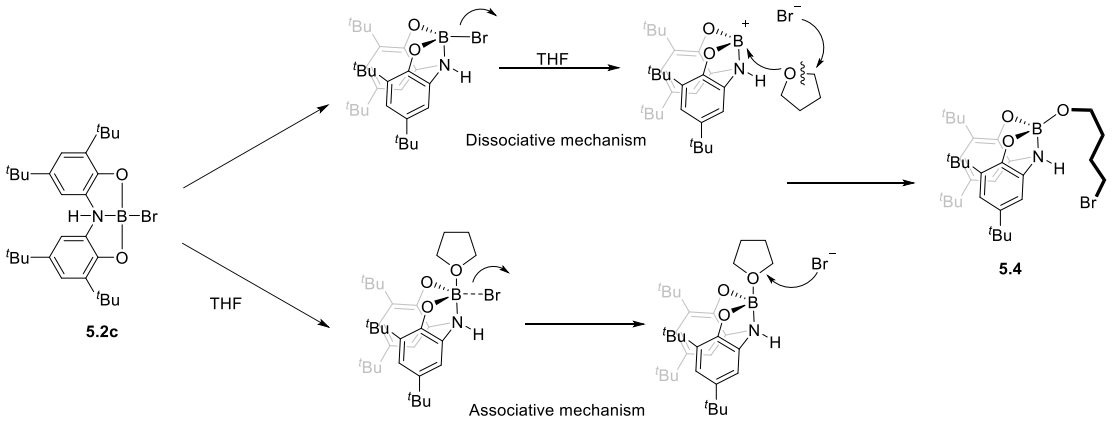


5.2c **5.4** **5.5**

Scheme 5.9: Synthesis of **5.4** and **5.5**.

Computational studies on the mechanism of boron tribromide mediated C−O bond cleavage were previously carried out by Silva and co-workers, and they suggested two possible mechanisms for this type of reactions.[7] The C−O bond could either be activated through a dissociative monomolecular mechanism (with dissociation of B−Br bond) or an associative bimolecular mechanism which has a five-coordinate transition state. According to DFT computations, it is possible that there is competition between these two mechanisms, and in some substrates (such as $PhCH_2OMe$), the energy barriers of two mechanisms are very close.

In view of this, two possible mechanisms are proposed for THF ring-opening (Scheme 5.10): (i) cleavage of B−Br bond and synchronous coordination of THF to the boron centre; and (ii) interaction between THF and the boron centre to give a five-coordinate transition state, both of which are followed by bromide mediated C−O bond cleavage of THF.



Scheme 5.10: Proposed mechanisms for THF activation.

With compound **5.4** in hand, its reactivity was explored. Upon addition of base (e.g. as *n*-propylamine) at room temperature in benzene, complex **5.4** eliminates the bromide and amine-proton, forming *n*-propylammonium bromide and complex **5.5**. The ^{1}H NMR spectrum reveals two ligand backbone signals at 7.31 and 7.19 ppm, four resonances attributed to the methylene moieties at 3.99, 3.17, 1.36 and 1.17 ppm, and two *tert*-butyl signals at 1.53 and 1.26 ppm. The ^{11}B{^{1}H} NMR resonances of **5.4** at 13.2 ppm shifts to 14.7 ppm. Single crystals of **5.5** were previously grown by Dr Siu-Kwan Lo via the diffusion of hexane into a toluene solution of the product.[15] The crystal structure of **5.5** reveals the pincer stabilised boron consists of a seven-membered ring with an N−B−O moiety (Figure 5.5).

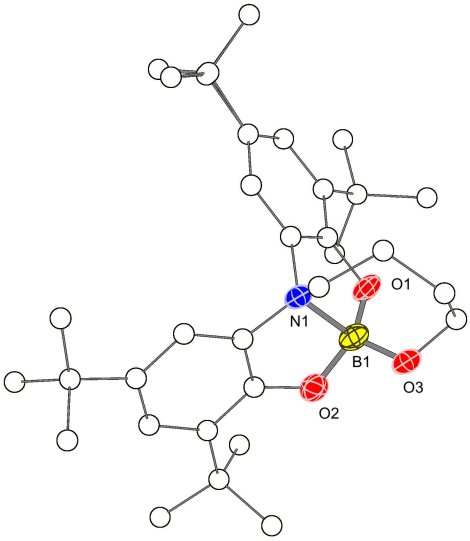
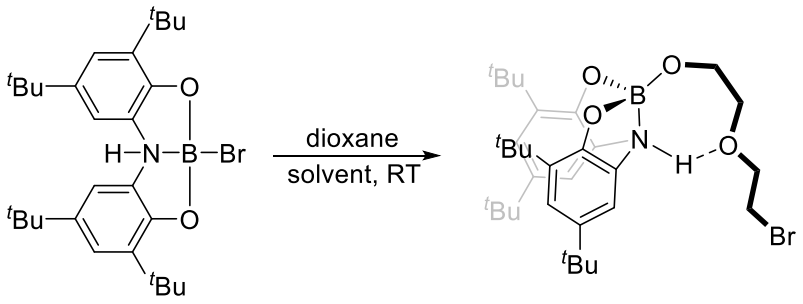


Figure 5.5: Single crystal X-ray structure of **5.5**. Anisotropic displacement ellipsoids are set at 50% probability. Hydrogen atoms have been omitted for clarity. All carbon atoms are pictured as spheres of arbitrary radius. Selected interatomic distances [Å] and angles [°]: B1–N1 1.763(5), B1–O1 1.452(5), B1–O2 1.450(6), B1–O3 1.394(6); O1-B1-N1 100.6(3), O2-B1-N1 100.4(3), O2-B1-O1 113.0(4), O3-B1-N1 112.9(3), O3-B1-O1 116.7(4), O3-B1-O2 111.5(4).[15]

Dioxane is symmetric, and therefore less polar than THF, and more difficult to undergo ring-fission. The addition of **5.2c** into excess amount of dioxane overnight afforded the formation of a single new product **5.6** (Scheme 5.11). The solution ^{1}H NMR spectrum of **5.6** revealed a broad resonance at 8.31 ppm, which is attributed to the amine (N−H) moiety of the ligand backbone. This is significantly downfield shifted when compared to the N−H resonance of **5.2c** at 6.43 ppm or **5.4** at 5.94 ppm. This shift is caused by a weak hydrogen bonding interaction between the amine proton and the oxygen atom of a 2-(2-bromoethoxy)ethoxy moiety (see Scheme 5.11).

Besides the amine resonance, the ^{1}H NMR spectrum also shows the protons attributed to the aromatic ligand backbone of **5.6** at 7.73 and 7.36 ppm (as two doublets), *tert*-butyl groups at 1.56 and 1.30 ppm, and of the 2-(2-bromoethoxy)ethoxy moiety at 3.85,

2.96 and 2.75 ppm. The $^{11}B\{^{1}H\}$ NMR resonance of **5.6** was observed at 13.6 ppm, which is very close to that of **5.4** at 13.2 ppm.



5.2c **5.6**

Scheme 5.11: Synthesis of **5.6** in toluene.

Single crystals of **5.6** were obtained from a concentrated pentane solution. Single crystal X-ray diffraction reveals that a C−O bond of the dioxane ring has been cleaved, affording the 2-(2-bromoethoxy)ethoxy boron complex shown in Figure 5.6. The bond length for the N−H···O interaction is 2.048(1) Å, and it falls in the range of a strong hydrogen bonding interaction, which is in agreement with the observed downfield shifted N−H moiety in the ^{1}H NMR spectrum.[19]

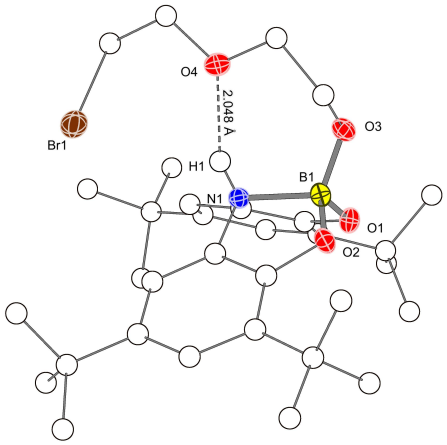
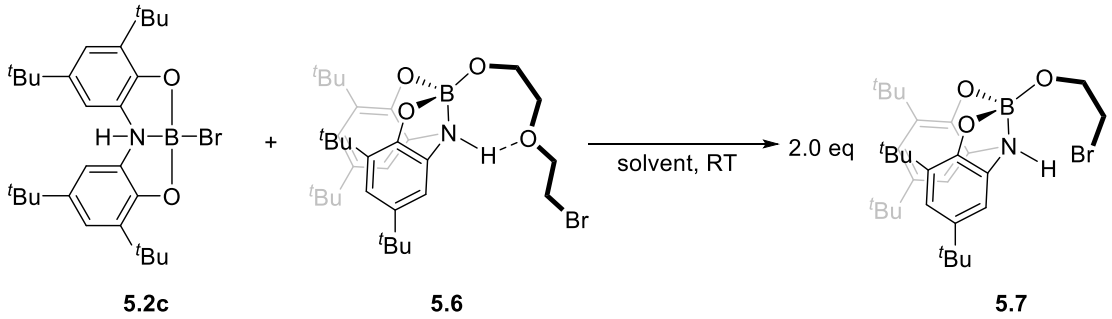


Figure 5.6: Single crystal X-ray structure of **5.6**. Anisotropic displacement ellipsoids are set at 50% probability. Hydrogen atoms have been omitted for clarity (with the exception of H1). All carbon atoms are pictured as spheres of arbitrary radius. Selected interatomic distances [Å] and angles [°]: B1–N1 1.6961(18), B1–O1 1.4594(17), B1–O2 1.4571(17), B1–O3 1.4124(17); O1-B1-N1 101.24(10), O2-B1-N1 101.69(10), O2-B1-O1 113.95(12), O3-B1-N1 113.19(11), O3-B1-O1 110.10(11), O3-B1-O2 115.53(11).

Unlike the reaction of **5.4** with a base, the reaction of **5.6** and *n*-propylamine did not afford a similar product, probably due to the unfavourable formation of an eight-membered ring.

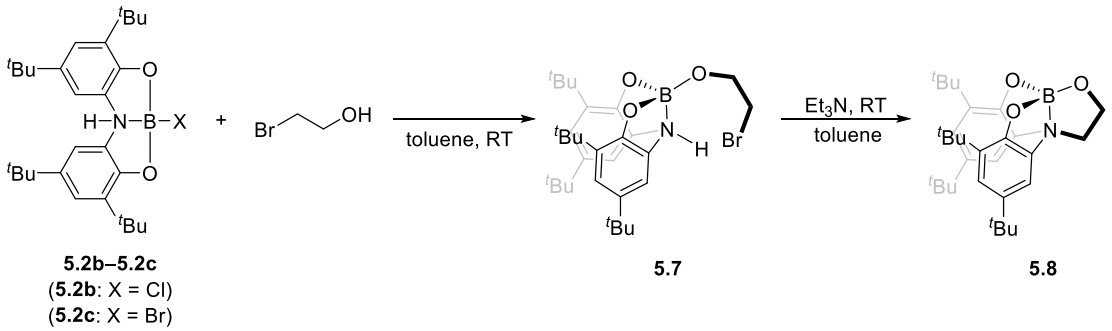
As complex **5.6** has a 2-(2-bromoethoxy)ethoxy moiety, in principle, it could potentially undergo additional C−O bond cleavage reactions (with **5.2c**). When **5.6** was added to a C_6D_6 solution with a stochiometric amount of **5.2c** (1: 1 ratio), only a single product was observed by NMR spectroscopy (Scheme 5.12). The resulting product is the 2-bromoethoxy boron complex **5.7**, which is a boron alkoxy complex similar to that of **5.4** and **5.6**. The solution ^{1}H NMR spectrum displays resonances for the ligand backbone at 7.30 and 7.07 ppm (as two doublets), an amine resonance at 6.41 ppm, and two methylene resonances arising from the bromoethoxy moiety at 4.02 and 3.29 ppm.

The $^{11}B\{^{1}H\}$ NMR signal appears at 13.2 ppm, as expected for four-coordinate bromoalkoxy boron complexes and is similar to those observed for **5.4** and **5.6**.



Scheme 5.12: Synthesis of **5.7**.

Another synthetic pathway for complex **5.7** is via dehydrocoupling of amine-borane complex **4.6** and 2-bromoethanol (Scheme 5.13), however, an elevated temperature of 80 ℃ is needed for this transformation. The reaction of **5.2b** and **5.2c** with 2-bromoethanol at room temperature through dehydrohalogenation could also generate the product (Scheme 5.13). Single crystals of **5.7** suitable for single crystal X-ray diffraction were obtained by crystallisation of the crude product from a concentrated hexane solution (Figure 5.7). The B1−N1 bond length of **5.7** is 1.681(3) Å and it is similar to that of **5.6** (1.6961(18) Å). The B1−O3 bond of **5.6**, 1.4124(17) Å, also compares favourably with that observed for **5.7** (1.423(3) Å).



Scheme 5.13: Synthesis of **5.7** and **5.8**.

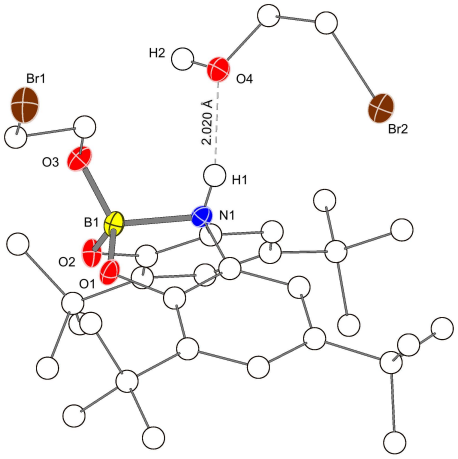


Figure 5.7: Single crystal X-ray structure of **5.7**. Anisotropic displacement ellipsoids are set at 50% probability. Hydrogen atoms have been omitted for clarity (with the exception of H1 and H2). All carbon atoms are pictured as spheres of arbitrary radius. Selected interatomic distances [Å] and angles [°]: B1–N1 1.681(3), B1–O1 1.455(3), B1–O2 1.456(3), B1–O3 1.423(3); O1-B1-N1 102.16(15), O1-B1-O2 115.18(19), O2-B1-N1 102.01(16), O3-B1-O1 113.52(18), O3-B1-N1 113.81(18), O3-B1-O2 109.50(17).

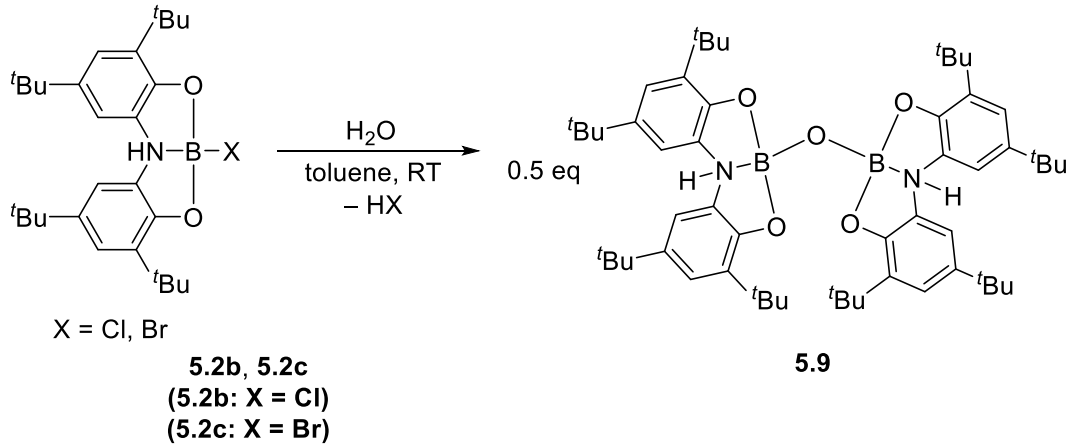
Addition of triethylamine to a toluene solution of **5.7** gives the five-membered ring containing product **5.8** (Scheme 5.13). The five-membered ring strain leads to a more distorted tetrahedral structure of **5.8** compared to **5.7**. The $^{11}B\{^{1}H\}$ NMR spectrum of **5.8** shows a signal at 18.2 ppm which is more downfield than the seven-membered ring complex **5.5**. The solution ^{1}H NMR spectrum in C_6D_6 reveals resonances for the ligand backbone at 7.32 and 7.29 ppm (two doublets), methylene resonances at 3.63 and 3.00 ppm, and two *tert*-butyl resonances at 1.51 and 1.26 ppm.

As a brief summary, compound **5.2c** has been found to activate cyclic ethers, such as THF and dioxane, to give borate ester complexes **5.4** and **5.6**. The reaction of amine-borane **4.6** or boron halides **5.2b**−**5.2c** with alcohols also affords the borate ester complex **5.7**. Upon the addition of a base, borate ester complexes **5.4** and **5.7** are subjected to dehydrobromination and give ring-closed products **5.5** and **5.6**,

respectively. This provides a new methodology for N−B−O ring formation which may have future synthetic uses.

5.6 Boron halides in water activation

In Section 5.5, the reactivity of boron halides with 2-bromoethanol was reported, which exemplified the use of **5.2b**−**5.2c** in O−H bond activation reactions. As another example, the reactivity of boron halides **5.2b** and **5.2c** towards water was investigated. In a toluene solution of **5.2b**, a stochiometric amount of degassed water was added, resulting in a colourless solution (Scheme 5.14). Solution ^{1}H NMR spectroscopy revealed resonances attributed to the ligand (ArH: 7.22, 6.96 ppm; NH: 6.09 ppm, ^{t}Bu: 1.36, 1.29 ppm) and ^{11}B{^{1}H} NMR spectroscopy showed a broad resonance at 12.3 ppm which is similar to the previously listed boron complexes. The formation of complex **5.9** was occasionally encountered during the preparation of some of the boron complexes described previously, as many of them are sensitive towards water.[15]



Scheme 5.14: Synthesis of **5.9**.

Crystallisation of the crude product from hexane afforded colourless single crystals suitable for single crystal X-ray diffraction (Figure 5.8). The structure of **5.9** is a dimeric

amine boron complex with an oxo-bridge. Intramolecular hydrogen bonding interactions between the N−H moiety with the oxygen atom of an adjacent ligand were observed.

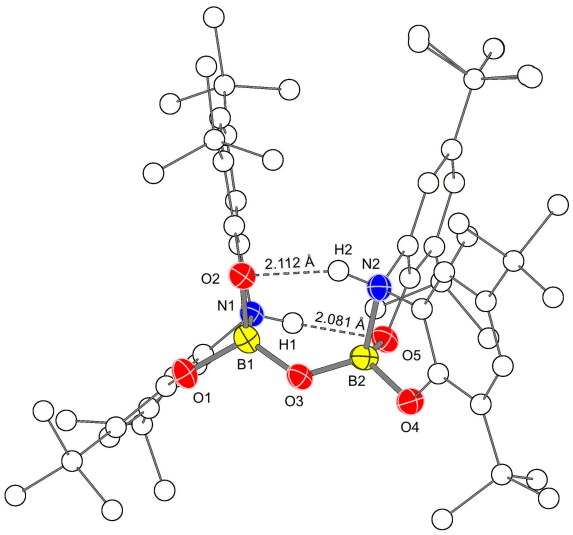


Figure 5.8: Single crystal X-ray structure of **5.9**. Anisotropic displacement ellipsoids are set at 50% probability. Hydrogen atoms have been omitted for clarity (with the exception of H1 and H2). All carbon atoms are pictured as spheres of arbitrary radius. Selected interatomic distances [Å] and angles [°]: B1–N1 1.688 (3), B1–O1 1.464 (3), B1–O2 1.485(3), B1–O3 1.394(3), B2–N2 1.691(3), B2–O3 1.390(3), B2–O4 1.463(3), B2–O5 1.495(3); O1-B1-N1 100.92(17), O1-B1-O2 112.2(2), O2-B1-N1 101.09(18), O3-B1-O1 114.4(2), O3-B1-N1 112.35(19), O3-B1-O2 114.3(2), O3-B2-N2 112.4(2), O3-B2-O4 114.0(2), O3-B2-O5 114.6(2), O4-B2-N2 101.14(18), O4-B2-O5 112.2(2), O5-B2-N2 100.95(18).[15]

5.7 Conclusions

Employing the pincer ligand [H_3(ONO)], novel boron halides [ON(H)O]BX, **5.2a**−**5.2c** have been synthesised. With different B−X (X = F, Cl, Br) bonds, complexes **5.2a**−**5.2c** have variable reactivity. In the presence of nucleophilic amines, **5.2b** can undergo dehydrohalogenation (−HCl) and converts to corresponding amine-boron adducts **5.3b** and **5.3c**. Boron halides **5.2b**−**5.2c** react with water to give a boron oxide complex

{[ON(H)O]B}$_2$O, **5.9**, or react with alcohols (such $BrCH_2CH_2OH$) to give alkoxyboron complexes. Bromoborane **5.2c** can activate THF or dioxane to give ring-opened products **5.4** and **5.6**. Complexes **5.4** and **5.7** were subjected to ring-closure reactions upon the adding of base to give **5.5** and **5.8**. The reaction from **5.2c** to **5.5** is very interesting, and can be considered as a B−N moiety insertion into the C−O bond of the THF molecule.

5.8 References

[1] C. Camacho-Camacho, G. Merino, F. J. Martínez-Martínez, H. Nöth, R. Contreras, *Eur. J. Inorg. Chem.* **1999**, *1999*, 1021–1027.

[2] B. C. Ranu, S. Bhar, *Org. Prep. Proced. Int.* **1996**, *28*, 371–409.

[3] J. Zakzeski, P. C. A. Bruijnincx, A. L. Jongerius, B. M. Weckhuysen, *Chem. Rev.* **2010**, *110*, 3552–3599.

[4] F. L. Benton, T. E. Dillon, *J. Am. Chem. Soc.* **1942**, *64*, 1128–1129.

[5] H. C. Brown, P. V. Ramachandran, J. Chandrasekharan, *Heteroat. Chem.* **1995**, *6*, 117–131.

[6] J. B. Heilmann, Y. Qin, F. Jäkle, H.-W. Lerner, M. Wagner, *Inorg. Chim. Acta* **2006**, *359*, 4802–4806.

[7] C. Sousa, P. J. Silva, *Eur. J. Org. Chem.* **2013**, *2013*, 5195–5199.

[8] C. Bonnier, T. P. Bender, *Molecules* **2015**, *20*, 18237–18245.

[9] Y. Wang, M. Y. Abraham, R. J. Gilliard, D. R. Sexton, P. Wei, G. H. Robinson, *Organometallics* **2013**, *32*, 6639–6642.

[10] H. Lyu, I. Kevlishvili, X. Yu, P. Liu, G. Dong, *Science* **2021**, *372*, 175–182.

[11] S. Aldridge, R. J. Calder, D. L. Coombs, C. Jones, J. W. Steed, S. Coles, M. B. Hursthouse, *New J. Chem.* **2002**, *26*, 677–686.

[12] R. K. Bartlett, H. S. Turner, R. J. Warne, M. A. Young, I. J. Lawrenson, *J. Chem. Soc. A* **1966**, 479–500.

[13] H. S. Turner, R. J. Warne, *J. Chem. Soc.* **1965**, 6421–6450.

[14] B. Cordero, V. Gómez, A. E. Platero-Prats, M. Revés, J. Echeverría, E. Cremades, F. Barragán, S. Alvarez, *Dalton Trans.* **2008**, 2832–2838.

[15] S.-K. Lo, *Geometry Constrained Main-Group Compounds for the Activation of Small Molecules*, Thesis (D.Phil.) − University of Oxford, 2018, (Department of Inorganic Chemistry), Oxford, **2018**.

[16] G. S. Hammond, T. D. Nevitt, *J. Am. Chem. Soc.* **1954**, *76*, 4121–4123.

[17] P. J. Kropp, K. A. Daus, S. D. Crawford, M. W. Tubergen, K. D. Kepler, S. L. Craig, V. P. Wilson, *J. Am. Chem. Soc.* **1990**, *112*, 7433–7434.

[18] S. Colin, L. Vaysse-Ludot, J. P. Lecouvé, J. Maddaluno, *J. Chem. Soc., Perkin Trans. 1* **2000**, 4505–4511.

[19] T. K. Harris, A. S. Mildvan, *Proteins: Struct., Funct., Bioinf.* **1999**, *35*, 275–282.

Chapter Six

Experimental Details

6.1 General considerations and starting materials

General synthetic methods. All reactions were performed under an inert atmosphere of argon using standard Schlenk-line or glovebox techniques (MBraun UNIlab glovebox, maintained at < 0.1 ppm H_2O and < 0.1 ppm O_2). *n*-Heptane (Fluka Analytical) was degassed with nitrogen before use. Hexane (Sigma Aldrich, HPLC grade), pentane (Sigma Aldrich, HPLC grade), toluene (Sigma Aldrich, HPLC grade), and benzene (Sigma Aldrich, HPLC grade) were purified using an MBraun SPS-800 solvent system. Tetrahydrofuran (THF; Sigma Aldrich, ≥ 99.9%) and 1,4-dioxane (dioxane, Alfa Aesar, 99+%) were distilled over a sodium metal/benzophenone mixture and freeze-pump-thaw degassed. Pyridine (Sigma Aldrich, HPLC grade) was distilled over CaH_2 and freeze-pump-thaw degassed. Chloroform (Sigma Aldrich, HPLC grade), C_6D_6 (Sigma Aldrich, 99.6%), toluene-d_8 (Sigma Aldrich, 99.6%), and $CDCl_3$ (Fluorochem Ltd, 99.8%) were freeze-pump-thaw degassed, and stored over activated 3 Å molecular sieves. THF-d_8 (Euriostop, 99.5%), triethylamine (Alfa Aesar, 99%), and *n*-propylamine (Sigma Aldrich, 99%) were dried over CaH_2 and vacuum distilled before use. DBU (Alfa Aesar, 98%) was dried over CaH_2 and freeze-pump-thaw degassed before use.

All dry solvents were stored over activated 3 Å molecular sieves under argon in gas-tight ampoules. 3,5-Di-*tert*-butylcatechol (Sigma Aldrich, 98%) was used as received without further purification. [H_3(ONO)] was prepared via a previously reported synthesis with some modifications.[1] [Na(dioxane)$_{1.4}$](PCO) was synthesised according to literature procedures.[2] The synthetic procedures for the isolation of complexes **2.1**, **2.7**·1.5BH_3:py, **2.11a**, **2.11b**, **4.10**, **5.3c**, **5.5** and **5.9** were carried out as described in the theses of Cory Smith and Siu-Kwan Lo with minor modifications.[3,4]

Liquid aldehydes, ketones, alcohols, imines and isocyanates were dried over activated 3 Å molecular sieves and freeze-pump-thaw degassed prior to use. All other reagents were used as received.

Table 6.1: Suppliers and purification procedures for commercially purchased chemicals.

Reagents	Suppliers	Purity	Purification
2-(Trifluoromethyl)phenyl isocyanate	Alfa Aesar	97%	Used as received
2,4,6-Trimethylphenyl isocyanate	Alfa Aesar	98%	Used as received
2-Bromoethanol	Sigma-Aldrich	95%	Used as received
3,5-Di-*tert*-butylcatechol	Sigma-Aldrich	98%	Used as received
4'-Bromoacetophenone	Alfa Aesar	98%	Used as received
4-Bromobenzaldehyde	Sigma-Aldrich	99%	Used as received
4-Bromophenyl isocyanate	Alfa Aesar	99%	Used as received
4'-Chloroacetophenone	Sigma-Aldrich	98+%	Used as received
4-Fluorobenzaldehyde	Sigma-Aldrich	98%	Used as received
4'-Iodoacetophenone	Sigma-Aldrich	97%	Used as received
4'-Methoxyacetophenone	Alfa Aesar	98%	Used as received
4-Methoxybenzaldehyde	Sigma-Aldrich	98%	Used as received
4-Methylbenzaldehyde	Sigma-Aldrich	97%	Used as received
4'-Nitroacetophenone	Sigma-Aldrich	98%	Used as received
9-BBN dimer	Sigma-Aldrich	99%	Used as received
Acetone	Sigma-Aldrich	97%	Used as received
Allyl isocyanate	Sigma-Aldrich	98%	Used as received
BCF	Sigma-Aldrich	95%	Used as received
Benzaldehyde	Sigma-Aldrich	99.50%	Used as received

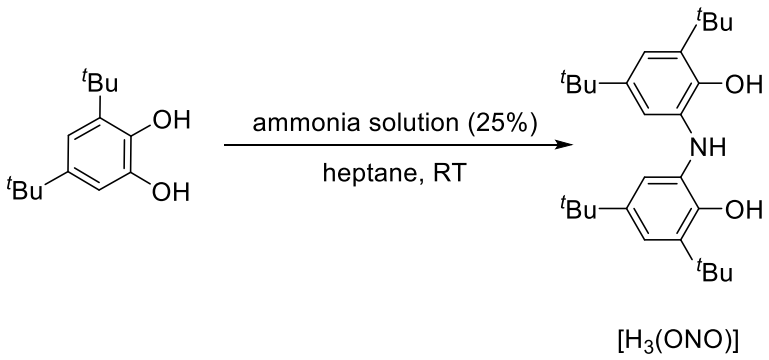
Benzophenone	Sigma-Aldrich	99+%	Used as received
Benzyl isocyanate	Sigma-Aldrich	99%	Used as received
Borane dimethylsulfide	Alfa Aesar	94%	Used as received
Borane trimethylamine complex	Sigma-Aldrich	97%	Used as received
Borane triphenylphosphine complex	Sigma-Aldrich	97%	Used as received
Boron tribromide	Sigma-Aldrich	99+%	Used as received
Boron trichloride	Sigma-Aldrich	(1.0 M in toluene)	Used as received
Boron trifluoride etherate	Sigma-Aldrich	98+%	Used as received
Carbon dioxide gas	BOC	CP grade	Used as received
Cyclohexyl isocyanate	Sigma-Aldrich	98%	Used as received
Cyclohexylmethanol	Fluorochem	98%	Used as received
Dimethyl sulfoxide	Sigma-Aldrich	99.9%	Used as received
Ethanol	Sigma-Aldrich	99.50%	Used as received
Gallium trichloride	Sigma-Aldrich	99.99%	Used as received
Hexamethylcyclotrisiloxane	Sigma-Aldrich	98%	Used as received
Isobutyraldehyde	Sigma-Aldrich	99.50%	Used as received
Mesitaldehyde	Alfa Aesar	97%	Used as received
N,*N*-Diisopropylethylamine	Sigma-Aldrich	99.00%	Used as received
N-Benzylidenemethylamine	Alfa Aesar	98%	Used as received
N-Benzylidene-*tert*-butylamine	Sigma-Aldrich	98%	Used as received
n-Propylamine	Sigma-Aldrich	99%	Distilled from CaH_2 prior to use
Phenyl isocyanate	Sigma-Aldrich	98%	Used as received
Phenylacetylene	Sigma-Aldrich	98%	Used as received
Pinacol borane	Sigma-Aldrich	97%	Used as received
Potassium *tert*-butoxide	Sigma-Aldrich	≥98%	Used as received

p-Tolyl isocyanate	Sigma-Aldrich	99%	Used as received
Sodium borohydride	Sigma-Aldrich	98%	Used as received
Sodium *tert*-butoxide	Acros Organics	98%	Used as received
Triethylamine	Alfa Aesar	99%	Distilled from CaH_2 prior to use
Triethylphosphine oxide	Sigma-Aldrich	97%	Used as received
Triphenylborane	Alfa Aesar	96%	Used as received

Additional characterisation techniques. All NMR spectra and two-dimensional experiments (NOESY, DOSY, HSQC, HMBC) were collected on solution J. Young NMR tubes on either a Bruker Avance III HD nanobay NMR equipped with a 9.4T magnet (^{1}H 400.2 MHz, ^{11}B 128.4 MHz, ^{13}C 100.6 MHz, ^{19}F 376.5 MHz, ^{31}P 162.0 MHz), a Bruker Avance III NMR equipped with a 11.75 T, magnet (^{1}H 499.9 MHz, ^{11}B 160.4 MHz, ^{13}C 125.7 MHz, ^{19}F 470.4 MHz, ^{31}P 202.4 MHz), or a Bruker Avance NMR equipped with a 11.75 T magnet and a ^{13}C detect cryoprobe (^{1}H 500.3 MHz, ^{13}C 125.8 MHz) at 298 K unless otherwise stated. Chemical shifts (δ) were referenced to internal solvent resonances (except ^{11}B, ^{19}F, ^{31}P NMR).[5] Data were processed using MestReNova or TopSpin software. Coupling constants (*J*) are reported in Hertz (Hz). The following abbreviations are used to define multiplets: s (singlet), d (doublet), t (triplet), q (quadruplet), sept. (septet), dd (doublet of doublets), m (multiplet), br (broad signal).

Elemental analyses were carried out by Elemental Microanalyses Ltd. (Devon, U.K.). Samples (approx. 10 mg) were submitted in sealed Pyrex ampoules.

6.2 Experimental details for Chapter Two

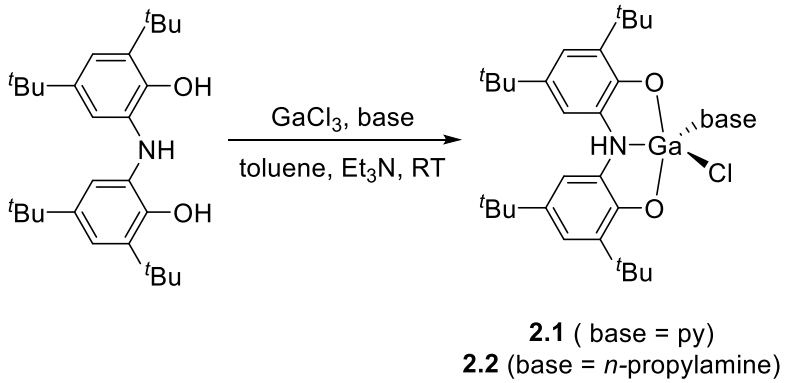


Scheme 6.1: Synthesis of [H_3(ONO)].

6.2.1 Synthesis of [H_3(ONO)]

[H_3(ONO)] was prepared via a modified literature procedure.[1] 3,5-Di-*tert*-butylcatechol (25 g, 112.5 mmol) and an ammonia solution (25%, 15 mL, 201 mmol) were stirred in a heptane (30 mL) at room temperature for 10 days, forming a white precipitate. The filtrate was removed with a filter cannula and the remaining solid was washed with pentane (3 × 15 mL) yielding *N*,*N*-bis-(3,5-di-*tert*-butyl-2-phenol)amine as a white solid (16 g, 37.6 mmol; 67% yield).

^{1}H NMR (400 MHz, C_6D_6): δ (ppm) 7.22 (d, $^4J_{H–H}$ = 2.3 Hz, 2H; Ar-*H*), 6.77 (d, $^4J_{H–H}$ = 2.2 Hz, 2H; Ar-*H*), 5.04 (s, 2H; O*H*), 4.59 (s, 1H; N*H*), 1.53 (s, 18H; C(CH_3)$_3$), 1.21 (s, 18H; C(CH_3)$_3$).



Scheme 6.2: Synthesis of compounds **2.1** and **2.2**.

6.2.2 Synthesis of Ga[ON(H)O]Cl(py) (**2.1**)

$[H_3(ONO)]$ (850 mg, 2.0 mmol) and $GaCl_3$ (350 mg, 2.0 mmol) were dissolved in pyridine (25 mL). The solution turned yellow-orange. Triethylamine (0.5 mL, 3.1 mmol) was then added to the solution, producing a viscous orange-brown solution. The solution was stirred for two hours at room temperature. All volatiles were removed *in vacuo* and the product was extracted into hot hexane, followed by filtration. The solution was then reduced to dryness *in vacuo* and product was purified by recrystallisation from a hot hexane solution, affording **2.1** as a compositionally pure white solid (1050 mg, 1.73 mmol, 87% yield). Elemental analysis calculated for $C_{33}H_{46}ClGaN_2O_2$: C, 65.20%; H, 7.63%; N, 4.61%; found: C, 65.12%; H, 7.73%; N, 4.78%.

^{1}H NMR (400 MHz, C_6D_6): δ (ppm) 9.16 – 9.10 (m, 2H; py-*H*), 7.41 (d, $^4J_{H–H}$ = 2.3 Hz, 2H; Ar-*H*), 7.22 (d, $^4J_{H–H}$ = 2.3 Hz, 2H; Ar-*H*), 6.75 (m, 1H; py-*H*), 6.52 (m, 2H; py-*H*), 4.61 (s, 1H; N*H*), 1.53 (s, 18H; C(C*H*$_3$)$_3$), 1.38 (s, 18H; C(C*H*$_3$)$_3$).

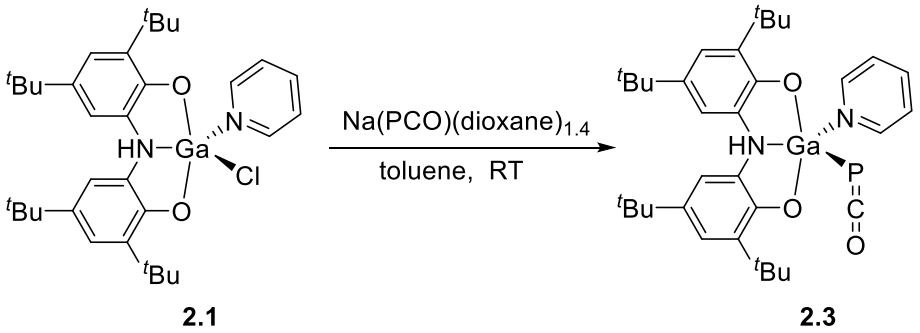
$^{13}C\{^{1}H\}$ NMR (101 MHz, C_6D_6): δ (ppm) 154.76 (Ar-*C*), 147.67 (py-*C*), 139.95 (py-*C*), 138.73 (Ar-*C*), 137.26 (Ar-*C*), 130.87 (Ar-*C*), 124.90 (py-*C*), 122.90 (Ar-*C*), 120.76 (Ar-*C*), 35.56 (*C*$(CH_3)_3$), 34.48 (*C*$(CH_3)_3$), 31.98 (C(*C*$H_3)_3$), 29.79 (C(*C*$H_3)_3$).

6.2.3 Synthesis of Ga[ON(H)O]Cl($NH_2{}^n$Pr) (**2.2**)

Toluene (10 mL) was added to a Schlenk tube containing [H_3(ONO)] (1.0 g, 2.35 mmol) and $GaCl_3$ (414 mg, 2.35 mmol), resulting in a pale pink solution. *n*-Propylamine (0.77 mL, 9.4 mmol) was then added, and the solution was stirred overnight at room temperature. All volatiles were removed *in vacuo*, and the crude product was extracted with hot hexane. Further recrystallisation from pentane afforded **2.2** as colourless crystals (920 mg, 1.74 mmol, 74%). Elemental analysis calculated for $C_{31}H_{50}ClGaN_2O_2$: C 63.33%, H 8.57%, N 4.76%; found: C 63.01%, H 8.60%, N 5.09%.

^{1}H NMR (500 MHz, C_6D_6): δ (ppm) 7.39 (d, $^{4}J_{H–H}$ = 2.3 Hz, 2H; Ar-*H*), 7.14 (d, $^{4}J_{H–H}$ = 2.3 Hz, 2H; Ar-*H*), 4.42 (s, 1H; N*H*), 2.67 (m, 2H; $NH_2CH_2CH_2CH_3$), 2.19 (t, $^{3}J_{H–H}$ = 7.2 Hz, 2H; $NH_2CH_2CH_2CH_3$), 1.55 (s, 18H; C(C$H_3)_3$), 1.36 (s, 18H; C(C$H_3)_3$), 0.93 (m, 2H; $NH_2CH_2CH_2CH_3$), 0.48 (t, $^{3}J_{H–H}$ = 7.4 Hz, 3H, $NH_2CH_2CH_2CH_3$).

$^{13}C\{^{1}H\}$ NMR (126 MHz, C_6D_6): δ (ppm) 154.52 (Ar-*C*), 138.66 (Ar-*C*), 137.06 (Ar-*C*), 130.80 (Ar-*C*), 122.90 (Ar-*C*), 120.67 (Ar-*C*), 44.04 ($NH_2CH_2CH_2CH_3$), 35.59 (*C*$(CH_3)_3$), 34.44 (*C*$(CH_3)_3$), 31.95 (C(*C*$H_3)_3$), 29.83 (C(*C*$H_3)_3$), 24.09 ($NH_2CH_2CH_2CH_3$), 10.76 ($NH_2CH_2CH_2CH_3$).



2.1 **2.3**

Scheme 6.3: Synthesis of compound **2.3**.

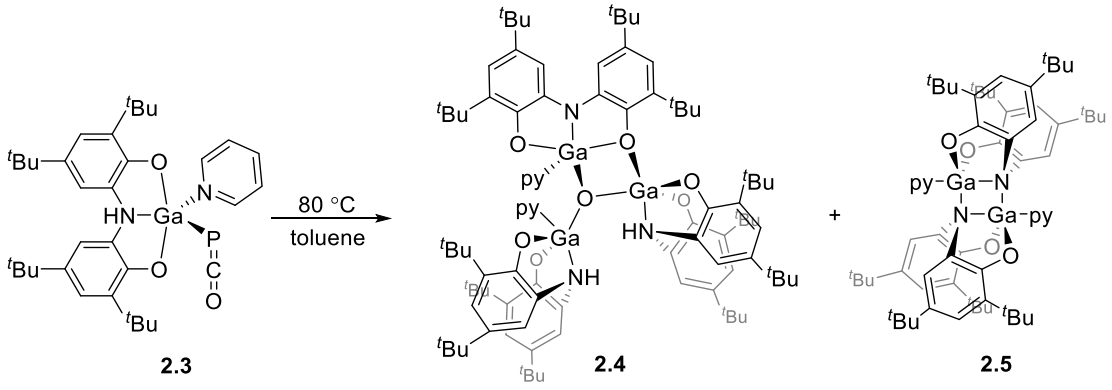
6.2.4 Synthesis of Ga[ON(H)O]py(PCO) (**2.3**)

Toluene (5 mL) was added to an ampoule containing [Na(dioxane)$_{1.4}$](PCO) (821 mg, 4.0 mmol) and **2.1** (1.0 g, 1.64 mmol). The solution was stirred overnight at room temperature, then filtrated. The filtrate was dried *in vacuo* to give the crude product. The crude product was washed by pentane (5 mL) and *dried in vacuo*, affording yellow solids as the product (970 mg, 1.54 mmol, 93%).

^{1}H NMR (500 MHz, C_6D_6): δ (ppm) 9.27 – 9.09 (m, 2H; py-*H*), 7.40 (d, $^{4}J_{H–H}$ = 2.4 Hz, 2H; Ar-*H*), 7.28 (d, $^{4}J_{H–H}$ = 2.4 Hz, 2H; Ar-*H*), 6.80 (m, 1H; py-*H*), 6.61 (m, 2H; py-*H*), 4.29 (s, 1H; N*H*), 1.54 (s, 18H; C(C*H*$_3$)$_3$), 1.38 (s, 18H; C(C*H*$_3$)$_3$).

^{13}C{^{1}H} NMR (126 MHz, C_6D_6): δ (ppm) 182.56 (d, $^{1}J_{P–C}$ = 94.7 Hz, P*C*O), 154.69 (Ar-*C*), 147.58 (py-*C*), 139.38 (py-*C*), 138.38 (Ar-*C*), 137.14 (Ar-*C*), 131.10 (Ar-*C*), 124.67 (py-*C*), 122.67 (Ar-*C*), 120.57 (Ar-*C*), 35.36 (*C*(CH$_3$)$_3$), 34.28 (*C*(CH$_3$)$_3$), 31.79 (C(*C*H$_3$)$_3$), 29.60 (C(*C*H$_3$)$_3$).

^{31}P{^{1}H} NMR (202 MHz, C_6D_6): δ (ppm) −374.5 (*P*CO).



Scheme 6.4: Synthesis of **2.4** and **2.5**.

6.2.5 Synthesis of $Ga_3[ON(H)O]_2[ONO]py_2$ (**2.4**) and $[Ga(ONO)py]_2$ (**2.5**)

Toluene (5 mL) was added to an ampoule with **2.3** (500 mg, 0.79 mmol). The solution was heated in an oil bath at 80 °C overnight, resulting into an orange solution with yellow crystals. The solution was filtered, and the filtrate was dried *in vacuo* to give **2.4** (206 mg, 0.14 mmol, 52%) as an orange solid, while the residue (as yellow crystals) was dried to give **2.5** (105 mg, 0.11 mmol, 27%).

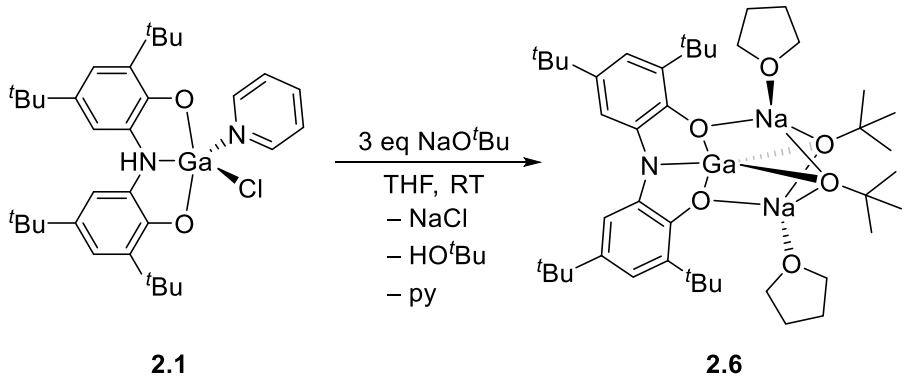
2.4: ^{1}H NMR (400 MHz, C_6D_6): δ (ppm) 8.72 – 8.61 (m, 2H; py-*H*), 7.43 (br, 4H; Ar-*H*), 7.35 (d, $^4J_{H–H}$ = 2.3 Hz, 2H; Ar-*H*), 7.27 (d, $^4J_{H–H}$ = 2.3 Hz, 2H; Ar-*H*), 7.09 (d, $^4J_{H–H}$ = 2.2 Hz, 2H; Ar-*H*), 7.04 (d, $^4J_{H–H}$ = 2.2 Hz, 2H; Ar-*H*), 6.55 (m, 1H; py-*H*), 6.31 (s, 1H; N*H*), 6.29 (m, 2H; py-*H*), 6.06 (s, 1H; N*H*), 1.84 (s, 18H; C(CH_3)$_3$), 1.62 (s, 18H; C(CH_3)$_3$), 1.56 (s, 18H; C(CH_3)$_3$), 1.25 (s, 18H; C(CH_3)$_3$), 1.23 (s, 18H; C(CH_3)$_3$), 1.17 (s, 18H; C(CH_3)$_3$).

^{13}C{^{1}H} NMR (126 MHz, C_6D_6): δ (ppm) 154.87 (Ar-*C*), 154.52 (Ar-*C*), 152.75 (Ar-*C*), 147.38 (py-*C*), 140.23 (py-*C*), 139.88 (Ar-*C*), 137.82 (Ar-*C*), 137.62 (Ar-*C*), 137.58 (Ar-*C*), 136.96 (Ar-*C*), 136.25 (Ar-*C*), 132.66 (Ar-*C*), 131.02 (Ar-*C*), 130.77 (Ar-*C*),

124.69 (py-*C*), 123.09 (Ar-*C*), 122.32 (Ar-*C*), 122.28 (Ar-*C*), 121.02 (Ar-*C*), 120.14 (Ar-*C*), 119.86 (Ar-*C*), 35.78 (*C*(CH_3)$_3$), 35.64 (*C*(CH_3)$_3$), 35.61 (*C*(CH_3)$_3$), 34.36 (*C*(CH_3)$_3$), 34.32 (*C*(CH_3)$_3$), 34.30 (*C*(CH_3)$_3$), 31.97 (C(*C*H_3)$_3$), 31.81 (C(*C*H_3)$_3$), 31.66 (C(*C*H_3)$_3$), 30.23 (C(*C*H_3)$_3$), 29.97 (C(*C*H_3)$_3$), 29.78 (C(*C*H_3)$_3$).

2.5: ^{1}H NMR (500 MHz, $CDCl_3$): δ (ppm) 9.11 (m, 2H; py-*H*), 8.19 (m, 1H; py-*H*), 7.75 – 7.66 (m, 2H; py-*H*), 6.89 (d, $^4J_{H–H}$ = 2.3 Hz, 2H; Ar-*H*), 6.78 (d, $^4J_{H–H}$ = 2.3 Hz, 2H; Ar-*H*), 1.17 (s, 18H; C(C*H*$_3$)$_3$), 1.15 (s, 18H; C(C*H*$_3$)$_3$).

^{13}C{^{1}H} NMR (126 MHz, $CDCl_3$): δ (ppm) 153.56 (Ar-*C*), 150.14 (py-*C*), 140.72 (py-*C*), 136.81 (Ar-*C*), 136.78 (Ar-*C*), 135.56 (Ar-*C*), 125.14 (py-*C*), 119.40 (Ar-*C*), 118.64 (Ar-*C*), 35.09 (*C*(CH_3)$_3$), 34.16 (*C*(CH_3)$_3$), 31.94(C(*C*H_3)$_3$), 29.45(C(*C*H_3)$_3$).



2.1 **2.6**

Scheme 6.5: Synthesis of **2.6**.

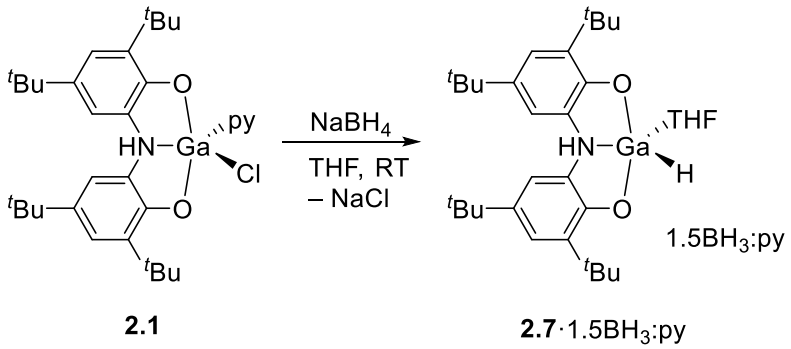
6.2.6 Synthesis of [ONO]Ga(Na_2)(THF)$_2$(O^{t}Bu)$_2$ (**2.6**)

THF (5mL) was added to an ampoule with NaO^{t}Bu (500 mg, 5.20 mmol) and **2.1** (1.0 g, 1.58 mmol). The solution was stirred overnight at room temperature. Removal of solvent afforded a yellow oil, which was extracted into pentane (5 mL) and filtered. The product crystallised from the filtrate, as yellow crystals (520 mg, 0.63 mmol, 38%).

Elemental analysis calculated for $C_{44}H_{74}GaNNa_2O_6$: C 63.77%, H 9.00%, N 1.69%; found: C 63.76%, H 8.82%, N 2.11%.

^{1}H NMR (400 MHz, C_6D_6): δ (ppm) 8.38 (br, 2H; Ar-*H*), 7.13 (br, 2H; Ar-*H*), 3.50 – 3.34 (m, 8H; OC*H*$_2$), 1.74 (s, 18H; C(C*H*$_3$)$_3$), 1.67 (s, 18H; C(C*H*$_3$)$_3$), 1.34 – 1.27 (m, 8H; OCH$_2$C*H*$_2$), 1.00 (s, 18H; OC(C*H*$_3$)$_3$)).

^{13}C{^{1}H} NMR (101 MHz, C_6D_6): δ (ppm) 149.60 (Ar-*C*), 136.88 (Ar-*C*), 136.22 (Ar-*C*), 124.35 (Ar-*C*), 110.01 (Ar-*C*), 108.25 (Ar-*C*), 68.14 (O-*C*H$_2$), 67.98 (O*C*(CH$_3$)$_3$), 35.25 (*C*(CH$_3$)$_3$), 34.99 (*C*(CH$_3$)$_3$), 34.20 (OC(*C*H$_3$)$_3$), 32.75 (C(*C*H$_3$)$_3$), 31.16 (C(*C*H$_3$)$_3$), 25.54 (O-CH$_2$*C*H$_2$).



Scheme 6.6: Synthesis of **2.7**·1.5BH$_3$:py.

6.2.7 Synthesis of HGa(THF)[ON(H)O]·1.5BH$_3$:py (**2.7**·1.5BH$_3$:py)

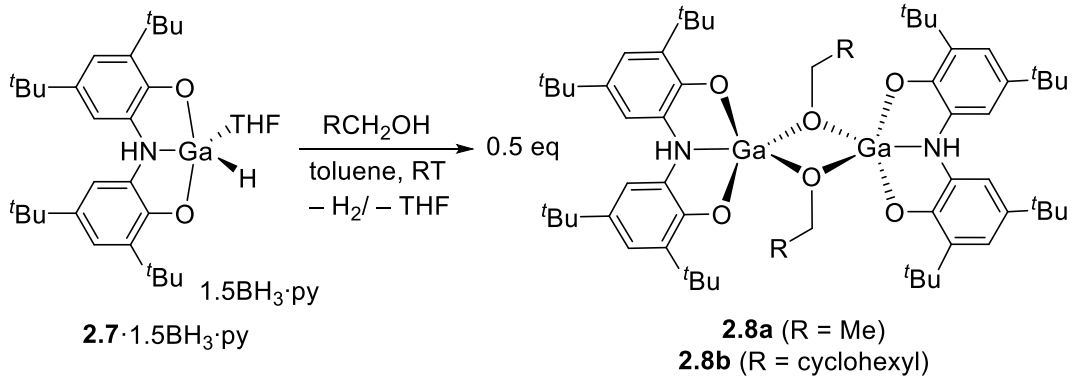
2.1 (525 mg, 0.86 mmol) and sodium borohydride (170 mg, 4.5 mmol) were dissolved in THF (20 mL), affording a colourless solution. The solution was stirred overnight resulting in the formation of a white precipitate of NaCl. All volatiles were removed *in vacuo*, and the product was extracted into toluene and filtered. The solvent was subsequently removed *in vacuo*, yielding the crude product. The product was purified by recrystallisation from concentrated toluene and pentane, yielding the product as a white solid. (360 mg, 0.51 mmol, 59% yield). Colourless crystals suitable for X-ray

diffraction analysis were obtained by layering a concentrated toluene with pentane at 4 °C. Note that borane-pyridine cannot be removed by washing. Elemental analysis calculated for $C_{39.5}H_{62}B_{1.5}GaN_{2.5}O_3$: C, 67.21%; H, 8.85%; N, 4.96%; found: C, 67.56%; H, 8.89%; N; 4.55%.

^{1}H NMR (400 MHz, C_6D_6): δ (ppm) 8.13 (d, $^3J_{H–H}$ = 5.6 Hz, 2H; py-*H*), 7.35 (d, $^4J_{H–H}$ = 2.4 Hz, 2H; Ar-*H*), 7.20 (d, $^4J_{H–H}$ = 2.4 Hz, 2H; Ar-*H*), 6.52 (t, $^3J_{H–H}$ = 7.7 Hz, 1H; py-*H*), 6.15 (t, $^3J_{H–H}$ = 6.9 Hz, 2H; py-*H*), 5.67 (br, 1H; Ga*H*), 4.01 (s, 1H; N*H*), 3.91 (m, 4H; OCH_2), 3.76 – 3.11 (m, 3H; BH_3), 1.59 (s, 18H; C(CH_3)$_3$), 1.45 (m, 4H; OCH$_2$CH_2), 1.35 (s, 18H; C(CH_3)$_3$).

^{13}C{^{1}H} NMR (101 MHz, C_6D_6): δ (ppm) 156.11(Ar-*C*), 147.27 (py-*C*),, 137.87(py-*C*), 137.80(Ar-*C*), 137.42 (Ar-*C*), 132.09 (Ar-*C*), 124.66 (py-*C*), 122.61 (Ar-*C*), 120.36 (Ar-*C*), 68.72 (O*C*H$_2$), 35.63 (*C*(CH$_3$)$_3$), 34.36 (*C*(CH$_3$)$_3$), 32.00 (C(*C*H$_3$)$_3$), 29.76 (C(*C*H$_3$)$_3$), 25.53 (OCH$_2$*C*H$_2$).

^{11}B NMR (128 MHz, C_6D_6): δ (ppm) –10.8 (q, $^1J_{B–H}$ = 100.4 Hz).



Scheme 6.7: Synthesis of compounds **2.8a** and **2.8b**.

6.2.8 Synthesis of {Ga[ON(H)O](OCH$_2$CH$_3$)}$_2$ (**2.8a**)

2.7·1.5BH$_3$:py (2.82 g, 4.0 mmol) was stirred in ethanol (5 mL) overnight yielding a white precipitate. The solution was filtered and the white solid was washed with ethanol (4 × 10 mL) and pentane (1 × 10 mL). The solid was dried *in vacuo*, affording **2.8a**

(1.6 g, 1.49 mmol, 75% yield). Colourless crystals suitable for single crystal X-ray diffraction were obtained from a concentrated benzene solution at room temperature. Elemental analysis calculated for $C_{60}H_{92}Ga_2N_2O_6$: C, 66.92%; H, 8.61%; N, 2.60%; found: C, 66.51%; H, 8.73%; N, 2.54%.

^{1}H NMR (500 MHz, C_6D_6): δ (ppm) 7.46 (d, $^4J_{H–H}$ = 2.4 Hz, 4H; Ar-*H*), 7.42 (d, $^4J_{H–H}$ = 2.4 Hz, 4H; Ar-*H*), 4.70 (s, 2H; N*H*), 4.05 (br, 4H; OCH_2), 1.40−1.29 (overlapped singlets, 78H; C(CH_3)$_3$ and CH_2CH_3).

^{13}C{^{1}H} NMR (126 MHz, C_6D_6): δ (ppm) 154.60 (Ar-*C*), 139.00 (Ar-*C*), 138.40 (Ar-*C*), 130.52 (Ar-*C*), 123.43 (Ar-*C*), 119.73 (Ar-*C*), 61.85 (O*C*H_2), 35.74 (*C*(CH$_3$)$_3$), 34.49 (*C*(CH$_3$)$_3$), 31.94 (C(*C*H$_3$)$_3$), 29.68 (C(*C*H$_3$)$_3$), 19.07 (OCH$_2$*C*H$_3$).

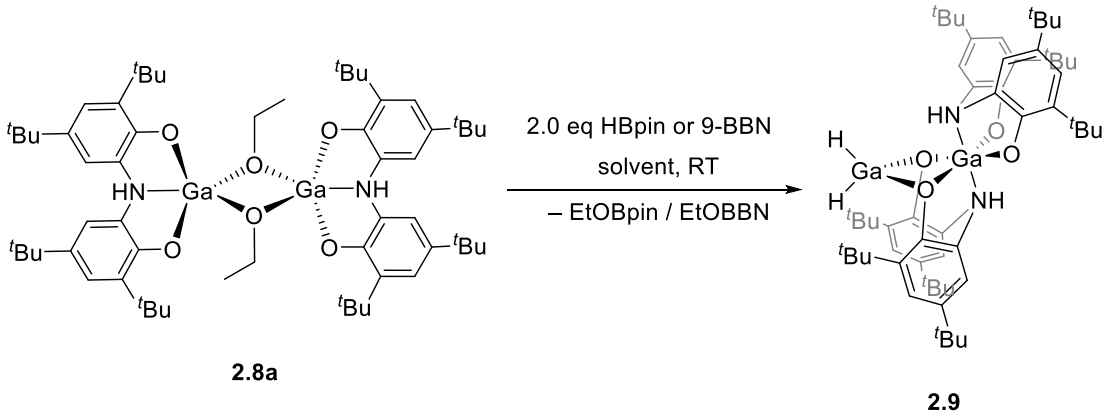
6.2.9 Synthesis of {Ga[ON(H)O](OCH$_2$Cy)}$_2$ (**2.8b**)

Cyclohexylmethanol (21 mg, 0.18 mmol) was added to a toluene solution (2.0 mL) of **2.7** (100 mg, 0.18 mmol) in an ampoule under argon and the mixture was stirred overnight. The solvent was removed *in vacuo* and the solid residue was washed with pentane (2 mL), then dried *in vacuo*, affording the desired product as white solid. X-ray quality crystals were obtained from concentrated toluene or chloroform solutions, yielding colourless crystals. (60 mg, 0.05 mmol, 56%). Elemental analysis calculated for $C_{70}H_{108}N_2O_6Ga_2$: C, 69.31%; H, 8.97%; N, 2.31%; found: C, 69.28%; H, 9.20%; N, 2.49%.

^{1}H NMR (500 MHz, $CDCl_3$): δ (ppm) 7.52 (br, 4H; Ar-*H*), 7.21 (br, 4H; Ar-*H*), 4.97 (s, 2H; N*H*), 3.82 (s, 4H; OCH_2), 1.82 (s, 2H; OCH$_2$C*H*), 1.54 (s, 8H; OCH$_2$CHCH_2), 1.39 (s, 36H; C(CH_3)$_3$), 1.33 (s, 36H; C(CH_3)$_3$), 1.16 (s, 8H; OCH$_2$CHCH$_2$CH_2), 0.67 (s, 4H; OCH$_2$CHCH$_2$CH$_2$CH_2).

^{13}C{^{1}H} NMR (126 MHz, $CDCl_3$): δ (ppm) 154.33 (Ar-*C*), 138.67 (Ar-*C*), 138.04 (Ar-*C*), 129.54 (Ar-*C*), 123.32 (Ar-*C*), 119.39 (Ar-*C*), 71.83 (O*C*H_2), 40.01 (OCH$_2$*C*H),

35.51 ($C(CH_3)_3$), 34.41 ($C(CH_3)_3$), 31.83 ($C(CH_3)_3$), 29.98 (OCH_2CHCH_2), 29.47($C(CH_3)_3$), 26.74 ($OCH_2CHCH_2CH_2$), 25.66 ($OCH_2CHCH_2CH_2CH_2$).



2.8a **2.9**

Scheme 6.8: Synthesis of **2.9**.

6.2.10 Synthesis of $H_2Ga[\mu^2\text{-}ON(H)O]Ga[ON(H)O]$ (**2.9**)

Method 1: In the glovebox, HBpin (17 μL, 15.0 mg, 0.117 mmol) was added to a solution of **2.8a** (60 mg, 0.056 mmol) in toluene (2 mL) using a micro-syringe. This afforded a colourless solution after stirring for 2 mins. After storing at –30 ℃ in a freezer for 5 days colourless crystals formed. However, using this method we were unable to separate the product from EtOBpin, as EtOBpin has similar solubility to **2.9**.

Method 2: **2.8a** (180 mg, 0.168 mmol) was stirred in hexane (4 mL) with 9-BBN (9-borabicyclo(3.3.1)nonane) (42 mg, 0.172 mmol) at room temperature overnight giving a colourless solution. The solution was stored at –30 ℃ in a freezer for 3 days, affording colourless crystals. The supernatant was decanted and the remaining solid was washed with *n*-pentane (3 × 2 mL) and subsequently dried *in vacuo* to afford **2.9** as a white powder (25 mg, 0.025 mmol, 15%). Elemental analysis calculated for $C_{56}H_{84}Ga_2N_2O_4$: C, 68.03%; H, 8.56%; N, 2.83%; found: C, 67.46%; H, 8.50%; N, 2.82%. Room temperature ^{1}H NMR spectra indicate the existence of at least four isomers of compound **2.9**, and here only the ^{1}H NMR spectroscopic data for isomer **2.9$_{\mathbf{I}}$** and **2.9$_{\mathbf{II}}$**,

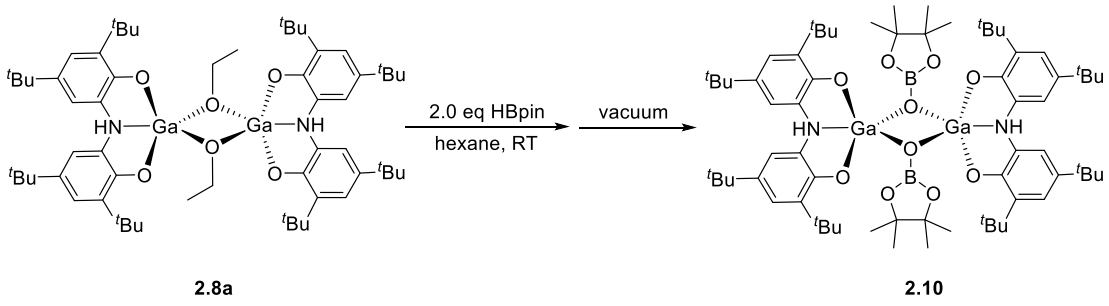
the ^{13}C NMR spectroscopic data for **2.9$_{I}$** are presented. The NMR resonances for other isomers are difficult to assign due to their low abundance in solution.

Isomer **2.9$_{I}$**: ^{1}H NMR (500 MHz, C_6D_6): δ (ppm) 7.32 (d, $^{4}J_{H–H}$ = 2.4 Hz, 4H; Ar-*H*), 7.05 (d, $^{4}J_{H–H}$ = 2.4 Hz, 4H; Ar-*H*), 5.55 (s, 2H; Ga*H*), 4.02 (s, 2H; N*H*), 1.58 (s, 36H; C(C*H*$_3$)$_3$), 1.30 (s, 36H; C(C*H*$_3$)$_3$).

^{13}C NMR (126 MHz, C_6D_6): δ (ppm) 155.59 (Ar-*C*), 138.96 (Ar-*C*), 138.57 (Ar-*C*), 131.25 (Ar-*C*), 123.50 (Ar-*C*), 118.76 (Ar-*C*), 35.72 (*C*(CH$_3$)$_3$), 34.36 (*C*(CH$_3$)$_3$), 31.84 (C(*C*H$_3$)$_3$), 29.54 (C(*C*H$_3$)$_3$).

Isomer **2.9$_{II}$**: ^{1}H NMR (500 MHz, C_6D_6): δ (ppm) 7.55 (d, $^{4}J_{H–H}$ = 2.4 Hz, 2H; Ar-*H*), 7.33 (m, 4H; Ar-*H*), 6.81 (d, $^{4}J_{H–H}$ = 2.4 Hz, 2H; Ar-*H*), 5.94 (s, 1H; Ga*H*), 5.86 (s, 1H; Ga*H*), 5.11 (s, 1H; N*H*), 4.82 (s, 1H; N*H*), 1.43 (s, 18H; C(C*H*$_3$)$_3$), 1.32 (s, 18H; C(C*H*$_3$)$_3$), 1.25 (s, 18H; C(C*H*$_3$)$_3$), 1.24 (s, 18H; C(C*H*$_3$)$_3$).

6.2.11 Synthesis of {Ga[ON(H)O](OBpin)}$_2$ (**2.10**).



Scheme 6.9: Synthesis of **2.10**.

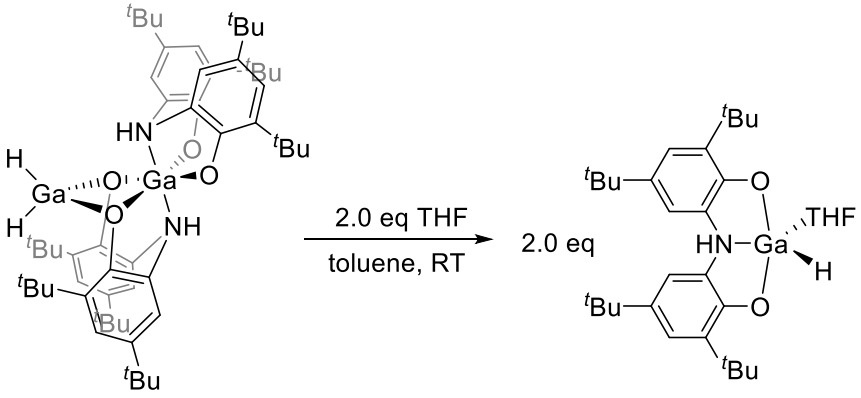
In glovebox, HBpin (17 μL, 15.0 mg, 0.117mmol) was added to a suspension of **2.8a** (60 mg, 0.056 mmol) in hexane (5 mL) using a micro-syringe. This afforded a colourless solution after stirring for 2 mins. The solution was then dried *in vacuo*, and dissolved into *n*-pentane (5 mL) and stored at –30 °C in a freezer for 5 days until

colourless crystals formed. The supernatant was decanted and the remaining solid was washed with *n*-pentane (3 × 2 mL) and subsequently dried *in vacuo* to afford **2.10** as a white powder (12 mg, 0.009 mmol, 17%). Elemental analysis calculated for $C_{68}H_{106}B_2Ga_2N_2O_{10}$: C, 64.18%; H, 8.40%; N, 2.20%; found: C, 63.99%; H, 8.35%; N, 1.93%.

^{1}H NMR (500 MHz, $CDCl_3$): δ (ppm) 7.51 (d, $^4J_{H–H}$ = 2.4 Hz, 4H; Ar-*H*), 7.19 (d, $^4J_{H–H}$ = 2.4 Hz, 4H; Ar-*H*), 6.36 (s, 2H; N*H*), 1.36 (s, 36H; C(C*H*$_3$)$_3$), 1.33 (s, 36H; C(C*H*$_3$)$_3$), 1.09 (s, OC(C*H*$_3$)$_2$, 24H).

^{13}C{^{1}H} NMR (126 MHz, $CDCl_3$): δ (ppm) 154.59 (Ar-*C*), 138.23 (Ar-*C*), 137.78 (Ar-*C*), 129.49 (Ar-*C*), 122.81 (Ar-*C*), 119.58 (Ar-*C*), 83.54 (O*C*(CH$_3$)$_2$), 35.54 (*C*(CH$_3$)$_3$), 34.37 (*C*(CH$_3$)$_3$), 31.86 (C(*C*H$_3$)$_3$), 29.66 (C(*C*H$_3$)$_3$), 24.44 (OC(*C*H$_3$)$_2$).

^{11}B NMR (128 MHz, $CDCl_3$): δ (ppm) 22.5.



2.9 **2.7**

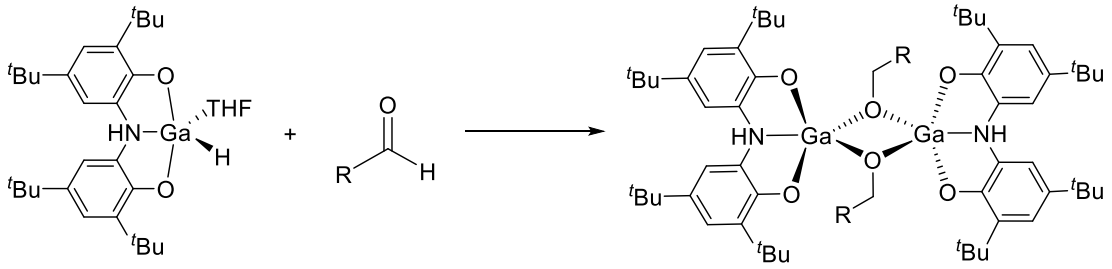
Scheme 6.10: Synthesis of **2.7**.

6.2.12 Synthesis of HGa(THF)[ON(H)O] (**2.7**)

In a glovebox, HBpin (17 μL, 15.0 mg, 0.117 mmol) was added to a suspension of **2.8a** (60 mg, 0.056 mmol) in hexane (2 mL) using a micro-syringe, which afforded a

colourless solution after stirring for 2 minutes. THF (10 μL, 0.123 mmol) was added and the solution was stored at –30 °C overnight, resulting in precipitation of a white solid. The supernatant was decanted and the remaining solid was washed with *n*-pentane (3 × 2 mL) and subsequently dried *in vacuo* to afford **2.7** as a white powder (35 mg, 0.062 mmol, 55% yield). Elemental analysis calculated for $C_{32}H_{50}GaNO_3$: C, 67.85%; H, 8.90%; N, 2.47%; found: C, 67.83%; H, 8.89%; N, 2.53%.

^{1}H NMR (400 MHz, C_6D_6): δ (ppm) 7.35 (d, $^4J_{H–H}$ = 2.4 Hz, 2H; Ar-*H*), 7.15 (d, $^4J_{H–H}$ = 2.4 Hz, 2H; Ar-*H*), 5.65 (s, 1H; Ga*H*), 3.92 (s, 1H; N*H*), 3.90 – 3.81 (m, 4H; OCH_2), 1.59 (s, 18H; C(CH_3)$_3$), 1.48 – 1.41 (m, 4H; OCH$_2$CH_2), 1.35 (s, 18H; C(CH_3)$_3$). ^{13}C{^{1}H} NMR (101 MHz, C_6D_6): δ (ppm) 155.92 (Ar-*C*), 138.19 (Ar-*C*), 137.78 (Ar-*C*), 131.76 (Ar-*C*), 122.91 (Ar-*C*), 119.82 (Ar-*C*), 68.55 (O*C*H$_2$), 35.67 (*C*(CH$_3$)$_3$), 34.35 (*C*(CH$_3$)$_3$), 31.94 (C(*C*H$_3$)$_3$), 29.69 (C(*C*H$_3$)$_3$), 25.56 (OCH$_2$*C*H$_2$).



Scheme 6.11: Synthetic route to compounds **2.11a**–**2.11e**.

6.2.13 General synthesis and characterisation data for {Ga[ON(H)O](OCH$_2$R)}$_2$ (**2.11a**−**e**).

2.7 (100 mg, 0.18 mmol) was dissolved in toluene (2 mL) giving a colourless solution. One equivalent of aldehyde or ketone (0.18 mmol) was added to the solution, and kept stirring overnight for all samples (note: benzophenone requires stirring for 5 days). The solvent was pumped and the solid remnants were washed with pentane (2 mL), then dried *in vacuo*, affording the desired products as white solids. X-ray quality crystals were obtained from concentrated toluene, $CDCl_3$ or C_6D_6 solutions, yielding colourless crystals.

6.2.14 Synthesis of {Ga[ON(H)O](OCH$_2$Ph)}$_2$ (**2.11a**)

In accordance with the general procedure using benzaldehyde (19 mg, 0.18 mmol) as the substrate to afford **2.11a**. (85 mg, 0.07 mmol, 82% yield). Elemental analysis calculated for $C_{70}H_{96}Ga_2N_2O_6$: C, 70.01%; H, 8.06%; N, 2.33%; found: C, 70.00%; H, 7.96%; N, 2.25%.

^{1}H NMR (500 MHz, $CDCl_3$): δ (ppm) 7.53 (d, $^3J_{H–H}$ = 6.9 Hz, 4H; Ar-*H*), 7.19 – 7.04 (m, 10H; Ar-*H*), 7.01 (d, $^4J_{H–H}$ = 2.3 Hz, 4H; Ar-*H*), 5.22 (s, 4H; C*H*$_2$), 3.93 (s, 2H; N*H*), 1.39 (s, 36H; C(C*H*$_3$)$_3$), 1.27 (s, 36H; C(C*H*$_3$)$_3$).

^{13}C{^{1}H} NMR (126 MHz, $CDCl_3$): δ (ppm) 153.96 (Ar-*C*), 140.53 (Ar-*C*), 138.36 (Ar-*C*), 137.65 (Ar-*C*), 129.54 (Ar-*C*), 128.86 (Ar-*C*), 128.28 (Ar-*C*), 126.78 (Ar-*C*), 123.03 (Ar-*C*), 119.25 (Ar-*C*), 67.63 (O*C*H$_2$), 35.52 (*C*(CH$_3$)$_3$), 34.30 (*C*(CH$_3$)$_3$), 31.80 (C(*C*H$_3$)$_3$), 29.43 (C(*C*H$_3$)$_3$).

6.2.15 Synthesis of {Ga[ON(H)O](OCH$_2$CHMe$_2$)}$_2$ (**2.11b**)

In accordance with the general procedure described above using **2.7** (100 mg, 0.18 mmol) and isobutyraldehyde (17 μL, 0.19 mmol) to afford product **2.11b** (57 mg, 0.050 mmol, 57% yield). Elemental analysis calculated for $C_{64}H_{100}Ga_2N_2O_6$: C, 67.85%; H, 8.90%; N, 2.47%; found: C, 67.68%; H, 8.85%; N, 2.57%.

^{1}H NMR (400 MHz, $CDCl_3$): δ (ppm) 7.53 (br, 4H; Ar-*H*), 7.21 (br, 4H; Ar-*H*), 5.01 (br, 2H; N*H*), 3.79 (br, 4H; OC*H*$_2$), 2.09 (br, 2H; C*H*Me$_2$), 1.38 (s, 36H; C(C*H*$_3$)$_3$), 1.33 (s, 36H; C(C*H*$_3$)$_3$), 1.03 – 0.66 (m, 12H; CH(C*H*$_3$)$_2$).

^{13}C{^{1}H} NMR (101 MHz, $CDCl_3$): δ (ppm) 154.25 (Ar-*C*), 138.66 (Ar-*C*), 137.98 (Ar-*C*), 129.56 (Ar-*C*), 123.39 (Ar-*C*), 119.39 (Ar-*C*), 72.81 (O*C*H$_2$), 35.47 (*C*(CH$_3$)$_3$), 34.43 (*C*(CH$_3$)$_3$), 31.83 (C(*C*H$_3$)$_3$), 30.74 (O*C*H(CH$_3$)$_2$), 29.41 (C(*C*H$_3$)$_3$), 19.32 (OCH(*C*H$_3$)$_2$).

6.2.16 Synthesis of {Ga[ON(H)O](OCH$_2$C$_6$H$_4$-4-OMe)}$_2$ (**2.11c**)

In accordance with general procedure described above using 4-methoxybenzaldehyde (30 mg, 0.18 mmol) as the substrate to afford **2.11c** (52 mg, 0.04 mmol, 47% yield). Elemental analysis calculated for $C_{84}H_{112}Ga_2N_2O_8$: C, 71.19%; H, 7.97%; N, 1.98%; found: C, 70.62%; H, 7.88%; N, 1.98%.

^{1}H NMR (400 MHz, $CDCl_3$): δ (ppm) 7.48 (d, $^3J_{H–H}$ = 8.2 Hz, 4H, Ar-*H*), 7.14 (d, $^4J_{H–H}$ = 2.2 Hz, 4H; Ar-*H*), 7.08 (d, $^4J_{H–H}$ = 2.3 Hz, 4H; Ar-*H*), 6.65 (d, $^3J_{H–H}$ = 8.1 Hz, 4H, Ar-*H*), 5.15 (s, 4H; C*H*$_2$), 4.00 (s, 2H; N*H*), 3.68 (s, 6H; OC*H*$_3$), 1.39 (s, 36H; C(C*H*$_3$)$_3$), 1.27 (s, 36H; C(C*H*$_3$)$_3$).

$^{13}C\{^{1}H\}$ NMR (101 MHz, $CDCl_3$): δ (ppm) 159.46 (Ar-*C*), 154.02 (Ar-*C*), 138.32 (Ar-*C*), 137.60 (Ar-*C*), 132.58 (Ar-*C*), 129.71 (Ar-*C*), 128.20 (Ar-*C*), 122.98 (Ar-*C*), 119.15 (Ar-*C*), 114.26 (Ar-*C*), 67.22 (O*C*H_2), 55.22 (O*C*H_3), 35.53 (*C*$(CH_3)_3$), 34.28 (*C*$(CH_3)_3$), 31.73 (C(*C*$H_3)_3$), 29.45 (C(*C*$H_3)_3$).

6.2.17 Synthesis of {Ga[ON(H)O]($OCH_2C_6H_4$-4-Br)}$_2$ (**2.11d**)

In accordance with the general procedure described above using 4-bromobenzaldehyde (33 mg, 0.18 mmol) to afford **2.11d** (70 mg, 0.051 mmol, 58% yield). Elemental analysis calculated for $C_{70}H_{94}Br_2Ga_2N_2O_6$: C, 61.88%; H, 6.97%; N, 2.06%; C, 61.43%; H, 7.22%; N, 2.19%.

^{1}H NMR (500 MHz, $CDCl_3$): δ (ppm) 7.44 (d, $^{3}J_{H–H}$ = 8.1 Hz, 4H, Ar-*H*), 7.29 (d, $^{3}J_{H–H}$ = 8.1 Hz, 4H, Ar-*H*), 7.20 (d, $^{4}J_{H–H}$ = 2.4 Hz, 4H; Ar-*H*), 7.15 (d, $^{4}J_{H–H}$ = 2.4 Hz, 4H; Ar-*H*), 5.21 (s, 4H, C*H*$_2$), 4.02 (s, 2H; N*H*), 1.40 (s, 36H; C(C*H*$_3)_3$), 1.32 (s, 36H; C(C*H*$_3)_3$).

$^{13}C\{^{1}H\}$ NMR (126 MHz, $CDCl_3$): δ (ppm) 153.73 (Ar-*C*), 139.18 (Ar-*C*), 138.98 (Ar-*C*), 137.81 (Ar-*C*), 132.07 (Ar-*C*), 129.40 (Ar-*C*), 128.17 (Ar-*C*), 123.38 (Ar-*C*), 122.00 (Ar-*C*), 119.05 (Ar-*C*), 66.85 (O*C*H_2), 35.53 (*C*$(CH_3)_3$), 34.34 (*C*$(CH_3)_3$), 29.71 (C(*C*$H_3)_3$), 29.40 (C(*C*$H_3)_3$).

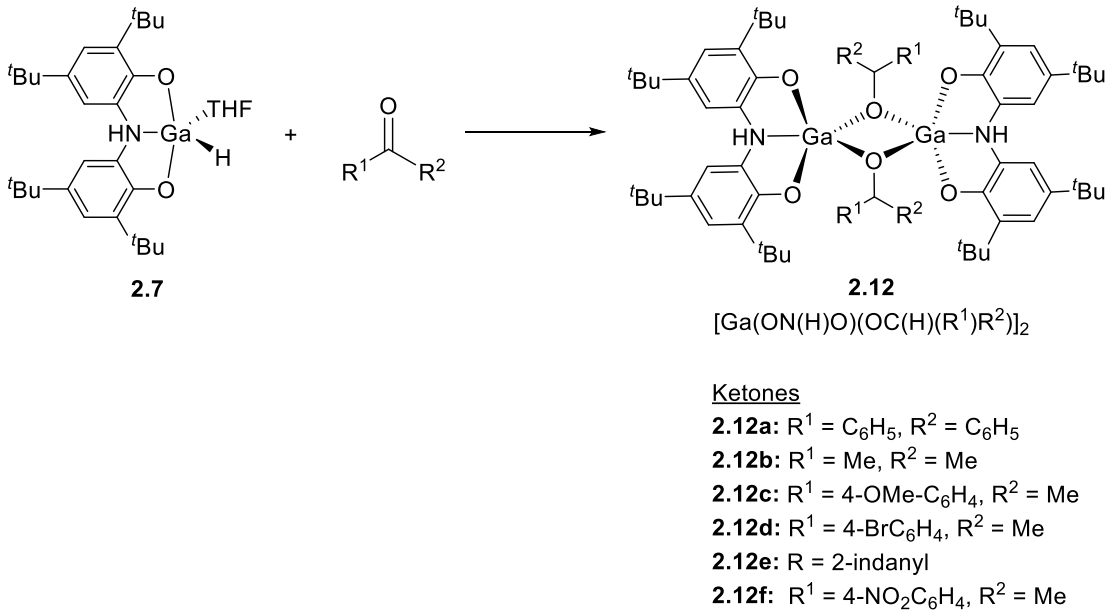
6.2.18 Synthesis of {Ga[ON(H)O]($OCH_2C_6H_2Me_3$)}$_2$ (**2.11e**)

In accordance with the general procedure described above using 2,4,6-trimethylbenzaldehyde (27 mg, 0.18 mmol) to give afford **2.11e** (41 mg, 0.032 mmol, 36% yield).

Elemental Analysis calculated for $C_{76}H_{108}Ga_2N_2O_6$: C, 71.03%; H, 8.47%; N, 2.18%; found: C, 71.02%; H, 8.62%; N, 2.30%.

^{1}H NMR (500 MHz, $CDCl_3$): δ (ppm) 7.10 (d, $^4J_{H–H}$ = 2.3 Hz, 4H; Ar-*H*), 6.97 (d, $^4J_{H–H}$ = 2.3 Hz, 4H; Ar-*H*), 6.78 (s, 4H; Ar-*H*), 5.35 (s, 4H; C*H*$_2$), 2.49 (s, 6H; $C_6H_2CH_3$), 2.18 (s, 12H; $C_6H_2(CH_3)_2$), 1.39 (s, 36H; $C(CH_3)_3$), 1.31 (s, 36H; $C(CH_3)_3$).

^{13}C{^{1}H} NMR (126 MHz, $CDCl_3$): δ (ppm) 153.87 (Ar-*C*), 139.16 (Ar-*C*), 138.16 (Ar-*C*), 137.89 (Ar-*C*), 136.97 (Ar-*C*), 133.56 (Ar-*C*), 130.17 (Ar-*C*), 130.04 (Ar-*C*), 122.34 (Ar-*C*), 119.08 (Ar-*C*), 62.98 (OCH_2), 35.41 ($C(CH_3)_3$), 34.25 ($C(CH_3)_3$), 31.87 ($C(CH_3)_3$), 29.35 ($C(CH_3)_3$), 21.46 ($C_6H_2CH_3$), 19.13 ($C_6H_2CH_3$).



Scheme 6.12: Synthetic route to compounds **2.12a**–**2.12f**.

6.2.19 Synthesis of {Ga[ON(H)O](OCH(Ph)$_2$)}$_2$ (**2.12a**)

In accordance with general procedure described above using benzophenone (33 mg, 0.18mmol) to afford **2.12a** (86 mg, 0.064 mmol, 72% yield). Elemental Analysis

calculated for $C_{82}H_{104}Ga_2N_2O_6$: C, 72.78%; H, 7.75%; N, 2.07%; found: C, 72.26%; H, 7.75%; N, 2.30%.

^{1}H NMR (500 MHz, $CDCl_3$): δ (ppm) 7.48 – 7.41 (m, 8H; Ar-*H*), 7.11 – 6.99 (m, 16H; Ar-*H*), 6.86 (d, $^4J_{H–H}$ = 2.3 Hz, 4H; Ar-*H*), 6.71 (s, 2H; OC*H*), 3.75 (s, 2H; N*H*), 1.22 (s, 36H; C(CH_3)$_3$), 1.19 (s, 36H; C(CH_3)$_3$).

^{13}C{^{1}H} NMR (126 MHz, $CDCl_3$): δ (ppm) 153.28 (Ar-*C*), 142.48 (Ar-*C*), 138.24 (Ar-*C*), 137.59 (Ar-*C*), 129.34 (Ar-*C*), 128.58 (Ar-*C*), 127.72 (Ar-*C*), 127.14 (Ar-*C*), 122.76 (Ar-*C*), 119.01 (Ar-*C*), 77.86 (O*C*H), 35.13 (*C*(CH$_3$)$_3$), 34.20 (*C*(CH$_3$)$_3$), 31.76 (C(*C*H$_3$)$_3$), 29.13 (C(*C*H$_3$)$_3$).

6.2.20 Synthesis of {Ga[ON(H)O](OCH(Me)$_2$)}$_2$ (**2.12b**)

In accordance with the general procedure described above using acetone (13 μL, 0.18 mmol) to give **2.12b** (64 mg, 0.058 mmol, 65% yield). Elemental Analysis calculated for $C_{62}H_{96}Ga_2N_2O_6$: C, 67.40%; H, 8.76%; N, 2.54%; found: C, 66.81%; H, 8.78%; N, 2.68%.

^{1}H NMR (500 MHz, $CDCl_3$): δ (ppm) 7.59 (d, $^4J_{H–H}$ = 2.4 Hz, 4H; Ar-*H*), 7.23 (d, $^4J_{H–H}$ = 2.4 Hz, 4H; Ar-*H*), 5.02 (s, 2H; N*H*), 4.39 (sept, $^3J_{H–H}$ = 6.3 Hz, 2H; C*H*(CH$_3$)$_2$), 1.43 (d, $^3J_{H–H}$ = 6.3 Hz, 12H; CH(CH_3)$_2$), 1.40 (s, 36H; C(CH_3)$_3$), 1.34 (s, 36H; C(CH_3)$_3$).

^{13}C{^{1}H} NMR (101 MHz, $CDCl_3$): δ (ppm) 154.16 (Ar-*C*), 138.51 (Ar-*C*), 138.02 (Ar-*C*), 129.73 (Ar-*C*), 123.42 (Ar-*C*), 119.58 (Ar-*C*), 69.59 (O*C*H(CH$_3$)$_2$), 35.49 (*C*(CH$_3$)$_3$), 34.42 (*C*(CH$_3$)$_3$), 31.84 (C(*C*H$_3$)$_3$), 29.75 (C(*C*H$_3$)$_3$), 25.38 (OCH(*C*H$_3$)$_2$).

6.2.21 Synthesis of {Ga[ON(H)O][OCH(CH_3)(C_6H_4-4-OMe)]}$_2$ (**2.12c**)

In accordance with general procedure described above using 4'-methoxyacetophenone (27 mg, 0.18 mmol) to afford **2.12c** (90 mg, 0.070 mmol, 79% yield). Elemental Analysis calculated for $C_{74}H_{104}Ga_2N_2O_8$: C, 68.95%; H, 8.13%; N, 2.17%; found: C, 69.06%; H, 8.01%; N, 2.23%.

^{1}H NMR (500 MHz, $CDCl_3$): δ (ppm) 7.63 (overlapped singlets, 4H; Ar-*H*), 7.12 (m, 6H; Ar-*H*), 7.03 (d, $^4J_{H–H}$ = 2.3 Hz, 2H; Ar-*H*), 6.70 – 6.57 (m, 4H; Ar-*H*), 5.46 (q, $^3J_{H–H}$ = 6.4 Hz, 2H; OC*H*CH_3), 4.03 (s, 1H; N*H*), 3.96 (s, 1H; N*H*), 3.63 (s, 6H; OCH_3), 3.62 (s, 6H; OCH_3), 1.79 (m, 6H; OCHCH_3), 1.41 (overlapped singlets, 36H; C(CH_3)$_3$), 1.27 (overlapped singlets, 36H; C(CH_3)$_3$).

^{13}C{^{1}H} NMR (126 MHz, $CDCl_3$): δ (ppm) 159.03 (overlapped singlets, Ar-*C*), 154.16 – 153.38 (overlapped singlets, Ar-*C*), 138.42 – 137.90 (overlapped singlets, Ar-*C*), 137.60 – 137.01 (overlapped singlets, Ar-*C*), 129.62 (overlapped singlets, Ar-*C*), 129.26 (overlapped singlets, Ar-*C*), 128.40 – 127.62 (overlapped singlets, Ar-*C*), 126.97 (overlapped singlets, Ar-*C*), 122.85 (overlapped singlets, Ar-*C*), 119.98 – 117.95 (overlapped singlets, Ar-*C*), 114.10 (s, Ar-*C*), 72.14 (overlapped singlets, O*C*H), 55.12 (overlapped singlets, O*C*H_3), 35.45 (overlapped singlets, *C*(CH_3)$_3$), 34.25 (overlapped singlets, *C*(CH_3)$_3$), 31.74 (overlapped singlets, C(*C*H_3)$_3$), 29.42 (overlapped singlets, C(*C*H_3)$_3$), 24.04 (overlapped singlets, O*C*HCH_3).

6.2.22 Synthesis of {Ga[ON(H)O][OCH(CH_3)(C_6H_4-4-Br)]}$_2$ (**2.12d**)

In accordance with the general procedure described above using 4-bromoacetophenone (36 mg, 0.18 mmol) to give **2.12d** (54 mg, 0.039 mmol, 44% yield). Elemental Analysis

calculated for $C_{72}H_{98}Br_2Ga_2N_2O_6$: C, 62.36%; H, 7.12%; N, 2.02%; found: C, 62.10%; H, 7.32%; N, 2.14%.

^{1}H NMR (500 MHz, $CDCl_3$): : δ (ppm) 7.60 – 7.52 (m, 4H; Ar-*H*), 7.25 (d, $^4J_{H–H}$ = 1.6 Hz, 2H; Ar-*H*), 7.23 (d, $^4J_{H–H}$ = 1.6 Hz, 2H; Ar-*H*), 7.16 (d, $^4J_{H–H}$ = 2.3 Hz, 1H; Ar-*H*), 7.15 (d, $^4J_{H–H}$ = 2.3 Hz, 2H; Ar-*H*), 7.14 (d, $^4J_{H–H}$ = 2.3 Hz, 1H; Ar-*H*), 7.13 (d, $^4J_{H–H}$ = 2.3 Hz, 2H; Ar-*H*), 7.07 (d, $^4J_{H–H}$ = 2.3 Hz, 1H; Ar-*H*), 7.06 (d, $^4J_{H–H}$ = 2.3 Hz, 1H; Ar-*H*), 5.44 (q, $^3J_{H–H}$ = 6.5 Hz, 2H; OC*H*CH_3), 3.92 (s, 1H; N*H*), 3.86 (s, 1H; N*H*), 1.94 – 1.64 (m, 6H, CHC*H*$_3$), 1.46 – 1.21 (overlapped singlets, 72H, C(C*H*$_3$)$_3$).

^{13}C{^{1}H} NMR (126 MHz, $CDCl_3$): δ (ppm) 153.82 – 153.10 (overlapped singlets, Ar-*C*), 144.14 (overlapped singlets, Ar-*C*), 139.07 – 138.61 (overlapped singlets, Ar-*C*), 137.77–137.30 (overlapped singlets, Ar-*C*), 132.01, 129.36–128.85 (overlapped singlets, Ar-*C*), 128.22 – 127.68 (overlapped singlets, Ar-*C*), 127.40 (overlapped singlets, Ar-*C*), 123.28 (overlapped singlets, Ar-*C*), 118.97 (overlapped singlets, Ar-*C*), 72.21 (overlapped singlets, O*C*H), 35.46 (overlapped singlets, *C*(CH$_3$)$_3$), 34.31 (overlapped singlets, *C*(CH$_3$)$_3$), 31.79 (overlapped singlets, C(*C*H$_3$)$_3$), 29.38 (overlapped singlets, C(*C*H$_3$)$_3$), 24.28 (overlapped singlets, CH*C*H$_3$).

6.2.23 Synthesis of {Ga[ON(H)O](OCHC$_8$H$_8$)}$_2$ (**2.12e**)

In accordance with the general procedure described above using 2-indanone (24 mg, 0.18 mmol) to give **2.12e** (73 mg, 0.058 mmol, 66% yield). Elemental Analysis calculated for $C_{74}H_{100}Ga_2N_2O_6$: C, 70.93%; H, 8.04%; N, 2.24%; found: C, 71.18%; H, 7.72%; N, 2.26%.

^{1}H NMR (500 MHz, $CDCl_3$): δ (ppm) 7.34 (m, 4H; Ar-*H*), 7.17 – 7.06 (m, 8H; Ar-*H*), 6.85 (d, $^4J_{H–H}$ = 2.3 Hz, 4H; Ar-*H*), 5.33 (m, 2H; OC*H*C$_8$H$_8$), 3.66 (s, 2H; N*H*), 3.52 (d,

$^{3}J_{H–H}$ = 7.6 Hz, 2H; OCHCH_2), 3.48 (d, $^{3}J_{H–H}$ = 7.6 Hz, 2H; OCHCH_2), 3.05 (d, $^{4}J_{H–H}$ = 1.9 Hz, 2H; OCHCH$_2$CH_2), 3.01 (d, $^{4}J_{H–H}$ = 1.9 Hz, 2H; OCHCH$_2$CH_2),1.39 (s, 36H; C(CH_3)$_3$), 1.29 (s, 36H; C(CH_3)$_3$).

^{13}C{^{1}H} NMR (126 MHz, $CDCl_3$): δ(ppm) 153.90 (Ar-*C*), 141.39 (Ar-*C*), 137.84 (Ar-*C*), 137.24 (Ar-*C*), 129.29 (Ar-*C*), 127.45 (Ar-*C*), 125.88 (Ar-*C*), 122.72 (Ar-*C*), 119.81 (Ar-*C*), 75.40 (O*C*H), 44.03 (O*C*H$_2$), 35.48 (*C*(CH$_3$)$_3$), 34.33 (*C*(CH$_3$)$_3$), 31.84 (C(*C*H$_3$)$_3$), 29.39 (C(*C*H$_3$)$_3$).

6.2.24 Synthesis of {Ga[ON(H)O][OCH(CH$_3$)(C$_6$H$_4$-4-NO$_2$)]}$_2$ (**2.12f**)

In accordance with the general procedure described above using 4′-nitroacetophenone (30 mg, 0.18 mmol) to give **2.12f**. (64 mg, 0.049 mmol, 55% yield). Elemental Analysis calculated for $C_{72}H_{98}Ga_2N_2O_6$: C, 65.56%; H, 7.49%; N, 4.25%; found: C, 65.35%; H, 7.45%; N, 4.47%.

^{1}H NMR (500 MHz, $CDCl_3$): δ (ppm) 7.96 (m, 4H, Ar-*H*), 7.87 (m, 4H, Ar-*H*), 7.15 (m, 4H, Ar-*H*), 7.09 – 6.95 (m, 4H, Ar-*H*), 5.58 (q, $^{3}J_{H–H}$ = 6.5 Hz, 2H; OC*H*CH$_3$), 3.96 (s, 1H; N*H*), 3.94 (s, 1H; N*H*), 1.91 (m, 6H, CHCH_3), 1.39 (overlapped singlets, 36H, C(CH_3)$_3$), 1.22 (overlapped singlets, 36H, C(CH_3)$_3$).

^{13}C{^{1}H} NMR (126 MHz, $CDCl_3$): δ (ppm) 153.23 (overlapped singlets, Ar-*C*), 152.15 (overlapped singlets, Ar-*C*), 147.29 (overlapped singlets, Ar-*C*), 139.29 (overlapped singlets, Ar-*C*), 137.77 (overlapped singlets, Ar-*C*), 128.84 (overlapped singlets, Ar-*C*), 126.54 (overlapped singlets, Ar-*C*), 124.10 (overlapped singlets, Ar-*C*), 123.66 (overlapped singlets, Ar-*C*), 118.89 (overlapped singlets, Ar-*C*), 72.45 (overlapped singlets, O*C*H), 35.50 (overlapped singlets, *C*(CH$_3$)$_3$), 34.26 (overlapped singlets,

C(CH_3)$_3$), 31.61 (overlapped singlets, C(*C*H_3)$_3$), 29.43 (overlapped singlets, C(*C*H_3)$_3$), 24.37 (overlapped singlets, CH*C*H_3).

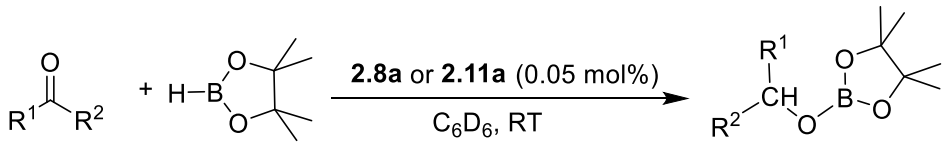
^{1}H NMR (500 MHz, C_6D_6): δ (ppm) 7.86 (d, $^3J_{H–H}$ = 8.6 Hz, 4H; Ar-*H*), 7.42 (d, $^3J_{H–H}$ = 8.4 Hz, 4H; Ar-*H*), 7.37 (d, $^4J_{H–H}$ = 2.3 Hz, 2H; Ar-*H*), 7.35 (d, $^4J_{H–H}$ = 2.3 Hz, 2H; Ar-*H*), 7.29 (d, $^4J_{H–H}$ = 2.3 Hz, 2H; Ar-*H*), 7.24 (d, $^4J_{H–H}$ = 2.3 Hz, 2H; Ar-*H*), 5.13 (q, $^3J_{H–H}$ = 6.6 Hz, 2H; Ar-*H*), 3.90 (s, 2H; N*H*), 1.72 (d, $^3J_{H–H}$ = 6.6 Hz, 6H; CHC*H*$_3$), 1.58 (s, 18H; C(C*H*$_3$)$_3$), 1.55 (s, 18H; C(C*H*$_3$)$_3$), 1.33 (s, 18H; C(C*H*$_3$)$_3$), 1.28 (s, 18H; C(C*H*$_3$)$_3$). Compound **2.12f** is poorly soluble in C_6D_6, consequently a ^{13}C NMR spectrum for **2.12f** could not be obtained.

6.3 Experimental details for Chapter Three

6.3.1 General procedure for the catalytic hydroboration of aldehydes and ketones

To a dried ampoule containing the pre-catalyst **2.8a** (27 mg) or **2.11a** (30 mg) and HMCTS (1.11 g), C_6D_6 (50 mL) was added. This gave a stock solution containing 0.0005 mol·L^{-1} of catalyst and 0.1 mol·L^{-1} of HMCTS.

To the stock solution (500 μL, with 0.00025 mmol **2.8a** or **2.11a**), neat aldehyde or ketone substrate (ca. 0.5 mmol) and neat HBpin (80 μL, 0.55 mmol) was added using a (100 μL) gastight syringe (Scheme 6.12).



Scheme 6.13: Catalytic hydroboration of aldehydes and ketones.

6.3.2 $PhCH_2OBpin$: product from hydroboration of benzaldehyde.

^1H NMR (400 MHz, C_6D_6): δ (ppm) 7.41 (d, $^3J_{H–H}$ = 7.5 Hz, 2H; Ar-*H*), 7.31 – 7.22 (m, 2H; Ar-*H*), 7.21 – 7.14 (m, 1H; Ar-*H*), 5.05 (s, 2H; OC*H*$_2$), 1.16 (s, 12H; Bpin-C*H*$_3$).

$^{11}B\{^1H\}$ NMR (128 MHz, C_6D_6): δ (ppm) 22.8.

6.3.3 4-Br-$C_6H_4CH_2OBpin$: product from hydroboration of 4-bromobenzaldehyde

^1H NMR (400 MHz, C_6D_6): δ (ppm) 7.27 – 7.18 (m, 2H; Ar-*H*), 6.94 (m, 2H; Ar-*H*), 4.72 (s, 2H; OC*H*$_2$), 1.03 (s, 12H; Bpin-C*H*$_3$).

$^{11}B\{^1H\}$ NMR (128 MHz, C_6D_6): δ (ppm) 22.7.

6.3.4 4-MeO-$C_6H_4CH_2OBpin$: product from hydroboration of 4-methoxybenzaldehyde

^1H NMR (400 MHz, C_6D_6): δ (ppm) 7.23 (d, $^3J_{H–H}$ = 6.5 Hz, 2H; Ar-*H*), 6.82 – 6.60 (m, 2H; Ar-*H*), 4.90 (s, 2H; OC*H*$_2$), 3.30 (s, 3H; OC*H*$_3$), 1.04 (s, 12H; Bpin-C*H*$_3$).

$^{11}B\{^1H\}$ NMR (128 MHz, C_6D_6): δ (ppm) 22.8.

6.3.5 2,4,6-$Me_3C_6H_2CH_2OBpin$: product from hydroboration of mesitaldehyde

^1H NMR (400 MHz, C_6D_6): δ (ppm) 6.71 (s, 2H; Ar*H*), 5.00 (s, 2H; OC*H*$_2$), 2.35 (s, 6H; C_6H_2(C*H*$_3$)$_2$), 2.11 (s, 3H; C_6H_2C*H*$_3$), 1.04 (s, 12H; Bpin-C*H*$_3$).

$^{11}B\{^{1}H\}$ NMR (128 MHz, C_6D_6): δ (ppm) 22.6.

6.3.6 4-F-C_6H_4-CH_2OBpin: product from hydroboration of 4-fluorobenzaldehyde

^{1}H NMR (400 MHz, C_6D_6): δ (ppm) 7.14 – 7.00 (m, 2H; Ar-*H*), 6.84 – 6.70 (m, 2H; Ar-*H*), 4.78 (s, 2H; OCH_2), 1.04 (s, 12H; Bpin-CH_3).

$^{11}B\{^{1}H\}$ NMR (128 MHz, C_6D_6): δ (ppm) 22.7.

6.3.7 4-Me-$C_6H_4CH_2$OBpin: product from hydroboration of 4-methylbenzaldehyde

^{1}H NMR (500 MHz, C_6D_6): δ (ppm) 7.25 (d, $^{3}J_{H–H}$ = 7.9 Hz; Ar-*H*), 6.96 (d, $^{3}J_{H–H}$ = 7.8 Hz, 2H; Ar-*H*), 4.94 (s, 2H; OCH_2), 2.09 (s, 3H; C_6H_4CH_3), 1.05 (s, 12H; Bpin-CH_3).

$^{11}B\{^{1}H\}$ NMR (128 MHz, C_6D_6): δ (ppm) 22.8.

6.3.8 (4-Br-C_6H_4)(CH_3)C(H)OBpin: product from hydroboration of 4'-bromoacetophenone

^{1}H NMR (400 MHz, C_6D_6): δ (ppm) 7.47 – 7.16 (m, 2H; Ar-*H*), 7.06 – 6.90 (m, 2H; Ar-*H*), 5.20 (q, $^{3}J_{H–H}$ = 6.5 Hz, 1H; OC*H*), 1.32 (d, $^{3}J_{H–H}$ = 6.5 Hz, 3H; CH_3), 1.06 – 0.99 (s, 12H; Bpin-CH_3).

$^{11}B\{^{1}H\}$ NMR (128 MHz, C_6D_6): δ (ppm) 22.4.

6.3.9 (4-MeO-C_6H_4)(CH_3)C(H)OBpin: product from hydroboration of 4'-methoxyacetophenone

^{1}H NMR (400 MHz, C_6D_6): δ (ppm) 7.50 – 7.20 (m, 2H; Ar-*H*), 6.89 – 6.60 (m, 2H; Ar-*H*), 5.37 (q, $^3J_{H–H}$ = 6.5 Hz, 1H; OC*H*), 3.32 (s, 3H; OCH_3), 1.46 (d, $^3J_{H–H}$ = 6.5 Hz, 3H; CHCH_3), 1.03 (s, 12H; Bpin-CH_3).

^{11}B{^{1}H} NMR (128 MHz, C_6D_6): δ (ppm) 22.7.

6.3.10 (CH_3)$_2$C(H)OBpin: product from hydroboration of acetone

^{1}H NMR (400 MHz, C_6D_6): δ (ppm) 4.43 (hept, $^3J_{H–H}$ = 6.2 Hz, 1H; OC*H*), 1.15 (d, $^3J_{H–H}$ = 6.1 Hz, 6H; CH(CH_3)$_2$), 1.06 (s, 12H; Bpin-CH_3).

^{11}B{^{1}H} NMR (128 MHz, C_6D_6): δ (ppm) 22.5.

6.3.11 (CH_3)$_2$C(H)CH_2OBpin: product from hydroboration of isobutyraldehyde

^{1}H NMR (400 MHz, C_6D_6): δ (ppm) 3.69 (d, $^3J_{H–H}$ = 6.5 Hz, 2H; OCH_2), 1.96 – 1.61 (m, 1H; C*H*), 1.06 (s, 12H; Bpin-CH_3), 0.83 (d, $^3J_{H–H}$ = 6.7 Hz, 6H; CH_3).

^{11}B{^{1}H} NMR (128 MHz, C_6D_6): δ (ppm) 22.5.

6.3.12 (4-NO_2-C_6H_4)C(H)(CH_3)OBpin: product from hydroboration of 4'-nitroacetophenone

^{1}H NMR (400 MHz, C_6D_6): δ (ppm) 8.12 – 7.58 (m, 2H; Ar-*H*), 7.07 – 7.01 (m, 2H; Ar-*H*), 5.19 (q, $^3J_{H–H}$ = 6.5 Hz, 1H; OC*H*), 1.27 (d, $^3J_{H–H}$ = 6.5 Hz, 3H; CHCH_3), 1.03 (s, 12H; Bpin-CH_3).

$^{11}B\{^{1}H\}$ NMR (128 MHz, C_6D_6): δ (ppm) 22.4.

6.3.13 (4-I-C_6H_4)C(H)(CH_3)OBpin: product from hydroboration of 4'-iodoacetophenone

^{1}H NMR (400 MHz, C_6D_6): δ (ppm) 7.55 – 7.35 (m, 2H; Ar-*H*), 7.01 – 6.73 (m, 2H; Ar-*H*), 5.18 (q, $^{3}J_{H–H}$ = 6.5 Hz, 1H; OC*H*), 1.32 (d, $^{3}J_{H–H}$ = 6.5 Hz, 3H; CHCH_3), 1.04 – 0.95 (s, 12H; Bpin-CH_3).

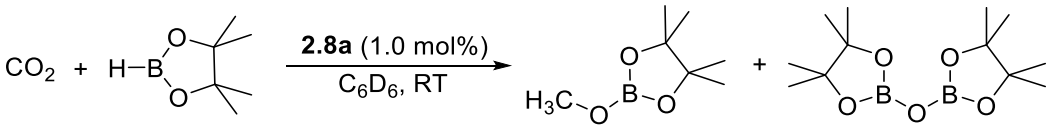
$^{11}B\{^{1}H\}$ NMR (128 MHz, C_6D_6): δ (ppm) 22.5.

6.3.14 (4-Cl-C_6H_4)C(H)(CH_3)OBpin: product from hydroboration of 4'-chloroacetophenone

^{1}H NMR (400 MHz, C_6D_6): δ (ppm) 7.07 (m, 4H; Ar-*H*)), 5.22 (q, $^{3}J_{H–H}$ = 6.5 Hz, 1H; OC*H*), 1.33 (d, $^{3}J_{H–H}$ = 6.5 Hz, 3H; CHCH_3), 1.04 – 0.96 (s, 12H, CH_3; Bpin-CH_3).

$^{11}B\{^{1}H\}$ NMR (128 MHz, C_6D_6): δ (ppm) 22.4.

6.3.15 Preparation of a stock solution for carbon dioxide hydroboration



Scheme 6.14: Catalytic hydroboration of carbon dioxide.

To a dried ampoule containing the pre-catalyst **2.8a** (40 mg) and HMCTS (0.444 g) as an internal standard, was added 20 mL of C_6D_6. This gave a stock solution containing 0.0019 mol·L^{-1} of catalyst **2.8a** and 0.1 mol·L^{-1} of HMCTS.

To the stock solution (500 μL, with 0.00093 mmol **2.8a**), neat HBpin (13.5 μL, 0.093 mmol) was added using a gastight syringe, then degassed via freeze-pump-thaw method three times prior to exposure to ~2 bar pressure carbon dioxide at room temperature. The ampoule was sealed and kept stirring at room temperature, and NMR data were collected after 20 and 38 hours separately.

6.3.16 MeOBpin: product from the hydroboration of carbon dioxide

^{1}H NMR (400 MHz, C_6D_6): δ (ppm) 3.50 (s, 3H; OC*H*$_3$)), 1.04 (s, 12H, CH_3; Bpin-C*H*$_3$).

^{11}B{^{1}H} NMR (128 MHz, C_6D_6): δ (ppm) 22.7.

6.3.17 O(Bpin)$_2$: side product from the hydroboration of carbon dioxide

^{1}H NMR (400 MHz, C_6D_6): δ (ppm) 1.01 (s, 24H, CH_3; Bpin-C*H*$_3$).

^{11}B{^{1}H} NMR (128 MHz, C_6D_6): δ (ppm) 21.8.

6.3.18 General procedure for the catalytic hydroboration of isocyanates

To a dried ampoule containing the pre-catalyst **2.8a** (86 mg) and HMCTS (445 mg) as an internal standard, was added 20 mL of C_6D_6. This gave a stock solution containing 0.004 mol·L^{-1} of catalyst and 0.1 mol·L^{-1} of HMCTS.

To the stock solution (500 μL, with 0.002 mmol **2.8a**), the neat isocyanate substrate (ca. 0.2 mmol) and neat HBpin (90 μL, 0.62 mmol) were added using a gastight syringe. ^{13}C{^{1}H} NMR spectroscopic studies were only carried for the unreported compounds RN(Me)Bpin (R− = 2-$CF_3C_6H_4$−, 4-MeC_6H_4−, CH_2=$CHCH_2$−, $PhCH_2$−), the rest of the products have been previously reported by Hill and Nembenna.[6,7]



Scheme 6.15: Catalytic hydroboration of isocyanates.

6.3.19 PhN(Me)Bpin: product from hydroboration of phenyl isocyanate.

^{1}H NMR (400 MHz, C_6D_6): δ (ppm) 7.48 – 7.41 (m, 2H; Ar-*H*), 7.24 – 7.17 (m, 2H; Ar-*H*), 6.90 – 6.84 (m, 1H; Ar-*H*), 3.00 (s, 3H; NC*H*$_3$), 1.08 (s, 12H; Bpin-C*H*$_3$).

^{11}B{^{1}H} NMR (128 MHz, C_6D_6): δ (ppm) 24.6.

6.3.20 MesN(Me)Bpin: product from hydroboration of 2,4,6-trimethylphenyl isocyanate

^{1}H NMR (400 MHz, C_6D_6): δ (ppm) 6.75 (s, 2H; Ar-*H*), 2.83 (s, 3H; Ar-C*H*$_3$), 2.24 (s, 6H; Ar-C*H*$_3$), 2.09 (s, 3H; NC*H*$_3$), 1.21 – 1.04 (m, 12H; Bpin-C*H*$_3$).

^{11}B{^{1}H} NMR (128 MHz, C_6D_6): δ (ppm) 23.9.

6.3.21 2-$CF_3C_6H_4$N(Me)Bpin: product from hydroboration of 2-(trifluoromethyl)phenyl isocyanate

^{1}H NMR (400 MHz, C_6D_6): δ (ppm) 7.40 (m, 1H; Ar-*H*), 7.07 – 7.05 (m, 1H; Ar-*H*), 7.04 (m, 1H; Ar-*H*), 6.83 – 6.77 (m, 1H; Ar-*H*), 2.99 (s, 3H; NC*H*$_3$), 1.14 – 1.05 (s, 12H; Bpin-C*H*$_3$).

^{13}C{^{1}H} NMR (101 MHz, C_6D_6): δ (ppm) 146.80 (q, $^{3}J_{F–C}$ = 2.1 Hz; *C*-N(Me)Bpin), 133.00 (q, $^{4}J_{F–C}$ = 1.4 Hz; *C*(H)-C(H)-C-CF_3), 131.74 (Ar-*C*), 129.17 (q, $^{2}J_{F–C}$ = 29.3

Hz; *C*-CF_3), 127.16 (q, $^3J_{F–C}$ = 5.3 Hz; *C*(H)-C-CF_3), 126.16 (Ar-*C*), 82.92 (BO*C*H), 38.82 (N*C*H_3), 24.65 (Bpin-*C*H_3), (*C*F_3 was not observed due to the low intensity).

$^{19}F\{^1H\}$ NMR (377 MHz, C_6D_6): δ (ppm) −60.14.

$^{11}B\{^1H\}$ NMR (128 MHz, C_6D_6): δ (ppm) 23.9.

6.3.22 4-MeC_6H_4N(Me)Bpin: product from hydroboration of *p*-tolyl isocyanate

^1H NMR (400 MHz, C_6D_6): δ (ppm) 7.40 – 7.32 (m, 2H; Ar-*H*), 7.06 – 6.96 (m, 2H; Ar-*H*), 3.02 (s, 3H; Ar-C*H*$_3$), 2.14 (s, 3H; NC*H*$_3$), 1.08 (s, 12H; Bpin-C*H*$_3$).

$^{13}C\{^1H\}$ NMR (101 MHz, C_6D_6): δ (ppm) 145.57 (Ar-*C*), 129.98 (Ar-*C*), 129.41 (Ar-*C*), 119.57 (Ar-*C*), 82.22 (BO*C*H), 34.57 (N*C*H_3), 24.79 (Bpin-*C*H_3).

$^{11}B\{^1H\}$ NMR (128 MHz, C_6D_6): δ (ppm) 24.6.

6.3.23 CH_2=$CHCH_2$N(Me)Bpin: product from hydroboration of allyl isocyanate

^1H NMR (400 MHz, C_6D_6): δ (ppm) 5.70 (m, 1H; CH_2=C*H*CH_2), 5.10 – 4.95 (m, 2H; C*H*$_2$=$CHCH_2$), 3.53 (m, 2H; CH_2=CHC*H*$_2$), 2.60 (s, 3H; NC*H*$_3$), 1.10 (s, 12H; Bpin-C*H*$_3$).

$^{13}C\{^1H\}$ NMR (101 MHz, C_6D_6): δ (ppm) 137.11 (CH_2=*C*HCH_2), 115.19 (*C*H_2=$CHCH_2$), 82.22 (BO*C*H), 51.81 (CH_2=CH*C*H_2), 33.39 (N*C*H_3), 24.98 (Bpin-*C*H_3).

$^{11}B\{^1H\}$ NMR (128 MHz, C_6D_6): δ (ppm) 24.3.

6.3.24 $PhCH_2N(Me)Bpin$: product from hydroboration of benzyl isocyanate or *N*-benzylidenemethylamine

^1H NMR (400 MHz, C_6D_6): δ (ppm) 7.25 – 7.19 (m, 2H; Ar-*H*), 7.17 – 7.10 (m, 2H; Ar-*H*), 7.08 – 7.02 (m, 1H; Ar-*H*), 4.10 (s, 2H; PhCH_2), 2.54 (s, 3H; NCH_3), 1.10 (s, 12H; Bpin-CH_3).

$^{13}C\{^1H\}$ NMR (101 MHz, C_6D_6): δ (ppm) 140.75 (Ar-*C*), 128.62 (Ar-*C*), 128.05 (Ar-*C*), 127.01 (Ar-*C*), 82.41 (BO*C*H), 53.25 (Ph*C*H_2), 33.32 (N*C*H_3), 24.86 (Bpin-*C*H_3).

$^{11}B\{^1H\}$ NMR (128 MHz, C_6D_6): δ (ppm) 24.6.

6.3.25 $4\text{-}BrC_6H_4N(Me)Bpin$: product from hydroboration of 4-bromophenyl isocyanate

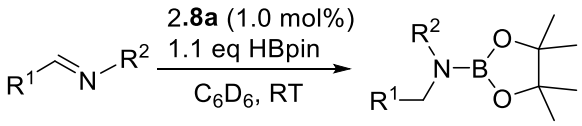
^1H NMR (400 MHz, C_6D_6): δ (ppm) 7.30 – 7.26 (m, 2H; Ar-*H*), 7.17-7.13 (m, 2H; Ar-*H*), 2.85 (s, 3H; NCH_3), 1.06 (s, 12H; Bpin-CH_3).

$^{11}B\{^1H\}$ NMR (128 MHz, C_6D_6): δ (ppm) 24.5.

6.3.26 General procedure for the catalytic hydroboration of imines

To a dried ampoule containing the pre-catalyst **2.8a** (44 mg) and HMCTS (445 mg), C_6D_6 (20 mL) was added. This gives rise to a stock solution containing 0.002 $mol \cdot L^{-1}$ of catalyst and 0.1 $mol \cdot L^{-1}$ of HMCTS.

To the stock solution (500 μL, with 0.001 mmol **2.8a**), the neat imine substrate (ca. 0.1 mmol) was added, and neat HBpin (16 μL, 0.11 mmol) was added using a gastight syringe.



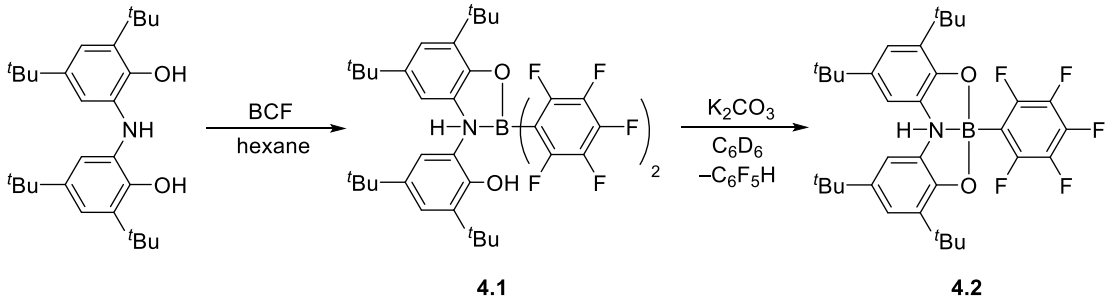
Scheme 6.16: Catalytic hydroboration of imines.

6.3.27 $PhCH_2N(^tBu)Bpin$: product from hydroboration of *N*-benzylidene-*tert*-butylamine

^1H NMR (400 MHz, C_6D_6): δ (ppm) 7.31 (m, 1H; Ar-*H*), 7.25 – 7.03 (m, 1H; Ar-*H*), 4.35 (s, 2H; $PhCH_2$), 1.28 (s, 9H; $C(CH_3)_3$), 1.11 (s, 12H; Bpin-CH_3).

$^{11}B\{^1H\}$ NMR (128 MHz, C_6D_6): δ (ppm) 25.1.

6.4 Experimental details for Chapter Four



Scheme 6.17: Synthesis of **4.1** and **4.2**.

6.4.1 Synthesis of $[O(H)N(H)O]B(C_6F_5)_2$ (**4.1**)

In a glovebox, a hexane solution (10 mL) of BCF (240 mg, 0.47 mmol) was added to a hexane solution (5 mL) of $[H_3(ONO)]$ (200 mg, 0.47 mmol). After stirring at room temperature overnight, colourless crystals formed. The solution was then filtered and the crystals are subsequently dried *in vacuo*, affording white solids as the product (92

mg, 0.12 mmol, 26%). Elemental analysis calculated for $C_{40}H_{42}BF_{10}NO_2$: C 62.43%, H 5.50%, N 1.82%; found: C 62.13%, H 5.36%, N 1.83%.

^{1}H NMR (400 MHz, C_6D_6): δ (ppm) 9.97 (br, 1H; O*H*), 7.44 (d, $^3J_{H–H}$ = 2.1 Hz, 1H; Ar-*H*), 7.29 (d, $^3J_{H–H}$ = 2.1 Hz, 1H; Ar-*H*), 7.10 (d, $^3J_{H–H}$ = 2.2 Hz, 1H; Ar-*H*), 6.91 (d, $^3J_{H–H}$ = 2.2 Hz, 1H; Ar-*H*), 4.73 (s, 1H; N*H*), 1.70 (s, 9H; C(C*H*$_3$)$_3$), 1.01 (s, 9H; C(C*H*$_3$)$_3$), 0.99 (s, 9H; C(C*H*$_3$)$_3$), 0.94 (s, 9H; C(C*H*$_3$)$_3$).

^{13}C{^{1}H} NMR (126 MHz, C_6D_6): δ (ppm) 153.31 (Ar-*C*), 149.28 (m, *C*$_6$F$_5$), 147.39 (m, *C*$_6$F$_5$), 145.47 (Ar-*C*), 143.80 (Ar-*C*), 142.32 (Ar-*C*), 141.60 (m, *C*$_6$F$_5$), 139.62 (m, *C*$_6$F$_5$), 138.62 (m, *C*$_6$F$_5$),137.94 (Ar-*C*), 136.60 (m, *C*$_6$F$_5$), 136.34 (Ar-*C*), 132.47 (Ar-*C*), 132.25 (Ar-*C*), 125.10 (Ar-*C*), 122.83 (Ar-*C*), 118.25 (Ar-*C*), 115.17 (Ar-*C*), 35.17 (*C*(CH$_3$)$_3$), 34.67 (*C*(CH$_3$)$_3$), 34.45 (*C*(CH$_3$)$_3$), 34.07 (*C*(CH$_3$)$_3$), 31.45 (C(*C*H$_3$)$_3$), 30.81 (C(*C*H$_3$)$_3$), 29.78 (C(*C*H$_3$)$_3$), 29.37 (C(*C*H$_3$)$_3$).

^{19}F NMR (377 MHz, C_6D_6): δ (ppm) −131.49 (br, C_6F_5), −133.38 (br, C_6F_5), −137.04 (br, C_6F_5), −155.81 (m, C_6F_5), −156.41 (m, C_6F_5), −162.68 (m, C_6F_5), −163.02 (br, C_6F_5), −165.26 (br, C_6F_5).

^{11}B{^{1}H} NMR (128 MHz, C_6D_6): δ (ppm) 8.6.

6.4.2 Synthesis of [ON(H)O]B(C_6F_5) (**4.2**)

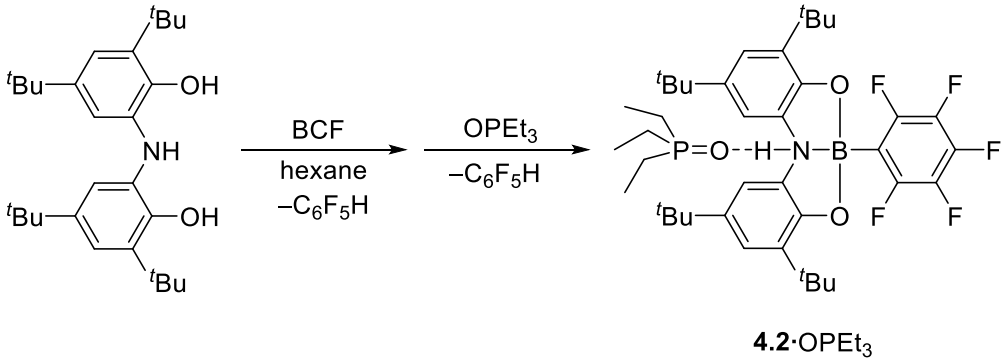
To an NMR tube fitted with a J. Young tap, K_2CO_3 (3 mg, 0.022 mmol) was added to a C_6D_6 solution (0.5 mL) of **4.1** (10 mg, 0.013 mmol). After overnight reaction, the formation of the product (**4.2**) was confirmed by solution NMR studies (NMR conversion: 99%).

^{1}H NMR (400 MHz, C_6D_6): δ (ppm) 7.33 (d, $^{4}J_{H–H}$ = 2.1 Hz, 2H; Ar-*H*), 6.98 (d, $^{4}J_{H–H}$ = 2.1 Hz, 2H; Ar-*H*), 6.12 (s, 1H; N*H*), 1.49 (s, 18H; C(C*H*$_3$)$_3$), 1.24 (s, 18H; C(C*H*$_3$)$_3$).

^{13}C{^{1}H} NMR (126 MHz, C_6D_6): δ (ppm) 153.17 (Ar-*C*), 149.77 (m, *C*$_6$F$_5$), 147.83 (m, *C*$_6$F$_5$), 142.19 (m, *C*$_6$F$_5$), 142.01 (Ar-*C*), 140.26 (m, *C*$_6$F$_5$), 138.60 (m, *C*$_6$F$_5$), 136.73 (Ar-*C*), 136.42 (m, *C*$_6$F$_5$), 130.24 (Ar-*C*), 124.46 (Ar-*C*), 115.31 (Ar-*C*), 35.12 (*C*(CH$_3$)$_3$), 34.67 (*C*(CH$_3$)$_3$), 31.74 (C(*C*H$_3$)$_3$), 29.28 (C(*C*H$_3$)$_3$).

^{19}F NMR (377 MHz, C_6D_6): δ (ppm) −132.83 (m, C_6F_5), −155.23 (m, C_6F_5), −162.97 (m, C_6F_5).

^{11}B{^{1}H} NMR (128 MHz, C_6D_6): δ (ppm) 13.0.



4.2·OPEt$_3$

Scheme 6.18: Synthesis of **4.2**·OPEt$_3$.

6.4.3 Synthesis of OPEt$_3$·[ON(H)O]B(C$_6$F$_5$) (**4.2**·OPEt$_3$)

In a glovebox, a hexane solution (5 mL) of BCF (120 mg, 0.23 mmol) was added to a hexane solution (5 mL) of [H$_3$(ONO)] (100 mg, 0.23 mmol). To the resultant solution, triethylphosphine oxide (35 mg, 0.26 mmol) was added. After stirring at room temperature overnight, the solution was filtered. The filtrate was stored at 4 ℃ for 3 days until colourless crystals formed. Following filtration afforded white solids as the product (84 mg, 0.11 mmol, 49%).

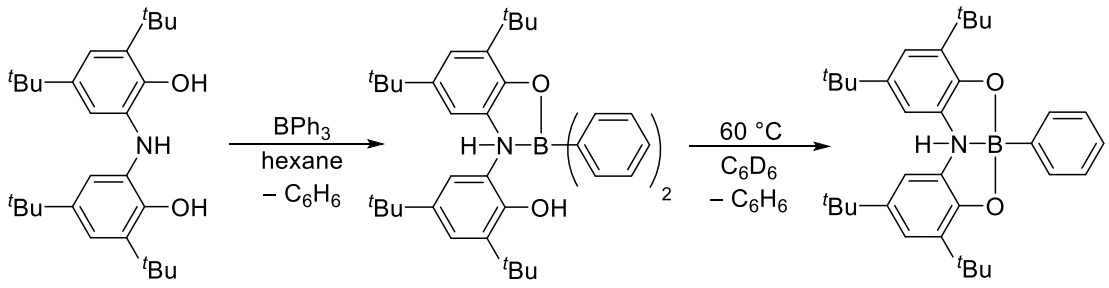
^{1}H NMR (500 MHz, C_6D_6): δ (ppm) 11.85 (s, 1H; N*H*), 7.57 (d, $^{4}J_{H–H}$ = 2.1 Hz, 2H; Ar-*H*), 7.37 (d, $^{4}J_{H–H}$ = 2.1 Hz, 2H; Ar-*H*), 1.60 (s, 18H; C(C*H*$_3$)$_3$), 1.31 (s, 18H; C(C*H*$_3$)$_3$), 0.86 (m, 6H; OPC*H*$_2$CH$_3$), 0.56 (m, 9H; OPCH$_2$C*H*$_3$).

^{13}C{^{1}H} NMR (126 MHz, C_6D_6): δ (ppm) 153.81 (Ar-*C*), 150.42 (m, B*C*$_6$F$_5$), 148.45 (m, B*C*$_6$F$_5$), 141.81 (m, B*C*$_6$F$_5$), 141.08 (Ar-*C*), 139.83 (m, B*C*$_6$F$_5$), 138.42 (m, B*C*$_6$F$_5$), 136.46 (m, B*C*$_6$F$_5$), 135.96 (Ar-*C*), 132.82 (Ar-*C*), 123.37 (Ar-*C*), 115.56 (Ar-*C*), 35.11 (*C*(CH$_3$)$_3$), 34.62 (*C*(CH$_3$)$_3$), 31.87 (C(*C*H$_3$)$_3$), 29.47 (C(*C*H$_3$)$_3$), 19.33 (d, $^{1}J_{P–C}$ = 66.5 Hz), 5.24 (d, $^{2}J_{P–C}$ = 4.9 Hz).

^{19}F NMR (377 MHz, C_6D_6): δ (ppm) −131.20 (m), −158.06 (m), −164.79 (m).

^{31}P{^{1}H} NMR (162 MHz, C_6D_6): δ (ppm) 51.3 (O*P*Et$_3$).

^{11}B{^{1}H} NMR (128 MHz, C_6D_6): δ (ppm) 13.0.



4.3 **4.4**

Scheme 6.19: Synthesis of **4.3** and **4.4**.

6.4.4 Synthesis of [ON(H)OH]B(C$_6$H$_5$)$_2$ (**4.3**)

In a glovebox, a hexane solution (15 mL) of BPh$_3$ (57 mg, 0.23 mmol) was added to a hexane solution (5 mL) of [H$_3$(ONO)] (100 mg, 0.23 mmol). After stirring at room temperature overnight, the solution was concentrated to 5 mL and stored at 4 °C for 3 days until colourless crystals formed. The solution was then filtered and afforded

product as white solid (25 mg, 0.04 mmol, 18%). Elemental analysis calculated for $C_{40}H_{52}BNO_2$: C, 81.48%; H, 8.89%; N, 2.38%; found: C, 80.98%, H, 8.92%, N, 2.41%.

^{1}H NMR (400 MHz, C_6D_6): δ (ppm) 8.00 (s, 1H; O*H*), 7.96 (m, 4H; Ar-*H*), 7.46 (d, $^4J_{H–H}$ = 2.2 Hz, 1H; Ar-*H*), 7.20 (t, $^3J_{H–H}$ = 7.3 Hz, 4H; Ar-*H*), 7.10 (t, $^3J_{H–H}$ = 7.3 Hz, 2H; Ar-*H*), 6.95 (d, $^4J_{H–H}$ = 2.3 Hz, 1H; Ar-*H*), 6.76 (d, $^4J_{H–H}$ = 2.2 Hz, 1H; Ar-*H*), 6.45 (d, $^4J_{H–H}$ = 2.3 Hz, 1H; Ar-*H*), 4.20 (s, 1H; N*H*), 1.79 (s, 9H; C(C*H*$_3$)$_3$), 1.06 (s, 9H; C(C*H*$_3$)$_3$), 1.05 (s, 9H; C(C*H*$_3$)$_3$), 1.04 (s, 9H; C(C*H*$_3$)$_3$).

^{13}C{^{1}H} NMR (101 MHz, C_6D_6): δ (ppm) 156.27 (Ar-*C*), 146.20 (m, Ar-*C*),144.58 (Ar-*C*), 142.91 (Ar-*C*), 141.72 (Ar-*C*), 136.94 (Ar-*C*), 136.24 (Ar-*C*), 134.33 (Ar-*C*), 133.03 (Ar-*C*), 129.79 (Ar-*C*), 127.67 (Ar-*C*), 127.25 (Ar-*C*), 124.14 (Ar-*C*), 121.05 (Ar-*C*), 118.85 (Ar-*C*), 117.22 (Ar-*C*), 35.31 (*C*(CH$_3$)$_3$), 34.51 (*C*(CH$_3$)$_3$), 34.46 (*C*(CH$_3$)$_3$), 34.25 (*C*(CH$_3$)$_3$), 31.65 (C(*C*H$_3$)$_3$), 31.23 (C(*C*H$_3$)$_3$), 29.94 (C(*C*H$_3$)$_3$), 29.85 (C(*C*H$_3$)$_3$).

^{11}B{^{1}H} NMR (128 MHz, C_6D_6): δ (ppm) 13.5.

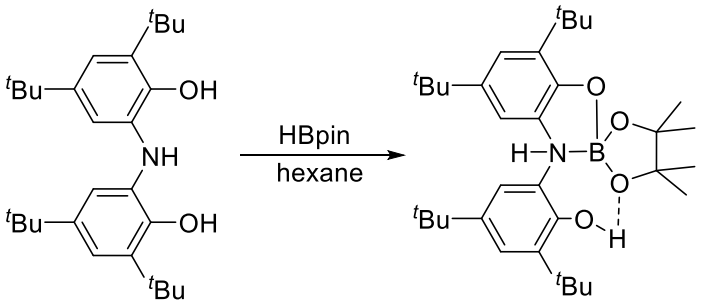
6.4.5 Synthesis of [ON(H)O]B(C_6H_5) (**4.4**)

To an NMR tube fitted with a J. Young tap, a C_6D_6 solution (0.5 mL) of **4.3** (10 mg, 0.017 mmol) was heated at 60 ℃ overnight. The formation of the product (**4.4**) was confirmed by solution NMR studies (NMR yield: 99%).

^{1}H NMR (400 MHz, $CDCl_3$): δ (ppm) 7.55 – 7.48 (m, 2H; Ar-*H*), 7.20 (d, $^4J_{H–H}$ = 2.5 Hz, 2H; Ar-*H*), 7.19 – 7.18 (m, 1H; Ar-*H*), 7.16 (d, $^4J_{H–H}$ = 2.2 Hz, 2H; Ar-*H*), 7.12 (d, $^4J_{H–H}$ = 2.2 Hz, 2H; Ar-*H*), 6.18 (s, 1H; N*H*), 1.38 (s, 18H; C(C*H*$_3$)$_3$), 1.20 (s, 18H; C(C*H*$_3$)$_3$).

$^{13}C\{^{1}H\}$ NMR (126 MHz, $CDCl_3$): δ (ppm) 154.45 (Ar-*C*), 141.40 (Ar-*C*), 136.07 (Ar-*C*), 132.54 (Ar-*C*), 129.51 (Ar-*C*), 128.62 (Ar-*C*), 127.95 (br, B-*C*), 127.92 (Ar-*C*), 124.21 (Ar-*C*), 115.47 (Ar-*C*), 35.07 ($C(CH_3)_3$), 34.67 ($C(CH_3)_3$), 31.81 ($C(CH_3)_3$), 29.30 ($C(CH_3)_3$).

$^{11}B\{^{1}H\}$ NMR (128 MHz, C_6D_6): δ (ppm) 14.7.



4.5

Scheme 6.20: Synthesis of **4.5**.

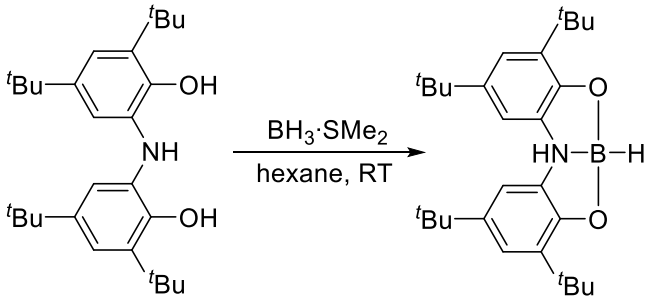
6.4.6 Synthesis of [O(H)N(H)O]B(pin) (**4.5**)

In an ampoule, neat HBpin (34 μL, 0.23 mmol) was added to a hexane solution (5 mL) of [H_3(ONO)] (100 mg, 0.23 mmol) using a microsyringe. This resulted in visible gas formation. After standing at room temperature overnight, colourless crystals of the product formed. The solution was then filtered affording **4.5** as white solid (88 mg, 0.16 mmol, 68%). Elemental analysis calculated for $C_{34}H_{54}BNO_4$: C, 74.03%; H, 9.87%; N, 2.54%; found: C, 73.97%, H, 10.01%, N, 2.60%.

^{1}H NMR (400 MHz, C_6D_6): δ (ppm) 7.45 – 7.35 (br, 1H; Ar-*H*), 7.12 (br, 1H; Ar-*H*), 6.69 (br, 1H; Ar-*H*), 6.66 – 6.58 (br, 1H; Ar-*H*), 4.72 (s, 1H; N*H*), 1.67 (s, 9H; $C(CH_3)_3$), 1.63 (s, 9H; $C(CH_3)_3$), 1.33 (s, 9H; $C(CH_3)_3$), 1.10 (s, 9H; $C(CH_3)_3$), 1.02 (s, 12H, Bpin-CH_3).

$^{13}C\{^{1}H\}$ NMR (101 MHz, C_6D_6): δ (ppm) 148.63 (Ar-*C*), 146.17 (Ar-*C*), 142.17 (Ar-*C*), 141.97 (Ar-*C*), 139.09 (Ar-*C*), 137.31 (Ar-*C*), 136.00 (Ar-*C*), 128.63 (Ar-*C*), 121.03 (Ar-*C*), 120.75 (Ar-*C*), 116.60 (Ar-*C*), 113.26 (Ar-*C*), 84.10 (O*C*H(CH_3)$_2$), 35.43 (*C*(CH_3)$_3$), 35.22 (*C*(CH_3)$_3$), 34.68 (*C*(CH_3)$_3$), 34.56 (*C*(CH_3)$_3$), 31.94 (C(*C*H_3)$_3$), 31.48 (C(*C*H_3)$_3$), 30.60 (C(*C*H_3)$_3$), 29.94 (C(*C*H_3)$_3$), 24.44 (OCH(*C*H_3)$_2$).

$^{11}B\{^{1}H\}$ NMR (128 MHz, C_6D_6): δ (ppm) 23.0.



4.6

Scheme 6.21: Synthesis of **4.6**.

6.4.7 Synthesis of [ON(H)O]BH (**4.6**)

To a hexane solution (10 mL) of [H_3(ONO)] (1.00 g, 2.35 mmol) in an ampoule fitted with a J. Young tap, was added neat BH_3·SMe_2 (223 μL, 2.35 mmol), and the mixture stirred at room temperature overnight, forming white precipitate. The filtrate was removed with a filter cannula and the residue was washed with pentane (5 mL) yielding **4.6** as a white solid (800 mg, 1.84 mmol, 78%). Elemental analysis calculated for $C_{34}H_{55}BN_2O_2$: C, 77.23%; H, 9.72%; N, 3.22%; found: C, 76.97%, H, 9.81%, N, 3.21%.

^{1}H NMR (400 MHz, C_6D_6): δ (ppm) 7.29 (d, $^{4}J_{H–H}$ = 2.1 Hz, 2H; Ar-*H*), 6.88 (d, $^{4}J_{H–H}$ = 2.1 Hz, 2H; Ar-*H*), 5.41 (s, 1H; N*H*), 1.52 (s, 18H; C(CH_3)$_3$), 1.25 (s, 18H; C(CH_3)$_3$).

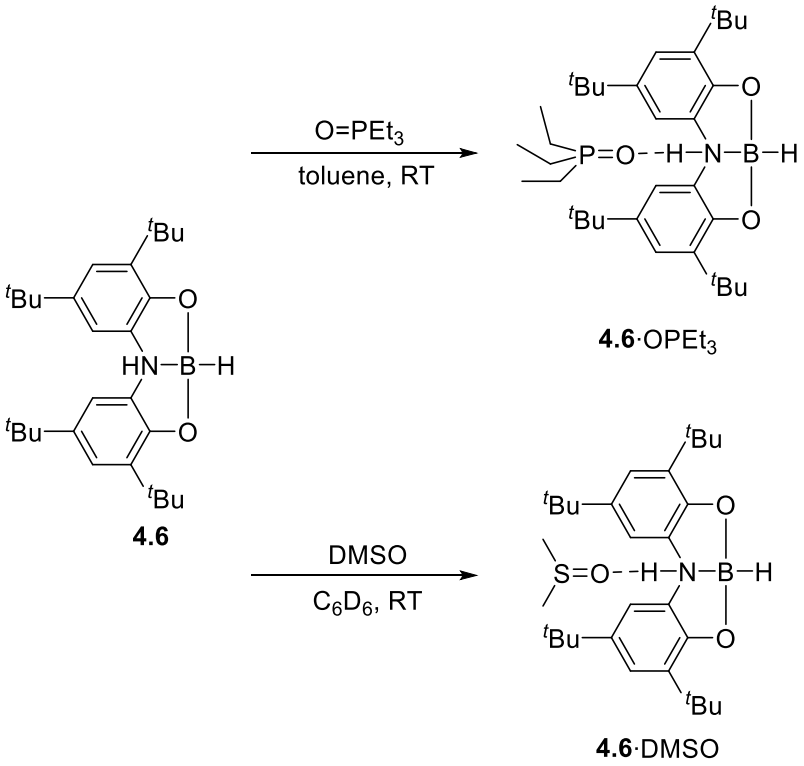
$^{11}B\{^{1}H\}$ NMR (128 MHz, C_6D_6): δ (ppm) 11.8.

Note: the **4.6** is poorly soluble in C_6D_6, so no ^{13}C NMR spectrum was acquired.

Or in $CDCl_3$:

^1H NMR (500 MHz, $CDCl_3$): δ (ppm) 7.29 (d, $^4J_{H–H}$ = 2.1 Hz, 2H; Ar-*H*), 7.21 (d, $^4J_{H–H}$ = 2.2 Hz, 2H; Ar-*H*), 6.70 (s, 1H; N*H*), 1.39 (s, 18H; C(C*H*$_3$)$_3$), 1.30 (s, 18H; C(C*H*$_3$)$_3$).

$^{13}C\{^1H\}$ NMR (126 MHz, $CDCl_3$): δ (ppm) 153.71 (Ar-*C*), 141.31 (Ar-*C*), 136.16 (Ar-*C*), 129.34 (Ar-*C*), 124.24 (Ar-*C*), 115.12 (Ar-*C*), 34.95 (*C*(CH$_3$)$_3$), 34.65 (*C*(CH$_3$)$_3$), 31.80 (C(*C*H$_3$)$_3$), 29.18 (C(*C*H$_3$)$_3$).



Scheme 6.22: Synthesis of **4.6**·OPEt$_3$ and **4.6**·DMSO.

6.4.8 Synthesis of [ON(H)O]BH·OPEt$_3$ (**4.6**·OPEt$_3$)

Toluene (6 mL) was added to a gas-tight ampoule containing **4.6** (200 mg, 0.46 mmol) and triethylphosphine oxide (62 mg, 0.46 mmol). The resulting solution was stirred at

room temperature for 2 hours. All volatiles were removed under vacuum, and the crude product was extracted with hexane. Recrystallisation from the hexane solution resulted in the isolation of **4.6**·$OPEt_3$ (100 mg, 0.18 mmol, 38%) as white solid. Elemental analysis calculated for $C_{34}H_{57}BNO_3P$: C, 71.69%; H, 10.09%; N, 2.46%; found: C, 71.15%, H, 10.02%, N, 2.54%.

^{1}H NMR (400 MHz, C_6D_6): δ (ppm) 11.62 (s, 1H; N*H*), 7.58 (d, $^4J_{H–H}$ = 2.2 Hz, 2H; Ar-*H*), 7.32 (d, $^4J_{H–H}$ = 2.2 Hz, 2H; Ar-*H*), 5.59 − 4.43 (br, 1H; B*H*), 1.59 (s, 18H; C(C*H*$_3$)$_3$), 1.28 (s, 18H; C(C*H*$_3$)$_3$), 0.99 (m, 6H; PC*H*$_2$CH$_3$), 0.64 (m, 9H; PCH$_2$C*H*$_3$).

^{13}C{^{1}H} NMR (101 MHz, C_6D_6): δ (ppm) 154.69 (Ar-*C*), 140.57 (Ar-*C*), 135.49 (Ar-*C*), 132.52 (Ar-*C*), 123.04 (Ar-*C*), 116.01 (Ar-*C*), 35.08 (*C*(CH$_3$)$_3$), 34.56 (*C*(CH$_3$)$_3$), 31.89 (C(*C*H$_3$)$_3$), 29.48 (C(*C*H$_3$)$_3$), 19.34 (d, $^1J_{P–C}$ = 66.1 Hz; OP(*C*H$_2$CH$_3$)$_3$), 5.48 (d, $^2J_{P–C}$ = 4.9 Hz; OP(CH$_2$*C*H$_3$)$_3$).

^{11}B{^{1}H} NMR (128 MHz, C_6D_6): δ (ppm) 10.9.

^{31}P{^{1}H} NMR (162 MHz, C_6D_6): δ (ppm) 52.7 (O*P*Et$_3$).

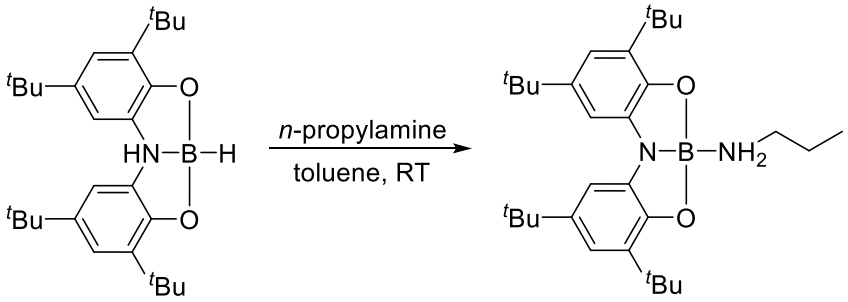
6.4.9 Synthesis of [ON(H)O]BH·DMSO (**4.6**·DMSO)

In an NMR tube fitted with a J. Young tap, DMSO (2 μL, 0.028 mmol) was added to a solution of **4.6** (12 mg, 0.028 mmol) in C_6D_6 (0.5 mL). This afforded a colourless solution after an hour. The formation of the product (**4.6**·DMSO) was confirmed by solution phase NMR spectroscopy (NMR conversion: 99%).

^{1}H NMR (400 MHz, C_6D_6): δ (ppm) 10.65 (s, 1H; N*H*), 7.57 (d, $^4J_{H–H}$ = 2.2 Hz, 2H; Ar-*H*), 7.31 (d, $^4J_{H–H}$ = 2.2 Hz, 2H; Ar-*H*), 5.60 − 4.20 (br, 1H; B*H*), 1.77 (s, 6H; S(C*H*$_3$)$_2$), 1.56 (s, 18H; C(C*H*$_3$)$_3$), 1.25 (s, 18H; C(C*H*$_3$)$_3$).

$^{13}C\{^{1}H\}$ NMR (101 MHz, C_6D_6): δ (ppm) 154.55 (Ar-*C*), 140.96 (Ar-*C*), 135.64 (Ar-*C*), 131.96 (Ar-*C*), 123.32 (Ar-*C*), 116.01 (Ar-*C*), 40.69 (S(*C*H_3)$_2$), 35.07 (*C*(CH_3)$_3$), 34.57 (*C*(CH_3)$_3$), 31.84 (C(*C*H_3)$_3$), 29.44 (C(*C*H_3)$_3$).

$^{11}B\{^{1}H\}$ NMR (128 MHz, C_6D_6): δ (ppm) 11.4.



4.6 **4.7**

Scheme 6.23: Synthesis of **4.7**.

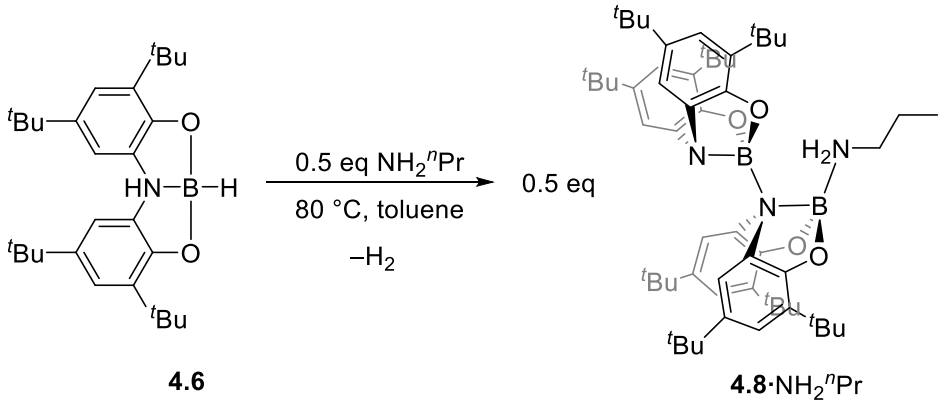
6.4.10 Synthesis of [ONO]B($NH_2{}^n$Pr) (**4.7**)

Neat *n*-propylamine (57 μL, 0.69 mmol) was added to a gas-tight ampoule containing a solution of **4.6** (200 mg, 0.46 mmol) in toluene (5 mL). After stirring for 2 hours, all volatiles were removed under vacuum. The resulting residue was washed with pentane (5 mL), affording **4.7** (120 mg, 0.24 mmol, 53%) as white solid. Dessolving **4.7** into C_6D_6 solution results into the formation of **4.8**·$NH_2{}^n$Pr and *n*-propylamine. With excess *n*-propylamine, dimerisation was not observed. This compound can also be synthesised by reaction of *n*-propylamine with **4.8**·$NH_2{}^n$Pr.

^{1}H NMR (400 MHz, C_6D_6): δ (ppm) 7.62 (d, $^{4}J_{H–H}$ = 2.1 Hz, 2H; Ar-*H*), 7.16 (d, $^{4}J_{H–H}$ = 2.1 Hz, 2H), 4.28 (br, 2H; N*H*$_2$CH$_2$CH$_2$CH$_3$), 2.39 (br, 2H; NC*H*$_2$CH$_2$CH$_3$), 1.65 (s, 18H; C(C*H*$_3$)$_3$), 1.46 (s, 18H; C(C*H*$_3$)$_3$), 0.87 – 0.79 (m, 2H; NCH$_2$C*H*$_2$CH$_3$), 0.32 (t, $^{3}J_{H–H}$ = 7.4 Hz, 3H; NCH$_2$CH$_2$C*H*$_3$).

$^{13}C\{^{1}H\}$ NMR (101 MHz, C_6D_6): δ (ppm) 151.09 (Ar-*C*), 143.10 (Ar-*C*), 141.79 (Ar-*C*), 131.74 (Ar-*C*), 115.78 (Ar-*C*), 111.78 (Ar-*C*), 41.85 (N*C*$H_2CH_2CH_3$), 34.79 (*C*$(CH_3)_3$), 34.76 (*C*$(CH_3)_3$), 32.26 (*C*$(CH_3)_3$), 30.01 (C(*C*$H_3)_3$), 22.26 (NCH_2*C*H_2CH_3), 11.39 (NCH_2CH_2*C*H_3).

$^{11}B\{^{1}H\}$ NMR (128 MHz, C_6D_6): δ (ppm) 14.2.



4.6 **4.8**·$NH_2{}^n$Pr

Scheme 6.24: Synthesis of **4.8**·$NH_2{}^n$Pr.

6.4.11 Synthesis of [ONO]B[ONO]B·($NH_2{}^n$Pr) (**4.8**·$NH_2{}^n$Pr)

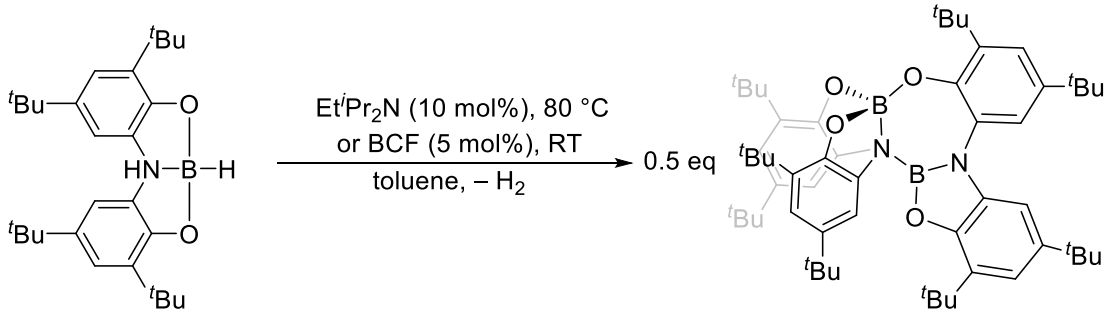
Neat *n*-propylamine (19 μL, 0.23 mmol) was added to a gas-tight ampoule containing **4.6** (200 mg, 0.46 mmol) in toluene (5 mL). After heating at 80 °C overnight, the solution was cooled to room temperature, leading to growth of colourless crystals. These were filtered, dried and washed with pentane (5 mL), yielding **4.8**·$NH_2{}^n$Pr (25 mg, 0.027 mmol, 12%) as a white solid. Elemental analysis calculated for $C_{59}H_{89}B_2N_3O_4$: C, 76.53%; H, 9.69%; N, 4.54%; found: C, 76.32%, H, 9.86%, N, 4.45%.

^{1}H NMR (400 MHz, $CDCl_3$): δ (ppm) 7.60 (d, $^{4}J_{H–H}$ = 2.1 Hz, 2H; Ar-*H*), 7.31 (d, $^{4}J_{H–H}$ = 2.1 Hz, 2H; Ar-*H*), 6.92 (d, $^{4}J_{H–H}$ = 2.1 Hz, 2H; Ar-*H*), 6.62 (d, $^{4}J_{H–H}$ = 2.1 Hz, 2H; Ar-*H*), 5.66 (s, 2H; N*H*$_2CH_2CH_2CH_3$), 3.65 – 3.47 (m, 2H; NH_2C*H*$_2CH_2CH_3$), 1.96 (h,

$^{3}J_{H–H}$ = 7.2 Hz, 2H; $NH_2CH_2CH_2CH_3$), 1.34 (s, 18H; $C(CH_3)_3$), 1.32 (s, 18H; $C(CH_3)_3$), 1.23 – 1.19 (m, 3H; $NH_2CH_2CH_2CH_3$), 1.02 (s, 18H; $C(CH_3)_3$), 0.96 (s, 18H; $C(CH_3)_3$).

$^{13}C\{^{1}H\}$ NMR (101 MHz, $CDCl_3$): δ (ppm) 151.30 (Ar-*C*), 150.15 (Ar-*C*), 142.58 (Ar-*C*), 142.47 (Ar-*C*), 141.66 (Ar-*C*), 135.00 (Ar-*C*), 133.34 (Ar-*C*), 130.82 (Ar-*C*), 121.61 (Ar-*C*), 116.22 (Ar-*C*), 115.32 (Ar-*C*), 111.33 (Ar-*C*), 43.69 ($NCH_2CH_2CH_3$), 34.53-34.62 (two overlapped $C(CH_3)_3$), 34.45 ($C(CH_3)_3$), 34.00 ($C(CH_3)_3$), 32.10 ($C(CH_3)_3$), 31.48 ($C(CH_3)_3$), 29.76 ($C(CH_3)_3$), 29.55 ($C(CH_3)_3$), 22.91 ($NCH_2CH_2CH_3$), 11.09 ($NCH_2CH_2CH_3$).

$^{11}B\{^{1}H\}$ NMR (128 MHz, $CDCl_3$): δ (ppm) 15.9, 12.6.



4.6 **4.9**

Scheme 6.25: Synthesis of **4.9**.

6.4.12 Preparation of $[B(ONO)]_2$ (**4.9**)

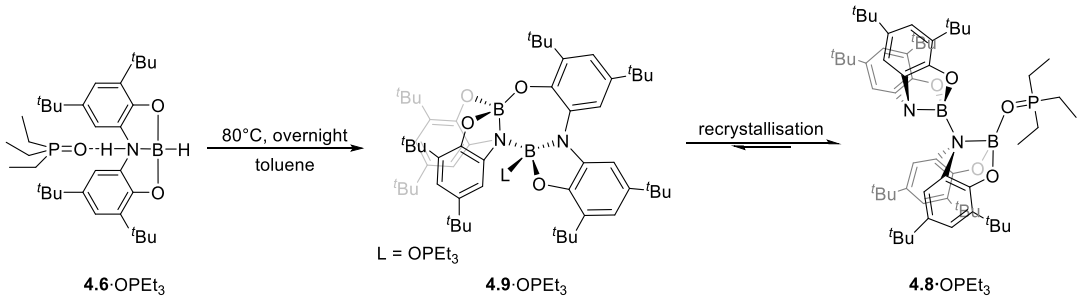
Toluene (6 mL) was added to a gas-tight ampoule containing **4.6** (200 mg, 0.46 mmol) and *N*,*N*-diisopropylethylamine (8 µL, 0.046 mmol). After heating at 80 °C for 4 hours, all volatiles were removed *in vacuo*, and the crude product was extracted with hexane and filtered. Recrystallisation from the filtrate afforded **4.9** as colourless crystals (126 mg, 0.145 mmol, 63%). The reaction of **4.6** with BCF (5 mol%) in toluene at room temperature also afford **4.9** as the product (NMR conversion: 99%). Elemental analysis

calculated for $C_{36}H_{49}BN_2O_5 \cdot C_5H_{12}$: C, 78.02%; H, 9.88%; N, 2.98%; found: C, 77.90%, H, 9.84%, N, 3.01%.

^{1}H NMR (400 MHz, C_6D_6): δ (ppm) 8.44 (br, 1H; Ar-*H*), 7.74 (br, 1H; Ar-*H*), 7.51 (d, $^4J_{H–H}$ = 2.4 Hz, 1H; Ar-*H*), 7.49 (br, 1H; Ar-*H*), 7.37 (d, $^4J_{H–H}$ = 1.9 Hz, 1H; Ar-*H*), 7.21 (d, $^4J_{H–H}$ = 1.9 Hz, 1H), 7.20 (br, 1H; Ar-*H*), 7.04 (d, $^4J_{H–H}$ = 2.4 Hz, 1H; Ar-*H*), 1.90 (s, 9H; C(C*H*$_3$)$_3$), 1.65 (s, 9H; C(C*H*$_3$)$_3$), 1.58 (s, 9H; C(C*H*$_3$)$_3$), 1.55 (s, 9H; C(C*H*$_3$)$_3$), 1.34 (s, 9H; C(C*H*$_3$)$_3$), 1.23 (s, 9H; C(C*H*$_3$)$_3$), 1.20 (s, 9H; C(C*H*$_3$)$_3$), 1.00 (s, 9H; C(C*H*$_3$)$_3$).

^{13}C{^{1}H} NMR (126 MHz, C_6D_6): δ (ppm) 153.35 (Ar-*C*), 152.59 (Ar-*C*), 146.79 (Ar-*C*), 146.03 (Ar-*C*), 144.11 (Ar-*C*), 143.79 (Ar-*C*), 143.15 (Ar-*C*), 142.63 (Ar-*C*), 141.97 (Ar-*C*), 136.74 (Ar-*C*), 136.64 (Ar-*C*), 135.90 (Ar-*C*), 134.93 (Ar-*C*), 133.29 (Ar-*C*), 133.19 (Ar-*C*), 129.36 (Ar-*C*), 123.98 (Ar-*C*), 123.93 (Ar-*C*), 121.59 (Ar-*C*), 118.76 (Ar-*C*), 117.83 (Ar-*C*), 116.13 (Ar-*C*), 116.04 (Ar-*C*), 108.37 (Ar-*C*), 36.09 (*C*(CH$_3$)$_3$), 35.28 (*C*(CH$_3$)$_3$), 35.17 (*C*(CH$_3$)$_3$), 35.05 (*C*(CH$_3$)$_3$), 34.74 (*C*(CH$_3$)$_3$), 34.67 (*C*(CH$_3$)$_3$), 34.51 (*C*(CH$_3$)$_3$), 34.45 (*C*(CH$_3$)$_3$), 32.12 (C(*C*H$_3$)$_3$), 31.93 (C(*C*H$_3$)$_3$), 31.64 (C(*C*H$_3$)$_3$), 31.37 (C(*C*H$_3$)$_3$), 30.99 (C(*C*H$_3$)$_3$), 30.12 (C(*C*H$_3$)$_3$), 29.39 (C(*C*H$_3$)$_3$), 28.93 (C(*C*H$_3$)$_3$).

^{11}B{^{1}H} NMR (128 MHz, C_6D_6): δ (ppm) 26.0, 14.6.



4.6·OPEt$_3$ **4.9**·OPEt$_3$ **4.8**·OPEt$_3$

Scheme 6.26: Synthesis of **4.8**·OPEt$_3$ and **4.9**·OPEt$_3$.

6.4.13 Synthesis of **4.8**·$OPEt_3$ and **4.9**·$OPEt_3$

A toluene solution (6 mL) of **4.6**·$OPEt_3$ (100 mg, 0.38 mmol) was heated at 80 ℃ in an oil bath for 4 hours, resulting into the formation of **4.9**·$OPEt_3$ (confirmed by NMR spectroscopy). Subsequent recrystallisation from toluene afford **4.8**·$OPEt_3$ as white solid (42 mg, 0.042 mmol, 22%). The NMR of **4.9**·$OPEt_3$ could be acquired by heating **4.6**·$OPEt_3$ in C_6D_6 at 80 ℃, or from the reaction of stoichiometric amounts of **4.8** and $OPEt_3$.

4.8·$OPEt_3$

The solubility of **4.8**·$OPEt_3$ is very low in common commerically available deuterated solvents, and therefore no high resolution ^1H and ^{13}C NMR spectra could be acquired. Elemental analysis calculated for $C_{62}H_{95}B_2N_2O_5P$: C, 74.39%; H, 9.57%; N, 2.80%; found: C, 74.48%, H, 9.62%, N, 2.85%.

$^{31}P\{^1H\}$ NMR (162 MHz, $CDCl_3$): δ (ppm) 80.0 (O*P*Et_3).

$^{11}B\{^1H\}$ NMR (128 MHz, $CDCl_3$): δ (ppm) 16.3, 13.1.

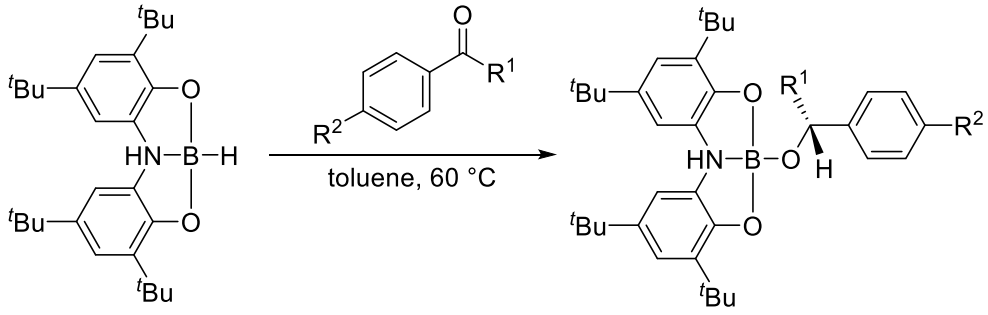
4.9·$OPEt_3$:

^1H NMR (400 MHz, C_6D_6): δ (ppm) 8.16 (d, $^4J_{H–H}$ = 2.1 Hz, 1H; Ar-*H*), 7.72 (d, $^4J_{H–H}$ = 2.1 Hz, 1H; Ar-*H*), 7.67 (d, $^4J_{H–H}$ = 2.3 Hz, 1H; Ar-*H*), 7.46 (d, $^4J_{H–H}$ = 2.0 Hz, 1H; Ar-*H*), 7.28 (d, $^4J_{H–H}$ = 2.1 Hz, 1H; Ar-*H*), 7.22 (d, $^4J_{H–H}$ = 2.3 Hz, 1H; Ar-*H*), 7.06 (d, $^4J_{H–H}$ = 2.1 Hz, 1H; Ar-*H*), 6.98 (d, $^4J_{H–H}$ = 2.0 Hz, 1H; Ar-*H*), 1.98 (s, 9H; C(C*H*$_3$)$_3$), 1.89 (s, 9H; C(C*H*$_3$)$_3$), 1.61 (s, 9H; C(C*H*$_3$)$_3$), 1.48 (s, 9H; C(C*H*$_3$)$_3$), 1.40 (s, 9H; C(C*H*$_3$)$_3$), 1.37 (s, 9H; C(C*H*$_3$)$_3$), 1.32 (s, 9H; C(C*H*$_3$)$_3$), 1.21 – 1.14 (m, 6H, PC*H*$_2$CH$_3$), 1.13 (s, 9H; C(C*H*$_3$)$_3$), 0.47 – 0.38 (m, 9H, OCH$_2$C*H*$_3$).

$^{13}C\{^{1}H\}$ NMR (126 MHz, C_6D_6): δ (ppm) 154.03 (Ar-*C*), 153.51 (Ar-*C*), 147.75 (Ar-*C*), 144.23 (Ar-*C*), 142.43 (Ar-*C*), 141.43 (Ar-*C*), 141.12 (Ar-*C*), 140.21 (Ar-*C*), 140.06 (Ar-*C*), 139.06 (Ar-*C*), 137.80 (Ar-*C*), 135.54 (Ar-*C*), 135.32 (Ar-*C*), 133.81 (Ar-*C*), 133.46 (Ar-*C*), 130.29 (Ar-*C*), 121.65 (Ar-*C*), 121.05 (Ar-*C*), 117.71 (Ar-*C*), 117.54 (Ar-*C*), 115.78 (Ar-*C*), 113.53 (Ar-*C*), 112.57 (Ar-*C*), 107.69 (Ar-*C*), 36.08 (*C*(CH_3)$_3$), 35.06 (*C*(CH_3)$_3$), 35.00 (*C*(CH_3)$_3$), 34.88 (*C*(CH_3)$_3$), 34.85 (*C*(CH_3)$_3$), 34.81 (*C*(CH_3)$_3$), 34.76 (*C*(CH_3)$_3$), 34.67 (*C*(CH_3)$_3$), 32.34 (C(*C*H_3)$_3$), 32.21 (C(*C*H_3)$_3$), 32.06 (C(*C*H_3)$_3$), 31.98 (C(*C*H_3)$_3$), 31.43 (C(*C*H_3)$_3$), 30.98 (C(*C*H_3)$_3$), 29.70 (C(*C*H_3)$_3$), 29.40 (C(*C*H_3)$_3$), 17.19 (d, $^{1}J_{C-P}$ = 65.5 Hz; OP(*C*H_2CH$_3$)$_3$), 5.08 (d, $^{2}J_{C-P}$ = 4.7 Hz; OP(CH$_2$*C*H$_3$)$_3$).

$^{11}B\{^{1}H\}$ NMR (128 MHz, C_6D_6): δ (ppm) 13.8, 8.0.

$^{31}P\{^{1}H\}$ NMR (162 MHz, C_6D_6): δ (ppm) 73.6 (O*P*Et$_3$).



Scheme 6.27: Synthesis of **4.11** and **4.12**.

6.4.14 Synthesis of [ON(H)O]B(OCH$_2$-*p*-C$_6$H$_4$CH$_3$) (**4.11**)

In a gas-tight ampoule, **4.6** (200 mg, 0.46 mmol) was dissolved in toluene (5 mL), followed by addition of 4-methylbenzaldehyde (54 µL, 0.46 mmol). The mixture was stirred at 60 °C overnight. All volatiles were removed *in vacuo*, and the product was

extracted into hexane (8 mL) and filtered. The solution was transferred to a Schlenk tube via a filter cannula and the product was purified by crystallisation from hexane solution at room temperature, affording colourless crystals. The supernatant was decanted and the colourless crystals were subsequently dried *in vacuo* to afford **4.11** (87 mg, 0.16 mmol, 46%). Elemental analysis calculated for $C_{36}H_{50}BNO_3$: C, 77.82%; H, 9.07%; N, 2.52%; found: C, 77.78%, H, 9.06%, N, 2.61%.

^{1}H NMR (400 MHz, C_6D_6): δ (ppm) 7.43 – 7.37 (m, 2H; Ar-*H*), 7.30 (d, $^4J_{H–H}$ = 2.2 Hz, 2H; Ar-*H*), 7.02 (d, $^3J_{H–H}$ = 7.8 Hz, 2H; Ar-*H*), 6.92 (d, $^4J_{H–H}$ = 2.2 Hz, 2H; Ar-*H*), 6.37 (s, 1H; N*H*), 5.04 (s, 2H; OCH_2), 2.13 (s, 3H; ArCH_3), 1.49 (s, 18H; C(CH_3)$_3$), 1.24 (s, 18H; C(CH_3)$_3$).

^{13}C{^{1}H} NMR (126 MHz, C_6D_6): δ (ppm) 153.57 (Ar-*C*), 141.32 (Ar-*C*), 139.09 (Ar-*C*), 136.53(Ar-*C*), 136.01 (Ar-*C*), 130.61 (Ar-*C*), 129.37 (Ar-*C*), 127.25 (Ar-*C*), 123.81 (Ar-*C*), 116.15 (Ar-*C*), 65.16 (O*C*H$_2$), 35.08 (*C*(CH$_3$)$_3$), 34.57 (*C*(CH$_3$)$_3$), 31.76 (C(*C*H$_3$)$_3$), 29.37 (C(*C*H$_3$)$_3$), 21.17 (C*C*H$_3$).

^{11}B{^{1}H} NMR (128 MHz, C_6D_6): δ (ppm) 13.8.

6.4.15 Synthesis of [ON(H)O]B[OCH(CH$_3$)-*p*-C$_6$H$_4$NO$_2$] (**4.12**).

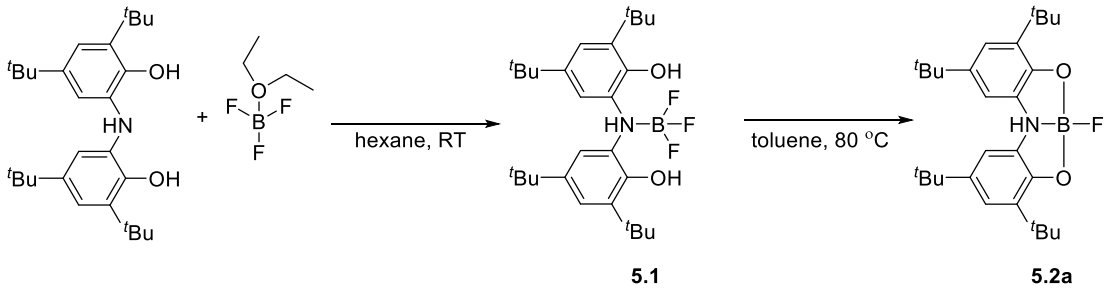
Toluene (6 mL) was added to an ampoule containing **4.6** (200 mg, 0.46 mmol) and 4'-nitroacetophenone (77 mg, 0.47 mmol), and the solution was stirred at 60 °C overnight. All volatiles were removed *in vacuo*, and the product was washed with hexane (5 mL). The resulting residue was dried *in vacuo*, affording **4.12** as an off-white powder (126 mg, 0.21 mmol, 34%). Elemental analysis calculated for $C_{36}H_{49}BN_2O_5$: C, 71.99%; H, 8.22%; N, 4.66%; found: C, 72.04%, H, 8.13%, N, 4.83%.

^{1}H NMR (400 MHz, $CDCl_3$): δ (ppm) 8.11 – 8.06 (m, 2H; Ar-*H*), 7.51 – 7.45 (m, 2H; Ar-*H*), 7.20 (m, 2H; Ar-*H*), 7.16 (d, $^{4}J_{H–H}$ = 2.1 Hz, 1H; Ar-*H*), 7.03 (d, $^{4}J_{H–H}$ = 2.1 Hz, 1H; Ar-*H*), 5.84 (s, 1H; N*H*), 5.18 (q, $^{3}J_{H–H}$ = 6.5 Hz, 1H; OC*H*), 1.52 (d, $^{3}J_{H–H}$ = 6.5 Hz, 3H), 1.41 (s, 9H; C(CH_3)$_3$), 1.35 (s, 9H; C(CH_3)$_3$), 1.27 (s, 9H; C(CH_3)$_3$), 1.25 (s, 9H; C(CH_3)$_3$).

^{13}C{^{1}H} NMR (126 MHz, $CDCl_3$): δ (ppm) 154.51 (Ar-*C*), 152.77 (Ar-*C*), 146.96 (Ar-*C*), 141.83 (Ar-*C*), 141.77 (Ar-*C*), 136.12 (Ar-*C*), 135.63 (Ar-*C*), 129.29 (Ar-*C*), 129.20 (Ar-*C*), 126.75 (Ar-*C*), 124.26 (Ar-*C*), 124.10 (Ar-*C*), 123.65 (Ar-*C*), 115.68 (Ar-*C*), 115.34 (Ar-*C*), 69.84 (O*C*HCH$_3$), 34.97 (*C*(CH$_3$)$_3$), 34.93 (*C*(CH$_3$)$_3$), 34.65 (*C*(CH$_3$)$_3$), 34.60 (*C*(CH$_3$)$_3$), 31.74 (*C*(CH$_3$)$_3$), 31.72 (*C*(CH$_3$)$_3$), 29.31 (*C*(CH$_3$)$_3$), 29.27 (*C*(CH$_3$)$_3$), 25.89 (OCH*C*H$_3$).

^{11}B{^{1}H} NMR (128 MHz, $CDCl_3$): δ (ppm) 12.9.

6.5 Experimental details for Chapter Five



Scheme 6.28: Synthesis of **5.1** and **5.2a**.

6.5.1 Synthesis of $[H_3(ONO)]\cdot BF_3$ (**5.1**)

Neat $BF_3\cdot Et_2O$ (90 μL, 0.73 mmol) was added to a hexane solution (5 mL) of $[H_3(ONO)]$ (300 mg, 0.70 mmol) in an ampoule equipped with a J. Young tap. White fumes were

immediately observed and the solution turned viscous and pale pink. After stirring overnight at room temperature, all the volatiles were removed *in vacuo* and the crude product was washed with pentane (3 × 5 mL), resulting in a white solid (218 mg, ~0.45 mol, 63%) as the product (a mixture of ~60% of **5.1** and ~40% of **5.2a**). We were unable to isolate a pure sample of **5.1** as it dehydrofluorinates in solution, and thus no ^{13}C NMR spectrum was recorded.

^{1}H NMR (400 MHz, C_6D_6): δ (ppm) 10.49 (s, 2H; O*H*), 7.92 (br, 2H; Ar-*H*), 7.32 (br, 2H; Ar-*H*), 6.93 (s, 1H; N*H*), 1.25 (s, 18H; C(C*H*$_3$)$_3$), 1.17 (s, 18H; C(C*H*$_3$)$_3$).

^{11}B{^{1}H} NMR (128 MHz, C_6D_6): δ (ppm) 0.1.

^{19}F{^{1}H} NMR (377 MHz, C_6D_6): δ (ppm) –145.79.

6.5.2 Synthesis of [ON(H)O]BF (**5.2a**)

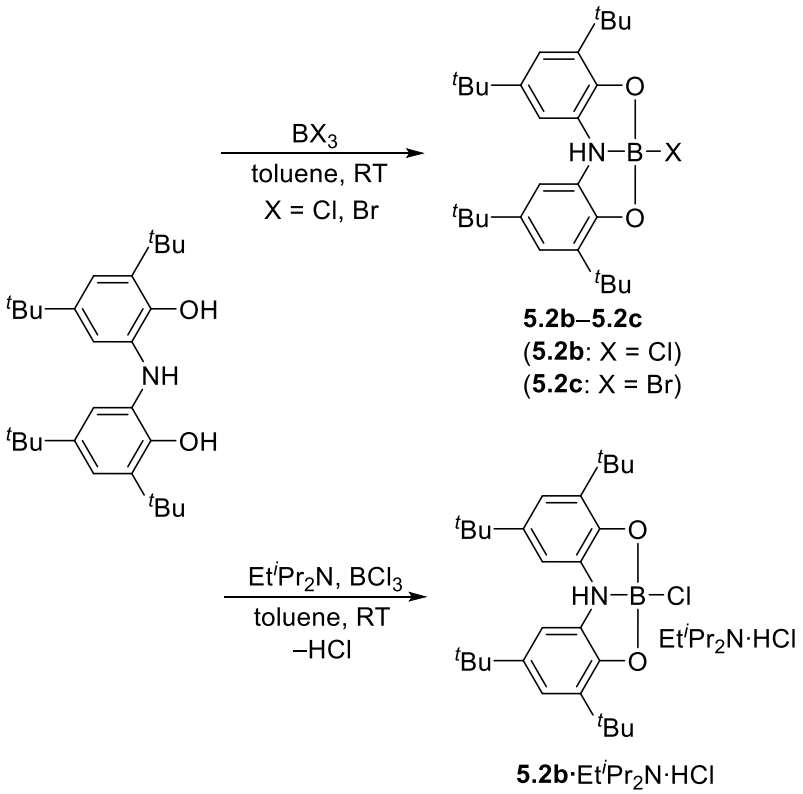
Neat $BF_3{\cdot}Et_2O$ (90 μL, 0.73 mmol) was added to a toluene solution (5 mL) of [H_3(ONO)] (300 mg, 0.70 mmol) in an ampoule fitted with a J. Young tap. White fumes were immediately observed and the solution turned a viscous pale pink. The solution was heated at 80 ℃ overnight, and all the volatiles were removed *in vacuo*. The crude product was washed with pentane (3 × 5 mL), affording a white solid (200 mg, 0.44 mol, 63%). Elemental analysis calculated for $C_{28}H_{41}BFNO_2$: C, 74.17%; H, 9.11%; N, 3.09%; found: C, 73.81%, H, 8.82%, N, 3.29%.

^{1}H NMR (400 MHz, C_6D_6): δ (ppm) 7.30 (d, $^{4}J_{H–H}$ = 2.2 Hz, 2H; Ar-*H*), 6.83 (d, $^{4}J_{H–H}$ = 2.2 Hz, 2H; Ar-*H*), 5.37 (s, 1H; N*H*), 1.47 (s, 18H; C(C*H*$_3$)$_3$), 1.23 (s, 18H; C(C*H*$_3$)$_3$).

$^{13}C\{^{1}H\}$ NMR (126 MHz, C_6D_6): δ (ppm) 153.26 (Ar-*C*), 141.76 (Ar-*C*), 136.47 (Ar-*C*), 129.83 (Ar-*C*), 124.21 (Ar-*C*), 115.86 (Ar-*C*), 35.08 (*C*$(CH_3)_3$), 34.58 (*C*$(CH_3)_3$), 31.72 (C(*C*$H_3)_3$), 29.25 (C(*C*$H_3)_3$).

$^{11}B\{^{1}H\}$ NMR (128 MHz, C_6D_6): δ (ppm) 12.2.

$^{19}F\{^{1}H\}$ NMR (377 MHz, C_6D_6): δ (ppm) –144.15.



Scheme 6.29: Synthesis of **5.2b**, **5.2c** and **5.2b**·Et^{i}Pr$_2$·HCl.

6.5.3 Synthesis of [ON(H)O]BCl (**5.2b**)

A toluene solution of BCl_3 (0.47 mL, 1.0 M, 0.47 mmol) was added to a toluene solution (5 mL) of [H_3(ONO)] (200 mg, 0.47 mmol) in an ampoule fitted with a J. Young tap. White fumes of HCl were generated immediately and the solution turned a pale-pink colour. The solution was stirred overnight at room temperature. All volatiles were

removed *in vacuo* and the product was washed with pentane (5 mL), resulting in **5.2b** as a white solid (110 mg, 0.23 mmol, 50%). Elemental analysis calculated for $C_{28}H_{41}BClNO_2$: C, 71.57%; H, 8.80%; N, 2.98%; found: C, 71.67%, H, 8.81%, N, 2.87%.

^{1}H NMR (500 MHz, C_6D_6): δ (ppm) 7.31 (d, $^{4}J_{H–H}$ = 2.1 Hz, 2H; Ar-*H*), 6.76 (d, $^{4}J_{H–H}$ = 2.1 Hz, 2H; Ar-*H*), 6.05 (s, 1H; N*H*), 1.44 (s, 18H; C(CH_3)$_3$), 1.23 (s, 18H; C(CH_3)$_3$).

^{13}C{^{1}H} NMR (126 MHz, C_6D_6): δ (ppm) 152.78 (Ar-*C*), 142.40 (Ar-*C*), 136.83 (Ar-*C*), 129.49 (Ar-*C*), 124.58 (Ar-*C*), 115.65 (Ar-*C*), 35.09 (*C*(CH$_3$)$_3$), 34.65 (*C*(CH$_3$)$_3$), 31.70 (C(*C*H$_3$)$_3$), 29.22 (C(*C*H$_3$)$_3$).

^{11}B{^{1}H} NMR (128 MHz, C_6D_6): δ (ppm) 14.7.

6.5.4 Synthesis of [ON(H)O]BBr (**5.2c**)

A hexane solution of boron tribromide (0.94 mL, 1.0 M, 0.94 mmol) was added to a hexane solution (5 mL) of [H_3(ONO)] (400 mg, 0.94 mmol) in an ampoule fitted with a J. Young tap. White fumes were generated immediately and the solution turned a pale-pink colour. After stirring overnight at room temperature, all the volatiles were removed *in vacuo*. The crude product was washed with hexane (3 × 2 mL), affording the product as pale white solid (245 mg, 0.52 mmol, 55%). Elemental analysis calculated for $C_{28}H_{41}BBrNO_2$: C, 65.38%; H, 8.03%; N, 2.72%; found: C, 65.52%, H, 8.39%, N, 2.76%.

^{1}H NMR (400 MHz, C_6D_6): δ (ppm) 7.30 (d, $^{4}J_{H–H}$ = 2.1 Hz, 2H; Ar-*H*), 6.73 (d, $^{4}J_{H–H}$ = 2.1 Hz, 2H; Ar-*H*), 6.30 (s, 1H; N*H*), 1.42 (s, 18H; C(CH_3)$_3$), 1.21 (s, 18H; C(CH_3)$_3$).

$^{13}C\{^{1}H\}$ NMR (101 MHz, C_6D_6): δ (ppm) 152.35 (Ar-*C*), 142.75 (Ar-*C*), 136.94 (Ar-*C*), 129.39 (Ar-*C*), 124.72 (Ar-*C*), 115.62 (Ar-*C*), 35.09 (*C*$(CH_3)_3$), 34.68 (*C*$(CH_3)_3$), 31.68 (C(*C*$H_3)_3$), 29.23 (C(*C*$H_3)_3$).

$^{11}B\{^{1}H\}$ NMR (128 MHz, C_6D_6): δ (ppm) 12.4.

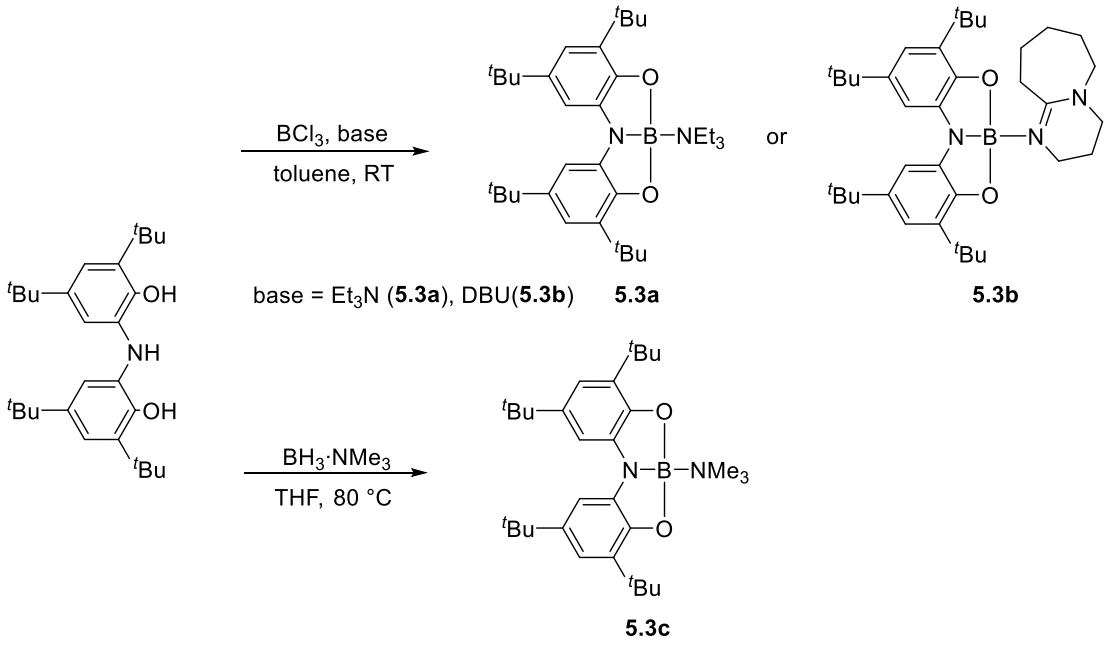
6.5.5 Synthesis of [ON(H)O]BCl·Et^{i}Pr$_2$N·HCl (**5.2b**·Et^{i}Pr$_2$N·HCl)

A toluene solution of BCl_3 (0.47 mL, 1.0 M, 0.47 mmol) was added to a toluene solution (5 mL) of [H_3(ONO)] (200 mg, 0.47 mmol) in an ampoule fitted with a J. Young tap. White fumes of HCl were generated immediately and the solution turned pale-pink. To the solution, neat Et^{i}Pr$_2$N (82 μL, 0.47 mmol) was added, and the mixture stirred overnight at room temperature. All volatiles were removed *in vacuo*, after which the product was washed with pentane (5 mL), resulting in **5.2b**·Et^{i}Pr$_2$N·HCl as a white solid (88 mg, 0.14 mmol, 29%).

^{1}H NMR (400 MHz, C_6D_6): δ (ppm) 12.17 (s, 1H; Et^{i}Pr$_2$N*H*), 11.44 (br, 1H; N*H*), 8.00 (d, $^{4}J_{H–H}$ = 2.1 Hz, 2H; Ar-*H*), 7.31 (d, $^{4}J_{H–H}$ = 2.1 Hz, 2H; Ar-*H*), 2.89 – 2.74 (m, 2H; NC*H*$(CH_3)_2$), 2.04 (m, 2H; NC*H*$_2$CH$_3$), 1.54 (s, 18H; C(C*H*$_3)_3$), 1.29 (s, 18H; C(C*H*$_3)_3$), 0.95 (t, $^{3}J_{H–H}$ = 7.4 Hz, 3H; NCH$_2$C*H*$_3$), 0.88 (d, $^{3}J_{H–H}$ = 6.7 Hz, 6H; NCH(C*H*$_3)_2$), 0.61 (d, $^{3}J_{H–H}$ = 6.7 Hz, 6H; NCH(C*H*$_3)_2$).

$^{13}C\{^{1}H\}$ NMR (126 MHz, C_6D_6): δ (ppm) 153.01 (Ar-*C*), 142.16 (Ar-*C*), 135.39 (Ar-*C*), 132.21 (Ar-*C*), 123.30 (Ar-*C*), 117.25 (Ar-*C*), 53.10 (N*C*H$(CH_3)_2$), 41.35 (N*C*H$_2$CH$_3$), 35.02 (*C*$(CH_3)_3$), 34.73 (*C*$(CH_3)_3$), 31.82 (C(*C*$H_3)_3$), 29.50 (C(*C*$H_3)_3$), 18.08 (NCH(*C*$H_3)_2$), 16.73 (NCH(*C*$H_3)_2$), 11.70 (NCH$_2$*C*H$_3$).

$^{11}B\{^{1}H\}$ NMR (128 MHz, C_6D_6): δ (ppm) 14.9.



Scheme 6.30: Synthesis of **5.3a**, **5.3b** and **5.3c**.

6.5.6 Synthesis of (ONO)BNEt$_3$ (**5.3a**)

A toluene solution of BCl_3 (470 μL, 1.0 M, 0.47 mmol) was added to a toluene solution (5 mL) of [H_3(ONO)] (200 mg, 0.47 mmol) in an ampoule fitted with a J. Young tap. White fumes of HCl were generated immediately and the solution turned pale pink. Triethylamine (200 μL, 1.43 mmol) was then added to the solution, and the mixture stirred overnight at room temperature. All volatiles were removed *in vacuo* and the product was extracted into hot hexane, followed by filtration. The volatiles were then removed under a dynamic vacuum and product was purified by crystallisation from hexane, affording **5.3a** as a white solid (108 mg, 0.20 mmol, 43%). Elemental analysis calculated for $C_{34}H_{55}BN_2O_2$: C, 76.38%; H, 10.37%; N, 5.24%; found: C, 76.34%, H, 10.36%, N, 5.23%.

^{1}H NMR (500 MHz, C_6D_6): δ (ppm) 7.63 (d, $^{4}J_{H–H}$ = 2.1 Hz, 2H; Ar-*H*), 7.16 (d, $^{4}J_{H–H}$ = 2.1 Hz, 2H; Ar-*H*), 2.57 (q, $^{3}J_{H–H}$ = 7.3 Hz, 6H; NC*H*$_2$CH$_3$), 1.60 (s, 18H; C(C*H*$_3$)$_3$), 1.43 (s, 18H; C(C*H*$_3$)$_3$), 0.78 (t, $^{3}J_{H–H}$ = 7.3 Hz, 9H; NCH$_2$C*H*$_3$).

^{13}C{^{1}H} NMR (126 MHz, C_6D_6): δ (ppm) 151.18 (Ar-*C*), 143.00 (Ar-*C*), 141.83 (Ar-*C*), 131.77 (Ar-*C*), 116.01 (Ar-*C*), 111.91 (Ar-*C*), 47.76 (N(*C*H$_2$CH$_3$)$_3$), 34.81 (*C*(CH$_3$)$_3$), 34.61 (*C*(CH$_3$)$_3$), 32.25 (C(*C*H$_3$)$_3$), 30.13 (C(*C*H$_3$)$_3$), 8.97(N(CH$_2$*C*H$_3$)$_3$).

^{11}B{^{1}H} NMR (128 MHz, C_6D_6): δ (ppm) 16.2.

6.5.7 Synthesis of (ONO)B(DBU) (**5.3b**)

A toluene solution of BCl_3 (470 μL, 1.0 M, 0.47 mmol) was added to a toluene solution (5 mL) of [H_3(ONO)] (200 mg, 0.47 mmol) in an ampoule fitted with a J. Young tap. White fumes of HCl were generated immediately and the solution turned pale-pink. 1,8-Diazabicyclo(5.4.0)undec-7-ene (DBU) (220 μL, 1.5 mmol) was then added to the solution, and the mixture was stirred overnight at room temperature. All volatiles were removed *in vacuo* and the product was washed with hexane (5 mL) and the residue dried, affording **5.3b** as a white solid (206 mg, 0.35 mmol, 75%). This compound could also be synthesised by reacting **5.2b** with 2 equivalents of DBU in a toluene solution, followed by filtration. The filtrate was then pumped down *in vacuo* and dissolved in toluene. Slow diffusion of pentane into this toluene solution afforded of **5.3b** as colourless crystals. Elemental analysis calculated for $C_{44}H_{64}BN_3O_2$: C, 77.97%; H, 9.52%; N, 6.20%; found: C, 77.84%, H, 9.46%, N, 6.36%.

^{1}H NMR (500 MHz, $CDCl_3$): δ (ppm) 7.18 (d, $^{4}J_{H–H}$ = 2.1 Hz, 2H; Ar-*H*), 6.79 (d, $^{4}J_{H–H}$ = 2.1 Hz, 2H; Ar-*H*), 3.53 (t, $^{3}J_{H–H}$ = 5.8 Hz, 2H; DBU), 3.48 – 3.41 (m, 2H; DBU),

3.28 (t, $^{3}J_{H–H}$ = 6.1 Hz, 2H; DBU), 3.23 – 3.12 (m, 2H; DBU), 1.90 – 1.72 (m, 6H; DBU), 1.65 (m, 2H; DBU), 1.37 (s, 18H; C(C*H*$_3$)$_3$), 1.32 (s, 18H; C(C*H*$_3$)$_3$).

^{13}C{^{1}H} NMR (126 MHz, $CDCl_3$): δ (ppm) 166.72 (Ar-*C*), 150.90 (Ar-*C*), 142.31 (Ar-*C*), 139.97 (Ar-*C*), 130.77 (Ar-*C*), 115.49 (Ar-*C*), 111.23 (Ar-*C*), 54.03 (DBU-*C*H$_2$), 49.31 (DBU-*C*H$_2$), 42.33 (DBU-*C*H$_2$), 34.59 (*C*(CH$_3$)$_3$), 34.43 (*C*(CH$_3$)$_3$), 32.16 (DBU-*C*H$_2$), 31.32 (DBU-*C*H$_2$), 29.80 (C(*C*H$_3$)$_3$), 29.18 (C(*C*H$_3$)$_3$), 27.04 (DBU-*C*H$_2$), 24.83 (DBU-*C*H$_2$), 21.50 (DBU-*C*H$_2$).

^{11}B{^{1}H} NMR (128 MHz, $CDCl_3$): δ (ppm) 14.6.

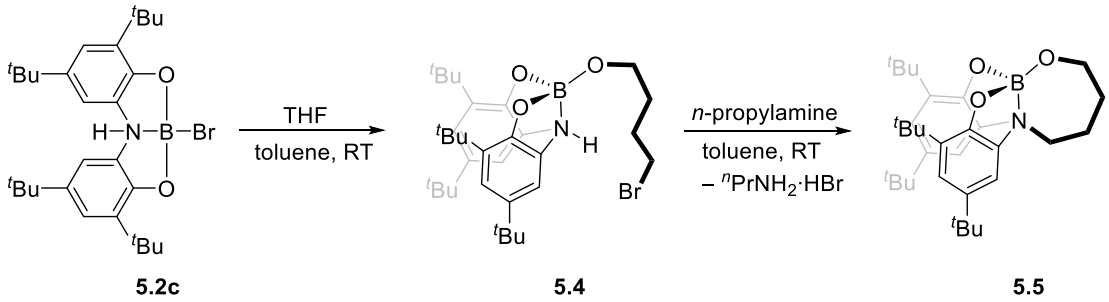
6.5.8 Sythesis of (ONO)BNMe$_3$ (**5.3c**)

Complex **5.3c** was prepared according to Dr Lo's D.Phil. thesis.[4] Elemental analysis calculated for $C_{34}H_{55}BN_2O_2$: C, 75.59%; H, 10.03%; N, 5.69%; found: C, 75.37%, H, 10.16%, N, 5.58%.

^{1}H NMR (400 MHz, C_6D_6): δ (ppm) 7.62 (d, $^{4}J_{H-H}$ = 2.1 Hz, 2H; Ar-*H*), 7.16 (d, $^{4}J_{H-H}$ = 2.1 Hz, 2H; Ar-*H*), 1.85 (s, 9H; N(C*H*$_3$)$_3$), 1.59 (s, 18H; C(C*H*$_3$)$_3$), 1.43 (s, 18H; C(C*H*$_3$)$_3$).

^{13}C{^{1}H} NMR (126 MHz, C_6D_6): δ (ppm) 151.19 (Ar-*C*), 143.18 (Ar-*C*), 142.00 (Ar-*C*), 131.97 (Ar-*C*), 115.98 (Ar-*C*), 111.74 (Ar-*C*), 45.11 (N*C*H$_3$), 34.80 (*C*(CH$_3$)$_3$), 34.75 (*C*(CH$_3$)$_3$), 32.24 (C(*C*H$_3$)$_3$), 30.01 (C(*C*H$_3$)$_3$).

^{11}B NMR (128 MHz, C_6D_6): δ (ppm) 15.7 (br).



Scheme 6.31: Synthesis of **5.4** and **5.5**.

6.5.9 Synthesis of [ON(H)O]BOC$_4$H$_8$Br (**5.4**)

THF (50 µL, 0.62 mmol) was added to an ampoule containing a solution of **5.2c** (200 mg, 0.39 mmol) in toluene (5 mL). This afforded a colourless solution. After stirring overnight at room temperature, all volatiles were removed *in vacuo*, the product was washed with pentane (5 mL) and the residue was dried, resulting in **5.4** as a white solid (180 mg, 0.31 mmol, 79%). Elemental analysis calculated for $C_{32}H_{49}BBrNO_3$: C, 65.54%; H, 8.42%; N, 2.39%; found: C, 66.44%, H, 8.42%, N, 2.29%.

^{1}H NMR (400 MHz, C_6D_6): δ (ppm) 7.30 (d, $^4J_{H–H}$ = 2.1 Hz, 2H; Ar-*H*), 6.97 (d, $^4J_{H–H}$ = 2.1 Hz, 2H; Ar-*H*), 5.94 (s, 1H; N*H*), 3.80 (t, $^3J_{H–H}$ = 6.2 Hz, 2H, OC*H*$_2$), 3.12 (t, $^3J_{H–H}$ = 6.7 Hz, 2H, BrC*H*$_2$), 1.95 – 1.83 (m, 2H, OCH$_2$C*H*$_2$), 1.80 – 1.70 (m, 2H, BrCH$_2$C*H*$_2$), 1.48 (s, 18H; C(C*H*$_3$)$_3$), 1.26 (s, 18H; C(C*H*$_3$)$_3$).

^{13}C{^{1}H} NMR (101 MHz, C_6D_6): δ (ppm) 153.58 (Ar-*C*), 141.29 (Ar-*C*), 136.05 (Ar-*C*), 130.42 (Ar-*C*), 123.88 (Ar-*C*), 116.18 (Ar-*C*), 62.08 (O*C*H$_2$), 35.07 (*C*(CH$_3$)$_3$), 34.60 (*C*(CH$_3$)$_3$), 34.22 (Br*C*H$_2$), 31.80 (C(*C*H$_3$)$_3$), 31.16 (OCH$_2$*C*H$_2$), 30.11 (BrCH$_2$*C*H$_2$), 29.34 (C(*C*H$_3$)$_3$).

^{11}B{^{1}H} NMR (128 MHz, C_6D_6): δ (ppm) 13.2.

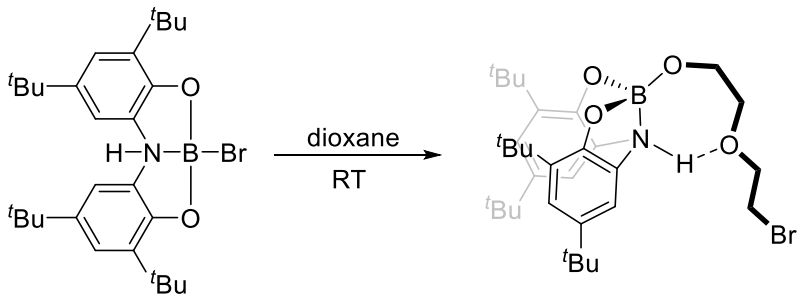
6.5.10 Synthesis of [ONO]BOC_4H_8 (**5.5**)

THF (50 μL, 0.62 mmol) was added to an ampoule containing a solution of **5.2c** (200 mg, 0.39 mmol) in toluene (5 mL). This afforded a colourless solution. After stirring overnight at room temperature, neat *n*-propylamine (50 μL, 0.61 mmol) was added, resulting in the precipitation of a white solid. The solution was filtered and the filtrate dried *in vacuo*, to yielding the crude product. After washing with pentane (5 mL), the residue was dried to afford **5.4** as a white solid (66 mg, 0.13 mmol, 34%). Elemental analysis calculated for $C_{32}H_{48}BNO_3$: C, 76.03%; H, 9.57%; N, 2.77%; found: C, 76.25%, H, 9.55%, N, 2.98%.

^{1}H NMR (400 MHz, C_6D_6): δ (ppm) 7.31 (d, $^4J_{H–H}$ = 2.1 Hz, 2H; Ar-*H*), 7.19 (d, $^4J_{H–H}$ = 2.1 Hz, 2H; Ar-*H*), 3.99 (t, $^3J_{H–H}$ = 5.1 Hz, 2H, OCH_2), 3.23 – 3.12 (m, 2H, NCH_2), 1.53 (s, 18H; C(CH_3)$_3$), 1.38 – 1.34 (m, 2H, OCH_2CH_2), 1.26 (s, 18H; C(CH_3)$_3$), 1.17 (m, 2H, NCH_2CH_2).

^{13}C{^{1}H} NMR (101 MHz, C_6D_6): δ (ppm) 153.49 (Ar-*C*), 141.47 (Ar-*C*), 136.17 (Ar-*C*), 135.52 (Ar-*C*), 123.45 (Ar-*C*), 113.94 (Ar-*C*), 63.61 (OCH_2), 59.30 (NCH_2), 35.14 (*C*$(CH_3)_3$), 34.68 (*C*$(CH_3)_3$), 32.67 (OCH_2CH_2), 31.81 (C(*C*H_3)$_3$), 29.30 (C(*C*H_3)$_3$), 24.83 (NCH_2CH_2).

^{11}B{^{1}H} NMR (128 MHz, C_6D_6): δ (ppm) 14.7.



5.2c **5.6**

Scheme 6.32: Synthesis of **5.6**.

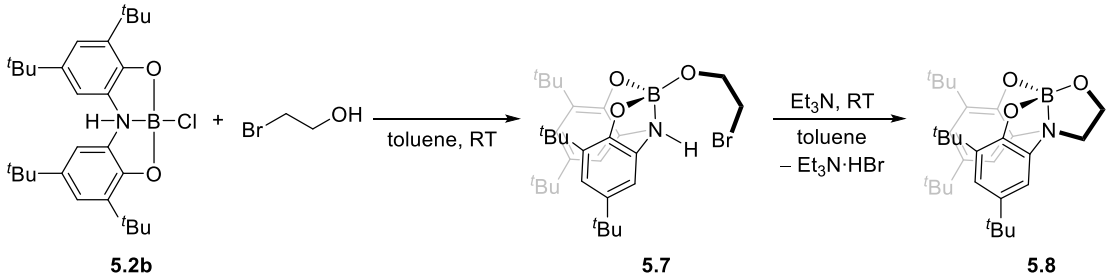
6.5.11 Synthesis of [ON(H)O]$BOC_2H_4OC_2H_4Br$ (**5.6**)

Dioxane (5 mL) was added to an ampoule containing **5.2c** (100 mg, 0.19 mmol) to afford a colourless solution. After stirring overnight at room temperature, all volatiles were removed *in vacuo* and the product was crystallised from pentane (3 mL) at room temperature. Colourless single crystals formed overnight. Further removal of the solvent through filtration and drying, resulted in the isolation of **5.6** as colourless crystals (44 mg, 0.073 mmol, 38%). Elemental analysis calculated for $C_{32}H_{49}BBrNO_4$: C, 63.80%; H, 8.20%; N, 2.32%; found: C, 63.95%, H, 8.23%, N, 2.49%.

^{1}H NMR (400 MHz, C_6D_6): δ (ppm) 8.31 (s, 1H; N*H*), 7.73 (d, $^4J_{H–H}$ = 2.2 Hz, 2H; Ar-*H*), 7.36 (d, $^4J_{H–H}$ = 2.2 Hz, 2H; Ar-*H*), 3.92 – 3.76 (m, 2H; BOCH_2), 3.02 – 2.92 (m, 2H; BrCH_2), 2.75 (m, 4H; $BOCH_2CH_2$ and $BrCH_2CH_2$), 1.56 (s, 18H; $C(CH_3)_3$), 1.30 (s, 18H; $C(CH_3)_3$).

$^{13}C\{^1H\}$ NMR (101 MHz, C_6D_6): δ (ppm) 154.37 (Ar-*C*), 141.38 (Ar-*C*), 135.93 (Ar-*C*), 131.09 (Ar-*C*), 123.58 (Ar-*C*), 116.64 (Ar-*C*), 73.29 ($BOCH_2$), 70.50 ($BOCH_2CH_2$), 61.60 ($BrCH_2CH_2$), 35.14 ($C(CH_3)_3$), 34.64 ($C(CH_3)_3$), 32.43 ($BrCH_2$), 31.84 ($C(CH_3)_3$), 29.37 ($C(CH_3)_3$).

$^{11}B\{^{1}H\}$ NMR (128 MHz, C_6D_6): δ (ppm) 13.6.



Scheme 6.33: Synthesis of **5.7** and **5.8**.

6.5.12 Synthesis of [ON(H)O]BOC_2H_4Br (**5.7**)

Neat 2-bromoethanol (30 μL, 0.43 mmol) was added to an ampoule containing a solution of **5.2b** (200 mg, 0.43 mmol) in toluene (5 mL). This afforded a colourless solution. After stirring overnight at room temperature, all volatiles were removed *in vacuo* and the product was washed with pentane (3 mL). The solvent was removed *in vacuo*, affording **5.7** as a white solid (100 mg, 0.18 mmol, 42%). Elemental analysis calculated for $C_{30}H_{45}BBrNO_3$: C, 64.53%; H, 8.12%; N, 2.51%; found: C, 64.91%, H, 8.09%, N, 2.65%.

^{1}H NMR (400 MHz, C_6D_6): δ (ppm) 7.30 (d, $^{4}J_{H–H}$ = 2.2 Hz, 2H; Ar-*H*), 7.07 (d, $^{4}J_{H–H}$ = 2.2 Hz, 2H; Ar-*H*), 6.41 (s, 1H; N*H*), 4.02 (t, $^{3}J_{H–H}$ = 6.0 Hz, 2H; BOCH_2), 3.29 (t, $^{3}J_{H–H}$ = 5.9 Hz, 2H ; BrCH_2), 1.48 (s, 18H; C(CH_3)$_3$), 1.24 (s, 18H; C(CH_3)$_3$).

$^{13}C\{^{1}H\}$ NMR (101 MHz, C_6D_6): δ (ppm) 153.05 (Ar-*C*), 141.25 (Ar-*C*), 135.71 (Ar-*C*), 130.08 (Ar-*C*), 123.62 (Ar-*C*), 115.85 (Ar-*C*), 63.50 (BO*C*H_2), 34.68 (*C*(CH$_3$)$_3$), 34.53 (Br*C*H_2), 34.24 (*C*(CH$_3$)$_3$), 31.39 (C(*C*H$_3$)$_3$), 28.95 (C(*C*H$_3$)$_3$).

$^{11}B\{^{1}H\}$ NMR (128 MHz, C_6D_6): δ (ppm) 13.2.

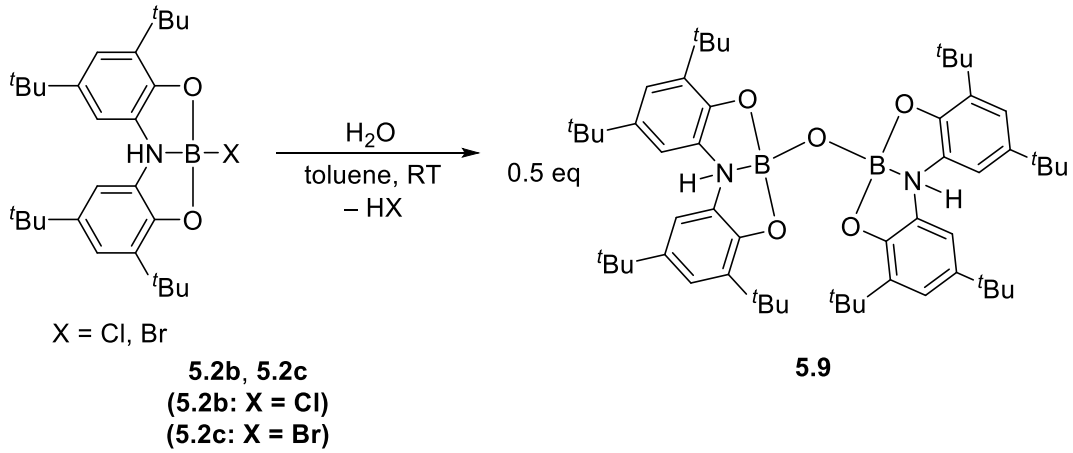
6.5.13 Synthesis of [ONO]BOC_2H_4 (**5.8**)

Triethylamine (30 μL, 0.22 mmol) was added to an ampoule containing a solution of **5.7** (100 mg, 0.18 mmol) in toluene (5 mL). This resulted in the precipitation of a white solid. After stirring overnight at room temperature, the solid product was isolated by filtration using a filter cannula. The filtrate was dried *in vacuo* and the crude product was washed with pentane (2 × 3 mL), affording **5.7** as a white solid (100 mg, 0.10 mmol, 58%). Elemental analysis calculated for $C_{30}H_{44}BNO_3$: C, 75.46%; H, 9.29%; N, 2.93%; found: C, 75.42%, H, 9.44%, N, 3.12%.

^{1}H NMR (400 MHz, C_6D_6): δ (ppm) 7.32 (d, $^4J_{H–H}$ = 2.2 Hz, 2H; Ar-*H*), 7.29 (d, $^4J_{H–H}$ = 2.2 Hz, 2H; Ar-*H*), 3.63 (t, $^3J_{H–H}$ = 5.9 Hz, 2H; OCH_2), 3.00 (t, $^3J_{H–H}$ = 5.9 Hz, 2H; NCH_2), 1.51 (s, 18H; C(CH_3)$_3$), 1.26 (s, 18H; C(CH_3)$_3$).

^{13}C{^{1}H} NMR (101 MHz, C_6D_6): δ (ppm) 155.24 (Ar-*C*), 142.09 (Ar-*C*), 136.78 (Ar-*C*), 135.87 (Ar-*C*), 124.15 (Ar-*C*), 114.98 (Ar-*C*), 64.68 (OCH_2), 62.74 (NCH_2), 35.20 (*C*(CH_3)$_3$), 34.66 (*C*(CH_3)$_3$), 31.79 (C(*C*H_3)$_3$), 29.29 (C(*C*H_3)$_3$).

^{11}B{^{1}H} NMR (128 MHz, C_6D_6): δ (ppm) 18.2.



Scheme 6.34: Synthesis of **5.9**.

6.5.14 Synthesis of {[ON(H)O]B}$_2$O (**5.9**)

The synthesis of complex **5.9** was previously described by Dr Siu-Kwan Lo.[4] Elemental analysis calculated for $C_{56}H_{82}B_2N_2O_5$: C, 76.01%; H, 9.34%; N, 3.17%; found: C, 75.98%, H, 9.53%, N, 3.19%.

^{1}H NMR (400 MHz, C_6D_6): δ (ppm) 7.22 (d, $^4J_{H–H}$ = 2.2 Hz, 4H; Ar-*H*), 6.96 (d, $^4J_{H–H}$ = 2.2 Hz, 24H; Ar-*H*), 6.09 (s, 2H; N*H*), 1.36 (s, 36H; C(C*H*$_3$)$_3$), 1.29 (s, 36H; C(C*H*$_3$)$_3$).

^{13}C{^{1}H} NMR (101 MHz, C_6D_6): δ (ppm) 154.03 (Ar-*C*), 140.69 (Ar-*C*), 135.43 (Ar-*C*), 131.04 (Ar-*C*), 123.62 (Ar-*C*), 116.39 (Ar-*C*), 34.94 (*C*(CH$_3$)$_3$), 34.54 (*C*(CH$_3$)$_3$), 31.84 (C(*C*H$_3$)$_3$), 29.28 (C(*C*H$_3$)$_3$).

^{11}B{^{1}H} NMR (128 MHz, C_6D_6): δ (ppm) 12.3.

6.6 References

[1] P. Chaudhuri, M. Hess, T. Weyhermüller, K. Wieghardt, *Angew. Chem., Int. Ed.* **1999**, *38*, 1095–1098.

[2] D. Heift, Z. Benkő, H. Grützmacher, *Dalton Trans.* **2014**, *43*, 831–840.

[3] C. D. Smith, *Synthesis and Reactivity of Geometrically Constrained Gallium(III) Complexes*, Thesis (M.Chem) − University of Oxford, (Department of Chemistry), Oxford, **2017**.

[4] S.-K. Lo, *Geometry Constrained Main-Group Compounds for the Activation of Small Molecules*, Thesis (D.Phil.) − University of Oxford, 2018, (Department of Inorganic Chemistry), Oxford, **2018**.

[5] G. R. Fulmer, A. J. M. Miller, N. H. Sherden, H. E. Gottlieb, A. Nudelman, B. M. Stoltz, J. E. Bercaw, K. I. Goldberg, *Organometallics* **2010**, *29*, 2176–2179.

[6] Y. Yang, M. D. Anker, J. Fang, M. F. Mahon, L. Maron, C. Weetman, M. S. Hill, *Chem. Sci.* **2017**, *8*, 3529–3537.

[7] R. K. Sahoo, N. Sarkar, S. Nembenna, *Angew. Chem., Int. Ed.* **2021**, *60*, 11991–12000.

Chapter Seven

Conclusions and perspective

7.1 Conclusions and perspective

In this thesis, we have discussed the application of the $[ON(H)O]^{2-}$ and $[ONO]^{3-}$ ligand for the synthesis of complexes of the group 13 elements, such as gallium and boron, and the use of such compounds in small molecule activation reactions. We have found that gallium hydrides **2.7** and **2.9** can hydrogallate aldehydes and ketones at room temperature to give gallium alkoxides **2.8**, **2.11** and **2.12**. The gallium alkoxide complex **2.8a** can act as an efficient catalyst for the hydroboration of substrates containing unsaturated C=O and C=N bonds. In general, this catalytic system is efficient. It is also a rare example of a gallium catalyst that can facilitate the hydroboration of carbon dioxide, imines and isocyanates at room temperature.

However, the transelementation of this gallium catalyst with boranes was observed when we attempted to use the catalyst for the hydroboration of alkenes and alkynes at elevated temperatures. To the best of our knowledge, there are no reported examples of gallium catalysts that are active in the hydroboration of unsaturated C=C or C≡C bonds. In order to do so, a more stable gallium complex needs to be developed to eliminate the possibility of transelementation reactions. Although we have carried out a mechanistic study of the **2.8a** catalysed hydroboration of aldehydes and ketones, the mechanisms for the hydroboration of carbon dioxide, imines, isocyanates have not been well explored. Understanding the mechanism for the catalytic hydroboration of these substrates is crucial, and more research needs to be carried out in this regard. Our research mainly focused on catalytic hydroboration, but for industrial use, hydrosilylation and hydrogenation are more economically attractive, so these processes are worth investigating in the future. Complexes **2.5** and **2.6** both have a fully deprotonated ligand backbone $[ONO^{cat}]^{3-}$, and hence they could potentially be used in

the cooperative activation of small molecules, such as dihydrogen, alcohols, amines, through heterolytic cleavage of the H−E (E = H, O, N) bonds. Complex **2.5** is geometrically unconstrained, while **2.6** is constrained, so they exhibit different reactivity, and the comparison of their similarities and differences is of interest Complex **2.5** is sparingly soluble in most organic solvents, so the modification of the coordinated pyridine moiety to a more lipophilic base will increase its solubility in organic solvents and make it easier to study this complex spectroscopically.

Ga−B transelementation was observed for gallium complexes on reaction with boranes in Chapter Four, however the reactions often afford multiple products, which are difficult to isolate. To fully characterise these products, we sought to synthesise them directly by reacting [H_3(ONO)] with boranes (e.g. BCF, BPh_3, HBpin, $BH_3{\cdot}SMe_2$), which afforded compounds **4.1**−**4.6**. Complexes **4.1** and **4.3** are found to undergo dehydroarylation (loss of H−R, R = C_6F_5, Ph) upon the addition of a base, and they may be used to hydroarylate substrates containing unsaturated bonds under certain conditions (e.g. in the presence of a catalyst). In principle, other boron complexes with the same general formula, [ON(H)O]BR, can be synthesised using a similar synthetic approach. It would be interesting to see if these species can be used in transfer hydroarylation reactions. Complex **4.6** has a hydridic B−H and an acidic N−H in the same molecule, and we have shown that it can dehydrogenate in the presence of acids or bases catalytically. The limitation of **4.6** as a potential energy source is that it has a low gravimetric density of dihydrogen (0.0046 kg H_2 per kg of **4.6**), however this might be overcome by modifying the ligand (i.e. changing the *tert*-butyls on the ligand backbone to methyl groups). We have also synthesised two novel Lewis acids, **4.8** and **4.9**, which are shown to have average and strong Lewis acidities, respectively, according to Gutmann–Beckett test. The modification of the $[ONO^{cat}]^{3-}$ ligand of **4.8**

and **4.9** from electron-donating *tert*-butyl groups to electron-withdrawing groups (such as $-NO_2$, $-Cl$, $-F$) is likely to give stronger Lewis acids.

In Chapter Five, the borylation of ethers (e.g. Et_2O, THF and dioxane) by **5.2c** through C−O bond cleavage was discussed. In the presence of a base, borate esters **5.4** and **5.7** can dehydrobrominate to give expanded (n+2)-membered (n = carbon atoms of the ether substrates) oxaborinanes **5.5** and **5.8**. These stepwise reactions feature a C−O bond insertion into cyclic ethers to give ring expanded products with an N−B−O moiety. These are conceptually similar to those proposed by Dong in 2021, albeit the latter needed a catalyst Ni(4-^{t}Bu-py)$_2$Br$_2$ at 60 °C.[1] This ring-expansion strategy is applicable to ring expansion of other cyclic ethers, and the reactivity of **5.2c** towards other cyclic systems containing C−X (X = S, N) bonds may also be worth exploring in the future.

7.2 References

[1] H. Lyu, I. Kevlishvili, X. Yu, P. Liu, G. Dong, *Science* **2021**, *372*, 175–182.

Appendix

Single crystal X-ray diffraction data

Identification code	**2.1**	**2.2**	**2.4**	**2.5**
Empirical formula	$C_{33}H_{46}ClGaN_2O_2$	$C_{31}H_{50}N_2O_2ClGa$	$C_{118.5}H_{160}N_5O_7Ga_3$	$C_{66}H_{90}Ga_2N_4O_4$
Formula weight	607.89	587.90	1975.67	1142.85
Temperature/K	150(2)	150(2)	150(2)	150(2)
Crystal system	monoclinic	orthorhombic	monoclinic	monoclinic
Space group	$P2_1/n$	$Pna2_1$	$C2/c$	$P2_1/c$
a/Å	10.3849(2)	20.8093(3)	37.1049(3)	14.1499(3)
b/Å	11.3817(2)	14.0715(2)	14.58360(10)	14.3165(2)
c/Å	27.6271(5)	10.82310(10)	41.7536(3)	17.0825(3)
α/°	90	90	90	90
β/°	100.686(2)	90	99.2530(10)	114.464(2)
γ/°	90	90	90	90
Volume/Å^3	3208.83(10)	3169.20(7)	22299.8(3)	3149.84(11)
Z	4	4	8	2
ρ_{calc}g/cm^3	1.258	1.232	1.177	1.205
μ/mm^{-1}	2.167	2.171	1.267	1.415
F(000)	1288.0	1256.0	8440.0	1216.0
Radiation	Cu Kα (λ = 1.54184)	Cu Kα (λ = 1.54184)	Cu Kα (λ = 1.54184)	Cu Kα (λ = 1.54184)
2θ range for data collection/°	6.512 to 132.966	7.584 to 154.55	5.92 to 152.974	8.396 to 152.282
Index ranges	$-12 \le h \le 12$, $-11 \le k \le 13$, $-32 \le l \le 16$	$-26 \le h \le 26$, $-17 \le k \le 17$, $-13 \le l \le 13$	$-40 \le h \le 46$, $-18 \le k \le 18$, $-51 \le l \le 52$	$-15 \le h \le 17$, $-12 \le k \le 17$, $-21 \le l \le 20$
Reflections collected	11938	54463	114828	22659
Independent reflections	5433 [R_{int} = 0.0260, R_{sigma} = 0.0314]	6679 [R_{int} = 0.0452, R_{sigma} = 0.0223]	23160 [R_{int} = 0.0274, R_{sigma} = 0.0205]	6424 [R_{int} = 0.0308, R_{sigma} = 0.0292]
Data/restraints/parameters	5433/0/356	6679/1/346	23160/355/1306	6424/0/355
Goodness-of-fit on F^2	1.020	1.034	1.055	1.020
Final R indexes [I>=2σ (I)]	R_1 = 0.0317, wR_2 = 0.0830	R_1 = 0.0238, wR_2 = 0.0614	R_1 = 0.0395, wR_2 = 0.1012	R_1 = 0.0283, wR_2 = 0.0695
Final R indexes [all data]	R_1 = 0.0354, wR_2 = 0.0856	R_1 = 0.0258, wR_2 = 0.0628	R_1 = 0.0443, wR_2 = 0.1051	R_1 = 0.0371, wR_2 = 0.0754
Largest diff. peak/hole / e Å^{-3}	0.38/−0.46	0.20/−0.18	0.79/−0.70	0.38/−0.27

Identification code	**2.6**	**2.7**	**2.7**·1.5BH_3:py	**2.8a**
Empirical formula	$C_{44}H_{74}GaNO_6Na_2$	$C_{32}H_{50}NO_3Ga$	$C_{39.5}H_{62}B_{1.5}GaN_{2.5}O_3$	$C_{84}H_{116}Ga_2N_2O_6$
Formula weight	828.74	566.45	705.85	1389.22
Temperature/K	150(2)	150(2)	150(2)	250(2)
Crystal system	orthorhombic	monoclinic	monoclinic	triclinic
Space group	*P*bca	$P2_1/n$	*C*2/c	*P*-1
a/Å	21.7502(7)	10.5108(4)	36.8096(17)	9.9279(4)
b/Å	19.5036(6)	11.7221(3)	12.9162(5)	14.2823(6)
c/Å	22.7241(6)	25.7484(8)	17.8272(7)	15.1222(8)
α/°	90	90	90	73.095(4)
β/°	90	94.700(3)	108.325(4)	88.710(4)
γ/°	90	90	90	86.042(3)
Volume/$Å^3$	9639.7(5)	3161.76(18)	8045.9(6)	2046.67(17)
Z	8	4	8	1
$\rho_{calc}g/cm^3$	1.142	1.19	1.165	1.127
μ/mm^{-1}	0.631	1.415	1.212	1.181
F(000)	3568.0	1216.0	3032.0	744.0
Radiation	Mo Kα (λ = 0.71073)	Cu Kα (λ = 1.54184)	Cu Kα (λ = 1.54178)	Cu Kα (λ = 1.54184)
2θ range for data collection/°	3.328 to 49.998	6.89 to 154.4	7.296 to 152.194	7.51 to 153.184
Index ranges	$-25 \le h \le 25$, $-23 \le k \le 13$, $-27 \le l \le 27$	$-13 \le h \le 13$, $-10 \le k \le 14$, $-32 \le l \le 32$	$-45 \le h \le 36$, $-13 \le k \le 15$, $-22 \le l \le 21$	$-12 \le h \le 12$, $-17 \le k \le 17$, $-19 \le l \le 18$
Reflections collected	40322	26500	23137	33243
Independent reflections	8489 [R_{int} = 0.1395, R_{sigma} = 0.1363]	6623 [R_{int} = 0.0563, R_{sigma} = 0.0476]	8256 [R_{int} = 0.0689, R_{sigma} = 0.0783]	8495 [R_{int} = 0.0616, R_{sigma} = 0.0481]
Data/restraints/parameters	8489/40/505	6623/0/354	8256/12/507	8495/138/496
Goodness-of-fit on F^2	0.980	1.084	1.034	1.051
Final R indexes [I>=2σ (I)]	R_1 = 0.0734, wR_2 = 0.1512	R_1 = 0.0537, wR_2 = 0.1415	R_1 = 0.0476, wR_2 = 0.1147	R_1 = 0.0621, wR_2 = 0.1563
Final R indexes [all data]	R_1 = 0.1592, wR_2 = 0.1792	R_1 = 0.0639, wR_2 = 0.1483	R_1 = 0.0922, wR_2 = 0.1323	R_1 = 0.0734, wR_2 = 0.1720
Largest diff. peak/hole / e $Å^{-3}$	0.66/−0.45	0.91/−0.61	0.59/−0.51	1.13/−0.53

Identification code	**2.8b**	**2.9**	**2.10**	**2.11a**
Empirical formula	$C_{84}H_{124}N_2O_6Ga_2$	$C_{66.5}H_{96}Ga_2N_2O_4$	$C_{84}H_{122}N_2O_{10}Ga_2$	$C_{91}H_{120}N_2O_6Ga_2$
Formula weight	1397.28	1126.89	1459.27	1477.32
Temperature/K	150(2)	150(2)	150(2)	150(2)
Crystal system	monoclinic	triclinic	triclinic	triclinic
Space group	$P2_1/c$	P-1	P-1	P-1
a/Å	14.1156(4)	13.2508(6)	10.0582(3)	10.1748(4)
b/Å	25.4954(5)	16.1097(7)	15.3516(4)	13.5915(7)
c/Å	11.7947(3)	16.2894(4)	28.3711(8)	16.6911(11)
α/°	90	100.939(3)	97.045(2)	73.425(5)
β/°	113.696(3)	95.296(3)	91.342(2)	87.080(4)
γ/°	90	110.593(4)	90.672(2)	71.718(4)
Volume/Å^3	3886.84(19)	3147.7(2)	4346.0(2)	2098.8(2)
Z	2	2	2	1
ρ_{calc}g/cm^3	1.194	1.189	1.115	1.169
μ/mm^{-1}	1.244	1.397	1.169	1.182
F(000)	1504.0	1206.0	1564.0	790.0
Radiation	Cu Kα (λ = 1.54184)	Cu Kα (λ = 1.54184)	Cu Kα (λ = 1.54184)	Cu Kα (λ = 1.54178)
2θ range for data collection/°	14.41 to 178.786	5.61 to 132.978	8.012 to 152.546	7.144 to 132.972
Index ranges	$-18 \le h \le 18$, $-33 \le k \le 33$, $-15 \le l \le 15$	$-15 \le h \le 15$, $-19 \le k \le 19$, $-19 \le l \le 16$	$-12 \le h \le 11$, $-18 \le k \le 19$, $-35 \le l \le 35$	$-12 \le h \le 9$, $-15 \le k \le 16$, $-19 \le l \le 19$
Reflections collected	67190	24362	48193	18902
Independent reflections	8876 [R_{int} = 0.0558, R_{sigma} = 0.0374]	11087 [R_{int} = 0.0509, R_{sigma} = 0.0703]	17952 [R_{int} = 0.0382, R_{sigma} = 0.0457]	7381 [R_{int} = 0.0650, R_{sigma} = 0.0825]
Data/restraints/parameters	8876/0/440	11087/134/743	17952/0/891	7381/51/570
Goodness-of-fit on F^2	1.061	1.057	1.148	0.853
Final R indexes [I>=2σ (I)]	R_1 = 0.0400, wR_2 = 0.0975	R_1 = 0.0487, wR_2 = 0.1178	R_1 = 0.0572, wR_2 = 0.1688	R_1 = 0.0518, wR_2 = 0.1149
Final R indexes [all data]	R_1 = 0.0527, wR_2 = 0.1032	R_1 = 0.0676, wR_2 = 0.1283	R_1 = 0.0709, wR_2 = 0.1802	R_1 = 0.0730, wR_2 = 0.1246
Largest diff. peak/hole / e Å^{-3}	0.61/−0.72	1.07/−0.74	0.51/−1.94	0.52/−0.69

Identification code	**2.11b**	**2.11c**	**2.11d**	**2.11e**
Empirical formula	$C_{85}H_{124}Ga_2N_2O_6$	$C_{84}H_{112}N_2O_8Ga_2$	$C_{82}H_{106}N_2O_6Ga_2Br_2$	$C_{78}H_{110}N_2O_6Ga_2Cl_6$
Formula weight	1409.29	1417.19	1514.94	1523.81
Temperature/K	150(2)	150(2)	150(2)	150(2)
Crystal system	triclinic	triclinic	triclinic	triclinic
Space group	*P*-1	*P*-1	*P*-1	*P*-1
a/Å	10.9400(4)	11.7351(3)	10.2092(5)	10.0474(6)
b/Å	10.9575(4)	13.6580(3)	14.1435(5)	13.9132(8)
c/Å	19.5421(8)	13.7914(4)	14.8323(4)	15.0745(7)
α/°	83.885(4)	118.346(3)	71.491(3)	73.849(5)
β/°	85.067(3)	91.183(2)	86.381(3)	89.590(4)
γ/°	61.298(4)	98.843(2)	81.607(3)	82.391(5)
Volume/Å^3	2041.45(15)	1911.12(10)	2008.84(14)	2005.3(2)
Z	1	1	1	1
ρ_{calc}g/cm^3	1.146	1.231	1.252	1.262
μ/mm^{-1}	1.189	1.297	2.369	3.046
F(000)	758.0	756.0	792.0	804.0
Radiation	Cu Kα (λ = 1.54178)	Cu Kα (λ = 1.54184)	Cu Kα (λ = 1.54184)	Cu Kα (λ = 1.54184)
2θ range for data collection/°	9.11 to 152.374	7.326 to 153.438	6.286 to 153.962	7.686 to 132.99
Index ranges	$-13 \le h \le 8$, $-13 \le k \le 11$, $-24 \le l \le 24$	$-14 \le h \le 14$, $-17 \le k \le 17$, $-17 \le l \le 17$	$-12 \le h \le 12$, $-16 \le k \le 17$, $-18 \le l \le 14$	$-11 \le h \le 11$, $-11 \le k \le 16$, $-17 \le l \le 17$
Reflections collected	19231	46696	16435	17880
Independent reflections	8342 [R_{int} = 0.0304, R_{sigma} = 0.0392]	7940 [R_{int} = 0.0318, R_{sigma} = 0.0196]	8349 [R_{int} = 0.0244, R_{sigma} = 0.0387]	7048 [R_{int} = 0.0423, R_{sigma} = 0.0542]
Data/restraints/parameters	8342/55/535	7940/0/506	8349/0/429	7048/0/443
Goodness-of-fit on F^2	1.084	1.034	1.024	1.031
Final R indexes [I>=2σ (I)]	R_1 = 0.0559, wR_2 = 0.1480	R_1 = 0.0299, wR_2 = 0.0777	R_1 = 0.0323, wR_2 = 0.0778	R_1 = 0.0421, wR_2 = 0.1041
Final R indexes [all data]	R_1 = 0.0618, wR_2 = 0.1523	R_1 = 0.0326, wR_2 = 0.0798	R_1 = 0.0404, wR_2 = 0.0828	R_1 = 0.0537, wR_2 = 0.1120
Largest diff. peak/hole / e Å^{-3}	1.97/−0.88	0.38/−0.36	0.41/−0.55	0.97/−0.58

Identification code	**2.12a**	**2.12b**	**2.12c**	**2.12d**
Empirical formula	$C_{86}H_{108}Cl_{12}Ga_2N_2O_6$	$C_{80}H_{114}N_2O_6Ga_2$	$C_{86}H_{116}N_2O_8Ga_2$	$C_{84}H_{110}Br_2Ga_2N_2O_6$
Formula weight	1830.58	1339.17	1445.24	1542.99
Temperature/K	150.15	150(2)	150(2)	150(2)
Crystal system	monoclinic	monoclinic	triclinic	orthorhombic
Space group	$P2_1/n$	$P2_1/c$	P-1	$Pca2_1$
a/Å	13.2386(2)	13.4385(2)	11.9141(4)	12.3203(6)
b/Å	23.2866(4)	25.7074(3)	13.7371(9)	17.7668(9)
c/Å	14.7290(3)	11.6672(2)	13.9224(9)	37.0079(14)
α/°	90	90	60.696(6)	90
β/°	98.551(2)	110.313(2)	80.943(4)	90
γ/°	90	90	80.598(4)	90
Volume/Å^3	4490.21(14)	3779.99(11)	1952.4(2)	8100.7(6)
Z	2	2	1	4
ρ_{calc}g/cm^3	1.354	1.177	1.229	1.265
μ/mm^{-1}	4.420	1.260	1.279	1.702
F(000)	1904.0	1436.0	772.0	3232.0
Radiation	Cu Kα (λ = 1.54184)	Cu Kα (λ = 1.54184)	Cu Kα (λ = 1.54184)	Mo Kα (λ = 0.71073)
2θ range for data collection/°	7.158 to 152.276	6.876 to 153.44	7.31 to 152.982	6.606 to 49.996
Index ranges	$-15 \le h \le 16$, $-29 \le k \le 23$, $-17 \le l \le 18$	$-16 \le h \le 16$, $-32 \le k \le 32$, $-14 \le l \le 13$	$-14 \le h \le 10$, $-16 \le k \le 17$, $-17 \le l \le 17$	$-14 \le h \le 13$, $-21 \le k \le 17$, $-41 \le l \le 44$
Reflections collected	26576	39859	17832	33972
Independent reflections	9303 [R_{int} = 0.0423, R_{sigma} = 0.0411]	7923 [R_{int} = 0.0464, R_{sigma} = 0.0317]	8068 [R_{int} = 0.0270, R_{sigma} = 0.0331]	13206 [R_{int} = 0.1107, R_{sigma} = 0.1629]
Data/restraints/parameters	9303/0/217	7923/114/481	8068/0/460	13206/1/891
Goodness-of-fit on F^2	2.877	1.017	0.945	0.911
Final R indexes [I>=2σ (I)]	R_1 = 0.1317, wR_2 = 0.3617	R_1 = 0.0316, wR_2 = 0.0791	R_1 = 0.0585, wR_2 = 0.1718	R_1 = 0.0625, wR_2 = 0.0932
Final R indexes [all data]	R_1 = 0.1474, wR_2 = 0.3823	R_1 = 0.0395, wR_2 = 0.0846	R_1 = 0.0657, wR_2 = 0.1818	R_1 = 0.1366, wR_2 = 0.1145
Largest diff. peak/hole / e Å^{-3}	4.22/−2.51	0.34/−0.34	2.72/−0.80	0.57/−0.50

Identification code	**2.12e**	**4.1**	**4.2**·$OPEt_3$	**4.5**
Empirical formula	$C_{76}H_{102}N_2O_6Ga_2Cl_6$	$C_{40}H_{42}BNO_2F_{10}$	$C_{40}H_{56}BNO_3F_5P$	$C_{34}H_{54}BNO_4$
Formula weight	1491.73	769.55	735.63	551.59
Temperature/K	150(2)	150(2)	150(2)	150(2)
Crystal system	monoclinic	monoclinic	monoclinic	orthorhombic
Space group	$P2_1/c$	$P2_1/n$	$C2/c$	$Pbca$
a/Å	17.7872(2)	17.8567(4)	36.3476(11)	18.7436(4)
b/Å	18.4325(2)	10.2266(2)	13.3235(3)	18.1246(3)
c/Å	12.10850(10)	43.2741(11)	19.8356(6)	19.7693(3)
α/°	90	90	90	90
β/°	104.5250(10)	95.693(2)	122.876(3)	90
γ/°	90	90	90	90
Volume/Å^3	3843.04(7)	7863.4(3)	8067.5(5)	6716.0(2)
Z	2	8	8	8
ρ_{calc}g/cm^3	1.289	1.300	1.211	1.091
μ/mm^{-1}	3.169	0.959	0.128	0.539
F(000)	1568.0	3200.0	3136.0	2416.0
Radiation	Cu Kα (λ = 1.54184)	Cu Kα (λ = 1.54184)	Mo Kα (λ = 0.71073)	Cu Kα (λ = 1.54184)
2θ range for data collection/°	7.026 to 152.372	7.524 to 132.998	6.59 to 49.998	8.128 to 153.222
Index ranges	$-22 \le h \le 22, -23 \le k \le 21, -15 \le l \le 12$	$-21 \le h \le 20, -12 \le k \le 12, -51 \le l \le 51$	$-43 \le h \le 41, -15 \le k \le 15, -23 \le l \le 23$	$-21 \le h \le 23, -22 \le k \le 17, -24 \le l \le 24$
Reflections collected	22979	171322	38091	27220
Independent reflections	7948 [R_{int} = 0.0348, R_{sigma} = 0.0391]	13841 [R_{int} = 0.1293, R_{sigma} = 0.0412]	7093 [R_{int} = 0.0800, R_{sigma} = 0.0540]	6988 [R_{int} = 0.0346, R_{sigma} = 0.0368]
Data/restraints/parameters	7948/0/419	13841/0/1005	7093/3/486	6988/0/385
Goodness-of-fit on F^2	1.037	1.041	1.062	1.019
Final R indexes [I>=2σ (I)]	R_1 = 0.0443, wR_2 = 0.1160	R_1 = 0.0846, wR_2 = 0.2397	R_1 = 0.0661, wR_2 = 0.1824	R_1 = 0.0443, wR_2 = 0.1022
Final R indexes [all data]	R_1 = 0.0562, wR_2 = 0.1266	R_1 = 0.1212, wR_2 = 0.2719	R_1 = 0.0899, wR_2 = 0.2010	R_1 = 0.0709, wR_2 = 0.1135
Largest diff. peak/hole / e Å^{-3}	1.19/−0.60	0.59/−0.50	0.57/−0.47	0.20/−0.21

Identification code	**4.6**·$OPEt_3$	**4.8**·$NH_2{}^nPr$	**4.8**·$OPEt_3$	**4.9**
Empirical formula	$C_{34}H_{57}BNO_3P$	$C_{59}H_{89}B_2N_3O_4$	$C_{68}H_{101}B_2N_2O_5P$	$C_{61}H_{92}B_2N_2O_4$
Formula weight	569.58	925.95	1079.09	938.98
Temperature/K	150(2)	150(2)	150(2)	150(2)
Crystal system	triclinic	monoclinic	monoclinic	triclinic
Space group	*P*-1	$P2_1/c$	$P2_1/c$	*P*-1
a/Å	10.5298(3)	10.03610(10)	13.52610(10)	14.1248(2)
b/Å	18.0514(3)	30.3554(2)	33.8755(3)	14.4384(3)
c/Å	19.3025(5)	18.8035(2)	14.9529(2)	17.1804(3)
α/°	104.010(2)	90	90	98.299(2)
β/°	90.602(2)	99.3320(10)	106.8430(10)	100.2560(10)
γ/°	100.192(2)	90	90	115.390(2)
Volume/$Å^3$	3498.19(15)	5652.67(9)	6557.56(12)	3017.26(10)
Z	4	4	4	2
$\rho_{calc}g/cm^3$	1.081	1.088	1.093	1.034
μ/mm^{-1}	0.926	0.508	0.732	0.477
F(000)	1248.0	2024.0	2352.0	1028.0
Radiation	Cu Kα (λ = 1.54184)	Cu Kα (λ = 1.54184)	Cu Kα (λ = 1.54184)	Cu Kα (λ = 1.54184)
2θ range for data collection/°	7.796 to 152.438	5.582 to 153.614	6.704 to 152.776	6.996 to 152.916
Index ranges	$-13 \le h \le 13$, $-22 \le k \le 14$, $-24 \le l \le 24$	$-12 \le h \le 12$, $-36 \le k \le 38$, $-23 \le l \le 23$	$-11 \le h \le 16$, $-41 \le k \le 42$, $-18 \le l \le 16$	$-17 \le h \le 17$, $-18 \le k \le 18$, $-21 \le l \le 19$
Reflections collected	40502	105563	41897	73047
Independent reflections	14453 [R_{int} = 0.0263, R_{sigma} = 0.0304]	11841 [R_{int} = 0.0364, R_{sigma} = 0.0163]	13562 [R_{int} = 0.0269, R_{sigma} = 0.0286]	12536 [R_{int} = 0.0402, R_{sigma} = 0.0206]
Data/restraints/parameters	14453/0/767	11841/0/670	13562/12/805	12536/106/699
Goodness-of-fit on F^2	1.034	1.026	1.066	1.059
Final R indexes [I>=2σ (I)]	R_1 = 0.0465, wR_2 = 0.1203	R_1 = 0.0517, wR_2 = 0.1430	R_1 = 0.0639, wR_2 = 0.1892	R_1 = 0.0484, wR_2 = 0.1291
Final R indexes [all data]	R_1 = 0.0557, wR_2 = 0.1282	R_1 = 0.0610, wR_2 = 0.1527	R_1 = 0.0704, wR_2 = 0.1946	R_1 = 0.0537, wR_2 = 0.1339
Largest diff. peak/hole / e $Å^{-3}$	1.08/−0.65	0.57/−0.42	0.80/−0.44	0.48/−0.33

Identification code	**4.10**	**4.11**	**5.2b** $Et^iPr_2N{\cdot}HCl$	**5.2c**
Empirical formula	$C_{60}H_{88}B_2N_2O_5$	$C_{36}H_{50}BNO_3$	$C_{39}H_{64}BCl_2N_2O_2$	$C_{34}H_{47}BNO_2Br$
Formula weight	938.94	555.58	674.63	592.44
Temperature/K	150(2)	150(2)	150(2)	150(2)
Crystal system	monoclinic	triclinic	monoclinic	monoclinic
Space group	$P2_1/n$	P-1	$P2_1/c$	$P2_1/c$
a/Å	10.95940(10)	11.5782(5)	10.2566(3)	10.10990(10)
b/Å	26.0177(2)	15.6776(6)	32.6154(6)	10.15310(10)
c/Å	20.0544(2)	18.8996(6)	13.1384(3)	31.2947(2)
α/°	90	93.687(3)	90	90
β/°	100.0660(10)	96.336(3)	111.546(3)	90.1850(10)
γ/°	90	97.313(3)	90	90
Volume/Å^3	5630.26(9)	3371.2(2)	4087.98(19)	3212.29(5)
Z	4	4	4	4
ρ_{calc}g/cm^3	1.108	1.095	1.096	1.225
μ/mm^{-1}	0.526	0.068	0.191	1.956
F(000)	2048.0	1208.0	1468.0	1256.0
Radiation	Cu Kα (λ = 1.54178)	Mo Kα (λ = 0.71073)	Mo Kα (λ = 0.71073)	Cu Kα (λ = 1.54184)
2θ range for data collection/°	8.138 to 152.632	6.746 to 50	3.56 to 49.998	8.746 to 152.34
Index ranges	$-13 \le h \le 13$, $-32 \le k \le 32$, $-18 \le l \le 25$	$-13 \le h \le 13$, $-18 \le k \le 18$, $-22 \le l \le 22$	$-12 \le h \le 10$, $-38 \le k \le 38$, $-15 \le l \le 15$	$-11 \le h \le 12$, $-12 \le k \le 12$, $-39 \le l \le 38$
Reflections collected	57491	54893	28220	33140
Independent reflections	11703 [R_{int} = 0.0232, R_{sigma} = 0.0154]	11848 [R_{int} = 0.0451, R_{sigma} = 0.0438]	7195 [R_{int} = 0.0461, R_{sigma} = 0.0459]	6681 [R_{int} = 0.0244, R_{sigma} = 0.0166]
Data/restraints/parameters	11703/6/697	11848/0/804	7195/0/440	6681/0/368
Goodness-of-fit on F^2	1.078	1.074	1.037	1.030
Final R indexes [I>=2σ (I)]	R_1 = 0.0526, wR_2 = 0.2180	R_1 = 0.0560, wR_2 = 0.1433	R_1 = 0.0436, wR_2 = 0.0960	R_1 = 0.0259, wR_2 = 0.0658
Final R indexes [all data]	R_1 = 0.0595, wR_2 = 0.2377	R_1 = 0.0822, wR_2 = 0.1553	R_1 = 0.0630, wR_2 = 0.1025	R_1 = 0.0274, wR_2 = 0.0670
Largest diff. peak/hole / e Å^{-3}	0.59/−0.33	1.18/−0.73	0.22/−0.20	0.32/−0.47

Identification code	**5.3b**	**5.3c**	**5.5**	**5.6**
Empirical formula	$C_{47}H_{71}BN_3O_2$	$C_{31}BN_2O_2H_{49}$	$C_{32}H_{48}BNO_3$	$C_{32}H_{49}BNO_4Br$
Formula weight	720.87	492.53	253.67	602.44
Temperature/K	150(2)	150(2)	293(2)	150(2)
Crystal system	monoclinic	monoclinic	triclinic	triclinic
Space group	$P2_1/n$	$P2_1/c$	P-1	P-1
a/Å	14.1198(4)	14.5737(5)	9.0527(11)	9.9868(4)
b/Å	16.8322(4)	19.0944(5)	11.2697(13)	13.3516(7)
c/Å	19.3478(4)	12.3383(4)	15.378(2)	13.8862(6)
α/°	90	90	84.060(10)	68.838(4)
β/°	106.965(3)	112.520(4)	74.468(11)	84.160(3)
γ/°	90	90	85.640(10)	73.455(4)
Volume/Å^3	4398.2(2)	3171.64(19)	1501.6(3)	1655.23(14)
Z	4	4	4	2
ρ_{calc}g/cm^3	1.089	1.031	1.122	1.209
μ/mm^{-1}	0.065	0.481	0.539	1.95
F(000)	1580.0	1080.0	554.0	640.0
Radiation	Mo Kα (λ = 0.71073)	Cu Kα (λ = 1.54184)	Cu Kα (λ = 1.54184)	Cu Kα (λ = 1.54184)
2θ range for data collection/°	3.172 to 50	8.036 to 152.108	7.898 to 153.574	6.826 to 152.076
Index ranges	$-16 \le h \le 16$, $-20 \le k \le 18$, $-23 \le l \le 23$	$-17 \le h \le 18$, $-15 \le k \le 23$, $-15 \le l \le 15$	$-9 \le h \le 11$, $-14 \le k \le 12$, $-19 \le l \le 19$	$-11 \le h \le 12$, $-16 \le k \le 16$, $-17 \le l \le 17$
Reflections collected	29374	17587	12895	16739
Independent reflections	7733 [R_{int} = 0.0415, R_{sigma} = 0.0479]	6549 [R_{int} = 0.0350, R_{sigma} = 0.0384]	5625 [R_{int} = 0.1177, R_{sigma} = 0.0974]	6847 [R_{int} = 0.0210, R_{sigma} = 0.0218]
Data/restraints/parameters	7733/7/509	6549/0/340	5625/42/380	6847/0/368
Goodness-of-fit on F^2	1.071	1.022	1.081	1.045
Final R indexes [I>=2σ (I)]	R_1 = 0.0645, wR_2 = 0.1686	R_1 = 0.0450, wR_2 = 0.1145	R_1 = 0.0963, wR_2 = 0.2687	R_1 = 0.0282, wR_2 = 0.0737
Final R indexes [all data]	R_1 = 0.0961, wR_2 = 0.1830	R_1 = 0.0617, wR_2 = 0.1257	R_1 = 0.1403, wR_2 = 0.2835	R_1 = 0.0306, wR_2 = 0.0758
Largest diff. peak/hole / e Å^{-3}	0.39/−0.41	0.26/−0.21	0.33/−0.29	0.36/−0.50

Identification code	**5.7**	**5.9**
Empirical formula	$C_{32}H_{50}BNO_4Br_2$	$C_{55}H_{82}B_2N_2O_5$
Formula weight	683.36	294.95
Temperature/K	150(2)	150(2)
Crystal system	triclinic	triclinic
Space group	*P*-1	*P*-1
a/Å	10.5077(6)	10.1623(4)
b/Å	10.5678(5)	15.1653(8)
c/Å	15.7884(8)	17.8497(9)
α/°	84.708(4)	88.964(4)
β/°	79.296(4)	89.282(3)
γ/°	84.268(4)	78.573(4)
Volume/Å^3	1709.20(16)	2695.8(2)
Z	2	6
ρ_{calc}g/cm^3	1.328	1.09
μ/mm^{-1}	3.269	0.522
F(000)	712.0	964.0
Radiation	Cu Kα (λ = 1.54184)	Cu Kα (λ = 1.54178)
2θ range for data collection/°	8.434 to 152.826	7.68 to 153.022
Index ranges	$-13 \le h \le 13$, $-13 \le k \le 12$, $-19 \le l \le 18$	$-11 \le h \le 12$, $-18 \le k \le 18$, $-21 \le l \le 22$
Reflections collected	17582	26501
Independent reflections	7063 [R_{int} = 0.0323, R_{sigma} = 0.0352]	11128 [R_{int} = 0.0530, R_{sigma} = 0.0660]
Data/restraints/parameters	7063/0/397	11128/6/742
Goodness-of-fit on F^2	1.031	1.176
Final R indexes [I>=2σ (I)]	R_1 = 0.0367, wR_2 = 0.0897	R_1 = 0.0507, wR_2 = 0.1416
Final R indexes [all data]	R_1 = 0.0438, wR_2 = 0.0953	R_1 = 0.0844, wR_2 = 0.1546
Largest diff. peak/hole / e Å^{-3}	1.87/−1.46	0.22/−0.21